Nature's Way: The Effects of Hydrogen Bond Networks on Acidities, Catalysis, and Molecular Recognition

A DISSERTATION
SUBMITTED TO THE FACULTY OF THE GRADUATE SCHOOL
OF THE UNIVERSITY OF MINNESOTA
BY

Alireza Shokri

IN PARTIAL FULFILLMENT OF THE REQUIREMENTS
FOR THE DEGREE OF
DOCTOR OF PHILOSOPHY

Steven R. Kass, Advisor

August 2013

Acknowledgements

I would like to express my sincere appreciation to my advisor Prof. Steven Kass for the continuous support of my Ph.D study, for his patience, motivation, enthusiasm, and immense knowledge. I could not have imagined having a better advisor and mentor for my research.

I would like to thank my wife, Marzieh, for her endless love, kindness and support she has shown during the past four years it has taken me to finalize this thesis.

Last but not the least, I would like to thank my family for their love and support.

To

My wife, Marzieh

Abstract

Hydrogen bond networks play a critical role in many biological processes. Herein, hydrogen bond arrays are studied and exploited. Their strengths are measured in compounds with multiple hydrogen bonds to better understand enzymatic reactions. Anion recognition abilities of synthetic hydrogen bonded receptors are studied to probe the role of hydrogen bonds in anion channels. At the same time, environmentally friendly green acids are developed and their catalytic reactivities in different organic reactions are explored. Hydrogen bonding networks provide a remarkable means for learning about fundamental biological reactions and synthesizing new anion receptors and novel Brønsted acid catalysts.

Table of Contents

List of Tables

Chapter 1

Chapter 2

Chapter 3

Chapter 5

Chapter 6

Chapter 7

Chapter 8

Appendix for chapter 3

Appendix for chapter 4

Appendix for chapter 5

Appendix for chapter 7

Appendix for chapter 8

List of Figures

Chapter 1

Chapter 2

Chapter 3

Chapter 4

Chapter 5

Chapter 6

Chapter 7

Chapter 8

Appendix for chapter 2

Appendix for chapter 3

Appendix for chapter 5

Appendix for chapter 6

Appendix for chapter 7

Appendix for chapter 8

List of Schemes

Chapter 1

Chapter 2

Chapter 7

List of Abbreviations

Å	angstrom
ACN	acetonitrile
BINAP	2,2'-bis(diphenylphosphino)-1,1'-binaphthyl
˚C	degrees Celsius
CF_3TMS	trimethyl(trifluoromethyl)silane
Calcd	calculated
δ	chemical shift in part per million
DIBAL-H	diisobutylaluminium hydride
DFT	density functional theory
ΔG°	change in free energy
ΔH°	change in free enthalpy
ΔS°	change in entropy
$\Delta C_p°$	change in heat capacity
DMSO	dimethyl sulfoxide
ε	dielectric constant
eV	electron volts
exptl	experimental
ESI	electrospray ionization
HRMS	high resolution mass spectrometry
h	hour(s)
IR	infrared spectroscopy
K	Kelvin
kcal mol^{-1}	kilocalorie per mole
M	molar (moles per liter)
m	minute(s)
g	gram

M06-2X	Minnesota 06 functional with double the amount of nonlocal exchange
MHz	megahertz
mL	milliliter
µL	microliter
mM	millimolar
mmol	millimole
MPLC	medium pressure liquid chromatography
m/z	mass to charge ratio
NMR	nuclear magnetic resonance
PEG	polyethylene glycol
Ph	phenyl
ppm	parts per million
Ref.	reference
TBAF	tetrabutylammonium fluoride
THF	tetrahydrofuran
TLC	thin layer chromatography
TOF	time of flight
s	second(s)
UV	ultraviolet
Vis	visible
zpe	zero-point energy

Chapter 1: Introduction

Hydrogen bonds

Hydrogen bonds play a critical role on our planet and are essential for life.[1] They are the reason that water is a liquid rather than a gas and are responsible for the base pairing in DNA and the three dimensional structures of proteins. They are also essential for the catalytic function of enzymes. A hydrogen bond between A−H and B can be defined as a simple electrostatic attraction between the positive end of an A−H bond dipole and the negative end of the dipole of B.[1-5,6] When A is a highly electronegative atom such as N, O, or F, H−A typically has a large dipole moment and these compounds are good hydrogen bond donors. When a hydrogen bond is formed, the A···B distance is less than the sum of the van der Waals radii of A and B, and the A− H distance increases. As a result, the fundamental vibrational frequency for A−H shows a substantial red shift (on the order of 100 cm^{-1}) and the proton signal in the ^{1}H NMR spectrum shifts to lower field regions because the magnetic shielding of the proton is reduced.[7,8] The latter change in hydrogen bonded systems is typically a few part per million.[9-11]

Three types of hydrogen bonds have been reported in the literature.[1-3] They correspond to weak (< 4 kcal mol^{-1}), moderate (4 - 15 kcal mol^{-1}), and strong (15 - 40 kcal mol^{-1}) interactions. Their properties are listed in Table 1 and a correlation between the hydrogen bond strength and the A···B bond length and the A−H···B bond angle have been noted. The strongest hydrogen bonds are observed when A−H···B is 180° but modest deviations from linearity up to 20° do not significantly affect their strength. On the other hand, the

Table 1. General characteristics of the three major hydrogen bond types.

H-Bond Parameters (A–H···B)	Weak	Moderate	Strong
A···B H-Bond length (Å)	> 3.2	2.5 - 3.2	2.2 - 2.5
A–H···B H-Bond angles (°)	> 90	> 130	170 - 180
H-Bond strength (kcal mol^{-1})	< 4	4 - 15	15 - 40
Relative infrared shift (cm^{-1})	< 10%	10 - 25%	25%

interaction energy is quite sensitive to the bond length and it decays exponentially with distance.

Normal hydrogen bond geometries

Hydrogen bond geometries in a variety of molecules such as proteins, nucleic acids, bio-macromolecules, and carbohydrates have been investigated by X-ray and neutron crystallography.[12,13] X-ray diffraction studies of A–H···B provide the distance between the two heavy atoms (i.e. A and B) very accurately but are not nearly as reliable in locating the bridging hydrogen atom position. As a result, hydrogen bond distances are commonly reported as d_{AB}. The length between the two heavy atoms can be related to potential-energy diagrams that describe the motion of a hydrogen atom between two acceptor groups (Figure 1).[14] Figure 1a corresponds to a typical hydrogen bond where d_{OO} is around 2.80 Å, the hydrogen atom is tightly bound to one of the two oxygens and the ΔH of formation is ∼5

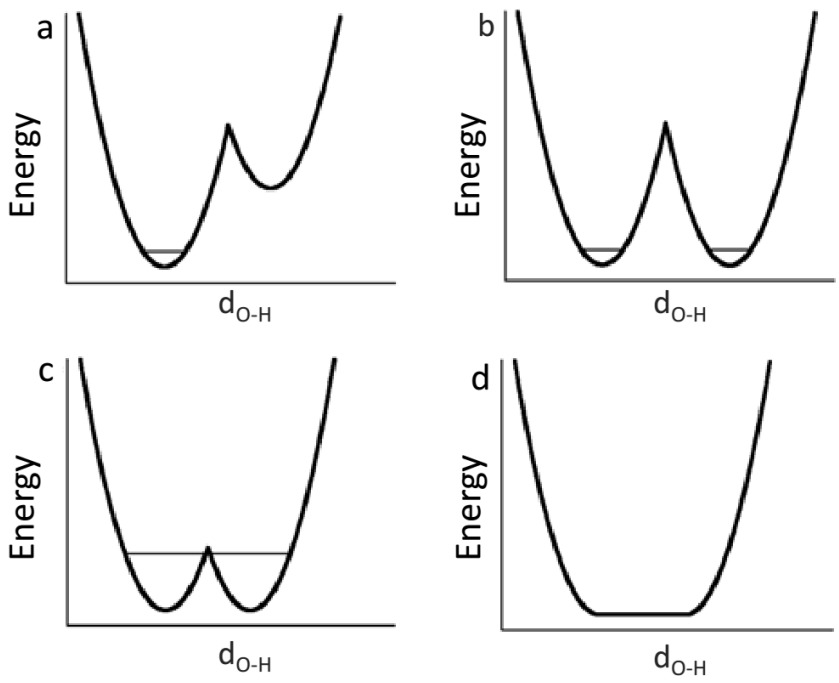

Figure 1. Potential energy diagrams for OHO hydrogen bonds: (a) asymmetric double-well, (b) symmetric double-well, (c) low-barrier, and (d) single-well hydrogen bonds.

kcal mol^{-1}. A symmetric hydrogen bond potential well with a high barrier for hydrogen transfer is illustrated in Figure 1b and typically is encountered when the hydrogen bonds are of moderate strength. In contrast, when strong hydrogen bonds (25 - 30 kcal mol^{-1}) are formed d_{OO} decreases to 2.50 Å and the energy barrier is close to the zero point energy (Figure 1c). In this case the hydrogen is essentially free to move between two heavy atoms and this situation is referred to as short strong or low barrier hydrogen bonds (LBHBs). Figure 1d shows a single well potential energy diagram where d_{OO} is shortened to 2.2 Å, and the barrier has disappeared. This situation also corresponds to a strong hydrogen bond.

Normal hydrogen bond energies in solution

The energies of ordinary hydrogen bonds in solution between uncharged groups typically are 1.0 - 2.0 kcal mol^{-1}, whereas the corresponding values involving a charged species are higher, 1.5 - 4.0 kcal mol^{-1}.[1,15] For example, the intramolecular hydrogen bond energy in an amide which has been studied by retardation of base-catalyzed proton exchange is 2.0 kcal mol^{-1}. In proteins the energetic effect of hydrogen bonds have been obtained by deletion studies where one amino acid residue that is capable of forming a hydrogen bond is removed and the effect of this change on the structural stability is obtained. Values of 0.5 - 2.0 kcal mol^{-1} for the protein barnase,[16] 2.2 kcal mol^{-1} for staphylococcal nuclease,[17] and 4.6 kcal mol^{-1} for triosephosphate isomerase have been reported.[18] It should be noted that these energies cannot be attributed to a single hydrogen bond because it's not possible to remove such an interaction without affecting other factors such as the conformation, bond dipoles, etc.

Low-barrier hydrogen bonds

Recently, low barrier hydrogen bonds have been invoked to explain the mechanism of catalyzed reactions by different enzymes such as liver alcohol dehydrogenase, zinc protease, triose-P isomerase, and steroid isomerase.[19-22] It has been proposed that LBHBs have a strength of ~ 25 - 30 kcal mol^{-1} in the gas phase and about half of this energy in organic solvents and water (i.e. 12 - 15 kcal mol^{-1}). The former quantities have been experimentally determined but strong hydrogen bonds in excess of ~ 8 kcal mol^{-1} have not been measured in solution to date.

LBHBs have several physiochemical properties in addition to their short heavy atom distances.[23] Proton NMR chemical shifts are quite downfield (16 - 25 ppm) and low deuterium fractionation factors have been reported. Red shifts of infrared vibrational stretching frequencies of hydroxyl groups down to ~ 3000 cm^{-1} were also noted, and these bands commonly are unusually broad. These situations arise when the pK_a values of the two heteroatoms involved in the hydrogen bond become comparable, whereas weaker interactions result when they do not match each other.

Ketosteroid isomerase interconverts non-conjugated and conjugated ketosteroids via a dienolate intermediate. Asp-38 removes a proton from C-4 of a Δ^5 ketosteroid to give the dienolate and puts the proton back on C-6 to give a Δ^4 product (Figure 2).[24] Gerlt and Gassman proposed that a LBHB formed between the intermediate and Tyr14 during the reaction. In the substrate-enzyme complex Tyr14 (pK_a = 11.6), which is in the enzyme active site, is hydrogen bonded to the carbonyl oxygen

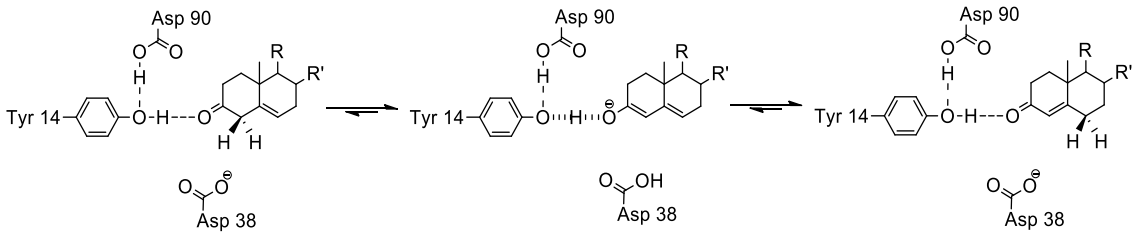

Figure 2. Reaction mechanism of Δ^5-ketosteroid isomerase in which a LBHB contributes to the differential stabilization of the dienolate intermediate.

in the substrate (pK_a = -7).[25] The enolization is facilitated by stabilization of the resulting dienolate through a low barrier hydrogen bonding with Tyr 14. This bond has three characteristics of a LBHB: matched pK_a values of the donor and acceptor, a low field proton signal at 18.15 ppm, and a fractionation factor of 0.34 for the hydrogen.

Another clear example of LBHBs in enzymatic catalysis is shown by serine proteases.[22] In their active sites His, Ser, and Asp residues are present, forming what is often called the "catalytic triad". The oxyanion "tetrahedral intermediate" is stabilized by formation of LBHBs with the peptidic NH of either Gly193 or Gly195 (Figure 3).[19] In addition, the general base His57 is hydrogen bonded with Asp102. The assigned chemical shift of the proton in the hydrogen bond between His57 and Asp102 is 18.3 ppm. A low fractionation factor for the proton was also found in support of the LBHB proposal.

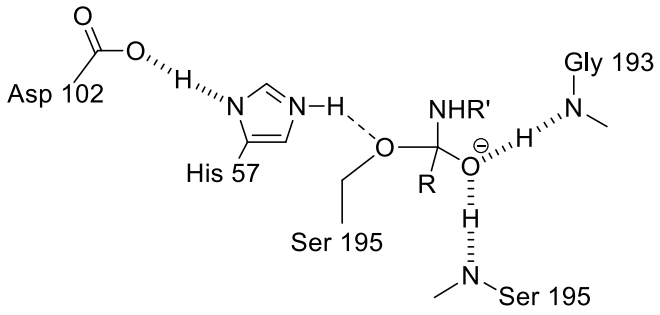

Figure 3. Low barrier hydrogen bonds in the catalytic triad of serine proteases.

Criticisms of low barrier hydrogen bonds

Warshel and co-worker have proposed that the polar environments in enzymes can stabilize the charges of asymmetric hydrogen bonds more than those with symmetric low barrier hydrogen bonds.[26] Calculations on the trypsin active site revealed that the dipoles of Gly193 and Ser195 provide electrostatic stabilization for the oxyanion hole. In contrast, proton transfer from His57 to Asp102 was calculated to be energetically unfavorable.[27,28] As a result, they concluded that enzymatic reactions can be explained without applying the LBHB proposal.

Although there are several physiochemical properties for LBHBs, there is no experimental evidence for their special strength in solution. For example, Kreevoy et al. have shown that the proton involved in the hydrogen bond between *p*-nitrophenol and its conjugate base has a ^{1}H NMR signal at 16.8 ppm in acetonitrile and a low fractionation factor of 0.31,[29] but the measured free energy for hydrogen bond formation is only 5.1 kcal mol^{-1}.[30] The FHF^- hydrogen bond, which is the shortest bond in the solid phase and the strongest one to be measured in the gas phase, is another example. In organic solvents it shows a ^{1}H NMR signal at 16.4 ppm and has a low fractionation factor of 0.66 for the hydrogen,[31] but its binding energy is just 0.82 kcal mol^{-1} in water.[32].

It was proposed in the original LBHB hypothesis that hydrogen bonds between an enzyme and its substrate may be weak because of a mismatch in the pK_a of the donor and acceptor. Factors that equalize the pK_a's in the transition state strengthen the hydrogen bond by 10 - 15 kcal mol^{-1}. The variation of ΔG for bond formation with ΔpK in solution

was investigated by Shan and Herschlag.[33] It was found that the slope of the log of formation constant (K_{form}) versus ΔpK is only 0.05 in water, which means that the hydrogen bond energy does not depend on the difference in the acidities of the donor and acceptor, and there is also no special energy at $\Delta pK_a = 0$. Scheiner et al. have also performed ab initio calculations on several hydrogen bonded models (carboxyl-imine, carbonyl-hydroxyl, and ammonia-hydrogen iodide) and observed that as the proton affinity of the less basic partner was enhanced, no particular stabilization was associated with the point of equal pK_a.[34] There was no dramatic or precipitous change in hydrogen bond strength that occurs when the acidities are equalized. Guthrie has also pointed out that having heteroatoms with similar pK_as involved in the bond might be the requirement for a short hydrogen bond, but it does not indicate how strong the hydrogen bond will be.[35a-35d] It should be noted that the strongest hydrogen bond that has ever been measured in solution is 7.5 kcal mol^{-1} in acetonitrile.[35e, 35f]

Although the effect of hydrogen bonds on the rates of enzyme-catalyzed reactions studied by site-directed mutagenesis experiments suggest the importance of LBHBs, there is no clear cut evidence in support of this proposal. It therefore has been suggested that instead of relying on a single extraordinarily strong interaction that multiple interactions are probably important.[33] That is, a network of hydrogen bonds and preorganization of catalytic groups in the active site can explain the high catalytic activities of enzymes.

Effect of multiple hydrogen bonds on acidity*

Alcohols are weak acids in protic solvents and their acidities vary with the medium. For instance, the pK_a value of ethanol is 15.9 in water, whereas in dimethyl sulfoxide (DMSO) it is 29.8.[36] The larger value in DMSO is due in large part to the lack of intermolecular hydrogen bonding and the resulting stabilization it brings about. Alcohols are weak acids in the gas phase too for the same reason, but substitution of a β hydrogen in ethanol with a hydroxyl group leads to a 13.6 ± 2.6 kcal mol^{-1} (i.e., 10 ± 2 pK_a units) enhancement in the deprotonation enthalpy. An even larger effect of 17.7 ± 2.8 kcal mol^{-1} (i.e., 13 ± 2 pK_a units) is observed for 1,3-propanediol relative to 1-propanol because of the increased flexibility in this compound.[37,38] These acidity enhancements for the diols are due to the strong intramolecular hydrogen bond in the conjugate base (Figure 4).

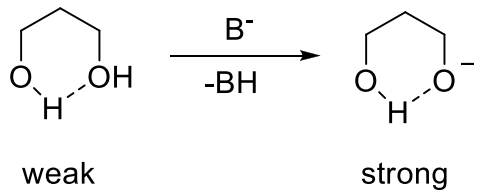

Figure 4. Effective intramolecular hydrogen bonding resulting in an acidity enhancement.

* This section has been taken nearly verbatim from my 2010 written preliminary examination at the University of Minnesota and this dossier was used as the template for the subsequent section.

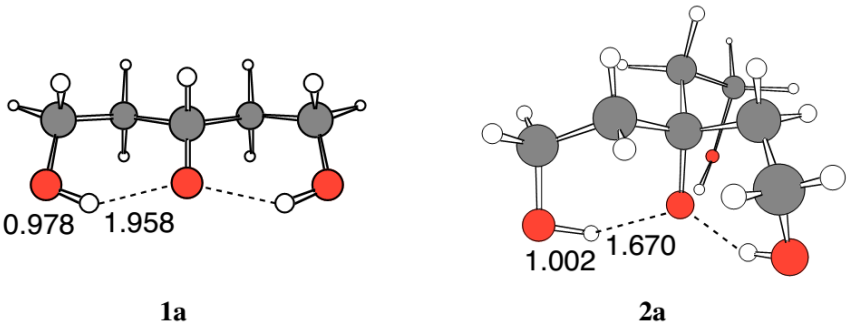

Figure 5. B3LYP/aug-cc-pVDZ geometries of the most stable structures of the conjugate bases of 1,3,5-pentanetriol (**1a**) and 3-(2-hydroxyethyl)-1,3,5-pentanetriol (**2a**).

Lewis structures of alkoxides have three lone pairs of electrons on the formally charged oxygen atom, all of which are capable of becoming hydrogen bond acceptors. Therefore, 1,3,5-pentanetriol (**1**) and 3-(2-hydroxyethyl)-1,3,5-pentanetriol (**2**) may have enhanced acidities in non-protic solvents as well as in the gas phase. Computed structures of the conjugate bases of **1** and **2** (**1a** and **2a**) revealed that their most stable conformers have two and three intramolecular hydrogen bonds respectively (Figure 5).[39]

Deprotonation enthalpies ($\Delta H°_{acid}$) of these polyols were also predicted by computational methods and subsequently were measured in the gas phase (Table 2).[39] There is good accord between the two and the results reveal that **1** and **2** have similar acidities to formic acid ($\Delta H°_{acid}$ = 346.2 ± 1.2 kcal mol $^{-1}$)[40] and hydrochloric acid ($\Delta H°_{acid}$ = 333.383 ± 0.002),[38] respectively. These values also indicate that **1** and **2** are 30.2 kcal mol^{-1} (22 pK_a units) and 41.0 kcal mol^{-1} (30 pK_a units) more acidic than 1-propanol.

Table 2. Computed B3LYP/aug-cc-pVDZ acidities of a series of alcohols at 298 K.[a]

Compound (ROH)	$\Delta H°_{acid}$(ROH)	
	Calcd.	Exptl.
$CH_3CH_2CH_2O\mathbf{H}$	374.4	375.7 ± 1.3
$HOCH_2CH_2CH_2O\mathbf{H}$	358.3	358.0 ± 2.5
$(HOCH_2CH_2)_2CHO\mathbf{H}$ (**1**)	344.2	344.3 ± 1.9
$(HOCH_2CH_2)_3CO\mathbf{H}$ (**2**)	333.7	333.0 ± 2.3
$(HOCH_2CH_2CH(OH)CH_2)_3CO\mathbf{H}$ (**3**)	318.9	-

[a]All values are in kcal mol^{-1} and come from Ref. 39.

The interaction of three hydroxyl groups to the single charged center in **2a** disperses the electron density and increases it at each of the hydroxyl oxygen atoms. This should make them better hydrogen bond acceptors than in the conjugate acid. As a result, adding additional hydrogen bond donors to **2** could increase its acidity. 5-(2,4-Dihydroxy-1-butyl)-1,3,5,7,9-nonanepentaol (**3**) was computationally examined in this regard, and the calculated structure of its most stable conjugate base has six hydrogen bonds (**3a** and Figure 6).[39] This leads to a predicted acidity of 318.9 kcal mol^{-1}, which corresponds to a 59.9 kcal mol^{-1} (44 pK_a units) acidity enhancement relative to 1-propanol. It also indicates that **3** should be a stronger acid than nitric acid ($\Delta H°_{acid}(HNO_3)$ = 324.5 ± 0.2 kcal mol^{-1})[38] in the gas phase. This is remarkable given that the heptaol **3** is a saturated acid made up of just C, O, and H atoms. Clearly, intramolecular hydrogen bond arrays can have large effects.

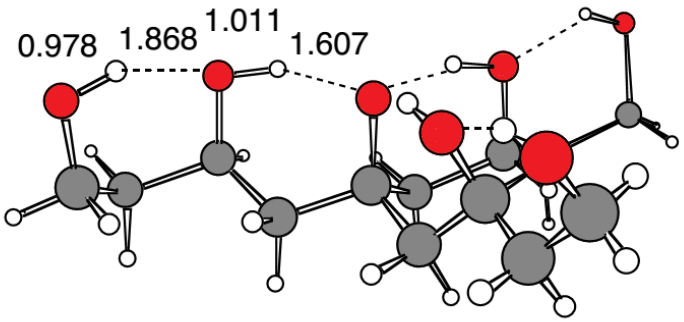

Figure 6. The B3LYP/aug-cc-pVDZ geometry of the most stable structure of the conjugate base of 5-(2,4-dihydroxy-1-butyl)-1,3,5,7,9-nonanepentaol (**3a**)

Acidities of 1,3-propanediol, triol **1** and tetraol **2** have been measured in DMSO (Table 3).[39] As expected, there is a systematic increase in the acidities with each additional hydroxyl group in the alcohol. More specially, the pK_a of 1,3-propanediol is approximately 4.6 pK_a units (i.e., 6.3 kcal mol^{-1}) more acidic than 1-propanol. The triol and tetraol are 10.3 and 13.9 pK_a units more acidic than 1-propanol, respectively, due to the presence of two and three intramolecular hydrogen bonds in their corresponding conjugate bases. As a result, triol **1** is more acidic than 2,2,2-trifluoroethanol (pK_a (CF_3CH_2OH) = 23.5)[41] and **2** is a stronger acid than imidazole (pK_a = 18.6)[42] and phenol (pK_a (PhOH) = 18).[43]

Table 3. DMSO acidities of a series of alcohols.[a]

Compound	pK_a	ΔpK_a (PrOH-ROH)
$CH_3CH_2CH_2O$**H**	30.0 [b]	0.0
$HOCH_2CH_2CH_2O$**H**	25.4 ± 0.3	4.6 [6.3][a]
$(HOCH_2CH_2)_2CHO$**H** (**1**)	19.7 ± 0.2	10.3 [14.0][a]
$(HOCH_2CH_2)_3CO$**H** (**2**)	16.1 ± 0.2	13.9 [19.0][a]

[a] Values in brackets are enthalpies based on the ΔpK_a at 25 °C and are in kcal mol^{-1}. [b] Estimated based on the pK_a values of MeOH (29.0),[36] EtOH (29.8),[36] and i-PrOH (30.3).[36]

The other significant finding of this study was the observation that there is a linear correlation between the experimentally determined pK_a values and the computed or measured gas-phase deprotonation enthalpies for 1,3-propanediol, triol **1** and tetraol **2** (Figure 7).[39] Using this plot, one can predict the pK_a of heptaol **3** in DMSO to be 10.5. This value is numerically smaller than that for acetic acid (pK_a (HOAc) = 12.3) and thus **3** is predicted to be the more acidic compound. There is no particular reason that the gas phase acidities and DMSO pK_a's should be linearly related, however, so this is a crude estimate that needs to be experimentally tested. The current SHEA acids (**1** and **2**) that have been prepared are soluble in polar solvents such as DMSO and acetonitrile, but are only slightly soluble in THF and diethyl ether and are insoluble in non-polar solvents such as hexanes or benzene. If this becomes problematic in future studies, then alkyl substituents can be incorporated to alter the solubility properties of the acids.

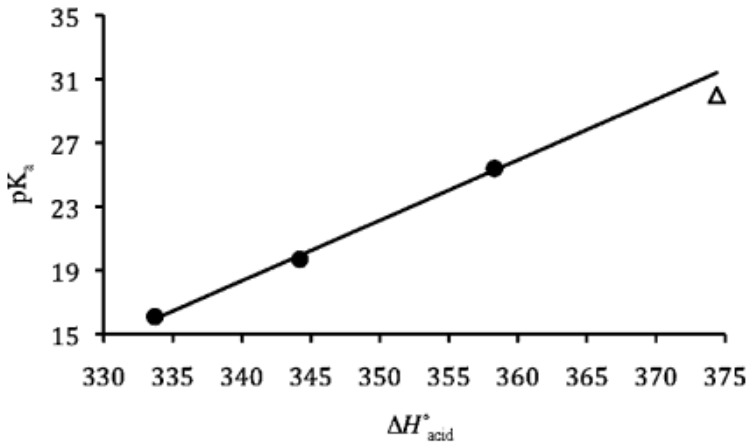

Figure 7. Measured DMSO pK_a values for 1,3-propanediol, triol **1**, and tetraol **2** versus their computed B3LYP acidities in kcal mol^{-1}; 1-propanol is given by the open triangle but was omitted from the linear fit of the data since its liquid phase pK_a value is an estimate.

The effect of electron withdrawing fluorine substituents on SHEA acids also has been examined (Table 4).[39] Results of the computational study revealed that the acidity of 1,1,1,5,5,5-hexafluoropentane-2,4-diol (**4**) is 334.4 kcal mol^{-1}, which is similar to the values for **2** and HCl. Perfluorinated derivatives of **1-3** (**1F-3F**) are predicted to be very strong acids with greater acidities than H_2SO_4 ($\Delta H°_{acid}$ = 306.3 ± 3.1 kcal mol^{-1})[44] and $HN(SO_2C_4F_9)_2$ ($\Delta H°_{acid}$ = 291.1 ± 2.2 kcal mol^{-1});[45] the latter compound is the strongest gas phase acid that has been accurately measured to date.[46] These results indicate that intramolecular hydrogen bonding networks and the incorporation of inductive effects lead to very strong acids in the gas phase.

Table 4. Computed B3LYP/aug-cc-pVDZ acidities of perfluorinated alcohols at 298 K.[a]

Compound	$\Delta H°_{acid}$
dl-$CF_3CH(OH)CH_2CH(OH)CF_3$ (**4**)	334.4
$(HOCF_2CF_2)_2CFOH$ (**1F**)	289.0
$(HOCF_2CF_2)_3COH$ (**2F**)	279.7
$(HOCF_2CF_2CF(OH)CF_2)_3COH$ (**3F**)	260.9

[a]All values are in kcal mol^{-1}.

Hydrogen bond catalysis

Hydrogen bonds have emerged as useful tools for catalysis. This is not surprising since many enzymes make use of hydrogen bonds to accelerate reactions. Chemists have attempted to design new and powerful catalysts that take advantage of this property, but the field is relatively undeveloped compared to Lewis and inorganic acid catalysis.

Lewis acid (LA) catalysts have several drawbacks. Many of them are insoluble in water or decompose violently in this medium. Heavy metals incorporated into LA structures are poisonous and consequently their use in chemical and pharmaceutical industry is largely avoided.[47] Moreover, when water is used as the solvent for a LA-catalyzed reaction additional effort is required to clean up the waste water. It is also difficult to immobilize traditional LAs on polymers or other stationary phases in order to facilitate catalyst removal by using flow processes that do not require extracting out the metal catalyst or byproducts.[48]

Although inorganic acids like H_2SO_4, HNO_3, and HCl are cheap, they have many disadvantages. For example, they are highly corrosive and when used in an industrial

setting expensive, glass-lined or titanium-clad steel vessels are needed. They are also harmful to plant growth due to their toxicity, sometimes cause oxidative side reactions and are incompatible with anhydrous reaction conditions, and their utility in organic synthesis is limited because of solubility issues.[49,50] Hydrogen bond acid catalysts, particularly chiral ones, therefore offer an attractive alternative.

Hydrogen bond catalysts can catalyze reactions in two different manners via general and specific acid catalysis.[51] If the rate of an acid-catalyzed reaction in solvent S is depend on the concentration of $[SH^+]$, the reaction is specific acid catalyzed. The acid might be weaker or stronger than the conjugate acid of the solvent but the rate is just affected by the concentration of SH^+ that is present in solution. The identity of the acid HA does not make any difference in the rate of reaction for specific acid catalyzed processes. In water SH^+ is commonly referred to as H_3O^+ but $H_{13}O_6^+$ is a better formulation of the structure.[52] All of the undissociated acids, however, play a role in general acid catalyzed reactions. This situation can be ascertained by increasing the buffer concentration at a constant pH, and if the reaction rate increases, then the transformation is subject to general acid catalysis.

Brønsted acids catalyze many organic reactions such as aldol condensations, dehydrations, and esterifications.[53,54] They also convert poor leaving groups such as -OH and -OR into good ones and routinely play a critical role in enzymatic reactions. For example, Asp121 in the active site of bovine RNase (a digestive enzyme) forms a hydrogen bond with His119, which serves as an acid during the catalytic cleavage of RNA (Figure 8).[55]

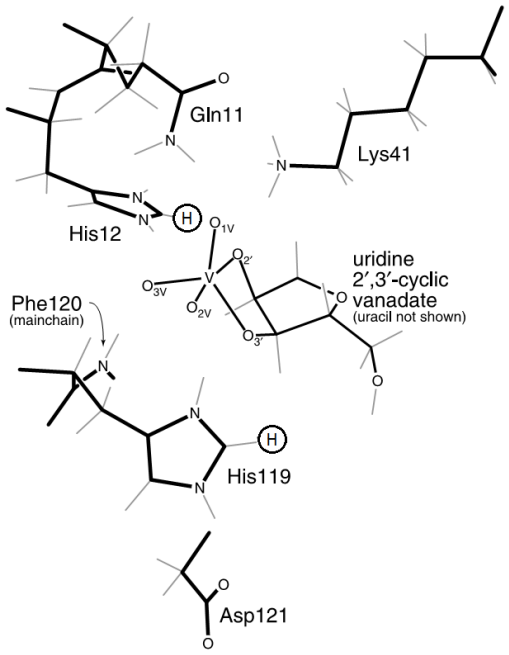

Figure 8. Crystalline structure of the active site of bovine RNase.

Hydrogen bond catalysts are currently receiving a great deal of attention.[56-59] Compounds such as thioureas serve as double hydrogen bond donors that facilitate nucleophilic additions. The added organization brought about by two hydrogen bonds also can lead to enantioselectivity and the formation of optically active products. For example, Berkessel and coworkers reported chiral isophoronediamine-derived bisthiourea **5** activates the Morita–Baylis–Hillman (MBH) reaction between cyclohexenone and cyclohexanecarbaldehyde (Scheme 1).[60] Using optimized conditions, enantioenriched allylic alcohols were produced with poor to excellent enantioselectivities (22-79% yield, 22-96% ee).

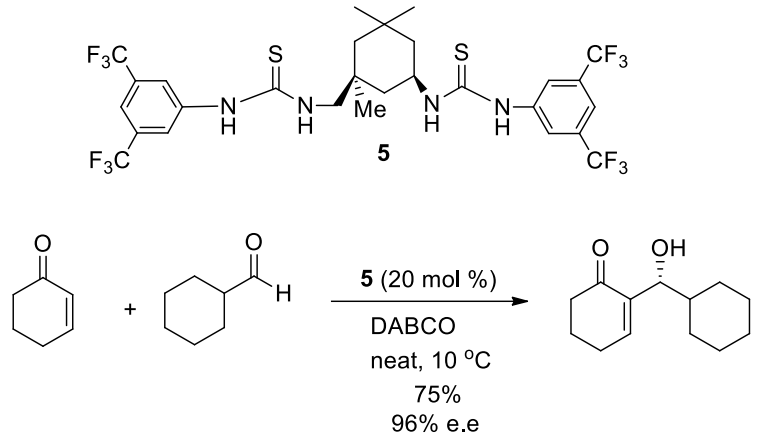

Scheme 1. Asymmetric Morita–Baylis–Hillman reaction catalyzed by a chiral bisthiourea.

Hydrogen bonds in anion recognition

Hydroxyl groups are among the best known of all hydrogen bond donor groups. Interactions involving hydroxyl subunits play a critical role in a broad range of recognition processes.[61] As an example, the recognition of carbohydrates by proteins relies on hydrogen bonding between hydroxyl groups of the carbohydrates and anionic proteins. Amino acids such as tyrosine (Tyr) that have hydrogen bond donor subunits are frequently found in the active sites of proteins that recognize carbohydrates. These sugar-protein interactions are important for many biological processes, and how carbohydrates are recognized by proteins is a fundamental question in biochemistry. As an example, it is well understood that they are involved in bacterial adhesion, toxins, viral glycoproteins, and in various amyloid-forming proteins such as those associated with Alzheimer, and Creutzfeldt diseases.[62]

Mutations of natural anion receptors have destructive effects on membrane transport and lead to a wide range of diseases such as cystic fibrosis and Startle disease.[63] Although the structures of natural ion channels and transporters are well known, there are no cures for most of these diseases. Low molecular weight synthetic receptors can mimic the action of natural ion channels and provide a useful means for studying membrane transport.

The design and synthesis of artificial anion receptors have been explored over the last two decades. Various hydrogen bond donors such as amides, ureas, thioureas, and pyrroles have been incorporated into rigid structures of macrocycles,[64] but less attention has been paid to hydroxyl-based anion receptors even though they play a key role in natural anion transporters and ion channels. Inspired by natural phenolic receptors, Smith and co-workers studied the anion binding abilities of phenolic-based compounds **6**-**8** (Figure 9) by carrying out ^{1}H NMR titrations.[65] The chloride binding constants of dihydroxybenzenes **7** and **8** were found to be high (K_a = 145 and 1015 M^{-1} in CD_3CN, respectively) given the structural simplicity of the "receptors". They also observed that increasing the acidity of the phenol leads to an enhancement of its chloride-affinity. For example, **6b** and **6c**, which contain electron withdrawing fluoro and nitro groups, have chloride affinities that are two and twelve times larger than phenol (i.e. K_a = 48 (**6a**), 95 (**6b**), and 555 (**6c**) M^{-1} in acetonitrile), respectively.

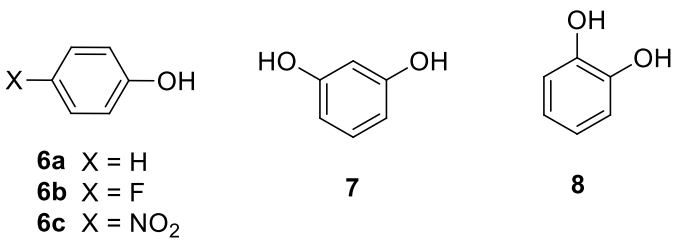

6a X = H
6b X = F
6c X = NO_2

7

8

Figure 9. Structure of several phenolic-based receptors.

Davis and co-workers employed a series of steroid anion receptors which made use of three hydroxyl groups to bind anions (Figure 10).[66] This relatively rigid structure preorganizes the hydrogen bond groups and prevents them from forming intramolecular hydrogen bonds. These receptors bind tridentate anions such as sulfonates in benzene, but were not found to associate with chloride.

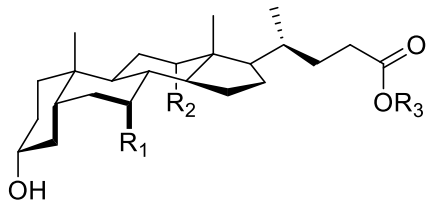

10a $R_1 = R_2 = OH$, $R_3 = Me$
10b $R_1 = R_2 = OH$, $R_3 = n\text{-Octyl}$

Figure 10. Steroid-based anion receptors.

Binding constants of the photoswitchable receptor **11**, containing two chiral 2,20-dihydroxy-1,10-binapthyl (BINOL) groups, with Cl^-, F^- and $H_2PO_4^-$ have been measured

by Shinmyozu and co-workers (Figure 11).[67] The resulting 1:1 association constants of trans-**11** with fluoride and chloride were found to be 1000 and 460 M^{-1} in $CDCl_3$. Based on this result, the author suggested that these anions form two hydrogen bonds with one BINOL group. However, dihydrogen phosphate showed 2:1 binding indicating that the each BINOL arm can associate one dihydrogen phosphate anion. The cis structure was also found to bind the same three anions, but in this case 1:1 complexes were found in all three instances. Association constants of 1000 M^{-1} (F^-), 50 M^{-1} (Cl^-), and 94 M^{-1} ($H_2PO_4^-$) were determined, but these values are similar or smaller than those for the trans structure. Even though computations indicated that dihydrogen phosphate can form four hydrogen bonds with cis-**11**, preorganization of the hydrogen bonds in the receptor did not lead to stronger associations. Many other factors such as cavity size, conformational issues, solvation, etc. are clearly important too.

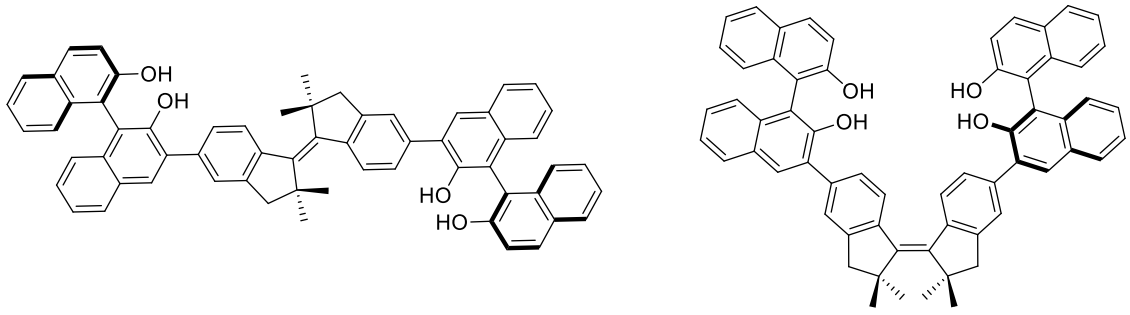

trans-**11** cis-**11**

Figure 11. Structure of BINOL-appended stiff-stilbene receptors.

In another study, Kondo and co-workers have reported the anion recognition ability for gem-silanediol (**12**), 1,3-disiloxane-1,3-diol (**13**) and 1,3-disiloxane-1,1,3,3-tetraols (**14a**

and **14b**) in acetonitrile (Table 5).[68] They observed that **12** and **13** can bind anions effectively via the hydrogen bonds of two silanol hydroxyl groups. A comparison of the anion recognition abilities of **14a** and **14b** to **12** and **13** revealed that cooperative hydrogen bonds in the tetraols lead to a 60-fold enhancement of the chloride anion association. This behavior makes the tetraols possible candidates for the development of ion selective electrodes.

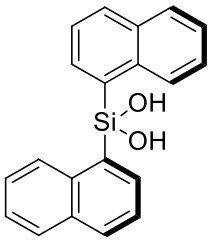

12

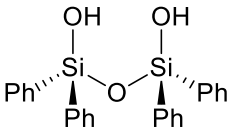

13

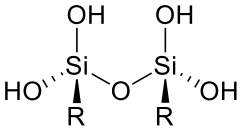

14a = 2,4,6-$^{i}PrC_6H_2$
14b = $(CH_3)_2CCH(CH_3)_2$

Table 5. Association constants of receptors **12 - 14** with anions in acetonitrile.

	K_a (M^{-1})			
	12	**13**	**14a**	**14b**
OAc^-	25000	ND	ND	ND
Cl^-	46	670	2480	2760
Br^-	6.4	52.5	128	77.7
I^-	0.7	4.3	8.6	10.1

Chapter 2: Hydrogen Bonded Arrays: The Power of Multiple Hydrogen Bonds*

Introduction

Many enzymes catalyze a wide variety of chemical processes by using two or even three hydrogen bonds to a single oxygen atom in what is commonly referred to as an oxyanion hole (Figure 1).[1] The strength of the individual hydrogen bonds can vary considerably and the presence of a strong low-barrier or single-well hydrogen bond has been used to explain a variety of enzyme mechanism pathways (e.g., mandelate racemase, triose-phosphate isomerase, citrate synthase, and glycolate oxidase).[2] Additive effects involving two and three hydrogen bonds to one charged center also have been shown in several enzyme model systems.[3,4] However, networks of hydrogen bonds are employed by enzymes, and the energies of these additional interactions are important in catalysis but are not well understood.[5] In this report, negative-ion photoelectron spectroscopy is used to directly probe the energetic consequences of hydrogen bond arrays in small covalently bound model compounds and the experimental results are compared to computational predictions. We find that in a series of monodeprotonated polyhydroxy alcohols (i.e., polyols) the strengths of the hydrogen bond arrays systematically increase with the number of hydroxyl groups from 1 – 3 and for 6. That is, an oxygen anion center is stabilized most effectively

* Shokri, A.; Schmidt, J.; Wang, X. B.; Kass, S. R., Hydrogen bonded arrays: the power of multiple hydrogen bonds. *J. Am. Chem. Soc.* **2012,** *134,* 2094-2099.

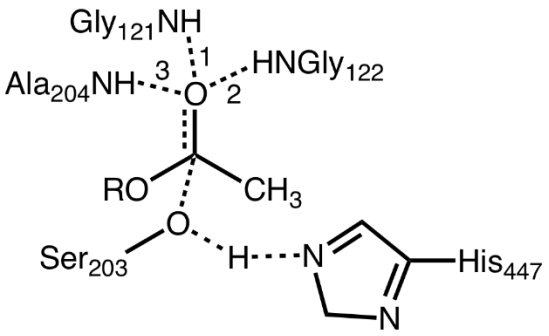

Figure 1. Proposed transition state for the enzymatic hydrolysis of acetylcholine with acetylcholinesterase via a three-pronged oxyanion hole (i.e., 1–3); see ref. 1d for additional details.

by up to 3 hydrogen bond donors, but in the process the donor groups become better hydrogen bond acceptors. The resulting hydrogen-bonded network can provide a large energetic stabilization that may lead to catalytic rate enhancements and greater acidities and basicities than those measured in water.

Experimental Section

General. ^{1}H and ^{13}C NMR spectra were recorded on Varian VI-300, VXR-300, and VI-500 spectrometers and are reported in parts per million (δ). High-resolution mass spectral analyses were performed with a Bruker BioTof II electrospray ionization–time of flight mass spectrometer with an internal standard; an aqueous solution of PEG polymer was used for this purpose. Medium pressure liquid chromatography (25-60 psi) was carried out on silica gel using a Biotage Isolera 1. Thin-layer chromatography (TLC) was performed on 0.25 mm Masherey-Nagel silica gel plates and compounds were visualized using aqueous potassium permanganate or *p*-anisaldehyde (1% EtOH solution) stains.

2-Benzyl-1,3-diphenylpropan-2-ol. A dry three-necked round-bottomed flask was equipped with a magnetic stirring bar and an addition funnel, a reflux condenser with an argon inlet, and a rubber septum. The flask was charged with 6.90 g (0.283 mol) of magnesium turnings and 200 mL of anhydrous diethyl ether. A solution of 17.56 g (0.156 mol) of benzyl chloride (Alfa Aesar) in 20 mL of diethyl ether was added dropwise over 45 min so as to maintain a gentle reflux. Subsequently, 4.504 g (0.050 mol) of dimethylcarbonate was added dropwise over a 20 min period and the resulting reaction mixture was stirred for an additional 20 h at room temperature before being quenched with 100 mL of 10% aqueous HCl. The resulting two layers were separated and the aqueous solution was extracted three times with 100 mL of diethyl ether. The combined organic material was dried with anhydrous $MgSO_4$, filtered, and concentrated under aspirator pressure. Recyrstallization of the resulting solid from absolute ethanol afforded 11.92 g (79%) of the tribenzyl alcohol as a white solid. ^{1}H NMR (300 MHz, $CDCl_3$) δ 1.51 (1H, s), 2.79 (6H, s), 7.28 (15H, m). ^{13}C NMR (75 MHz, $CDCl_3$) δ 45.7, 73.9, 126.4, 128.1, 131.0, 137.3. HRMS-ESI: calc for $C_{22}H_{22}NaO^+$ $(M + Na)^+$ 325.1563, found 325.1581.

1,3-Di(cyclohexa-1,4-dienyl)-2-(cyclohexa-1,4-dienylmethyl)propan-2-ol.

Tribenzylmethanol (2.0 g, 6.6 mmol) was placed in a 500 mL flask that was equipped with a Claisen adapter and a dry ice-acetone condenser. The reaction flask was charged with 200 mL of liquid ammonia followed by 40 g (0.54 mol) of *tert*-butanol and then 0.80 g (0.11 mol) of small pieces of lithium wire (Sigma Aldrich) were added over 4 h with stirring. By allowing the reaction mixture to warm to room temperature overnight, the ammonia was evaporated to afford a white solid. It was dissolved in 100 mL of water and

extracted three times with 100 mL of diethyl ether. The combined organic layers were dried over $MgSO_4$ and concentrated under reduced pressure, and the crude product was purified by flash column chromatography (20:1 hexanes/diethyl ether) to give 1.54 g (76%) of the desired alcohol as a colorless oil. ^{1}H NMR (300 MHz, $CDCl_3$) δ 1.76 (1H, s), 2.14 (6H, br s), 2.75 (12H, br s), 5.49 (3H, br s), 5.69 (6H, br s). ^{13}C NMR (75 MHz, $CDCl_3$) δ 26.7, 31.1, 48.0, 74.2, 123.1, 123.4, 124.5, 132.2. HRMS-ESI: calc for $C_{22}H_{28}NaO^+$ $(M + Na)^+$ 331.2032, found 331.2029.

5-(2,4-Dihydroxybutyl)nonane-1,3,5,7,9-pentaol (**4**). A solution of 1.23 g (4.00 mmol) of 1,3-di(cyclohexa-1,4-dienyl)-2-(cyclohexa-1,4-dienylmethyl)propan-2-ol in 100 mL of a 1:1 mixture of methanol : dichloromethane was cooled to -78 °C and then ozone was bubbled through it for 1 h until a blue color persisted. Excess ozone was removed from the reaction mixture by passing oxygen through it, and then 7.40 g (195 mmol) of sodium borohydride was slowly added with stirring over the course of 1 h all the while maintaining the temperature at -78 ˚C. The resulting solution was allowed to warm to room temperature and was maintained at 20 ˚C for 14 h. Acidification of the reaction mixture was carried out by slowly adding concentrated HCl until the pH was lowered to ~4 and a white precipitate formed. The resulting methanolic solution was filtered and concentrated at aspirator pressure with a rotary evaporator to afford a residue which was filtered, redissolved in 100 mL of methanol and concentrated again. This step was repeated several times to facilitate the removal of boron-containing compounds as volatile byproducts. The remaining material was purified on a silica gel column by flash chromatography (4:1 ethyl acetate/methanol) to afford 0.29 g (25%) of 5-(2,4-dihydroxybutyl)nonane-1,3,5,7,9-

pentaol as an ~3 : 1 mixture of the anti (RRS/SSR) and syn (RRR/SSS) isomers. ^{1}H NMR (300 MHz, CD_3OD) δ 1.80 (12H, m), 3.68 (6H, t, J = 6.0 Hz), 4.10 (3H, m). ^{13}C NMR (75 MHz, CD_3OD) δ 42.5 (anti), 42.6 (anti and syn), 42.7 (anti), 46.3 (anti), 46.6 (syn), 47.2 (anti), 47.9 (anti), 60.2 (syn), 60.3 (anti), 60.4 (anti), 60.5 (anti), 67.3 (syn), 67.57 (anti), 67.60 (anti), 77.0 (anti), 77.4 (syn); the syn isomer was isolated from its diastereomer by flash chromatography using a 4:1 dichloromethane/methanol solvent mixture after the PES experiments were carried out. HRMS-ESI: calc for $C_{13}H_{28}NaO_7^+$ $(M + Na)^+$ 319.1727, found 319.1732.

Photoelectron Spectroscopy. Photoelectron spectra were obtained at 20 K with a home-built variable temperature photoelectron spectrometer coupled with an electrospray ion source and a cryogenic ion-trap which has been previously described.[6] In this work, the alcohols were dissolved in a methanol : water solution (7:3 v/v) and electrospray ionization of ~10^{-3} M solutions afforded the $(M - 1)^-$ ions except for 1,3-propanediol. The ions were trapped and cooled for a period of 20-80 ms in the trap before being pulsed out into the extraction zone of a time-of-flight mass spectrometer with a repetition of 10 Hz. The desired $(M - 1)^-$ ions were mass-selected and decelerated before being intercepted by a probe laser beam in the photodetachment zone of a magnetic bottle photoelectron analyzer. An excimer laser (193 nm, 6.424 eV) and a Nd:YAG laser (266 nm, 4.661 eV) were used in this study and all three ions were examined at both wavelengths. The laser was operated at a 20 Hz repetition rate with the ion beam off on alternating laser shots to enable shot-by-shot background subtraction to be carried out. Photoelectrons were collected at nearly 100% efficiency with the magnetic bottle and analyzed in a 5.2 m long electron flight tube.

Time-of-flight photoelectron spectra were collected and converted to kinetic energy spectra, calibrated by the known spectra of I^- and ClO_2^-. The electron binding energy spectra were obtained by subtracting the kinetic energy spectra from the detachment photon energies. The resolution ($\Delta E/E$) of the resulting spectra was approximately 2% or 20 meV at 1 eV as measured for I^- at 355 nm. Photoelectron spectra for deprotonated triol **2** and tetraol **3** with the higher energy light source are given in Figure S1 in the Supporting Information.

Computational Methods. Extensive geometry optimizations were previously carried out on all of the anions studied in this work using the Becke three-parameter hybrid exchange and Lee-Yang-Parr correlation density functional (B3LYP)[7] along with the Dunning augmented correlation-consistent double-ζ basis set (aug-cc-pVDZ).[8] In this investigation, the lowest energy structure for each ion was re-optimized using the newer Minnesota 2006 density functional (M06-2X)[9] and served as the starting point for optimizing the structure of the corresponding radical with both functionals. The aug-cc-pVDZ basis set was used as before, but additional M06-2X single-point energies with the maug-cc-pVT(+d)Z basis set (i.e., M06-2X/maug-cc-pVT(+d)Z//M06-2X/aug-cc-pVDZ) were also computed.[10] Vibrational frequencies were calculated in both cases and the unscaled values provided zero-point energies and thermal corrections to the enthalpies. VDEs were calculated by taking the electronic energy differences between the different anions and their corresponding radicals with the same geometries as the ions. ADEs are reported as enthalpies at 0 K and were obtained using the optimized structures for both the anions and the radicals. All of the other energies reported in this work are given as enthalpies at 298

K. Gaussian 09[11] was used to carry out all of the calculations reported in this study, and the resulting geometries and energies are provided in the Supporting Information.

Results and Discussion

For an enzyme to catalyze a reaction, it must increase the rate relative to the uncatalyzed background process by reducing the energy difference between the reactant and the transition state. This can be accomplished by destabilizing the energy of the substrate in the enzyme bound complex or by lowering the transition state energy. In a similar manner, the electron binding energy of an anion can be increased by one or more hydrogen bonds if the stabilizing interaction(s) is greater in the ion than in the corresponding radical. To directly probe the effects of hydrogen bonds on a single-charged center, $HOCH_2CH_2CH_2OH$ (**1**), $(HOCH_2CH_2)_2CHOH$ (**2**), and $(HOCH_2CH_2)_3COH$ (**3**) were electrosprayed into a home-built variable temperature photoelectron spectrometer which has been described previously.[6] The $(M–1)^-$ ions of **2** and **3** (**2a** and **3a**) were produced but no signal was observed for the diol because it is not much more acidic than methanol.[12] In the triol and tetraol there are two hydroxyl groups that could be ionized but deprotonation of the internal one (i.e., the secondary and tertiary alcohol sites in **2** and **3**, respectively) leads to a more favorable hydrogen bonding network (Figure 2). For example, the primary alkoxide derived from the tetraol can only form two hydrogen bonds to the charged site whereas the tertiary alkoxide can form three. This leads to a computed 6.0 kcal mol^{-1} energy difference (B3LYP/aug-cc-pVDZ) between the two isomers, and

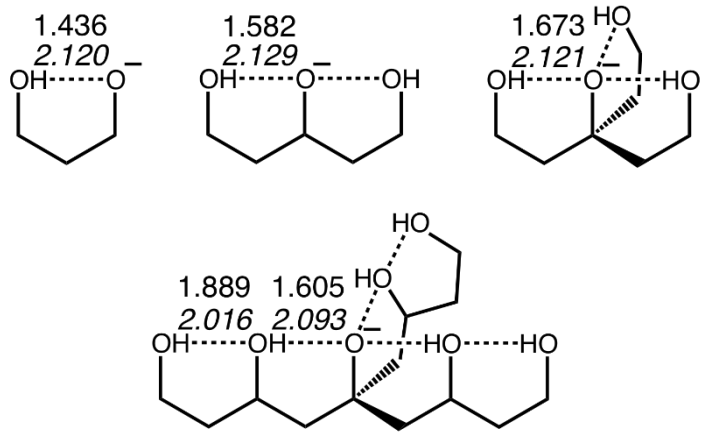

Figure 2. The most favorable hydrogen bonding patterns found for $HOCH_2CH_2O^-$ (**1a**), $(HOCH_2CH_2)_2CHO^-$ (**2a**), $(HOCH_2CH_2)_3CO^-$ (**3a**), and $(HOCH_2CH_2CH(OH)CH_2)_3CO^-$ (**4a**). Bond lengths for the anion and radical (in italics) are in Angstroms and are from the M06-2X/aug-cc-pVDZ geometries; the values for **3r**, **4a**, and **4r** are averages of the three different bond distances.

since they should be able to readily interconvert, it is reasonable to conclude that the ion composition is largely, if not entirely, made up of the more stable anion.

Photoelectron spectra were recorded for **2a** and **3a** at 193 nm (6.424 eV) and 266 nm (4.661 eV) at 20 K and the latter data are given in Figure 3; the 193 nm spectra have an additional band at higher energy corresponding to the formation of the radical in an excited state and are provided in the Supporting Information. The top of the bands in the 266 nm spectra provide the vertical detachment energies (VDEs) of the anions, and a linear extrapolation of the fast rising onset region leads to what should be a good estimate of the adiabatic detachment energies (ADEs).[13] The results are presented in Table 1 along with the literature value for 1-propoxide ($CH_3CH_2CH_2O^-$)[14] and B3LYP predictions with the aug-cc-pVDZ basis set (i.e., B3LYP/aug-cc-pVDZ).[7,8] and B3LYP predictions with

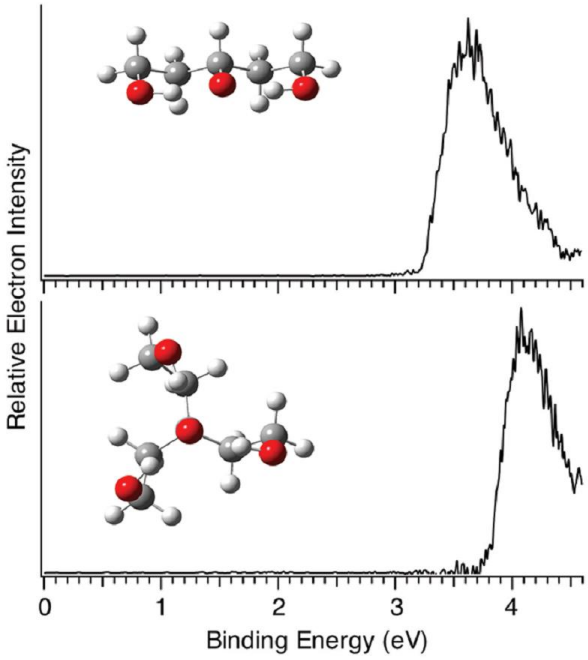

Figure 3. Low temperature (20 K) photoelectron spectra of $(HOCH_2CH_2)_2CHO^-$ (**2a**, top) and $(HOCH_2CH_2)_3CO^-$ (**3a**, bottom) at 266 nm (4.661 eV).

the aug-cc-pVDZ basis set (i.e., B3LYP/aug-cc-pVDZ).[7,8] The newer and apparently superior Minnesota 06 functional of Truhlar et al. was also used,[9] and since the energetics obtained using this method are more sensitive to the basis set, single-point energies were computed using the recently reported minimally augmented triple zeta + d basis set (i.e., maug-cc-pVT(+d)Z)[10] on the aug-cc-pVDZ geometries (i.e., M06-2X/maug-cc-pVT(+d)Z//M06-2X/aug-cc-pVDZ). In general, both computational methods do well in reproducing the experimental data, but the M06-2X approach with the maug-cc-pVT(+d)Z basis set gives the best results. These values, however, are consistently too small by 0.16

Table 1. Experimental and computed adiabatic (ADE) and vertical (VDE) electron binding energies for a series of alkoxides in eV.

Cmpd (RO^-)	Experimental ADE	VDE	Calculated[a] ADE	VDE
$CH_3CH_2CH_2O^-$	1789 ± 0.033		1.66 (1.57) [1.63]	1.81
$HOCH_2CH_2CH_2O^-$ (**1a**)			2.41 (2.40) [2.47]	2.69 (2.87)
$(HOCH_2CH_2)_2CHO^-$ (**2a**)	3.30	3.63	3.07 (3.09) [3.18]	3.53 (3.70)
$(HOCH_2CH_2)_3CO^-$ (**3a**)	3.85	4.18	3.53 (3.58) [3.66]	4.00 (4.18)
$(HOCH_2CH_2CH(OH)CH_2)_3CO^-$ (**4a**)	4.60	5.06	4.28 (4.36) [4.45]	4.76 (5.05)

a Computed values are at 0 K and correspond to B3LYP/aug-cc-pVDZ, M06-2X/aug-cc-pVDZ (in parentheses), and M06-2X/maug-cc-pVT(+d)Z//M06-2X/aug-cc-pVDZ (in brackets) energies; the difference between computed values at 0 and 20 K is negligible (i.e., < 0.01 eV).

eV (i.e., the errors span from 0.12 to 0.19 eV). As a result, this leads to an estimate of 2.63 eV for the ADE of $HOCH_2CH_2CH_2O^-$.[15]

The differences between the ADEs of the conjugate bases of 1-propanol and the polyols provide a direct measure of the consequences of multiple hydrogen bonds to a single charged center. This is not to say that these energy differences are the hydrogen bond strengths since there is no way to uniquely partition the various contributions that lead to the overall stability of the ion. In any case, total stabilizations as given by ADE ($(HOCH_2CH_2)_nCH_{3-n}O^-$ - $CH_3CH_2CH_2O^-$) for n = 1-3 lead to 19.4, 34.8, and 47.5 kcal mol^{-1}, respectively, and stabilization energies of 19.4, 17.4 and 15.8 kcal mol^{-1} per hydrogen bond; the latter numbers were obtained from the total stabilizations by dividing them by n,

the number of hydrogen bonds in the ion. These findings are in accord with earlier results by Herschlag et al. on ortho-substituted benzoic acids obtained by measuring their pK_a's in dimethysulfoxide (DMSO),[3] our earlier work on the acidities of **1**–**3** in DMSO and the gas phase,[4] and a variety of reports describing the stabilization of polyfunctional ions via hydrogen bonds.[16] Our data herein on simple covalently bound model systems for oxyanion holes with up to 3 hydrogen bonds reveal that up to 47.5 kcal mol^{-1} is available for catalysis to the extent that Nature can mimic the gas phase results. The energy gain is 44% of this value, however, if DMSO is used as the reference medium.[17]

To this point, only hydrogen bonds to a charged center are present, but additional interactions between non-charged groups may also contribute to an enzyme's catalytic ability. This can be energetically significant particularly since hydrogen bond donors to a charged group also will be better hydrogen bond acceptors than they would be in the absence of the charge. A more effective hydrogen bond array, consequently, could result. To assess the energetics that can be brought to bear in such a network, the conjugate base of an alcohol with 7 OH groups (i.e., $(HOCH_2CH_2CH(OH)CH_2)_3COH$, **4**) was examined. This ion (**4a**) can be stabilized by a total of 6 hydrogen bonds, and the most favorable structure that was computationally located has 3 hydrogen bonds to the charged center and 3 additional ones between non-charged OH groups (Figure 2). In this species the internal secondary hydroxyl groups serve as both hydrogen bond donors and acceptors. Conformers with 4 OH groups interacting with the oxyanion center were located, but the most favorable one is 7.0 (M06-2X/maug-cc-pVT(+d)Z//M06-2X/aug-cc-pVDZ) kcal

mol^{-1} less stable than the structure shown in Figure 2 (and Figure 4). This is consistent with a hydration shell number of 3 for hydroxide as determined by Meot-Ner and Speller.[18]

Heptaol **4** is an unknown compound but it can be prepared as a mixture of two diastereomers as outlined in Scheme 1. The resulting product affords an abundant $(M-1)^-$ ion signal via electrospray ionization, but irradiation at 266 nm does not lead to electron

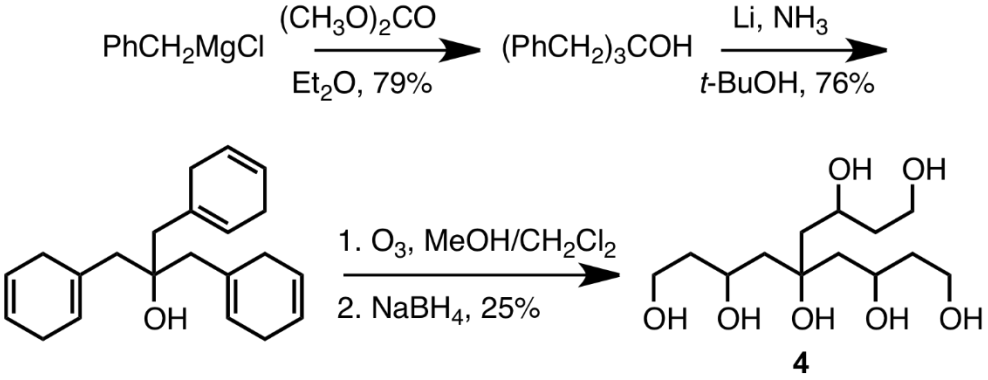

Scheme 1. Synthetic route for the preparation of heptaol **4**.

detachment. A low temperature spectrum at 20 K was recorded (Figure 4), however, when more energetic 193 nm photons were used. As with the smaller polyol anions at this wavelength, two features are apparent in the spectrum and the lower energy band provides the adiabatic and vertical electron detachment energies. These values are 4.60 (ADE) and 5.06 eV (VDE) which are remarkably large for a saturated alkoxide anion that lacks electron withdrawing groups and is not stabilized by resonance. To put these record breaking electron detachment energies in context, it is worth noting that the conjugate bases

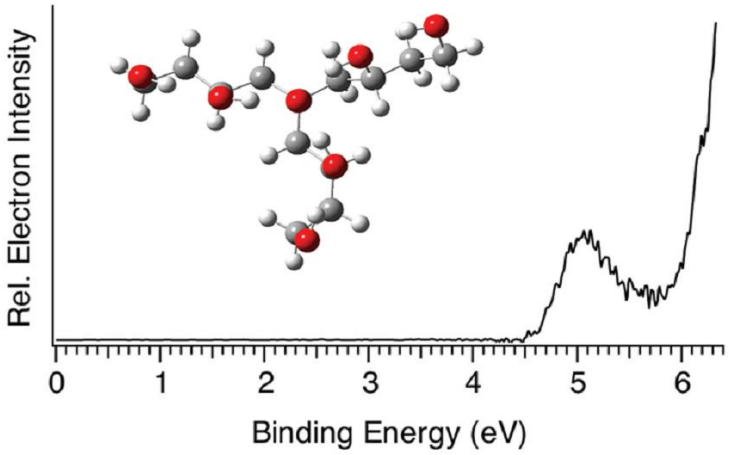

Figure 4. Low temperature (20 K) photoelectron spectrum of $(HOCH_2CH_2CH(OH)CH_2)_3CO^-$ **(4a)** at 193 nm (6.424 eV).

of strong acids such as CH_3CO_2H, HCl, HNO_3, and $HClO_3$ all have smaller ADEs (i.e., 3.470 ± 0.010, 3.613577 ± 0.000044, 3.937 ± 0.014, and 4.25 ± 0.10 eV, respectively)[19-22] than the deprotonated heptaol, whereas dihydrogen phosphate ($H_2PO_4^-$) has essentially the same value (i.e., 4.570 ± 0.010 eV).[23]

The hydrogen bond array in the conjugate base of **4** leads to a 64.8 kcal mol^{-1} stabilization relative to $CH_3CH_2CH_2O^-$, and 17.3 kcal mol^{-1} compared to the $(M - 1)^-$ ion of tetraol **3**. The latter difference can be attributed to the additional contribution from the 3 enhanced hydrogen bonds between the non-charged OH groups. These intramolecular interactions and those in the conjugate bases of **1**–**3** can be compared to the intermolecular hydrogen-bonded networks in $OH^-(H_2O)_n$, where n = 1 – 6 (Figure 5 and Table 2).[18,24,25] As can be seen for n = 1-3 in Figure 5, the intramolecular hydrogen bond system mirrors

Table 2. Energetic consequences of intramolecular vs intermolecular hydrogen bonds.[a]

n	ΔADE/n (intramolecular)	$\Delta H^{\circ}(RO^{-}(ROH)_n \rightarrow RO^{-} + nROH)/n$, R = H and CH_3 (intermolecular)[b]	intramol./ intermol. (%)[c]
1	(**1a** - $CH_3(CH_2)_2O^{-}$)/n = 19.4	26.5 [28.8]	73
2	(**2a** – **1a**)/n = 17.4	22.1 [25.1]	79
3	(**3a** – **1a**)/n = 15.8	20.1 [21.7]	79
4		12.0 [11.4]	
5		11.8	
6	(**4a** – **3a**)/(n-3) = 5.8	11.6	50

[a] All of the energies are in kcal mol^{-1} and come from ref. 17 and ref. 23. [b] The first value is for R = H and the latter one (in brackets) is for R = CH_3. When n ≥ 4 then the given energies are for $\Delta H^{\circ}(RO^{-}(ROH)_n \rightarrow RO^{-}(ROH)_3 + mROH)/m$, where m = n – 3. [c] The water cluster intermolecular values were used for this comparison.

the intermolecular interaction energies closely but are ~20 - 25% smaller. This is presumably because of geometric constraints in the polyols that restrict the O–H···O hydrogen bond angles from the ideal value of 180˚ to 153.0–158.5˚ (B3LYP) or 151.0–160.4˚ (M06-2X) when n = 1 - 3. The energy gap in Figure 5 is larger for n = 6, and it is tempting to attribute this to water-water interactions in $OH^{-}(H_2O)_6$, especially since computations indicate that the water molecules hydrogen bond with each other when n ≥ 3.[26] Methoxide-methanol cluster energies (the squares in Fig. 5),[24] however, follow the same trend as the hydroxide-water complexes even though the hydrogen-bonded network is more limited in the former case since alcohols have 1 less O–H bond than in water.

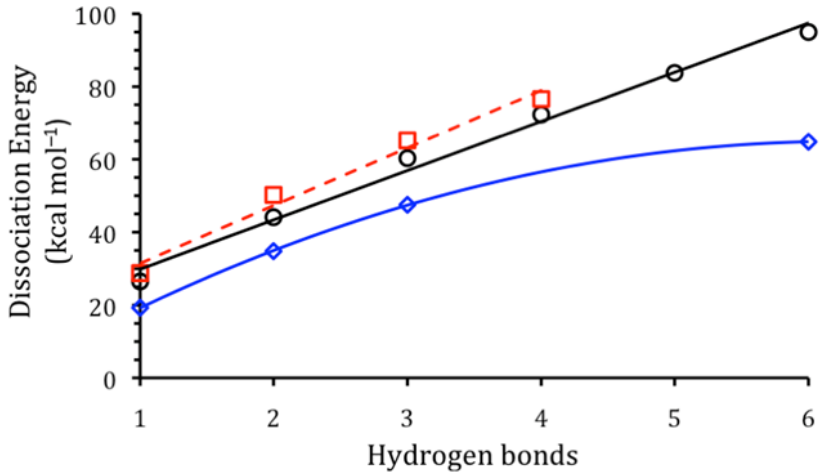

Figure 5. Dissociation energies versus hydrogen bond numbers. Diamonds are for polyol $(M–1)^-$ ion ΔADEs relative to $CH_3CH_2CH_2O^-$ (blue/diamond), circles represent the total dehydration energies of $OH^-(H_2O)_n$ (black/circle), and the squares are for the $CH_3O^-(CH_3OH)_n$ cluster energies (red/square).

This suggests that the fall off for **4a** is not due to water-water interactions in $OH^-(H_2O)_6$, but is instead the result of its more limited conformational flexibility. In accord with this hypothesis, the computed O–H···O hydrogen bond angles between the terminal hydroxyl groups and the oxygen atoms of the internal hydroxyl groups are 144 – 145˚ (B3LYP) and 142 – 143˚ (M06-2X) or ~10–15˚ smaller than the O–H···O$^-$ angles in **1a**-**4a**. This leads to weaker hydrogen bonds in the outer shell of **4a** that presumably can be strengthened by increasing the flexibility in **4** (e.g. by adding a CH_2 spacer between the primary and secondary OH groups).

Enzyme-substrate complexes enjoy a kinetic advantage over bimolecular processes because intramolecular reactions are generally favored over intermolecular ones.[27] Our simple covalently bound models for the former species reveal that intramolecular

hydrogen-bonded networks can be stabilized by the presence of a charged site, and this thermodynamic effect can be used to perturb acidities and basicities and catalyze enzyme reactions.[28] As a result, aqueous pK_a values may be a poor indication of the acidity or basicity of a given group in a biological context, and proton transfer processes that are currently viewed as being energetically unfavorable and inaccessible actually may take place. Careful control of hydrogen-bonded networks, consequently is an attractive design strategy for molecular recognition and artificial enzyme construction.[29]

Conclusions

The photoelectron spectra of a series of deprotonated polyhydroxyalcohols were obtained at 20 K and the adiabatic electron detachment energies for $HOCH_2CH_2CH_2O^-$ (**1a**), $(HOCH_2CH_2)_2CHO^-$ (**2a**), $(HOCH_2CH_2)_3CO^-$ (**3a**), and $(HOCH_2CH_2CH(OH)CH_2)_3CO^-$ (**4a**) are 2.63 (best estimate, see text for details), 3.30, 3.85, and 4.60 eV, respectively. These values are remarkably large and are bigger than the experimental ADE for $CH_3CH_2CH_2O^-$ (1.789 ± 0.033 eV) by 19.4, 34.8, 47.5, and 64.8 kcal mol^{-1}. These energy differences are a consequence of the hydrogen-bonded networks in the anions, and in the case of **4a** this leads to an ADE that is greater than the conjugate bases of CH_3CO_2H, HCl, and HNO_3. Its ADE is also 17.3 kcal mol^{-1} or 5.8 kcal mol^{-1} per hydrogen bond greater than for **3a**, and this difference can be attributed to the enhanced strength of the 3 hydrogen bonds between the non-charged OH groups in **4a**. The presence of a charged center leads to a considerable increase in the strength of a hydrogen-bonded

network, and this undoubtedly plays a key role in regulating the structure and function of a wide range of biomolecules.

Chapter 3: The Effect of Hydrogen Bonds on pK_a's: The Importance of Networking*

Introduction

Enzymes commonly make use of general acid and base catalysis to accelerate a wide range of chemical transformations, some of which require transition state stabilizations of 20 kcal mol^{-1} or more to account for the observed rates of reaction.[1] The bulk of this stabilization energy is typically provided by hydrogen bonds, which also serve as templates for proton transfer processes. Measured hydrogen bond strengths are less than 10 kcal mol^{-1} in solution,[2] however, and this difference (< 10 vs ≥ 20 kcal mol^{-1}) led Cleland, Gerlt and Gassman, Kreevoy, and Frey to propose stronger low-barrier hydrogen bonds (LBHBs) as a means by which enzymes can accelerate reactions.[3] These short-strong hydrogen bonds were invoked to account for the enzymatic reactions of chymotrypsin, serine protease, citrate synthase, and triose phosphate isomerase, among others. In this manuscript we propose a second stabilizing feature employed by enzymes to enhance catalysis is through outer-sphere solvating hydrogen bonding networks. This principle is demonstrated using a small molecule model system (i.e., $(HOCH_2CH_2CH(OH)CH_2CH_2)_3COH$ (**1**)).

Low barrier hydrogen bonds (LBHBs) are characterized by short A–B distances in A···H···B complexes, downfield chemical shifts in ^1H NMR spectra, low isotope

* Shokri, A.; Abedin, A.; Fattahi, A.; Kass, S. R., Effect of hydrogen bonds on pK_a values: importance of networking. *J. Am. Chem. Soc.* **2012**, *134*, 10646-10650.

fractionation factors, and broad vibrational stretching bands at reduced frequencies in infrared spectra. These physical characteristics are noncontroversial, but whether they arise in systems with unusually strong hydrogen bonds is contentious.[4,5] An alternative to the LBHB proposal is to use multiple but ordinary hydrogen bonds in the first or inner solvation shell. For example, Herschlag et al. measured the pK_a's of *ortho*–substituted benzoic acids with one or two hydrogen bond donating groups in dimethyl sulfoxide (DMSO), since this solvent has a smaller dielectric constant than water (i.e., 46.8 vs 78.4) and can serve as a better medium for modeling the active site of an enzyme.[6] The formation of 2 direct hydrogen bonds to the carboxylate anion center in the conjugate base was found to increase the acidity of the benzoic acid by up to 8.0 pK_a units (i.e., 10.9 kcal mol^{-1}). Subsequently, two and even three inner shell hydrogen bonds to a singly charged-site were found to dramatically increase the gas-phase acidity of acyclic aliphatic alcohols.[7] For example, the tertiary tetraol $(HOCH_2CH_2)_3COH$ was found to be as acidic as HCl and its deprotonation enthalpy is 43.2 ± 2.4 kcal mol^{-1} more favorable than that for *tert*–butanol.[8] This acidifying effect is due to the stronger hydrogen bonds in $(HOCH_2CH_2)_3CO^-$ (Figure 1) compared to its conjugate acid. The magnitude of this enhancement not surprisingly is reduced in condensed media, but the tetraol is still 16.1 pK_a units (i.e., 21.8 kcal mol^{-1}) more acidic than *tert*-butanol in DMSO; it is also a stronger acid than phenol by 2 pK_a units (i.e., 2.7 kcal mol^{-1}) in this solvent.[9]

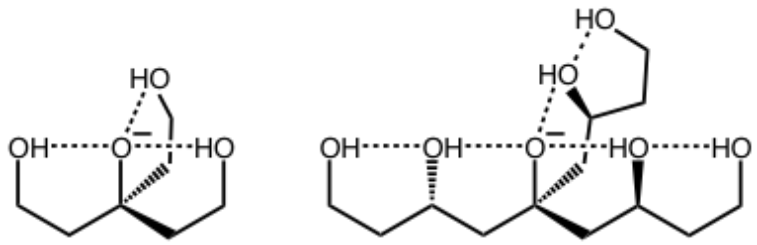

Figure 1. The most favorable hydrogen bonding arrangements for $(HOCH_2CH_2)_3CO^-$ and $(HOCH_2CH_2CH(OH)CH_2)_3CO^-$.

Intramolecular hydrogen bonds in folded proteins are known to be more stable than the corresponding hydrogen bonds to water in the proteins unfolded states.[10] There are no good available models, however, for addressing any stabilization beyond the first internal hydrogen bond shell in an enzyme's active site. As a result, it is difficult to predict or even account for many enzyme mutation studies.[11,12] Double mutant cycles offer a means to address this problem,[13] but to begin to investigate the hydrogen bond arrays employed by enzymes we decided to measure the DMSO acidity of a flexible polyol (i.e., **1**) whose conjugate base can be stabilized by two different types of hydrogen bonds (Figure 1). That is, an array where 3 hydrogen bonds can form to a tertiary alkoxide anion center and 3 additional interactions between hydroxyl groups can be produced. The latter type of hydrogen bond is often thought to be energetically unimportant since it is present in the acid and conjugate base (or analogously, in an enzyme–substrate bound complex and the corresponding reaction transition state), but this is not the case as will be shown.

Computations are also reported on **1** and related compounds to further probe the consequences of hydrogen bond networks and the influence electron withdrawing groups can have on these species.

Experimental Section

General. Glassware, syringes, NMR tubes, and needles were dried in ovens and stored in a desiccator containing rubber septa and phosphorus pentoxide. DMSO and DMSO-d_6 were dried under reflux at 1.7 torr over CaH_2 for several hours at 60–65 ˚C. Both solvents were also distilled under these conditions and stored on occasion for up to several days in dark vials that contained activated 3Å molecular sieves; activation of the sieves was carried out by heating in a furnace to 320 ˚C for 1 d. Pentane was dried and distilled over phosphorus pentoxide and used to triply rinse the mineral oil away from a 30% suspension of potassium hydride before the KH was used to make dimsyl anion. Dimsyl potassium was freshly prepared daily by reacting KH with DMSO or DMSO-d_6 at room temperature over a 30 m period. All of the dry solvents were degassed immediately before use by bubbling dry argon through them for approximately 20 minutes.

pK_a Determinations. Heptaol **1** was synthesized and purified by MPLC as previously described.[14] Each sample of the RRR/SSS diastereomer was dried overnight under high vacuum (~10^{-5} torr) and either used right away or stored in a desiccator for up to a few days. Millimolar concentrations of the heptaol were used to measure its pK_a by ^{1}H NMR spectroscopy as previously described.[7,15] Six determinations were carried out with 9-

carboxymethylfluorene serving as the reference compound (i.e., indicator) since it has a well-established pK_a value of 10.35.[9,16]

Gas Phase Measurements. Electrospray ionization of a methanol/water solution (3:1 v/v) of **1** afforded the M–1 ion at *m/z* 295 in a 3 T Ion Spec FTMS. This ion was isolated and cooled with a pulse of argon up to a pressure of ~10^{-5} Torr before being allowed to react with HBr and 2,4-dinitrophenol. In separate experiments, Br^- and 2,4-dinitrophenoxide where generated by electron ionization in the analyzer cell of a Finnegan dual cell FTMS instrument that was controlled with an Ion Spec data system. These ions were transferred to the source cell, cooled with a pulse of argon and isolated, and then were allowed to interact with heptaol **1** which was introduced into the instrument via the solid probe inlet.

Computations. Spartan 08 was used to carry out Monte Carlo and systematic conformational searches with the MMFF force field (molecular mechanics) and the AM1 Hamiltonian (semiempirical calculations) on a variety of alcohols and their conjugate bases.[17] B3LYP/6-311+G(d,p)[18] and M06-2X/maug-cc-pVT(+d)Z)[19-20] density functional theory single point energies were then obtained with the Gaussian 09 suite of programs[21] on all of the conformers that were found to be within 3–5 kcal mol^{-1} of the most favorable structures that had been located. The lowest energy species that resulted were fully optimized and harmonic vibrational frequencies were computed using the same two methods as employed for the single-point energy calculations. Gas phase acidities (ΔG°_{acid}) were subsequently calculated at 298 K using unscaled vibrational frequencies, but in carrying out the temperature correction all weak modes ≤ 260 cm^{-1} were replaced by

½(RT). The entropies of the alcohols were also corrected for an entropy of mixing term as reported by Gutherie[22] and previously assessed for these compounds.[7]

Liquid phase pK_a values in DMSO were computed using the conductor-like polarizable continuum model.[23] Both B3LYP/6-311+G(d,p) and M06-2X/maug-cc-pVT(+d)Z single point energies were obtained using 70 surface elements (tesserae) and an area of 0.2 Å for each sphere. The "iterative" keyword was used for solving the polarized continuum model electrostatic problem and calculating the polarization charges to a convergence threshold of 10^{-12} in a maximum number of steps set to 1000. Although it has previously been reported that solvent effects on the differences between gas- and liquid-phase geometries is negligible,[24] we decided to optimize the condensed phase structures and recompute the vibrational frequencies to compare the differences for the compounds studied herein. In accord with the literature, the resulting geometries and energies only led to small differences. In this work, relative pK_a's were computed using ethanol as the reference compound and they were converted to absolute values by using the experimental acidity of ethanol (pK_a = 29.8).[9] For the fluorinated polyols, B3LYP/6-31+G(d) computations were carried out on previously located structures to obtain their pK_a's.[7,25] In both cases noncorrected entropies were used.

Results and Discussion

Proton transfer processes play a key role in most enzymatic reactions and thus the acidities of different functional groups in enzymatic active sites are critically important for delineating detailed mechanistic pathways.[1,26] Changes in the dielectric constant of the

local environment, which typically is hydrophobic, will alter the aqueous pK_a values. This is well recognized but there is limited pK_a data available for compounds bound to an enzyme.[27] Enzymes are also replete with hydrogen bond donors and acceptors and, consequently, they have elaborate networks of hydrogen bonds. It is less well recognized that these hydrogen bond arrays can effect acidities, and very few investigations have been carried$_a$ out in this regard.[6,7] To probe the consequences of hydrogen bonding at non-charged sites in an acid and its conjugate base, the acidity of heptaol **1** was measured and computed in DMSO.

The acidity of heptaol **1** was determined by a previously reported ^{1}H-NMR method relative to 9-carbomethoxyfluorene,[7,15] since the latter compound is a suitable indicator and its pK_a value of 10.35 previously had been established.[9] Six determinations of the equilibrium constant revealed that it is independent of the heptaol concentration when this polyol is in the low millimolar range, and pK_a (**1**) = 11.4 ± 0.2. This is a remarkable finding in that **1** is an order of magnitude more acidic than acetic acid (pK_a = 12.3),[9] and it is the most acidic saturated alcohol of its kind that has been measured to date (i.e., an alcohol containing only C, H. and O atoms). Three different ionization sites can be envisioned for this polyol, but computations indicate that the tertiary alkoxide is significantly more stable than the secondary or primary anions both in the gas phase and in solution. That is, the relative M06-2X/maug-cc-pVT(+d)Z free energies for the 3˚, 2˚, and 1˚ ions are 0.0, 4.3, and 12.3 kcal mol^{-1} in the gas phase and 0.0, 3.7, and 10.9 kcal mol^{-1} in DMSO as predicted using the polarized continuum model (PCM).[23,28] The experimental pK_a is also in excellent accord with previous predictions of 10.5 and 11.7 based upon linear correlations between

the computed B3LYP gas-phase deprotonation enthalpies and free energies, respectively, at the tertiary hydroxyl group with the measured DMSO pK_a values of three polyols (i.e. $(HOCH_2CH_2)_3COH$) (**2**), $(HOCH_2CH_2)_2CHOH$ (**3**), and $HOCH_2CH_2CH_2OH$ (**4**)).[7] It is well reproduced too by the PCM calculations that follow.

In recent years advances in electronic structure theory have made it possible to reliably calculate pK_a values in different solvents.[29] This has been accomplished most commonly by computing gas-phase acidities and then using a polarized continuum model to obtain the energies of the acid and its conjugate base in a bulk dielectric environment consistent with the solvent of interest. In this study, B3LYP and the newer and often more superior M06-2X density functional were employed along with the 6-311+G(d,p) and maug-cc-pVT(+d)Z basis sets, respectively. Gas phase deprotonation free energies for methanol, ethanol, *tert*-butanol, polyols **1**–**4**, phenol and acetic acid are given in Table 1.[7,8,30] As expected, both methods do very well in reproducing the experimental values, but the M06-2X functional has the smaller average unsigned error (0.5 vs 1.5 kcal mol^{-1}) and the smaller maximum outlier (i.e., 1.4 vs 2.6 kcal mol^{-1}).

Table 1. Experimental and theoretical gas phase acidities (ΔG°_{acid}).[a]

Compound	B3LYP/6-311+G(d,p)	M062X/ maug-cc-pVT(+d)Z	Exptl[b]
CH_3OH	372.9	374.9	375.5 ± 0.6
CH_3CH_2OH	369.8	372.1	372.3 ± 0.8
$(CH_3)_3COH$	366.9	368.6	369.2 ± 0.7
$HOCH_2CH_2CH_2OH$ (**4**)	355.4	355.8	355.8 ± 2.0
$(HOCH_2CH_2)_2CHOH$ (**3**)	343.5	343.8	342.4 ± 1.2
$(HOCH_2CH_2)_3COH$ (**2**)	334.5	335.0	334.4 ± 1.7
$(HOCH_2CH_2CH(OH)CH_2)_3COH$ (**1**)	319.9[c]	320.2[c]	313.5 ± 5.0
$PhOH$	339.2	341.0	341.5 ± 1.0[d]
CH_3CO_2H	339.3	340.2	339.9 ± 1.7[d]
Avg. unsigned error	1.5	0.5	

[a]All values are in kcal mol^{-1}. [b]Refs. 7 and 8. [c]The same entropy correction for **2** given in ref. 7 was used. This point was not used in assessing errors because the experimental value has a large uncertainty. [d]See ref 30.

The gas-phase acidity of **1** has not been previously reported, but it is predicted to be about as acidic as HBr (ΔG°_{acid} = 318.3 ± 0.1 kcal mol^{-1})[8] and the adiabatic electron binding energy of its conjugate base was experimentally determined to be the same as that for dihydrogen phosphate (i.e., 4.60 ± 0.1 vs 4.57 ± 0.01 eV, respectively).[14,31] To assess the computational prediction, preliminary acidity measurements were carried out on the heptaol. Electrospray ionization of **1** afforded its conjugate base which was protonated by 2,4-dinitrophenol but not HBr (ΔG°_{acid} = 308.6 ± 2.0[32] and 318.3 ± 0.1 kcal mol^{-1}, respectively) even after a long reaction time (i.e., 5 minutes). In the reverse direction,

bromide anion was found to deprotonate the heptaol but 2,4-dinitrophenoxide did not. These results indicate that the acidity of **1** is between the values for HBr and 2,4-dinitrophenol. That is, ΔG°_{acid} (**1**) = 313.5 ± 5.0 kcal mol^{-1} which is in reasonable accord with our predictions, but suggests that when a more precise value is determined that it will be on the high end of the experimental range.

PCM computations were carried out using equation 1 to provide predictions of DMSO pK_a values, where ΔG°_{rxn} (kcal mol^{-1})/1.364 = pK_a (HX) – pK_a (CH_3CH_2OH) or pK_a (HX)

$$HX + CH_3CH_2O^- \rightarrow X^- + CH_3CH_2OH \quad (1)$$

= 29.8 + ΔG°_{rxn} (kcal mol^{-1})/1.364 (Table 2). This approach eliminates the difficulty in dealing with the solvation energy of the proton and takes advantage of the greater accuracy in computing relative energies compared to absolute values. Both the B3LYP and M06-2X predictions are in good accord with the experimental values and have average unsigned errors of 1.4 pK_a units. The maximum absolute deviation from experiment (3.2 vs 3.1 pK_a units, respectively) is also virtually the same for the two methods, and the overall results are similar in accuracy to a larger study of 105 organic acids previously reported.[29b]

Tetraol **2** has two kinds of hydroxyl groups, three primary OH substituents and one tertiary site. The latter position is predicted to be 4.7 (B3LYP/6-311+G(d,p)) and 4.2 (M06-2X/maug-cc-pVT(+d)Z) pK_a units more acidic than the primary alcohol sites, and consequently it is expected that the conjugate base is a tertiary alkoxide anion.

Table 2. Experimental and theoretical DMSO pK_a values.[a]

Compound	B3LYP/ 6-311+G (d,p)[b]	M062X/ maug-cc-pVT(+d)Z[b]	Exptl
CH_3OH	32.2 (-3.2)	30.0 (-1.0)	29.0[c]
$(CH_3)_3COH$	30.8 (1.4)	29.7 (2.5)	32.2[c]
$HOCH_2CH_2CH_2OH$ (**4**)	23.9 (1.5)	22.3 (3.1)	25.4 ± 0.3[d]
$(HOCH_2CH_2)_2CHOH$ (**3**)	20.1 (-0.4)	18.3 (1.4)	19.7 ± 0.2[d]
$(HOCH_2CH_2)_3COH$ (**2**)	16.4 (-0.3)	14.8 (1.3)	16.1 ± 0.2[d]
$(HOCH_2CH_2CH(OH)CH_2)_3COH$ (**1**)	13.6 (-2.2)	11.7 (-0.3)	11.4 ± 0.2
$(HOCF_2CF_2)_2CFOH$ (**3F**)	-3.6[e]	–	–
$(HOCF_2CF_2)_3COH$ (**2F**)	-4.4[e]	–	–
$(HOCF_2CF_2CF(OH)CF_2)_3COH$ (**1F**)	-17.3[e]	–	–
$PhOH$	18.2 (-0.8)	19.4 (-1.4)	18.0[c]
CH_3CO_2H	13.7 (-1.4)	12.8 (-0.5)	12.3[c]
Average unsigned error	1.4	1.4	

[a]Ethanol was used as a reference compound and its experimental pK_a (29.8) was employed as indicated in the text. [b]Parenthetical values correspond to the error in pK_a units (i.e., pK_a (expt – calc)). [c]See ref. 9. [d]See ref. 7. [e]These pK_a values were computed at the B3LYP/6-31+G(d) level.

Based upon the experimental pK_a values, the tetraol is found to be 16.1 pK_a units more acidic than *tert*-butanol. This difference is due to the three additional hydroxyl groups in **4**, and can be largely attributed to the stabilization of the conjugate base brought about by three intramolecular hydrogen bonds (Figure 1). On average this corresponds to an acidity enhancement of 5.4 pK_a units or 7.3 kcal mol^{-1} per hydrogen bond. Heptaol **1** is ~10^5 times more acidic than tetraol **2** (and a stronger acid than *tert*-butanol by a factor of 10^{21}!) indicating that the stabilization of the charge in the deprotonated anion goes beyond the

first internal hydrogen bond shell. As a result of the primary interactions between the alkoxide ion center and the three secondary hydroxyl groups, some of the excess electron density (charge) is delocalized on to the secondary OH substituents. This makes them better hydrogen bond acceptors than they would be otherwise. These outer or second solvation shell interactions between the uncharged primary and secondary hydroxyl groups are stronger in the conjugate base of **1** than in the acid resulting in an average stabilization of 1.6 pK_a units (i.e., 2.1 kcal mol^{-1}) per hydrogen bond. This corresponds to ~1/3 of the energy of the inner hydrogen bond shell, but more of these interactions can arise and they maybe used for transition state stabilization in enzyme-catalyzed reactions.[33] Both types of solvation shells also could alter the acidities and basicities of common functional groups when they are in a biological environment.

The hydrogen bond stabilization energies of the deprotonated aliphatic polyols **1–4** are not as large as they could be, in part, because the spacer length between the hydroxyl groups was not optimized. By incorporating two methylenes between the OH substituents, intramolecular six-membered rings are formed in the conjugate bases. These ring structures are too small to accommodate linear hydrogen bonds. For example, in the heptaol anion the M06-2X/maug-cc-pVT(+d)Z O–H···O bond angles span from 151-153˚ in the first solvation shell (i.e., in the O$^-$···H–O hydrogen bonds) and from 142-147˚ in the second (outer) solvation shell; similar values are observed in the B3LYP structures. Entropy also works against these acyclic anions, particularly when compared to an enzyme-bound substrate. If one corrects the experimental ΔpK_a (tetraol **2** – *tert*-butanol) energy difference to account for the entropies by using the computed ΔS values, the average

stabilization energy increases to 10 kcal mol^{-1} per hydrogen bond. In a lower dielectric constant (ε) medium than DMSO (ε = 46.8)[21] the hydrogen bond strength should be stronger.[34] Based upon the results of Chen et al. and Pan and McAllister, if ε is ~5, then the hydrogen bond strength would increase by 50%. These results suggest that strong hydrogen bonds can be formed in solution even though they have not been measured to date.

Brønsted acids are commonly employed as catalysts in many chemical transformations including non-biological processes.[35] Hydrogen bond enhanced acids such as **1** are interesting in this regard, particularly since they can be chiral and used, in principle, to carry out enantioselective protonations. To assess whether the conjugate bases of polyols can be further stabilized by incorporating electron withdrawing groups, the pK_a's of perfluorinated **1-3** (i.e., **1F- 3F)** were computed (Table 2).[36] All three of these compounds are predicted to have negative values for their pK_a's in DMSO which would make them more acidic than HCl (pK_a = 1.8), HBr (pK_a = 0.9), and CF_3SO_3H (pK_a = 0.3).[9] These Brønsted acids, consequently, represent a tunable system which can be exploited. The preparation, characterization, and catalytic ability of such species will be reported in a subsequent publication.

Conclusions

The pK_a of the heptaol **1** ($(HOCH_2CH_2CH(OH)CH_2)_3COH$) was measured in DMSO and this saturated aliphatic tertiary alcohol was found to be 10^{21} times more acidic than

tert-butanol and an order of magnitude more acidic than acetic acid. This remarkable acidity enhancement is largely attributable to the hydrogen bond network in the conjugate base of **1**. Three hydrogen bonds between the tertiary alkoxide center and the secondary hydroxyl groups result in a 22 kcal mol^{-1} stabilization. The oxygen atoms of the hydrogen bond donors are also better hydrogen bond acceptors than in the neutral acid because some of the excess charge is delocalized on to them. These secondary interactions (or second solvation shell) lead to an additional 6.4 kcal mol^{-1} stabilization, and as a result **1** is 10^5 times more acidic than $(HOCH_2CH_2)_3COH$ (**2**). Neutral-neutral hydrogen bonds such as this typically are ignored when accounting for enzyme catalysis because they are considered to be weak and are present in the substrate bound enzyme as well as the reaction transition state. However, our results indicate that the energetic consequences of hydrogen bonding in a charged species are not short range in nature, and that the movement of a charged center may lead to transition state stabilization in an enzyme-catalyzed process. The importance of hydrogen bond networks can be tested experimentally via double mutant cycles,[13] the incorporation of unnatural amino acids,[37] and the analyses of the molecular structures in the protein data bank. Computationalists and enzyme designers may also wish to look beyond the active site to tune hydrogen bond interactions.[38]

Application of the polarized continuum model provides predicted DMSO pK_a's that are in good accord with the experimental values (i.e., ± ~2 pK_a units). Electron withdrawing groups are found to increase the acidities of the polyols that were examined such that they are predicted to be stronger acids than HCl. As a result, it appears that the combination of hydrogen bonding and electron withdrawing substituents can lead to potent Brønsted acids

with adjustable acidities in nonprotic media. The characterization and utility of such species warrants further investigation and our initial results will be reported in due course.

Chapter 4: Characterization of a Saturated and Flexible Aliphatic Polyol Anion Receptor*

Anion transport plays a vital role in many cellular processes,[1] and enzymes that bind chloride, nitrate, phosphate, sulfate and oxyanions have been identified.[2-6] Multiple hydrogen bonds using both NH and OH donors are exploited for this purpose as illustrated for the Charcot-Leyden crystal (ClC) chloride channel, where Cl^- is coordinated to the hydroxyl groups of serine 107 and tyrosine 445 along with the backbone amides of isoleucine 356 and phenylalanine 357 (Figure 1).[2] To mimic this behavior, the cooperative action of hydrogen bond donors such as amides, ureas, thioureas, and pyrroles have been incorporated into rigid acyclic and macrocyclic structural frameworks.[7] Only limited examples of hydroxyl-based receptors, however, have been reported.[8] Davis and coworkers showed that cholic acid esters, a steroid with three OH groups, can weakly bind tridentate anions in non-polar media.[8a] Smith and coworkers explored the relative binding abilities of catechol and resorcinol (i.e., 1,2-$(HO)_2C_6H_4$ and 1,3-$(HO)_2C_6H_4$, respectively) with halide anions.[8b] Siloxanes that are capable of forming multiple hydrogen bonds also have been explored in acetonitrile (8d). Based upon these results and others, it is widely held that rigid

* Shokri, A.; Schmidt, J.; Wang, X. B.; Kass, S. R., Characterization of a saturated and flexible aliphatic polyol anion receptor. *J. Am. Chem. Soc.* **2012,** *134*, 16944-16947.

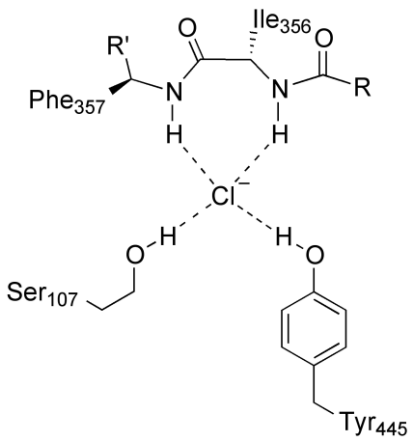

Figure 1. Schematic diagram of the Cl^- binding site of the ClC chloride ion channel.

receptors are needed to reduce the entropic penalty for anion complex formation and that intramolecular hydrogen bonding has a deleterious effect on binding.[8c,9] In this report, however, a flexible aliphatic alcohol with seven hydroxyl groups that does not meet either of these two criteria is found to bind to chloride anion. The resulting association complex was characterized in the gas phase by infrared photodissociation (IRPD) and photoelectron spectroscopy (PES), complementary computations were carried out, and binding constants were measured in a polar solvent as a function of temperature.

Heptaol **1** $[(HOCH_2CH_2CH(OH)CH_2)_3COH]$[10] was found to readily form a 1:1 complex with chloride anion upon its initial characterization by electrospray ionization (ESI) mass spectrometry. That is, an aqueous methanolic solution of **1** afforded an abundant $(M + Cl)^-$ anion (**1** • Cl^-) even though no chloride–containing salt was intentionally added. This suggests that **1** has a high chloride anion affinity, so we decided to characterize this

complex in the gas phase via IRPD spectroscopy. This was done because this technique is well-suited for providing structural information about hydrogen bonded systems.

IRPD spectra were obtained with a Fourier transform mass spectrometer (FTMS) equipped with an optical parametric oscillator (OPO)/optical parametric amplifier (OPA) laser system that previously was described.[11] Our instrument currently has a useful operating range from 2700 - 4000 cm^{-1} over which the energy increases in a roughly linear fashion from 5 mJ/pulse up to 26 mJ/pulse. Irradiation of **1** • Cl^- from 2800 to 3800 cm^{-1} in 5 cm^{-1} steps led to its cleavage and the loss of HCl at select wavelengths. A plot of the amount of fragmentation vs wavelength revealed four broad bands at 2945, 3260, 3395, and 3540 cm^{-1} (Figure 2). The highest of these frequencies is smaller than the ~3660 cm^{-1} O–H stretch of a simple alcohol in the gas phase, but is larger than the hydrogen-bond reduced value at ~3340 cm^{-1} in the liquid–phase.[12] This enables us to assign this band to an OH stretch that is slightly weakened by a hydrogen bond, presumably due to an OH • • OH interaction. The middle two frequencies at 3260 and 3395 cm^{-1} also undoubtedly correspond to O–H stretches, but these values are reduced by stronger hydrogen bonds most likely as a result of OH • • Cl^- interactions. As for the lowest energy mode at 2945 cm^{-1}, it may be the result of an even weaker OH stretch or alternatively could arise from C–H vibrations. To resolve this issue, **1** was sprayed from CH_3OD and D_2O so that all seven hydroxyl hydrogens in **1** • Cl^- were replaced by deuterium atoms. Given that isotopic substitution of a hydrogen by deuterium results in a reduction in the stretching frequency by a factor of ~1.41, all of the observed modes that are due to OH vibrations will move out of the experimentally accessible range and disappear from the spectrum. In accord with the

above assignments, only the vibrational mode at 2945 cm^{-1} remained in the spectrum of **1-*d*$_7$** • Cl^- (Figure 2), thereby indicating that this feature is the result of C–H stretching motions.

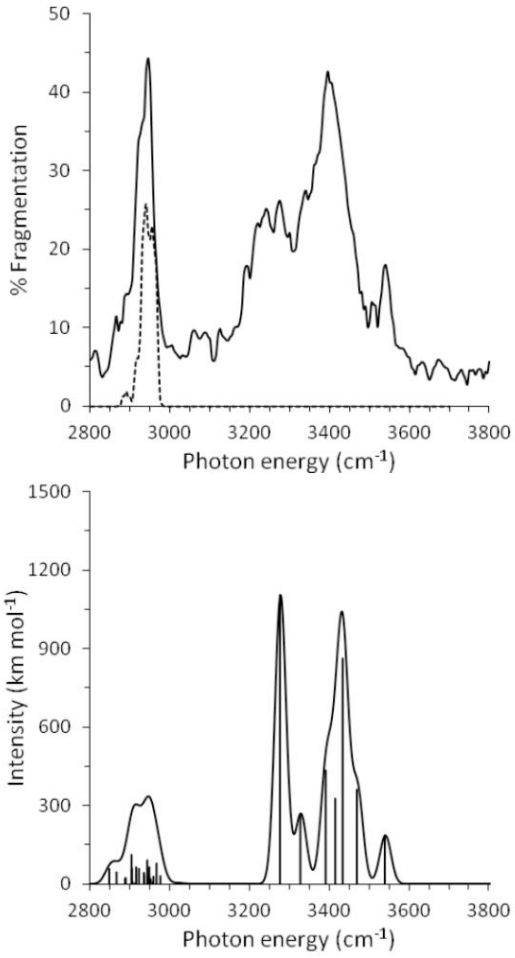

Figure 2. Experimenal IRPD spectrum of **1** • Cl^- (solid line) and its d_7–ion (dotted line) [top], and the B3LYP/aug-cc-pVDZ calculated spectrum [bottom]. Computed frequencies were scaled by 0.964 at all wavelengths and are depicted by vertical lines. The simulated spectrum was obtained by using a Gaussian function with a peak width at half height of 35 cm^{-1}.

Two limiting structures can be envisioned for the proton bound cluster **1** • Cl^- that differ in where a hydrogen atom is attached (i.e., ROH • Cl^- vs RO^- • HCl). It was anticipated that the latter structure would be more stable since the tertiary hydroxyl group of **1** is predicted to be more acidic than HCl by ~14 kcal mol^{-1}.[13] The inherent preference for the tertiary alkoxide–HCl complex might be overcome by differential solvation, however, and it is difficult to account for the band at 3540 cm^{-1} in a symmetric structure of this sort. To probe this point further, B3LYP geometry optimizations were carried out with the aug-cc-pVDZ basis set (i.e., B3LYP/aug-cc-pVDZ) and M06-2X/maug-cc-pVT(+d)Z single point energies were computed.[14-17] The most stable structure that was located is a chloride anion–heptaol complex in which two primary and two secondary hydroxyl groups coordinate to the chloride anion via four hydrogen bonds in a distorted tetrahedral arrangement (Figure 3). Many other ROH • Cl^- structures were located (see the appendix), but the only tertiary alkoxide–HCl cluster that we found is 22.2 kcal mol^{-1} higher in energy and in it the HCl interacts with one of the primary OH groups rather than the charged alkoxide center.

The B3LYP IR spectrum was computed for **1** • Cl^- (Figure 2). As can be seen, there is excellent accord between the predicted spectrum and the experimental results with the calculated bands (2949, 3265, 3434, and 3540 cm^{-1}) being within 4 to 39 cm^{-1} of the observed frequencies. The computed spectrum is also in accord with the band assignments that were deduced from the experimental data. That is, the calculated band at 2949 cm^{-1} corresponds to a combination of C-H stretching modes, the absorption at 3540 cm^{-1} is due to the O-H stretch of the primary (terminal) hydroxyl group that does not interact with the

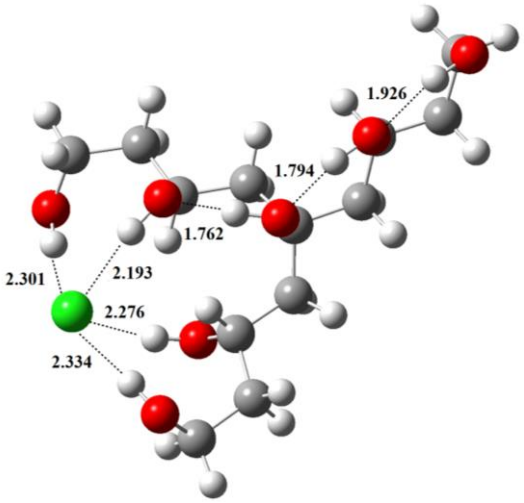

Figure 3. Lowest energy B3LYP/aug-cc-pVDZ structure for the addition complex of **1** and Cl^-.

chloride anion, and the two frequencies at 3265 and 3434 cm^{-1} correspond to overlapping O-H combination bands interacting with Cl^-.

To assess the stability of **1** • Cl^-, its negative ion photoelectron spectra were recorded at 193 nm (6.424 eV, ArF laser) and 157 nm (7.867 eV, F_2 laser) at 20 K (Figure 4).[18] One high energy band is seen, and based upon a linear extrapolation of the rapidly rising onset region, an estimate for the adiabatic electron detachment energy (ADE) of 6.0 eV is obtained. A M06-2X/maug-cc-pVT(+d)Z//B3LYP/aug-cc-pVDZ computational prediction of 6.02 eV is in excellent accord with the experimental result and is in keeping with previous reports showing that the M06-2X functional in combination with a large (i.e., triple zeta) basis set provides accurate ADEs;[10,16b,19] in contrast, B3LYP energies are

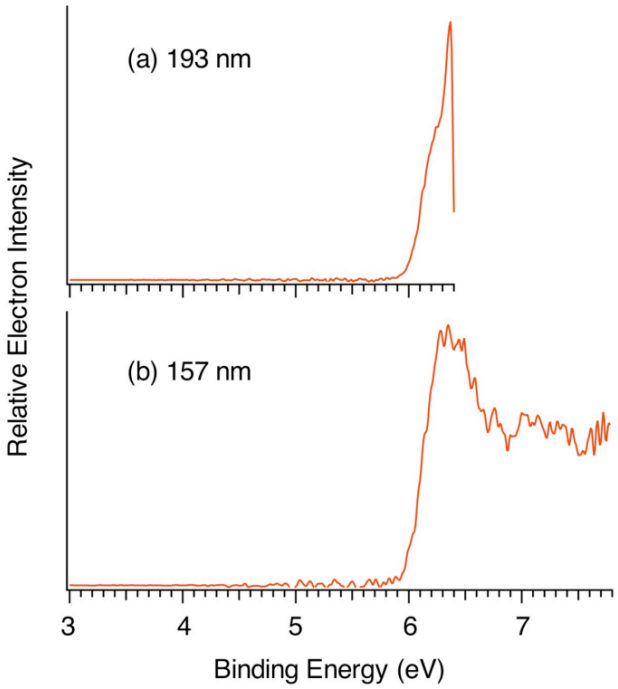

Figure 4. Low temperature (20 K) photoelectron spectra of **1** • Cl^- at 193 nm (6.424 eV) (a) and 157 nm (7.867 eV) (b).

sometimes too small by up to ~0.5 eV as is the case here (i.e., the B3LYP/aug-cc-pVDZ ADE is 5.33 eV which is too low by 0.67 eV).[20] Coordination of the chloride anion by **1** increases the electron binding energy relative to Cl^- (ADE = 3.6131 eV)[21] by 2.4 eV or 55 kcal mol^{-1}. This difference reflects the stabilization of chloride anion by multiple hydrogen bonds. Given that the hydration of Cl^- leads to a similar stabilization (i.e., ADE($Cl^-(H_2O)_4$) – ADE(Cl^-) = 2.31 eV or 53.3 kcal mol^{-1}),[22] the experimental data suggests that **1** forms four hydrogen bonds to the chloride anion in their association complex.[23,24] Computations are in accord with this structural assignment (Figure 3) and indicate that the enthalpy for

the fragmentation of **1** • Cl^- to its two separate constituents is endothermic by 48.8 kcal mol^{-1} at 298 K. Similarly, the complete dehydration of $Cl^-(H_2O)_4$ has been measured, and requires 50.1 kcal mol^{-1}.[25]

Our results to this point suggest that **1** is a good receptor for chloride ion in the gas phase, and that it might be one in solution as well. This runs counter to the paradigm in the field of anionic molecular receptors since **1** is flexible and can form intramolecular hydrogen bonds. The association of **1** with Cl^- in acetonitrile, consequently was examined by ^1H NMR spectroscopy.[26] Addition of increasing amounts of tetrabutylammonium chloride relative to **1** led to downfield shifts of all of the hydroxyl hydrogens due to complexation with the chloride anion, but only the resonance for the tertiary OH group was used to calculate the binding constant; the other hydroxyl signals are broader and overlap carbon-hydrogen resonances in some of the spectra. An x-reciprocal or Scatchard plot of the change in the chemical shift ($\Delta\delta$) divided by the chloride anion concentration versus Dd affords a straight line (Figure 5, $\Delta\delta/[Cl^-] = -362.0 \times \Delta\delta + 246.4$, $r^2 = 0.998$) where the association constant is given by the negative of the slope (i.e., -m) and the maximum value for the change in the chemical shift ($\Delta\delta_{max}$) is given by the intercept divided by –m.[27] That is, K = 362 M^{-1} and $\Delta\delta_{max}$ = 0.68 parts per million (ppm) at 22.0 ˚C. Alternatively, a nonlinear fit of the 1:1 binding isotherm gives the same result (K = 359 M^{-1} and $\Delta\delta_{max}$ = 0.68 ppm, supporting information), but is sometimes considered to be more accurate.[28]

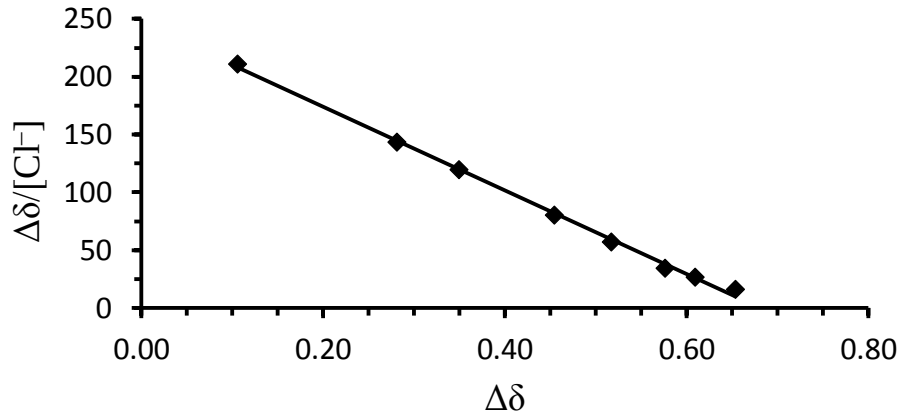

Figure 5. Scatchard x-reciprocal plot for the binding of **1** with chloride ion at 22.0 ˚C.

Similar data were obtained at -23.0 and 56.2 ˚C and the nonlinear approach affords K = 827 and 199 M^{-1}, respectively. Since the largest equilibrium constant was found at the lowest temperature that we examined, and the smallest equilibrium constant was obtained at the highest temperature that we studied, either the entropy for association must be negative or the heat capacity (ΔC_p°) has to have a negative value. A three point van't Hoff plot (RlnK = 2920/T + 1.71, r^2 = 0.997) affords ΔH° = -2.9 kcal mol^{-1} and DS˚ = 1.7 cal mol^{-1} K^{-1} indicating that ΔS˚ is positive (favorable) and that ΔC_p° is negative. This is consistent with previous anion binding studies that found entropically favored associations, presumably because of the poorer solvation of the bound complex.[29] Moreover, Anslyn and others found that the heat capacity changes with temperature in some such processes and is large and negative (unfavorable) in polar solvents (i.e., -30 to -560 cal mol^{-1} K^{-1}).[29b] When the change in the heat capacity is accounted for, then ΔH° = -3.1 kcal mol^{-1}, ΔS˚ = 1.3 cal mol^{-1} K^{-1} and ΔC_p° = -10.3 cal mol^{-1} K^{-1} are obtained. This suggests that the binding

enthalpy is worth ~1 kcal mol^{-1} per hydrogen bond to the chloride anion, and that the flexibility of the substrate leads to a less negative heat capacity than previously reported.

Larger association constants presumably can be obtained in a less polar solvent by increasing the acidity of the primary and secondary hydroxyl groups or optimizing the cavity size of the substrate so that a less distorted tetrahedral arrangement of hydrogen bonds can form around the chloride anion. A flexible polyhydroxy alkane that is capable of forming intramolecular hydrogen bonds, nevertheless, was found to bind to Cl^-. Additional anion receptors based upon such species, consequently, are worth exploring.

Chapter 5: Electron Withdrawing Trifluoromethyl Groups in Combination with Hydrogen Bonds in Polyols: Brønsted Acids, Hydrogen Bond Catalysts and Anion Receptors*

Introduction

In recent years the development and application of Brønsted acids has emerged as a fast growing branch of chemistry.[1] These compounds can be broadly classified into two categories, those with one acidic site such as BINOL-derived phosphoric acids,[2] bis(sulfonyl)imides,[3] *N*-triflyl phosphoric amides,[4] and carboranes,[5] and those with two acidic hydrogens such as thioureas,[6] biphenols,[7] and TADDOL derivatives.[8] These compounds are often employed as catalysts but sometimes require large loadings and are corrosive, harmful to plants and animals, and sensitive to heat.[9] We recently introduced a promising new variant that makes use of multiple hydrogen bonds to stabilize a charged center and enhance the acidity.[10] For example, 1,3,5-pentanetriol ($HOCH_2CH_2CH(OH)CH_2CH_2OH$), a simple aliphatic alcohol with three hydroxyl groups, was found to be more acidic than 2,2,2-trifluoroethanol (TFE) in DMSO and almost as acidic as phenol (i.e., the pK_a's of TFE, 1,3,5-pentanetriol, and PhOH are 23.4, 19.7, and 18.0, respectively). That is, the formation of two hydrogen bonds to the alkoxide center in

* Shokri, A.; Wang, X. B.; Kass, S. R., Electron-withdrawing trifluoromethyl groups in combination with hydrogen bonds in polyols: bronsted acids, hydrogen-bond catalysts, and anion receptors. *J. Am. Chem. Soc.* **2013,** *135*, 9525-9530.

the conjugate base of the triol leads to a 10.6 pK_a acidification relative to isopropanol. A larger hydrogen bonding network in a heptaol ($(HOCH_2CH_2CH(OH)CH_2CH_2)_3COH$) was found to result in a compound that is more acidic than acetic acid (pK_a = 11.4 vs 12.3) and 21 orders of magnitude stronger than *tert*-butanol.[11] Electron withdrawing groups can be incorporated into polyols of these sorts and should lead to even stronger Brønsted acids. To explore this possibility, three trifluoromethyl–containing polyols (**1**–**3**, Figure 1) were characterized by a number of means including aqueous and DMSO pK_a determinations, chloride anion binding association constants in acetonitrile, and gas-phase adiabatic electron detachment energies (ADEs) of their conjugate bases. The catalytic abilities of these compounds were also explored in a Friedel-Crafts alkylation and an aminolysis of an epoxide. These experimental results were supplemented with detailed computations as well.

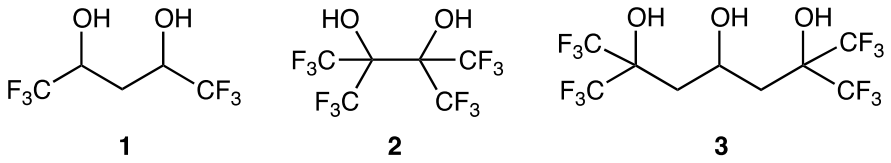

Figure 1. Trifluoromethyl group containing polyols.

Experimental Section

General. All glassware, needles, syringes, and NMR tubes were dried overnight in ovens at 110 ˚C and subsequently stored in a desiccator containing rubber septa and charged with phosphorus pentoxide. DMSO and DMSO-d_6 were dried under vacuum (1.5 Torr) over

CaH_2 at reflux for several hours and then were distilled under these conditions. The resulting solvents were stored in dark vials over 3Å molecular sieves that had been activated in a furnace at 320 ˚C for 1 day and then kept under an argon atmosphere for up to a few days. Pentane was dried and distilled over P_2O_5 and then used three times in succession to rinse mineral oil away from a 30% suspension of potassium hydride as part of the process for making the potassium salt of dimsyl anion (i.e., CH_3SOCH_2K). Fresh solutions of dimsyl potassium were prepared daily by reacting KH with DMSO or DMSO-d_6 at room temperature over a 30 min period. All of the dry solvents were routinely degassed immediately before use by bubbling dry argon through them for ~20 min. Chloroform-d was dried by storing it over activated 4Å molecular sieves, diol **2** was used as supplied (Matrix Scientific), and triol **3** was prepared as previously described,[12] but was purified by vacuum sublimation at 15 Torr and 70 ˚C rather than by recrystallization. NMR spectra were recorded on Varian VI-300 and VI-500 spectrometers at 295 K and the chemical shifts are given in parts per million (δ) relative to the residual solvent peak. Mass spectra were obtained with a Bruker BioTof II electrospray ionization–time of flight mass spectrometer using polyethylene glycol 200 as an internal standard.

meso-2-Phenyl-4,6-bis(trifluoromethyl)-1,3-dioxane. In a 500 ml round bottomed flask, 4.0 g (19 mmol) of a 40 : 60 mixture of *meso*- and *dl*-1,1,1,5,5,5-hexafluoropentane-2,4-diol,[13] 2.9 mL (3.0 g, 19 mmol) of benzaldehyde dimethylacetal, and 15 mg of *para*-toluenesulfonic acid were dissolved in 200 mL of dry methylene chloride freshly distilled from CaH_2. After magnetically stirring this solution at room temperature for 7 days, it was vigorously extracted with water (5 × 50 mL). The aqueous layers were combined and set

aside for later use because they contain the racemic 1,1,1,5,5,5-hexafluoropentane-2,4-diol. The organic layer was dried over $MgSO_4$ and concentrated with a rotary evaporator at water aspirator pressure to afford the crude ketal. It was then dissolved in ethanol, brought to a boil, and water was added until the solution turned cloudy. Upon slowly allowing the mixture to cool to room temperature, white needle-like crystals of *meso*-2-phenyl-4,6-bis(trifluoromethyl)-1,3-dioxane formed. They were filtered away from the mother liquor to yield 2.1 g (37% from the starting diol mixture and 92% when accounting for the diastereomeric ratio) of the title compound.[13a] ^{1}H NMR (300 MHz, DMSO-d_6): δ 1.85 (2H, m), δ 4.42 (2H, m), δ 5.69 (1H, s), δ 7.20-7.45 (5H, m). ^{13}C NMR (75 MHz, DMSO-d_6) δ 22.6, δ 73.4 (q, J = 33.2 Hz), 101.3, 126.3, 128.5, 129.9, 130.0 (q, J = 280 Hz), 136.2. ^{19}F NMR (282 MHz, DMSO-d_6) δ -80.3 (d, J = 5.9 Hz). HRMS-ESI: calc for $C_{12}H_{11}F_6O_2^+$ (M + H)$^+$ 301.0658, found 301.0665.

dl-1,1,1,5,5,5-Hexafluoropentane-2,4-diol. The combined aqueous material set aside earlier was vigorously extracted with diethyl ether (3 x 50 ml) and dried over $MgSO_4$. Removal of the ether at water aspirator pressure with a rotary evaporator gave an enriched diastereomeric mixture of *dl*-1,1,1,5,5,5-hexafluoropentane-2,4-diol (~95:5 of the desired *dl* isomer to the undesired *meso* compound).[13a] Further enrichment of the *dl* diastereomer was done by reketalizing the mixture as described above to afford 1.7 g of *dl*-1,1,1,5,5,5-hexafluoropentane-2,4-diol as a white solid in >99 : 1 diastereomeric purity. ^{1}H NMR (300 MHz, DMSO-d_6) δ 1.65 (2H, m), 4.1 (2H, m), 6.49 (2H, d, J = 6.9, OH). ^{13}C NMR (75 MHz, $CDCl_3$) δ 29.0 (s, CH_2), 66.7 (q, J = 32.9 Hz, *C*HCF_3), 125.6 (q, J = 280 Hz, CF_3).

^{19}F NMR (282 MHz, DMSO) δ -78.6 (d, J = 5.6 Hz). HRMS-ESI: calc for $C_5H_5F_6O_2^-$ (M – H)$^-$ 211.0199, found 211.0201.

pK_a Determinations. Aqueous acidities were measured by potentiometric titrations using a stock solution of NaOH (0.01 M) as the titrant after calibrating the pH meter with standard buffer solutions. DMSO pK_a's were measured by the overlapping indicator method at 20 – 25 °C by UV and ^{1}H NMR spectroscopy as previously described.[11,14] Multiple measurements were performed for each compound using two of the following indicators as long as they were within 2 pK_a units of the polyol being measured: 4-chloro-2,6-dinitrophenol (pK_a = 3.3), 2,4-dinitrophenol (pK_a = 5.1, Sigma Aldrich), 9-fluorenetriphenylphosphonium bromide (pK_a = 6.6), and 9-thiophenylfluorene (pK_a = 15.1).[15,16] Ion-pairing and self-association of the acids were minimized by working at low concentrations (10^{-5} – 10^{-3} M).

Binding Measurements. Diols **1** and **2** were mixed with CD_3CN and the resulting 2.5 mM solutions were placed in NMR tubes. Carefully measured volumes of 100 mM tetrabutylammonium chloride in CD_3CN were sequentially added and these titrations were monitored by recording an ^{1}H NMR spectrum at each point. The downfield chemical shifts of the OH signals were followed and nonlinear 1:1 fits of the binding isotherms were carried out using the solver add-on program for Excel to obtain the association equilibrium constants. Representative data and graphical fits of the results (Tables S1 and S2, and Figures S1 and S2) are provided in the supporting information.

Aminolysis of styrene oxide. A solution of 0.093 g (1.0 mmol) aniline, 0.12 g (1.0 mmol) styrene oxide and 5 mol% catalyst (0.05 mmol) in a 3 dram vial was stirred under argon at

60 ˚C for the indicated times. Reaction progress was monitored by TLC (6:1 hexanes/ethyl acetate) on 250 mm 60 F-254 silica gel plates and upon completion, 1 ml of $CDCl_3$ was added to the vial and the resulting mixture was placed in an NMR tube to obtain the ^1H NMR spectrum.

Friedel-Crafts reactions. β-Nitrostyrene (0.0074 g, 0.050 mmol), *N*-methylindole (0.020 g, 0.15 mmol) and 10 mol% of the catalyst (0.005 mmol) were dissolved in 0.6 ml of $CDCl_3$ and the ^1H NMR spectra of the reaction mixtures were recorded after 24 h.

Computations. Conformational searches were carried out using the MMFF force field and AM1 semiempirical calculations with Spartan 08.[17] Single-point B3LYP/6-311+G(d,p)[18] and M06-2X/maug-cc-pVT(+d)Z[19,20] energy computations were carried out on all of the resulting structures that were found to be within 3–5 kcal mol^{-1} of the most favorable species using Gaussian 09.[21] Full optimizations and vibrational frequency calculations were subsequently carried out using the same two DFT methods and basis sets on the most stable conformers of the acids and their conjugate bases.

The conductor-like polarizable continuum model (CPCM)[22] was used to predict pK_a values in DMSO using both computational approaches noted above. In this work, liquid-phase geometry optimizations and harmonic frequencies were computed in addition to single-point energies on the gas-phase structures. Relative pK_a values to TFE were obtained and converted to absolute values since pK_a (TFE) = 23.5 has been measured.[16]

Photoelectron Spectroscopy. Low temperature photoelectron spectra were recorded with a home-built variable temperature photoelectron spectrometer that has been previously described.[23] The conjugate bases of **1** and **2** were readily generated by electrospray

ionization from ~10^{-3} M methanol–water solutions and were trapped and cooled to 20 K over a period of 20–100 ms by blocking incoming anions for the final 20 ms of a 100 ms acquisition. These ions were then extracted into a time-of-flight mass spectrometer at a repetition rate of 10 Hz. Photoirradiation of the mass selected anions with an excimer laser at 193 nm (6.424 eV) operating at 20 Hz was carried out to enable shot-to-shot background subtraction for all of the reported spectra. Photoelectrons were collected at ~100% efficiency and analyzed with a 5.2 m long electron flight tube. This provided spectra with a resolution (ΔE/kinetic energy) of ~2% or 30 meV at 5 eV binding energy.

Results and Discussion

Hydrogen bonding is ubiquitous in biological systems and plays a critical role in molecular recognition and catalysis. Designing small molecules to mimic this behavior is a major challenge and the subject of much ongoing research. Brønsted acids and hydrogen bond catalysts can be exploited in this regard. We recently reported that hydrogen bond networks can be used to delocalize a charge site and increase the acidity or basicity of a compound.[24] Proof of concept computations on perfluoropolyols, species that are apt to be stable only at cryogenic temperatures, revealed that hydrogen bond arrays in conjunction with electron withdrawing groups lead to very strong Brønsted acids.[11] To test this prediction, three trifluoromethyl group containing polyols were examined.

Electrospray ionization of 1,3-bis(trifluoromethyl)-1,3-propanediol (**1**) and 1,1,2,2-tetra(trifluoromethyl)-1,2-ethanediol (**2**) afforded their corresponding $(M - 1)^-$ ions and the photoelectron spectra of these anions (**1a** and **2a**) were obtained at 20 K with an excimer

laser at 193 nm (Figure 2).[25] These broad spectra are similar to those of other deprotonated polyols, and the top of the bands give the vertical electron detachment energies (VDEs) whereas a linear extrapolation of the onset region affords the adiabatic electron detachment energies (ADEs, Table 1).[26] The resulting values are very large for alkoxide ions and correspond to enhancements relative to ethoxide and 2,2,2-trifluoroethoxide of up to 3.29

Table 1. Experimental and computed adiabatic (ADE) and vertical (VDE) electron detachment energies in eV for deprotonated alcohols and diols.

cmpd (RO^-)	expt		calc[a]	
	ADE	VDE	ADE	VDE
$CH_3CH_2O^-$	1.7120 ± 0.0040[b]		1.65 (1.58)	1.82 (1.72)
$CF_3CH_2O^-$	2.5541 ± 0.0043[b]		2.80 (2.79)	2.95 (2.88)
$CF_3CH(OH)CH_2CH(O^-)CF_3$ (**1a**)	4.00 ± 0.10	4.51 ± 0.10	3.73 (4.09)	4.31 (4.56)
$(CF_3)_2C(OH)C(O^-)(CF_3)_2$ (**2a**)	5.00 ± 0.10	5.51 ± 0.10	4.74 (4.82)	5.27 (5.37)
$((CF_3)_2C(OH)CH_2)_2CHO^-$ (**3a**)			4.45 (4.64)	5.27

[a]Computed values are at 0 K and correspond to B3LYP and M06-2X (in parentheses) energies. The aug-cc-pVDZ basis set was used for computing VDEs and ADEs with the former functional. M06-2X ADEs were computed with the larger maug-cc-pVT(+d)Z basis set. [b]See ref. 27.

and 2.45 eV (75.9 and 56.5 kcal mol^{-1}), respectively for **2a**.[27] This is due to the stabilization of **1a** and **2a** resulting from their strong intramolecular hydrogen bond and the presence of the electron withdrawing trifluoromethyl substituents. The latter effect is worth 16 kcal mol^{-1} per CF_3 group and was determined by comparing the ADEs of **1a** and **2a** to estimates for the conjugate bases of 1,3-propanediol (2.59 ± 0.14 eV) and 1,2-ethanediol (2.28 ± 0.14 eV).[28] It also results in electron binding energies that are larger than those for the conjugate bases of strong acids such as CH_3CO_2H (3.47 ± 0.01 eV),[29] HCl (3.613577 ± 0.000044

eV),[30] HNO_3 (3.937 ± 0.014 eV),[31] and in the later case, even for H_2SO_4 (4.75 ± 0.10 eV).[32] B3LYP/aug-cc-pVDZ and M06-2X/maug-cc-pVT(+d)Z calculations are in accord with these findings but the latter approach is more accurate. It reproduces the experimental ADEs with an average error of 0.16 eV, which is the same value that was previously reported for a different set of polyol anions.

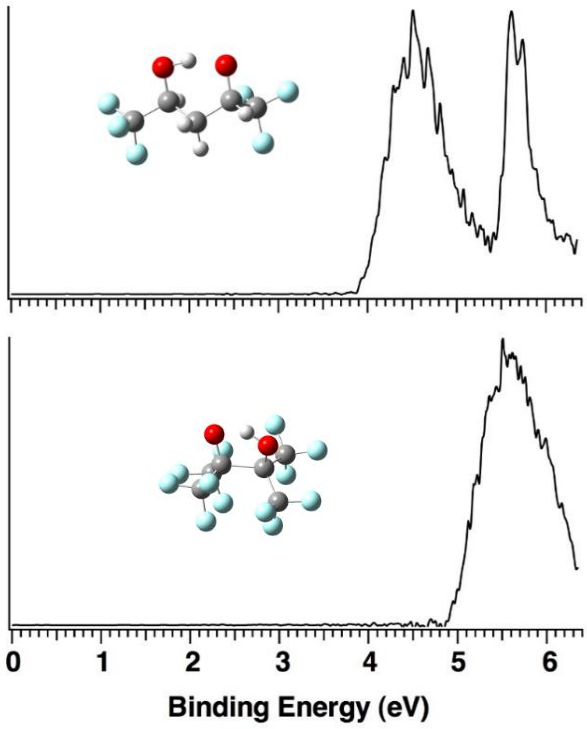

Figure 2. Low temperature (20 K) photoelectron spectra of $CF_3CH(OH)CH_2CH(O^-)CF_3$ (**1a**, top) and $(CF_3)_2C(OH)C(O^-)(CF_3)_2$ (**2a**, bottom) at 193 nm (6.424 eV).

The photoelectron spectra of **1a** and **2a** reveal that the combination of intramolecular hydrogen bonds and electron withdrawing groups can lead to very stable anions in the gas

phase. To assess the impact of this stabilization in solution, the pK_a's of **1**–**3** were measured in DMSO by ^{1}H NMR and UV spectroscopy (Table 2). The former values span from 4.8 to 16.0 which makes these compounds remarkably acidic alcohols. Diol **1** is the least acidic of the three but the two trifluoromethyl groups enhance its acidity by 9.4 pK_a units relative to 1,3-propanediol. As a result, it is a stronger acid than phenol by one hundred fold. Triol **3** is 8.9 orders of magnitude more acidic than **1** and 12.6 pK_a units more acidic than the unsubstituted polyol without any trifluoromethyl groups. It is also a little more than 10^5 times stronger than acetic acid even though it is a saturated compound. The most acidic compound of the series is diol **2**, which is 10^{23} times more acidic than ethylene glycol, 7.5 pK_a units stronger than acetic acid, and within 3 pK_a units of the value of HCl. These results reveal that the combination of intramolecular hydrogen bonding and electron withdrawing trifluoromethyl groups can lead to saturated polyols that are quite acidic in DMSO.

In protic solvents intramolecular hydrogen bond stabilization of polyol conjugate bases is relatively unimportant because the anions are stabilized by intermolecular hydrogen bonds with the solvent. As a result, the pK_a of ethylene glycol and ethanol in water differ by only 0.5 pK_a units (i.e., 15.4 vs 15.9).[33] The acidities of **2** and **3** consequently were measured in water as this presumably provides an opportunity to probe the effects of the trifluoromethyl group in the absence of intramolecular hydrogen bond stabilization. These compounds were found to be acidic (i.e., pK_a = 5.6 and 7.1, respectively) and are stronger acids than 1,1,1,3,3,3-hexafluoro-2-propanol (HFP, pK_a = 9.3), but neither one is as strong

Table 2. Calculated and experimental pK_a values.

cmpd (ROH)	B3LYP/6-311+G(d,p)	M06-2X/maug-cc-pVT(+d)Z	Expt DMSO
1	17.5	16.0	16.0 ± 0.1
2	0.6	2.3	4.8 ± 0.1
3	9.4	6.8	7.1 ± 0.3
$(CF_3)_3COH$	8.3	9.6	10.7[a]
$HOCH_2CH_2OH$[b]	24.7	24.1	28.0[c]
$HOCH_2CH_2CH_2OH$[b]	23.9	23.3	25.4 ± 0.3
$(HOCH_2CH_2)_2CHOH$[b]	20.1	18.3	19.7 ± 0.2
PhOH[b]	18.2	19.4	18.0
CH_3CO_2H[b]	13.7	12.8	12.3
HCl[a]			1.8

[a]See ref. 16. [b]See ref. 11. [c]This value was obtained from a linear correlation between ΔH°_{acid} and pK_a, see ref. 10.

as acetic acid (pK_a = 4.8). The acidity of **2** is not surprising in that the four trifluoromethyl groups are on adjacent carbons and exert a strong stabilizing inductive effect. That is, there is a 10^{10} times acidity enhancement of **2** relative to ethylene glycol which leads on average to a 2.5 pK_a unit effect per CF_3 group. In contrast, the four CF_3 groups in **3** are separated by three intervening carbons so little, if any, effect was expected from one of the geminal pairs of trifluoromethyl substituents. The 2.2 pK_a unit acidity enhancement relative to HFP, however, suggests that hydrogen bonds can transmit the inductive effect over distance even in an aqueous environment. This would provide an important long range stabilizing mechanism that may have far reaching implications in biological processes.

Liquid-phase DMSO pK_a values were calculated for $(CF_3)_3COH$ and **1-3**. This was accomplished by computing their gas-phase acidities (ΔG°_{acid}) and that of TFE (Table 3), and then calculating the solvation energies of the acids and their conjugate bases with a polarized continuum model (PCM). B3LYP/6-311+G(d,p) and M06-2X/maug-cc-pVT(+d)Z energies were used for this

Table 3. Calculated and experimental gas-phase acidities (ΔG°_{acid}, in kcal mol^{-1}).

cmpd (ROH)	B3LYP/6-311+G(d,p)	M06-2X/maug-cc-pVT(+d)Z	Expt
CF_3CH_2OH	351.4	354.0	354.1 ± 2.0[a]
$(CF_3)_3COH$	321.0	325.6	324.0 ± 2.0[a]
1	330.1	330.6	
2	302.8	307.6	
3	309.6	310.8	

[a]See ref. 27.

purpose and absolute pK_a's were derived from the relative values to TFE, and its experimentally measured acidity of 23.5. Both methods do well but the average unsigned errors for the gas-phase acidities (2.9 (B3LYP) and 0.9 (M06-2X) kcal mol^{-1}) and the DMSO pK_a's (2.6 (B3LYP) and 1.0 (M06-2X)) are noticeably smaller for the M06-2X density functional. The largest deviations from experiment (3.0 kcal mol^{-1} and 4.2 pK_a units (B3LYP) vs 1.6 kcal mol^{-1} and 2.5 pK_a units (M06-2X)) are also better for the meta hybrid generalized gradient approximation Minnesota 06 functional. Both methods are

least accurate for **2**, and this may be a reflection of the four CF_3 groups being in close proximity to each other.

Triol **3** has two ionization sites and our experiments do not indicate which one is more acidic. B3LYP/6-311+G(d,p) computations were carried out to address this issue. In the gas phase deprotonation of the internal hydroxyl group is energetically preferred over a terminal one, but only by 0.84 kcal mol^{-1}. This can be attributed to the formation of two direct hydrogen bonds to the charged center in the former case as opposed to one, along with a secondary hydrogen bond, in the latter instance (Figure 3). The same stability order is found in DMSO, but solvation reduces the predicted energy difference to 0.36 kcal mol^{-1}. As a result, the relative stabilities were also computed in water since it has a higher dielectric constant than that for DMSO (i.e. ε = 78.4 vs 46.8, respectively).[21] In this case

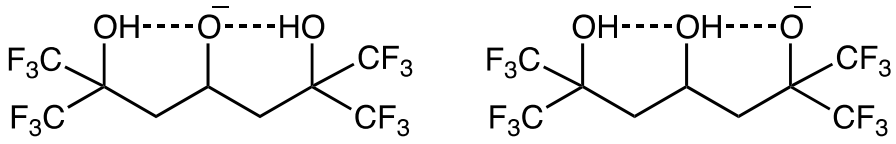

Figure 3. Isomeric conjugate bases of triol **3**.

there is a reversal, and now the terminal alkoxide anion is found to be more stable than the internal one by 0.81 kcal mol^{-1}. These results indicate that both the inductive effect and hydrogen bond stabilization are sensitive to the medium, and as a result the preferred ionization site can vary with the dielectric constant of the solvent. The energy differences here, however, are quite small, and the most stable structure may vary with the

computational approach; M06-2X/maug-cc-pVT(+d)Z calculations predict that the internal alkoxide anion is more stable in all three cases but the energy differences are 0.55 (gas phase), 0.71 (DMSO) and only 0.06 kcal mol^{-1} in water.

Molecular recognition of anions via ion channels and transporters is biologically important in stabilizing membrane potentials and controlling cell volumes, and is intimately connected to a number of debilitating diseases.[34] An acidic and flexible polyol ($HOCH_2CH_2CH(OH)CH_2)_3C$-OH, pK_a = 11.4 ± 0.2) was recently reported to bind chloride in acetonitrile with an association constant of 360 M^{-1} despite being an aliphatic alcohol that can form intramolecular hydrogen bonds.[35] Diols **1** and **2** bracket the acidity of this heptaol (i.e., **1** and **2** are 5-6 pK_a units less acidic and more acidic than it), and consequently their binding constants were also measured. The less acidic diol (**1**) was found to have an association constant with chloride of 3300 M^{-1} in acetonitrile. This is nine times larger than for the more acidic heptaol, 100 fold bigger than an α-D-ribose receptor in which the C1 and C5 hydroxyl groups are protected as their methyl and trityl (Ph_3C) ethers, respectively, and 14 times larger than for the corresponding β-anomer.[36] Our association constant is also greater than for phenols such as catechol (1,2-$(HO)_2C_6H_4$, ~3 fold) and resorcinol (1,3-$(HO)_2C_6H_4$, 23 times).[37] 1,1,2,2-Tetra(trifluoromethyl)ethylene glycol (**2**) has a binding constant with Cl^- of 6700 M^{-1} which is the largest measured value for an aliphatic alcohol to date, but it is only about twice as large as for **1** even though their acidities differ by 11 orders of magnitude in DMSO. This clearly indicates that there is only a loose relationship between the acidity of a compound and its anion binding affinity undoubtedly because the

cavity size of the receptor, steric interactions, and the solvation of the bound complex also play a role.

Our physical characterization of polyols **1**–**3** suggests that they could be good Brønsted acid catalysts, and since they are all capable of forming multiple hydrogen bonds in advance of proton transfer, they maybe more effective than other specific acid catalysts. To explore this possibility, their catalytic behavior in a Friedel-Crafts[38] reaction between β-nitrostyrene and *N*-methylindole (eq 1) was investigated. All three polyols promote this transformation and the reaction rates, as

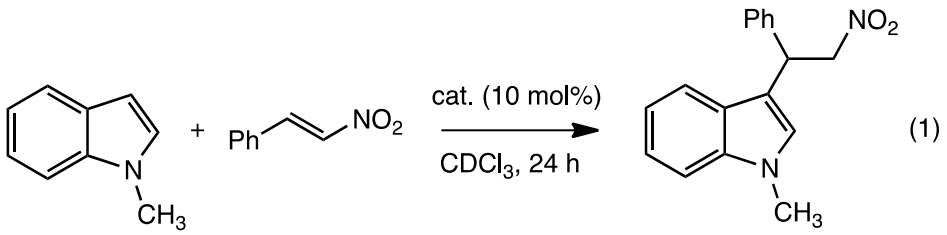

(1)

indicated by the percent conversion, correlate with their acidities not with the number of hydroxyl groups (Table 4). That is, 10 mol% of the strongest acid (**2**) leads to a 95% conversion at room temperature in 24 h whereas it is 19% with the weakest acid (**1**). Acetic acid does not catalyze this process, however, even though it is four pK_a units more acidic than **1** in DMSO. This indicates that general acid catalysis is involved and strongly suggests that more than one hydrogen bond is involved in this transformation (i.e., the reaction proceeds via hydrogen bond catalysis).

Table 4. Results for acid-catalyzed transformations.

catalyst	conversion (%)[a]		
	eq 1	eq 2[b]	**5** : **6**
1	19	89	73 : 27
2	95	100	88 : 12
3	53	100	81 : 19
no catalyst	4	5	43 : 57
HOAc	4	78	86 : 14

[a]Determined by ^{1}H NMR. [b]Reaction time = 2.75 h except for when **2** was used, then it was 20 min.

All three alcohols also catalyze the aminolysis of styrene oxide with aniline at 60 ˚C under solvent free conditions (SFC, eq 2, Table 4). The reactivity order again is in accord with the acidity of the three alcohols as is the selectivity. That is, the most acidic acid (**2**) catalyzes the reaction most efficiently and leads to the most selective transformation. It is also a more effective catalyst in this reaction than Shreiner's thiourea ((3,5-$(CF_3)_3C_6H_3NH)_2CS$) by about an order of magnitude.[39] Acetic acid is four orders of magnitude more acidic than **1** in DMSO but is a slightly less efficient catalyst. This indicates that general acid catalysis is also important in this reaction.

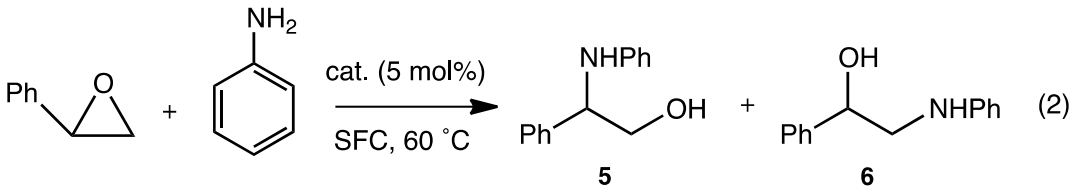

Conclusion

Diols **1** and **2** and triol **3** were found to be quite acidic in DMSO and water. The conjugate bases of the most acidic and least acidic compounds (i.e., **2** and **1**, respectively) are also remarkably stable in the gas phase as indicated by their ADEs, which in the former case exceeds that of deprotonated sulfuric acid. Taken together, these results suggest that the inductive effect can be transmitted via hydrogen bonds. Diols **1** and **2** also bind chloride anion in acetonitrile with the largest binding constants reported to date for an aliphatic alcohol (i.e., K = 3300 (**1**) and 6700 (**2**) M^{-1}), and are capable of acting as Brønsted acid and hydrogen bond catalysts (i.e., specific and general acid catalysts, respectively). As a result, hydrogen bonding in conjunction with electron withdrawing groups is a promising avenue for developing molecular recognition hosts and Brønsted acid and hydrogen bond catalysts.

Chapter 6: Hydrogen Bond Networks: The Strengths of Different Types of Hydrogen Bonds and An Alternative to the Low Barrier Hydrogen Bond Proposal*

Introduction

Hydrogen bonds can be used in synergy to provide catalytic power and enhance Brønsted acidities. For example, Shan and Herschlag reported that 2,6-dihydroxybenzoic acid is 10.9 kcal mol^{-1} (8.0 pK_a units) more acidic than benzoic acid in DMSO due to the presence of two hydrogen bonds in the conjugate base between the hydroxyl groups and the carboxylate anion.[1] We recently noted than an even larger acidification of 22 kcal mol^{-1} (16.1 pK_a units) in DMSO can be achieved by three hydrogen bonds to the tertiary alkoxide center in deprotonated 3-(2-hydroxyethyl)-1,3,5-pentanetriol [$(HOCH_2CH_2)_3COH$, **T4**].[2] In a similar way, enzyme active sites make use of hydrogen bonds to stabilize transition state structures by delocalizing negatively charged centers.[3-6] Extended networks of hydrogen bonds are employed, but many of the interactions are between non-charged groups. Triose phosphate isomerase (TPI) has such an arrangement (Figure 1),[7] but a single exceptionally strong low barrier hydrogen bond (LBHB) was proposed to account for the catalytic rate enhancement; this LBHB was originally proposed to be between His-95 and the enediolate but subsequently it was suggested that Glu-165 is the residue involved in the LBHB.[8]

*Shokri, A.; Wang, Y.; O'Doherty, G. A.; Wang, X. B.; Kass, S. R.; Hydrogen Bond Networks: The Strengths of Different Types of Hydrogen Bonds and An Alternative to the Low Barrier Hydrogen Bond Proposal. Submitted for publication.

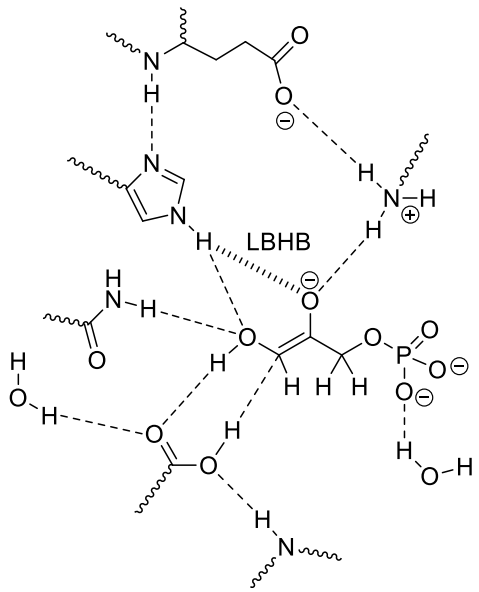

Figure 1. Hydrogen bonds in the active site of triose phosphate isomerase bound to an endiolate intermediate as indicated by computations. The proposed low barrier hydrogen bond is labeled.[8a]

LBHBs have been invoked in many additional processes (e.g., photoactive yellow protein, chymotrypsin, serine protease, and citrate synthase),[9] but this explanation is controversial.[10]

In the early 1990's some hydrogen bonds were found to have low H/D fractionation factors, downfield ^{1}H NMR signals of 10 δ or more, infrared spectra with low frequency and unusually broad O–H stretching bands, and short distances between the heteroatoms involved in the hydrogen bond (i.e., the X–Y distance in X···H···Y, where X and Y are nitrogen or oxygen centers).[11] Anionic $RO^-\cdots HOR'$ hydrogen bond strengths of 20 – 25 kcal mol^{-1} are common in the gas phase, and the dissociation energy of $F^-\cdots HF$ into F^- and HF is 45.8 ± 1.6 kcal mol^{-1}.[12] This led Gerlt and Gassman to propose that LBHBs can

provide 15 – 20 kcal mol^{-1} of stabilization in enzyme-catalyzed reactions.[8a,13] This remarkable hypothesis posited that hydrogen bonds in biological processes can be far stronger than previously considered possible. As a result, it has received considerable attention. No hydrogen bond, however, has been measured to be so strong in solution. The largest value to date is 7.5 kcal mol^{-1} for monodeprotonated phthalic acid (i.e., 1,2-$C_6H_4(CO_2H)CO_2^-$) in acetonitrile.[14] This critique of the LBHB proposal maybe a "red herring", however, because computations indicate that stronger hydrogen bonds can be formed in less polar media.

We have put forth a hydrogen bonding network (HBN) alternative to the LBHB proposal that suggests that a network of multiple hydrogen bond interactions can easily provide the required energy for enzyme-catalyzed transformations.[2,15] Primary (1˚) hydrogen bonds, which we define as those between a charged center and a donor or acceptor group, typically are the strongest ones. Secondary (2˚) and tertiary (3˚) hydrogen bonds, which involve non-charged groups (Figure 2) are common and their total energetic contributions may be quite significant. To assess this hypothesis, a small covalently bound model compound was investigated by negative ion photoelectron spectroscopy in the gas phase and pK_a measurements in DMSO. This experimental work was supplemented with extensive computations to probe the energetic consequences of different types of hydrogen bonds in different environments. Large stabilizations (> 15 kcal mol^{-1}) can be achieved, two 2˚ hydrogen bonds between non-charged donor and acceptor groups can be energetically more important than an $O^-\cdots H–O$ interaction, and their importance is enhanced with a decrease in the polarity of the environment.

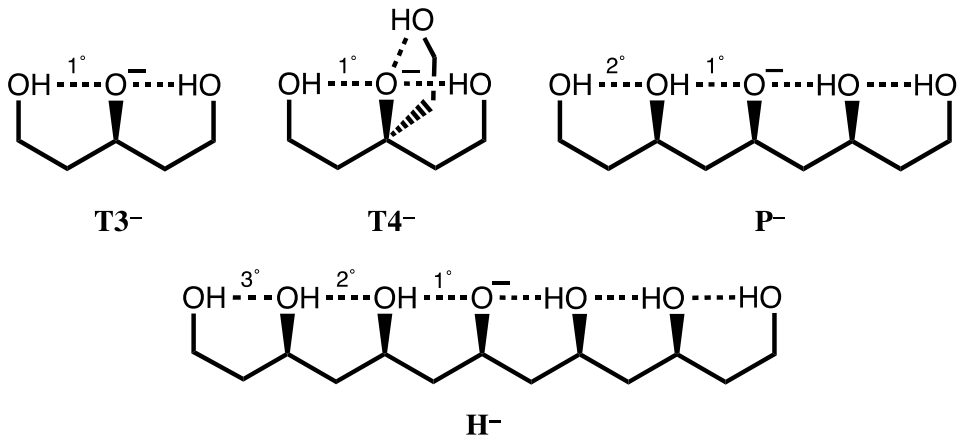

Figure 2. Most favorable hydrogen-bonding arrangements for the conjugate bases of several polyols and their different kinds of hydrogen bonds.

Experimental Section

General. ^{1}H and ^{13}C NMR spectra were recorded on Varian 300, 400 and 500 MHz spectrometers and the ^{1}H chemical shifts are reported relative to internal tetramethylsilane (0.00 δ) or residual proton signals in the deuterated solvents (i.e., 7.26 δ for $CDCl_3$ and 3.30 δ for CD_3OD). For the ^{13}C data, CD_3OD and $CDCl_3$ at 49.05 and 77.2 δ, respectively were used as the reference signals. Infrared (IR) spectra were obtained with a Nicolet iS5 FT-IR spectrometer. Mass spectra were recorded with a Bruker BioTof II electrospray ionization–time of flight mass spectrometer and optical rotations were measured with a Jasco P-2000 digital polarimeter.

Flash column chromatography was performed on 60-200 or 230-400 mesh silica gel. Analytical thin-layer chromatography was performed with precoated glass-backed plates

and visualized by quenching of fluorescence or by charring after treatment with *p*-anisaldehyde or potassium permanganate stain. Diethyl ether, tetrahydrofuran, dichloromethane and triethylamine were dried under argon by passing these solvents through activated alumina columns. Commercial reagents were used without purification unless otherwise noted. Air- and/or moisture-sensitive reactions were performed under an atmosphere of argon or nitrogen using oven- or flame-dried glassware and standard syringe/septa techniques.

pK_a Determination. The acidity of $(HOCH_2CH_2CH(OH)CH_2)_2CHOH$ (**P**) was measured in dry DMSO at room temperature (22 ˚C) by ^{1}H NMR spectroscopy as previously described.[2] 1-Acetylindolin-2-one (pK_a = 13.5)[16] was used as the reference indicator and five independent determinations were carried out to obtain the pK_a of the pentaol. In all of these experiments a low concentration of the polyol was used (i.e., 1 mM) to minimize ion pairing and self-association of the acid.

Photoelectron spectroscopy. A low temperature photoelectron spectrum of the conjugate base of $(HOCH_2CH_2CH(OH)CH_2)_2CHO^-$ **(P^-)** was recorded at 20 K with a photoelectron spectrometer that has been previously described.[17] The conjugate base of the pentaol was generated by electrospray ionization from an ~10^{-3} M methanol–water solution and the mass selected ion was photoirradiated with a F_2 excimer laser at 157 nm (7.867 eV) operating at 20 Hz to enable shot-to-shot background subtraction. Photoelectrons were collected with nearly perfect efficiency and analyzed with a 5.2 m long electron flight tube. This provided spectra with a resolution (ΔE/kinetic energy) of ~2% or 30 meV at 5 eV binding energy.

Computations. Monte Carlo and systematic conformational searches were carried out with Spartan 08 using the MMFF force field.[18] B3LYP/6-311+G(d,p)[19] and M06-2X/maug-cc-pVT(+d)Z[20,21] single point energy calculations were subsequently carried out with Gaussian 09[22] on all of the structures that were found within 7 kcal mol^{-1} of the most stable one. Full geometry optimizations and frequency calculations were then carried out on all of the species within 5 kcal mol^{-1} of the most favorable conformer using both density functional theory approaches. For computing the vertical and adiabatic detachment energies (i.e., VDEs and ADEs, respectively) both the anions and radicals were reoptimized with the B3LYP functional and the aug-cc-pVDZ basis set, and M06-2X/maug-cc-pVT(+d)Z single point energies were obtained too. The resulting ADEs are reported at 0 K.

Liquid phase pK_a values in various solvents were computed at 298 K using the conductor-like polarized continuum model (CPCM).[23] Single point energies were obtained with the B3LYP/6-311+G(d,p) and M06-2X/maug-cc-pVT(+d)Z methods on their optimized gas phase structures. The "iterative", "maxExtIt=1000", "mxIter=1000", and "QConv=VeryTight" keywords were employed to solve the PCM electrostatic problem and to compute the polarization charges to a convergence threshold of 10^{-12} within 1000 steps. For DMSO, 70 surface elements (tesserae) and an area of 0.2 Å for each sphere were used whereas the default parameters were employed for the other solvents.

Results and Discussion

To probe the energetic consequences of 1˚ and 2˚ hydrogen bonds, the all *syn*-pentaol [$(HOCH_2CH_2CH(OH)CH_2)_2CHOH$, **P**] was synthesized by a 3 step route starting from a previously reported precursor (Figure S1).[24] Electrospray ionization of the pentaol from an aqueous methanolic solution afforded the $(M - 1)^-$ ion ($\mathbf{P}^-$), and its photoelectron spectrum was recorded at 20 K using a F_2 excimer laser producing 157 nm (7.867 eV) photons (Figure 3). The spectrum is qualitatively similar to the previously reported one for the conjugate base of the related triol (i.e., $(HOCH_2CH_2)_2CHOH$, **T3**),[25] but the electron binding energy of $\mathbf{P}^-$ is much larger and additional bands at higher energies corresponding to excited states of the photoproduced radical are observed. A linear extrapolation of the onset region provides the adiabatic detachment energy (ADE) and the top of the first band gives the vertical detachment energy (VDE). These values are 4.05 and 4.45 eV, respectively, for $\mathbf{P}^-$ and are remarkable in that the ADE is larger than that for the conjugate bases of strong acids such as acetic, hydrochloric, and nitric acids (i.e., 3.470 ± 0.010, 3.613577 ± 0.000044, and 3.937 ± 0.014 eV, respectively).[26-28]

There are three different hydroxyl groups in the pentaol at C1, C3, and C5 that could be deprotonated but as expected the central alkoxide at C5 is predicted to be the most stable conjugate base (Figure 2). Its structure has two 1˚ and two 2˚ hydrogen bonds and is predicted to be 3.3 kcal mol^{-1} more stable than the alternative C3-deprotonated 2˚ alkoxide at the B3LYP/aug-cc-pVDZ level.[29] The computed B3LYP/aug-cc-pVDZ, M06-2X/maug-cc-pVT(+d)Z//B3LYP/aug-cc- pVDZ, and M06-2X/maug-cc-pVT(+d)Z ADEs for $\mathbf{P}^-$ are

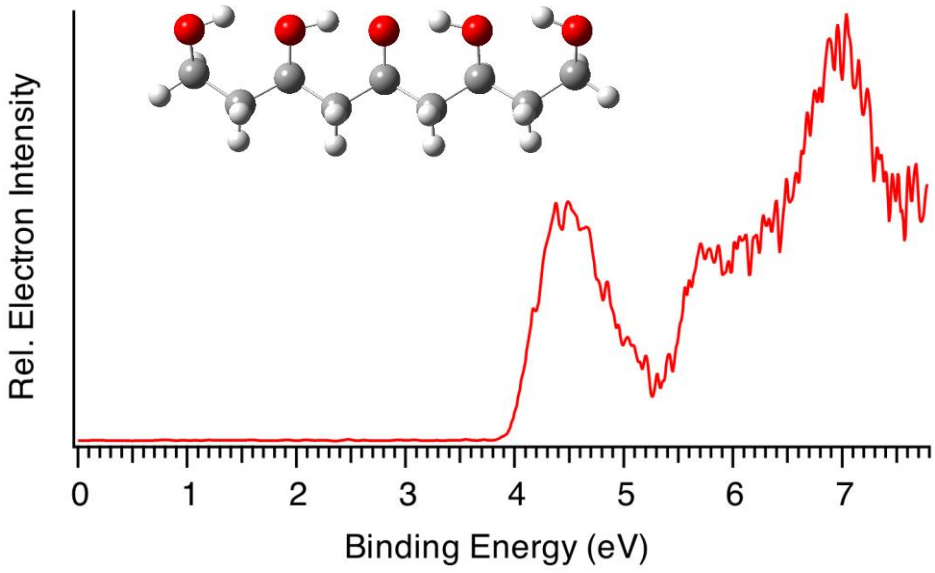

Figure 3. Low temperature (20 K) photoelectron spectrum of pentaol $\mathbf{P}^-$ at 157 nm (7.867 eV).

3.69, 3.80, and 3.82 eV, respectively, all of which reproduce the experimental result with accuracies that previously have been noted.[25]

The strength of the hydrogen bond network in $\mathbf{P}^-$ can be assessed by comparing its ADE to appropriate reference ions. For example, its ADE is 0.2 eV (4.6 kcal mol^{-1}) larger than for $(HOCH_2CH_2)_3CO^-$ ($\mathbf{T4}^-$, ADE = 3.85 eV),[25] which reveals that in this case two 1˚ and two 2˚ hydrogen bonds are more effective than three 1˚ hydrogen bonds. In other words, two 2˚ hydrogen bonds can exceed the strength of one strong ionic hydrogen bond. If one also compares $\mathbf{P}^-$ and $\mathbf{T3}^-$ (ADE = 3.30 eV),[25] the 0.75 eV (17.3 kcal mol^{-1}) difference

provides a direct measure of the total cooperative effect due to the presence of the two primary hydroxyl groups in the latter ion. Consequently, a 2˚ hydrogen bond in $\mathbf{P}^-$ can be considered to be worth 8.6 kcal mol^{-1} in the gas phase.

To assess the energetics of 2˚ hydrogen bonds in condensed media, the pK_a of the pentaol was measured in DMSO relative to 1-acetylindolin-2-one (pK_a = 13.5).[16] Five independent determinations of the equilibrium constant gave pK_a (**P**) = 14.7 ± 0.1 which is a striking result since it indicates that the pentaol is more acidic than hydrofluoric acid (pK_a = 15.0).[30] In accord with the gas phase results based upon the ADE determinations, the pentaol is 1.4 pK_a units (1.9 kcal mol^{-1}) more acidic than $(HOCH_2CH_2)_3COH$ (pK_a = 16.1 ± 0.2). This indicates that 2˚ hydrogen bonds are also important and provide a significant amount of stabilization in DMSO. By comparing the pK_a's of **P** and **T3** (19.7 ± 0.2),[2] the 2˚ hydrogen bonds are each found to be worth 2.5 pK_a units (3.4 kcal mol^{-1}) or 40% of the gas phase value. The strength of the 1˚ hydrogen bonds are additive in DMSO [i.e., 1/2 pK_a ($(CH_3)_2CHOH$ – **T3**) = 1/3 pK_a ($(CH_3)_2CHOH$ – **T4**)] and they are worth 5.3 pK_a units (7.2 kcal mol^{-1}) per hydrogen bond.[31] The 1˚ interactions consequently are worth about twice as much as the 2˚ ones in these compounds. A total stabilization of 15.6 pK_a units (21.1 kcal mol^{-1}) results due to all four hydrogen bonds in $\mathbf{P}^-$, and this is big enough to account for the missing energy that originally led to the LBHB proposal even though no single hydrogen bond contributes more than 7.2 kcal mol^{-1}.

Dimethyl sulfoxide has a large dielectric constant (46.7), and while it stabilizes cations more effectively than anions, the hydrogen bond network in $\mathbf{P}^-$ undoubtedly is energetically more important in less polar media. In enzyme active sites the local dielectric constant

varies from system to system, but values ranging from 3 to 35 are commonly cited[32] and they are all smaller than for DMSO. Consequently, the pK_a's of **T3** and **P** were computed using the CPCM model in different solvents (Table 1). Both the B3LYP and M06-2X results are in excellent accord with the measured values in DMSO, and while the former predictions are 1.5–1.9 pK_a units larger than the latter ones in the other solvents, the differences between the two compounds are only 0.2-0.3 pK_a units. Both functionals

Table 1. Calculated pK_a values for triol **T3** and pentaol **P** in solvents with different dielectric constants.[a]

Solvent	ε	B3LYP/6-311+G(d,p)			M062X/maug-cc-pVT(+d)Z		
		T3	**P**	**Δ (T3–P)**	**T3**	**P**	**Δ (T3–P)**
DMSO	46.7	16.9	14.4	2.5	17.3[19.7][b]	14.5[14.7][b]	2.8
Acetone	21.0	18.5	15.9	2.6	16.9	14.0	2.9
CH_2Cl_2	9.1	17.6	14.5	3.1	16.0	12.7	3.3
THF	7.5	17.2	14.0	3.2	15.7	12.2	3.5
$CHCl_3$	4.8	16.0	12.3	3.7	14.5	10.5	4.0
Benzene	2.3	12.6	7.3	5.3	11.1	5.5	5.6

[a]All acidities were computed relative to methanol, which has an experimental pK_a of 29.0 (ref. 29) in DMSO. [b]Experimental values are given in brackets and come from ref. 2.

indicate that the acidities of **T3** and **P** increase with a decrease in the dielectric constant of the solvent as anticipated. This change is 6.2 pK_a units (8.4 kcal mol^{-1}) for the triol in going

from DMSO to benzene based upon the more reliable M06-2X values. Consequently, the 1˚ hydrogen bond strength increases from 5.3 (expt) to a predicted value of 8.4 pK_a units (i.e., from 7.2 to 11.3 kcal mol^{-1}). The acidity differences between **P** and **T3** indicate that the 2˚ hydrogen bonds also become stronger and go from 2.5 to 3.9 pK_a units (i.e., from 3.4 to 5.3 kcal mol^{-1}). As a result, all four hydrogen bonds in **P**$^-$ provide a total stabilization of 24.6 pK_a units (31.9 kcal mol^{-1}) in benzene as opposed to 15.6 pK_a units (21.1 kcal mol^{-1}) in DMSO.

Given the strength of the 2˚ hydrogen bonds in **P**$^-$, computations in DMSO were carried out on the all syn linear heptaol **H** to probe the effect of hydrogen bonds that are one "solvent shell" further removed from the formally charged center. The predicted pK_a for this model compound is 13.7 (B3LYP) and 13.4 (M06-2X), and the latter value is 1.1 pK_a units (1.5 kcal mol^{-1}) more acidic than **P**. In benzene the predicted pK_a is 5.1 (B3LYP) and 3.3 (M06-2X), and both values indicate that in this solvent **H** is 2.2 pK_a units (3.0 kcal mol^{-1}) more acidic than **P**. These results indicates that the 3˚ hydrogen bonds in **H** are worth ~25% of the 2˚ ones in **P**, but a larger number of hydrogen bonds can be formed in each successive solvent shell so 3˚ interactions may make important contributions to the catalytic ability of enzymes in some instances.

Conclusions

Experimental and computational data on simple model polyhydroxyl alcohols reveal that hydrogen bonds to a charged center (i.e., 1˚ interactions) and those that are one solvent shell further away (i.e., 2˚ hydrogen bonds) both make significant energy contributions to

the stability of their conjugate bases. The former interactions are stronger and provide 5.3 pK_a units of stabilization in DMSO, which increases to 8.4 pK_a units in benzene for the compounds studied herein. Secondary hydrogen bonds are weaker, but stabilizations of 2.5 (DMSO) and 3.9 (benzene) pK_a units per hydrogen bond were found for the linear pentaol **P**. Tertiary hydrogen bonds in the linear heptaol **H** are even weaker, yet they still contribute 0.6 (DMSO) and 1.1 (benzene) pK_a units per hydrogen bond. These polyol model compounds provide the requisite energy required for enzyme catalysis via a network of hydrogen bonds, none of which is unusually strong. The stabilization brought about by multiple hydrogen bonds consequently provides an alternative to the LBHB proposal. It also indicates that acid-base processes leading to formation or elimination of charged centers alters the strength of hydrogen bond networks and provides a driving force for conformational changes including those involved in protein folding.

Chapter 7: Molecular Recognition: Preparation and Characterization of Two Tripodal Anion Receptors

Introduction

Molecular recognition of negative ions has attracted considerable attention in recent years because of the biological significance of the field, the potential applications in sensors, and the development of phase transfer reagents.[1-4] For example, negative ion gradients across lipid bilayer membranes brought about by transport proteins and anion channels are critical physiological processes.[5] The breakdown of this function leads to a wide range of diseases such a cystic fibrosis, nephrolithiasis, osteopetrosis, Angelman syndrome, and Bartter's syndrome type III.[6-8] There are no cures for most of these afflictions even though the structures of many charge carriers and anion channels are well established. Synthetic receptors can serve as models for the behavior of natural anion channels and provide a platform for probing the fundamental interactions in these species.[9] Given that the selectivity of peptide hosts arises in large part due to the displacement of water by hydrogen bond donors,[5a] multiple hydrogen bonds donor groups such as carbazoles, ureas, amides, sulfonamides, and hydroxyls have been incorporated into the structural frameworks of supramolecular hosts.[10,11] Two strategies often employed to increase selectivity and the binding ability of the receptor are to make use of rigid frameworks and to enhance the acidities of the hydrogen bond donating groups. Aromatic rings, particularly benzenoid structures, are most commonly used for the former purpose.[12] Intramolecular hydrogen bonds recently were also exploited to

further freeze the receptor into a preorganized conformation. Gale et al. incorporated two *ortho*-phenols into an isophthalamide-based receptor (**A**) to lock in the *syn-syn* conformer of the amide groups (Figure 1).[13] This resulted in enhanced binding of I^- by an order of magnitude. Similarly, Flood et al. showed that intramolecular hydrogen bonds in an aryl-1,2,3-triazole pentad (**B**) arising from the incorporation of two aromatic hydroxyl groups provides a more rigid backbone that amplifies the binding to Cl^- by a factor of more than 47.[14] This strategy also has been employed with a variety of different foldamers such as aromatic oligo-amides, -ureas, and -hydrazides.[15-18]

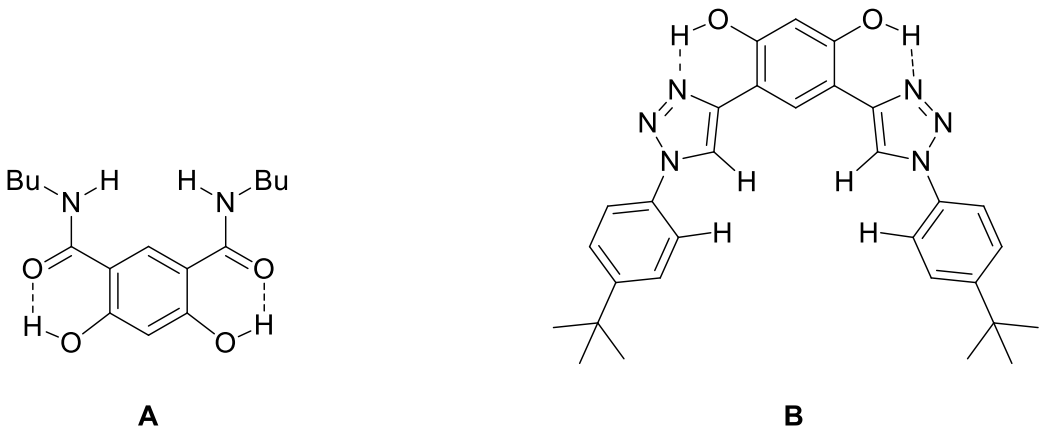

Figure 1. Hydrogen bond conformationally fixed receptors.

In general, the anion affinity of a host can be increased by enhancing its acidity,[19] but some exceptions such as ureas vs thioureas have been reported.[20] Electron withdrawing groups tend to further polarize O–H and N–H bonds leading to more favorable hydrogen bond interactions. For example, several orders of magnitude improvement were observed

when nitro groups were used to replace hydrogens on the aryl rings of *N*,*N*'-diaryl-(thio)ureas.[21] We recently reported that the incorporation of CF_3 substituents into a few polyols enhance their Cl^- association constants by a factor of 22 for each CF_3 group.[22] Hydrogen bond networks were also found to stabilize negatively charged centers, and the DMSO acidities of a series of polyols revealed that this stabilization can go beyond O^- ••• HO interactions (i.e., the primary hydrogen bonds).[23-25] This suggests that secondary hydrogen bonds (i.e., O^- ••• H*O* ••• *HO*) can be employed as a new strategy for enhancing anion binding since they were shown to increase acidity. Herein, two new hydroxyl-based anion receptors, **1** and **2** (Figure 2) are reported, their molecular complexes with Cl^-, $H_2PO_4^-$, and OAc^- and the $(M–1)^-$ anion of **1** (**1a)** were probed in the gas phase by photoelectron spectroscopy, binding constants with three of these anions and NO_3^- were measured in four different solvents, and the resulting experimental findings are supplemented with extensive computations. Taken together these results provide new perspectives in the field of supramolecular chemistry.

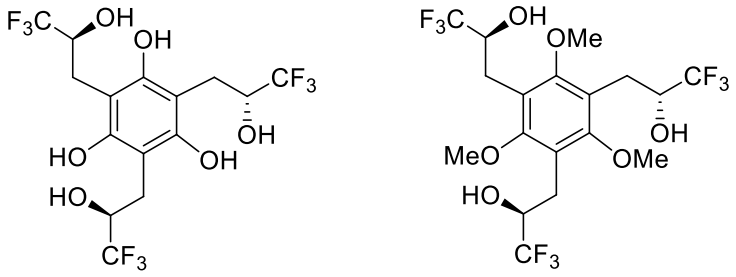

1 **2**

Figure 2. Trifluoromethyl-containing polyol receptors.

Experimental Section

General. All chemicals and solvents were purchased from Sigma-Aldrich and used as received except for the deuterated solvents (i.e., CD_3CN, CD_3COCD_3, CD_2Cl_2, and $CDCl_3$) which came from Cambridge Isotopes and were dried over activated 3 Å molecular sieves over the course of a few days. Nuclear magnetic resonance spectra were obtained with Varian VI-300 and VI-500 spectrometers, and all of the reported chemical shifts (δ) are referenced to the residual proton signals of the solvents. High resolution mass spectra were obtained with a Bruker BioTof II electrospray ionization–time-of-flight mass spectrometer using ethanolic PEG 300 and 425 solutions as internal standards. TLC analyses were carried out on precoated aluminum-backed 0.25 mm Masherey-Nagel silica gel plates. Medium pressure liquid chromatography (25−60 psi) was performed on silica gel using a Biotage Isolera 1. A Thomas Hoover capillary melting point apparatus was used to obtain the uncorrected melting point of **1**.

2,2',2''-(2,4,6-Trimethoxybenzene-1,3,5-triyl)triacetaldehyde (**3**). A 200 mL round-bottomed flask was equipped with a 2 cm magnetic stirring bar, argon inlet, and a rubber septum. The flask was charged with 3.0 g (10.5 mmol) of **4** and 100 mL of anhydrous CH_2Cl_2. A 1 M solution of DIBAL-H in hexanes (69.3 ml) was added dropwise over 30 min and the resulting reaction mixture was stirred for an additional 72 h at room temperature. The reaction mixture was quenched by addition of 25 ml of 1N H_2SO_4 and the resulting two layers were stirred for 3 h before being separated. The aqueous material was extracted three times with EtOAc using 50 ml portions and the combined organic layers were dried over $MgSO_4$, filtered, and concentrated under reduced pressure. The

resulting crude product was purified by flash column chromatography (1:2 hexanes/ethyl acetate) to give 1.2 g (40%) of **3** as a yellow oil. ^{1}H NMR (300 MHz, $CDCl_3$) δ 3.57 (9H, s), 3.67 (6H, s), 9.64 (3H, s). ^{13}C NMR (75 MHz, $CDCl_3$) δ 39.4, 60.8, 116.9, 157.9, 198.8. HRMS-ESI: calc for $C_{15}H_{18}NaO_6^+$ $(M + Na)^+$ 317.0996, found 317.0992.

3,3',3''-(2,4,6-Trimethoxybenzene-1,3,5-triyl)tris(1,1,1-trifluoropropan-2-ol) (**2**). A solution of 1.2 g (4.1 mmol) of **3** in 15 ml of monoglyme was cooled to 0 ˚C and 3.2 g (22.5 mmol) of CF_3TMS and 0.06 g (0.4 mmol) of CsF were sequentially added. The reaction flask was heated to 60 ˚C with stirring for 24 h and then the solvent was removed with a rotary evaporator. THF (15 ml) was added to the residue and then 30 ml of TBAF (1.0 M in THF) was slowly added. This solution was stirred for 3 h at room temperature before being concentrated under reduced pressure. The residue was extracted with three 50 ml portions of EtOAc and the combined organic material was dried by $MgSO_4$, filtered, and concentrated under vacuum. Flash column chromatography (2:1 hexanes/ethyl acetate) of the crude product on silica gel afforded 0.7 g (34%) of **2** as an ∼1:5 syn (RRR/SSS) and anti (RRS/SSR) mixture of diastereomers. *Anti*-**2**: ^{1}H NMR (300 MHz, $CDCl_3$) δ 3.04 (m, 6H), 3.31 (m, 3H), 3.82 (d, J = 0.8 Hz, 6H), 3.84 (d, J = 1.1 Hz, 3H), 4.21 (m, 3H). ^{13}C NMR (75 MHz, $CDCl_3$) δ 24.7, 24.8, 24.9, 61.2, 69.1 (q, *J* = 30.6 Hz), 69.2 (q, *J* = 30.6 Hz), 119.8, 119.9, 124.7 (q, *J* = 282.7 Hz), 157.7, 157.8. ^{19}F NMR (282 MHz, $CDCl_3$) -81.15 (d, J = 6.1 Hz), -81.12 (d, *J* = 8.5 Hz). HRMS-ESI: calc for $C_{18}H_{22}F_9O_6^+$ $(M + H)^+$ 505.1267, found 505.1257.

2,4,6-tris(3,3,3-Trifluoro-2-hydroxypropyl)benzene-1,3,5-triol (**1**). Boron tribromide (2.5 g, 10.0 mmol) was added dropwise to a solution of 0.50 g (1.0 mmol) of **2** in 50 ml of

CH_2Cl_2 at -78 ˚C. After 1 h of stirring the reaction mixture was warmed to room temperature and stirred for an additional 18 h, and then it was quenched by adding 50 ml of methanol. The volatile material was evaporated under reduced pressure and the residue was redissolved in 100 ml of methanol and reconcentrated. This process was repeated several times after which the residue was purified by flash column chromatography (2:1 hexanes/ethyl acetate) to afford 0.4 g (90%) of **1** as 1:5 mixture of syn and anti diastereomers. The anti diastereomer was subsequently separated from the syn isomer by flash column chromatography (2:1 hexanes/Et_2O) and was obtained as a white solid (m.p. 143-145 ˚C). ^{1}H NMR (300 MHz, CD_3CN) δ 2.61 (m, 3H), 3.05 (m, 3H), 3.96 (m, 3H), 5.30 (d, *J* = 3.8 Hz, 2H), 5.36 (d, *J* = 4.1 Hz, 1H), 7.47 (s, 1H), 7.49 (s, 1H), 7.50 (s, 1H). ^{13}C NMR (75 MHz, CD_3CN) δ 23.8, 23.8, 23.8, 70.4 (q, *J* = 29.6 Hz), 70.5 (q, *J* = 29.1 Hz), 104.5, 104.6, 124.9 (q, *J* = 283.0 Hz), 153.6, 153.7. ^{19}F NMR (282 MHz, CD_3CN) -81.1 (d, *J* = 7.7 Hz), -81.0 (d, *J* = 8.9 Hz). HRMS-ESI: calc for $C_{15}H_{15}F_9NaO_6^+$ $(M + Na)^+$ 485.0617, found 485.0640.

Titrations. One milliliter of dilute solutions (0.1–2.5 mM) of **1** or **2** in different solvents were placed in NMR tubes and capped with septa. More concentrated guest solutions (25–100 mM) containing the same dilute concentration of the initial host in all but three cases were subsequently added via syringe sequentially, and the course of the titration was followed by ^{1}H NMR spectroscopy. The signals of the aliphatic hydroxyl groups and methine hydrogens were monitored, and the data were fit with a 1:1 nonlinear binding isotherm using the Excel Solver add-on program to obtain the equilibrium association constants.

Photoelectron spectroscopy. Ions of interest were generated by electrospray ionization of ~10^{-3} M methanol–water solutions containing hexaol **1** or triol **2**, and except for the studies on the $(M–1)^-$ anion of the former compound (**1a**), a small amount of the ammonium salt of OAc^-, Cl^-, or $H_2PO_4^-$. A home-built photoelectron spectrometer that has been previously described was used in this work.[26] A F_2 excimer laser that emits 157 nm (7.867 eV) photons and which was operated at 20 Hz was employed and enabled shot-to-shot background subtraction of the data to be carried out. Photoelectrons were analyzed with a 5.2 m long flight tube and the resulting spectra obtained at 20 K had a resolution of ~2% or 50 meV at 5 eV.

Computations. Electronic structure calculations were carried out with the Gaussian 09 suite of programs.[27] To locate local and global minima, systematic conformational searches were carried out using Spartan 08 and the MMFF force field on hexaol **1** and triol **2**, both the conjugate bases and their anion-bound complexes.[28] Stable structures that were within 7 kcal mol^{-1} of the lowest energy structure were selected and B3LYP/6-311+G(d,p)[29] single point energies of these species were computed. Full optimizations were subsequently carried out on the most stable conformers and the lowest energy species were then minimized using the aug-cc-pVDZ basis set.[30] M06-2X/maug-cc-pVT(+d)Z[31,32] single point energies were also computed on these final geometries. To obtain the adiabatic and vertical detachment energies (ADEs and VDEs), the corresponding radicals were also optimized starting with the lowest energy anion structures. The ADEs are reported as enthalpies at 0 K, whereas all of the other energies were corrected to 298 K.

Results

Hydroxyl-based receptors **1** and **2** were synthesized as outlined in Scheme 1. Reduction of the previously reported tribenzylic nitrile **4**[33] with diisobutylaluminum hydride (DIBAL-H) afforded the trisaldehyde **3** in modest yield. Nucleophilic addition of three equivalents of

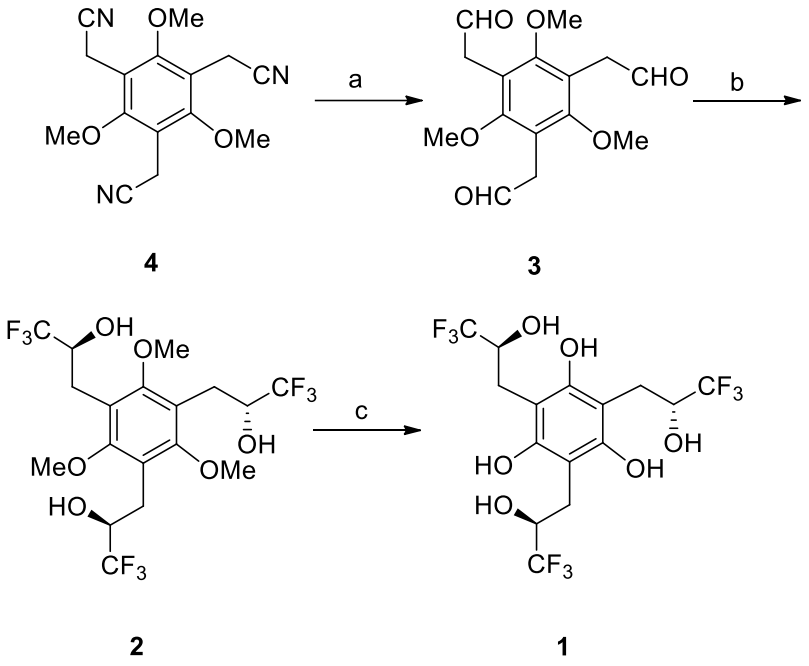

[a]DIBAL-H, CH_2Cl_2, 3 days; H_2SO_4, 3h, 40%. [b]CF_3TMS, CsF, monoglyme, 18h; TBAF, THF, 3h, 34%. [c] BBr_3, CH_2Cl_2, 90%.

Scheme 1. Synthesis of anion hosts **1** and **2**.

(trifluoromethyl)trimethylsilane in the presence of fluoride anion was subsequently carried out to give the desired triol **2** in a 34% yield. Cleavage of all three ethers with boron tribromide resulted in the formation of the desired hexaol receptor **1** in a very efficient (i.e., 90% yield) transformation.

Electrospray ionization of an aqueous methanolic solution of **1** afforded its conjugate base while spraying **1** and **2** in the presence of ammonium salts (i.e., NH_4X, X = Cl^-, OAc^-, and $H_2PO_4^-$) generated their corresponding 1:1 adduct ions. Photoelectron spectra of all seven of these species were recorded at 20 K with a F_2 excimer laser at 157 nm (7.867 eV, Figures 3 and 4). Each spectrum shows two or more broad features resulting from detachment of an electron to afford ground and excited states of the corresponding radical. The adiabatic electron detachment energies (ADEs) were obtained from the rapidly rising onset energies of the lowest energy features whereas the vertical detachment energies (VDEs) were obtained from the maxima of these bands. All of the results are summarized in Table 1.

Table 1. Experimental and computed adiabatic and vertical detachment energies in eV for (**1** – H^+) (**1a**) and 1:1 anion complexes of **1** and **2**.

anion	exptl		calc[a]		
	ADE	VDE	ADE		VDE
			B3LYP	M06-2X	B3LYP
1a	4.00 ± 0.10		3.72	3.91	4.03
1 • Cl^-	5.00 ± 0.10		4.58	5.02	4.76
1 • OAc^-	4.95 ± 0.10		4.68	4.87	5.11
1 • $H_2PO_4^-$	4.95 ± 0.10		4.73	4.92	5.18
2 • Cl^-	5.38 ± 0.10		4.83	5.11	5.36
2 • OAc^-	5.32 ± 0.10		4.76	5.01	5.28
2 • $H_2PO_4^-$	5.40 ± 0.10		4.78	4.97	5.48

[a]Computed values correspond to B3LYP/aug-cc-pVDZ and M06-2X/maug-cc-pVT(+d)Z energies at 0 K. Thermal corrections to 20 K are negligible (< 0.01 eV) and were omitted.

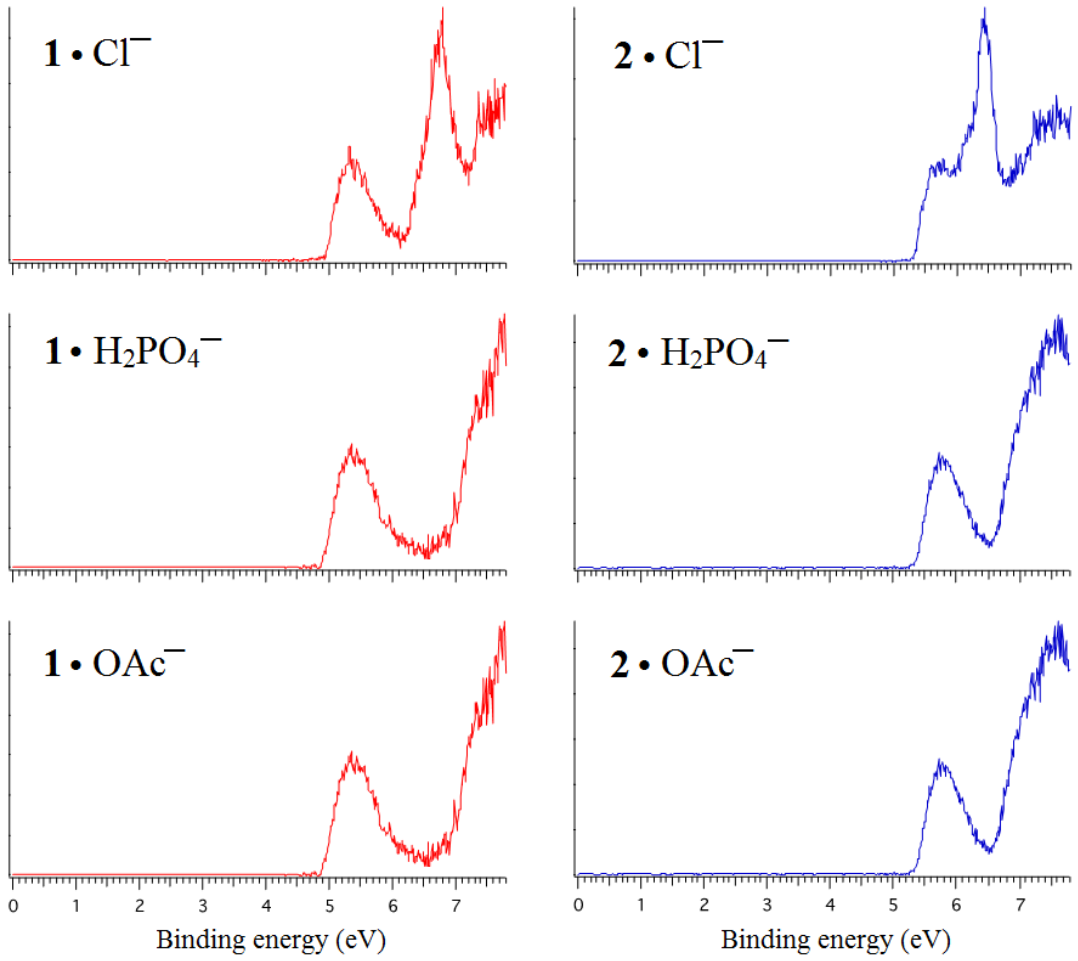

Figure 3. Low temperature (20 K) photoelectron spectra of hexaol **1** and triol **2** complexes with Cl^-, $H_2PO_4^-$, and OAc^- at 157 nm (7.867 eV).

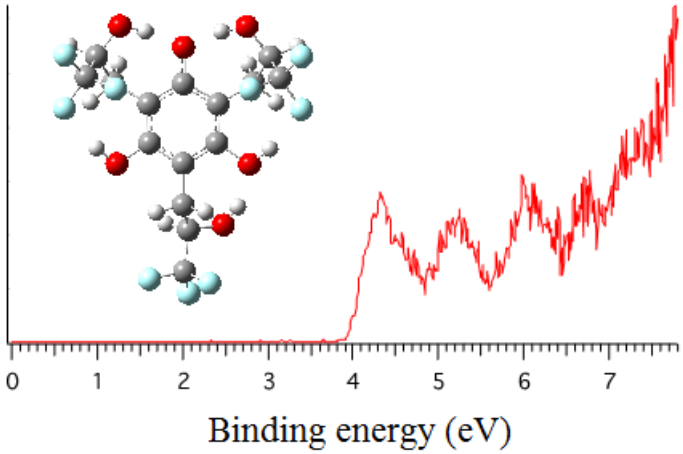

Figure 4. Low temperature (20 K) photoelectron spectrum of deprotonated hexaol **1a** at 157 nm (7.867 eV).

B3LYP geometry optimizations were carried out with the aug-cc-pVDZ basis set on all of the cluster ions, the conjugate base of **1** (**1a**), and their corresponding radicals. The structures of the chloride adducts are illustrated in Figure 5 and complete details for all of the structures (i.e., geometries and energies) are given in the supporting information. M06-2X single point energies with the maug-cc- pVT(+d)Z basis set were also computed and the resulting ADEs are provided in Table 1. As previously reported, B3LYP does reasonably well in reproducing the experimental values but the M06-2X functional is far superior. In this case, the errors span from 0.22 – 0.62 eV (B3LYP) and 0.02 – 0.43 eV (M06-2X) with average errors of 0.42 (B3LYP) and 0.18 (M06-2X) eV.

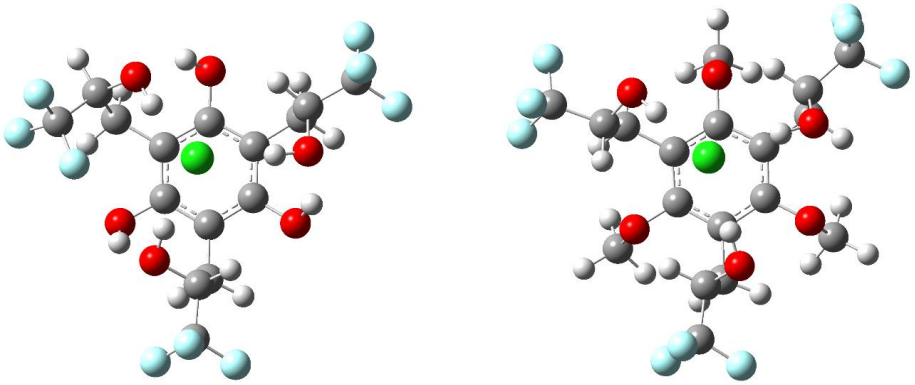

1 • Cl^- **2** • Cl^-

Figure 5. Computed B3LYP/aug-cc-pVDZ structures for **1** • Cl^- and **2** • Cl^-. The OH ••• Cl^- distances are 2.132, 2.191, and 2.245 Å in **1** • Cl^- and 2.133, 2.157, and 2.167 Å in **2** • Cl^-.

Binding affinities of **1** and **2** with Cl^-, $H_2PO_4^-$, NO_3^- and OAc^- were investigated in four different solvents (CD_3CN, acetone-d_6, CD_2Cl_2, and $CDCl_3$) by ^1H NMR spectroscopy, and the results are summarized in Table 2. Host concentrations were kept low over a range from 0.1 – 2.5 mM where there was no evidence for self aggregation while 25 – 100 mM guest solutions were used in carrying out the titrations. Anion-induced downfield shifts of the ^1H NMR signals of the aliphatic hydroxyl and methine groups were followed to obtain the binding isotherms and non-linear fits of the data provided the 1:1 association constants. Hexaol **1** was not soluble enough in $CDCl_3$ to measure its binding constants, it did not associate with $H_2PO_4^-$ and OAc^- in CD_3CN, and its titration profiles could not be fit in CD_2Cl_2. In contrast, the association constants of triol **2** with Cl^- and OAc^- were too large to measure by H NMR spectroscopy (> 10^5 M^{-1}) in acetone-d_6.

Table 2. Association constants for 1:1 complexes of **1** and **2** with tetrabutylammonium salts ($Bu_4N^+X^-$, $X^- = Cl^-$, $H_2PO_4^-$, NO_3^-, and OAc^-) in four different solvents at 22 ˚C.

anion	K_a (M^{-1})			
	$CDCl_3$	CD_2Cl_2	CD_3COCD_3	CD_3CN[a]
Cl^-	8,300	18,000	$> 10^5$	8,200 [667]
$H_2PO_4^-$	4,200	16,000	–[b]	4,200
NO_3^-	4,300	9,200	1,100	420 [164]
OAc^-	5,000	41,000	$> 10^5$	5,000

[a]Values in brackets are for **1**, the other results are for **2**. [b]Data could not be fit to a 1:1 binding isotherm.

Chloride affinities of **1** and **2** were also determined at three temperatures (i.e., -24.2, 22.0, and 51.3 or 59.1 ˚C) spanning up to an 83 ˚C temperature range in order to obtain the thermodynamic binding parameters (ΔG, ΔH, $T\Delta S$, and ΔC_p), which are given in Table 3.

Table 3. Titrations results of **1** and **2** with TBACl in CD_3CN at different temperatures.[a]

cmpd	T (˚C)	K (M^{-1})	ΔH	$T\Delta S$	ΔC_p	ΔG
1	-24.2	4,900				
	22.0	667	10.8	14.8	0.6	-4.0
	59.1	30,000				
2	-24.2	99,000				
	22.0	8,200	-2.1	3.0	0.2	-5.1
	51.3	6,000				

[a]Enthalpies, $T\Delta S$, and ΔG are in kcal mol^- whereas ΔC_p is in kcal mol^{-1} K^{-1}.

Discussion

To design molecular receptors, hydrogen bond donors are arranged in different orientations which are controlled by the covalent architecture of the host. Macrocycles and polyfused rings such as calixarenes, steroids, and *cis,cis*-1,3,5-substituted cyclohexanes are commonly employed subunits in molecular recognition studies.[34-36] Additional preorganization brought about by intramolecular hydrogen bonds has been employed to provide conformational control. It is also well know that increasing the acidity of a hydrogen bond donor in a receptor typically leads to enhanced binding of anions. As a result, computations were carried out on hexaol **1** and triol **2** since it was expected that they would benefit from several key features including a rigid central benzene moiety, three electron withdrawing trifluoromethyl groups to enhance the acidity of the aliphatic alcohols, and three phenolic substituents in the former compound to provide additional hydrogen bond stabilization of its anion–bound complexes. The B3LYP/aug-cc-pVDZ structures of the chloride clusters with the anti diastereomers of **1** and **2** (i.e., the RRS/SSR isomers) form three hydrogen bonds between the secondary hydroxyl groups and the chloride anion (Figure 5). As a result, the B3LYP/aug-cc-pVDZ and M06-2X/maug-cc-pVT(+d)Z clustering enthalpies (i.e., ΔH for Cl^- + **1** or **2** $\rightarrow$ **1** • Cl^- or **2** • Cl^-) are remarkably favorable. That is, ΔH = -41.2 (B3LYP) and –47.9 (M06-2X) kcal mol^{-1} (**2**) and -41.3 (B3LYP) and –51.2 (M06-2X) kcal mol^{-1} (**1**) whereas the binding of methanol to chloride anion is exothermic by –17.5 ± 0.3 kcal mol^{-1}.[37] The association of three molecules of methanol to Cl^-, however, has been determined to be –43.1 ± 0.5[37] which is similar to the computed values for **2**. The M06-2X binding affinity

for the hexaol is larger than for the triol and can be attributed to the presence of the three intramolecular hydrogen bonds between the aryl OH donors and the oxygen acceptors of the aliphatic hydroxyl groups in the chloride anion complex of **1**.

The experimentally determined ADEs for **1** and **2** clustered to Cl^-, OAc^- and $H_2PO_4^-$ (i.e., **1** • X^- and **2** • X^-) are well reproduced computationally, but the values for the triol are larger than those for the hexaol. This unexpected result is due to the fact that ADE(**2** • X^-) – ADE(**1** • X^-) corresponds to the difference in the clustering energies of **1** and **2** with X^- and $X^\bullet$. For example, Cl^- binds more favorably to the hexaol than the triol by 0.1 (B3LYP) and 3.3 kcal mol^{-1} (M06-2X) and this leads to a larger ADE for the former complex. This difference is offset and overcome by the greater preference for the association of **1** to $Cl^\bullet$ by 5.8 (B3LYP) and 5.4 kcal mol^{-1} (M06-2X). In retrospect maybe this is not surprising because the abstraction of a hydrogen atom from one of the secondary hydroxyl groups leads to an alkoxy radical that appears to rearrange to a stabilized phenoxyl radical with little or no barrier.[38]

In making clusters of **1**, but not **2**, its conjugate base (**1a**) was observed. The photoelectron spectrum of the $(M–1)^-$ ion consequently was recorded at 20 K (Figure 4). Computations indicate that the most acidic site in the hexaol is one of the phenolic hydroxyl groups and the resulting anion is stabilized by a total of five hydrogen bonds - two to the charged site, two O–H•••F interactions, and one O–H•••OH hydrogen bond. The ADE of **1a** is 4.00 ± 0.10 eV which is well reproduced by both the B3LYP (3.72 eV) and M06-2X (3.91 eV) predictions. It is also 1.75 eV (40.3 kcal mol^{-1}) larger than for phenoxide anion as a result of the hydrogen bond network in this ion.[39]

Hexaol **1** adopts a conformation(s) in acetonitrile where intramolecular hydrogen bonds are formed, and the secondary hydroxyl groups act as hydrogen bond donors and the phenolic oxygen atoms serve as hydrogen bond acceptors. This structural assignment is based on the downfield ^{1}H NMR chemical shifts of the aliphatic OH resonances at 5.47 ppm compared to those in the triol at 4.11 ppm. This preorganization might be expected to enhance the anion-binding of **1** by reducing the entropic penalty for association. Small equilibrium constants for 1:1 binding with Cl^- and NO_3^- were determined in CD_3CN contrary to expectation, but the entropy is quite favorable as anticipated and this can be viewed as a manifestation of the hydrophobic effect.[40,41] That is, binding results in the release of solvent molecules despite the unfavorable enthalpy for this process. In contrast, triol **2** was found to bind to all four anions (i.e., Cl^-, $H_2PO_4^-$, NO_3^- and OAc^-) and while it displays relatively little selectivity presumably because of the flexibility of its scaffold, to the best of our knowledge it is the strongest known hydoxyl-based receptor to date. This is due at least in the case of Cl^- to the favorable binding enthalpy and entropy. One can rationalize the thermochemical differences between **1** and **2** based upon their dipole moments and reorganization energies upon binding. That is, **1** and **2** have computed dipole moments of 1.58 and 3.80 D, respectively, so one would expect the solvent to organize more strongly around the triol. This should lead to a more favorable entropy of binding for **1**, which is what is observed (i.e., $T\Delta S$ = 14.8 (**1**) vs 3.0 kcal mol^{-1} (**2**)). The reorganization energies are analogous to vertical detachment energies (VDEs) in that they correspond to the difference between the energy for the adopted structure of the host in its bound complex and its free form. These energies were computed for the hexaol and

the triol and are 6.4 (B3LYP) and 4.9 kcal mol^{-1} (M06-2X) larger for the former compound. This is consistent with the binding enthalpies obtained from the Van't Hoff plots as the hexaol pays a larger energetic price than the triol to adopt its anion-bound conformation and ΔH is less favorable for **1**.

Solvents are well known to play a critical role in molecular recognition. Neutral receptors bind neutral guests much more effectively in lower dielectric constant media.[42] One might assume that the same situation would apply when a host binds an ion, but this need not be the case as charged species are always accompanied by a counterion in condensed media. A free ion would bind more tightly to a receptor in a non-polar solvent, but when a counterion is present the oppositely charged species will interact more strongly in this medium. To address this issue, 1:1 host-guest equilibrium constants were measured in four different solvents (i.e., $CDCl_3$, CD_2Cl_2, CD_3COCD_3 and CD_3CN) between **2** and Cl^-, $H_2PO_4^-$, NO_3^- and OAc^- (Table 2). The results in chloroform (ε = 4.7)[43] and acetonitrile (ε = 35.7)[43] are essentially the same except for nitrate, which binds ~10 times more strongly in the less polar solvent. In contrast, $CDCl_3$ and CD_2Cl_2 (ε = 8.9) are similar solvents but the equilibrium binding constants vary by factors of ~2 – 8. They are larger in the solvent with the bigger dielectric constant and this maybe due to greater ion separation of the tetrabutylammonium salts in dichloromethane. The most dramatic change in the complexation of **2** was observed in acetone-d_6. Equilibrium constants that are too big to measure by ^1H NMR spectroscopy were obtained with Cl^- and OAc^-. Acetone does have a larger solvent donor number than acetonitrile, chloroform, and dichloromethane (these values are 17, 14.1, 4.0, and 1.0 kcal mol^{-1},

respectively and correspond to the ability to solvate a cation),[44] but more work is needed to elucidate the key factors influencing host-guest binding of ions in different solvents and environments.

Conclusions

Two new hydroxyl-based hosts (**1** and **2**) were synthesized and their 1:1 anion-complexes along with the $(M–1)^-$ ion of **1** were characterized in the gas phase by negative ion photoelectron spectroscopy. The adiabatic detachment energies (ADEs) for all seven species are unusually large due to the stabilization resulting from the intramolecular hydrogen bond networks. Hexaol **1** • X^- (X = Cl, OAc, and H_2PO_4) appears to have the larger anion binding energies in the gas phase, but triol **2** has the bigger ADEs. This is because $X^{\bullet}$ interacts more strongly with **1** than **2** since the former species can lead to a more stable phenxoyl radical. Binding constants were also measured in four solvents. The preorganization in **1** arising from the intramolecular hydrogen bond network, which is absent in **2**, led to a poorer anion receptor. The binding entropy for hexaol **1** is more favorable than for triol **2**, at least in CD_3CN where the van't Hoff analysis was carried out, but the enthalpy difference dominates and it is less favorable for the hexaol. Given the flexibility of the cavity in **1** and **2**, these hosts are able to bind a variety of anions and the latter species is the strongest hydroxyl-based receptor reported to date.

Chapter 8: Solvent Effects on the Molecular Recognition of Anions

Anions play a critical role in living cells and their impact is often mediated by proteins in the form of molecular receptors.[1,2] The bound complexes initiate many biochemical processes such as enzymatic transformations, signal transductions and molecular transportation, and their stabilities are strongly affected by the properties of the recognition sites.[3-10] Anion selectivity is achieved via multiple hydrogen bond interactions and considerable effort has been spent mimicking natural receptors and designing synthetic analogs.[11-13] Little attention has been paid, however, to the solvent and environmental properties such as dielectric constants, dipole moments, lipophilicities and ET values (the normalized Dimroth–Reichardt parameter), even though they play a fundamental role in binding processes.[14-16] In this manuscript we report initial investigations of the formation of 1:1 host–anion complexes with two hydroxyl–based receptors (Figure 1) and 5 different anions with two different counterions in a range of solvents and solvent mixtures at different temperatures. These results reveal novel behavior for anion complexation in solvent mixtures and the effect of solvent media on binding selectivity.

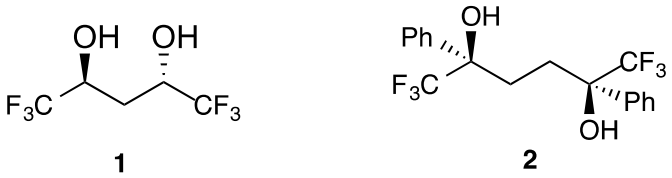

Figure 1. Hydroxyl–based anion receptors.

Anion association equilibrium constants of 1,3-diol **1**[17] were measured with tetrabutylammonium salts ($Bu_4N^+X^-$, X^- = Cl^-, $H_2PO_4^-$, NO_3^-, HSO_4^-, and OAc^-) in CD_3CN and $CDCl_3$ as representative examples of a polar and non–polar solvent, respectively. Sequential addition of the salts to the receptor led to significant downfield shifts of the hydroxyl group protons ($\Delta\delta$) and these were used to calculate the binding constants. Non–linear curves of $\Delta\delta$ versus the anion concentrations were cleanly fit to 1:1 binding isotherms to obtain the association constants (Table 1). To examine the role of a similar host with a different cavity size, 1,4-diol **2** was synthesized and its binding data are also displayed in Table 1. The 1,3-diol binds Cl^- and NO_3^- more strongly than the 1,4-diol whereas the order is reversed for $H_2PO_4^-$ and OAc^-, and there is little difference with HSO_4^-. In all cases the preference is less than an order of magnitude except for NO_3^- in chloroform, where the association constant is 23 times larger for **1** than **2**.

Table 1. Binding constants of **1** and **2** with $Bu_4N^+X^-$ salts in a polar and non-polar solvent at room temperature.[a]

X^-	K(**1**) (M^{-1})		K(**2**) (M^{-1})	
	CD_3CN	$CDCl_3$	CD_3CN	$CDCl_3$
Cl^-	3,300	4,000	1,000	1,900
NO_3^-	53	7,000	30	310
HSO_4^-	–	280	–	270
$H_2PO_4^-$	130	460	540	700
OAc^-	12,000	2,700	14,000	15,000

[a]T = 295.5 K and uncertainties in the measurements are estimated to be less than 25%.

Solvents play an important role in supramolecular chemistry, and it is well known that binding constants between noncharged species interacting via hydrogen bonds are typically orders of magnitude larger in nonpolar media than in polar ones.[18] The same trend has been reported for anions,[18] and is observed for **1** and **2** with Cl^-, HSO_4^-, and $H_2PO_4^-$ but the differences are remarkably small (i.e., $K_{CDCl_3}/K_{CD_3CN} < 4$). Two exceptions are for NO_3^-, where the ratio is much larger (i.e., 132 for **1** and 10.3 for **2**), and for OAc^-, where the equilibrium constant is 4 times bigger in the more polar solvent. These data show that there is no simple correlation between the stabilities of the complexes and bulk solvent properties such as the dielectric constant (ε), dipole moment (μ) and ET; note, ε, μ (in D), and ET (in kcal mol^{-1}) are 37.5, 3.92, and 0.46 (CH_3CN) and 4.8, 1.04, and 0.26 ($CHCl_3$), respectively.[19,20] Presumably, the binding constants are bigger in chloroform than acetonitrile because hydrogen bonds are stronger in non–polar organic solvents whereas polar solvents enhance the attraction between nonpolar groups.[21-23] The interactions of oppositely charged ions in salts, however, are undoubtedly larger in $CDCl_3$ and mitigates anion binding in this solvent.

To assess the impact of the tetrabutylammonium cation (Bu_4N^+), a different counterion for Cl^- was used in both solvents with the 1,3-diol (**1**). The bis(triphenylphosphine)iminium ion ($(Ph_3P)_2N^+$) was selected because it has been reported that the dissociation constant for $(Ph_3P)_2NCl$ is 21 times larger than for Bu_4NCl in dichloromethane.[24] A similar situation is expected in chloroform, whereas both salts are likely to be fully dissociated in acetonitrile but not necessarily free ions. One might therefore expect that K_{CDCl_3}/K_{CD_3CN} would be much larger when $(Ph_3P)_2N^+$ is used as the

counterion, since the associated chloride ion is freer in the non–polar solvent. The equilibrium constant ratio, however, is only 7 times larger than for Bu_4N^+ at room temperature (Table 2). This difference is not due primarily to enhanced complexation in $CDCl_3$, but rather to an unexpected drop in the association constant in CD_3CN.[20] These results were probed further by measuring the binding constants at lower and higher temperatures so that three point van't Hoff plots could be obtained to provide estimates of the enthalpies, entropies, and heat capacities. In CD_3CN the equilibrium constants are largest at low temperature (245 K) regardless of the counterion as is the case in $CDCl_3$ with $(Ph_3P)_2N^+$ but not for Bu_4N^+. The binding enthalpies and entropies have negative values in both solvents irrespective of counterion, and thus these association processes are enthalpically favorable but entropically unfavorable. As a result of the hydrophobic effect, ΔG has a downward curvature as a function of temperature and a positive value for the heat capacity in $CDCl_3$.[25-28] This behavior is reversed in CD_3CN when the tetrabutylammonium salt is used (i.e., ΔG has an upward curvature and C_p has a negative value) but not when bis(triphenylphosphine)iminium chloride is employed. These results indicate that the solvation of the reactants, which are more polar than the product, is more ordered than the host–guest complex in acetonitrile with Bu_4NCl whereas the opposite is the case with $(Ph_3P)_2NCl$ and in chloroform. This hydrophobic effect is in keeping with the relative polarity of the two solvents and is accord with the less polar nature of $(Ph_3P)_2N^+$ compared to Bu_4N^+. It also accounts for the unexpected drop in the binding constant when $(Ph_3P)_2NCl$ was used in acetonitrile.

Table 2. Binding constants and thermodynamic parameters for the association of **1** with MCl (where M = Bu_4N or $(Ph_3P)_2N$) in $CDCl_3$, CD_3CN, and a 1:1 mixture of these solvents.[a]

M^+	T (K)	K (M^{-1})		
		CD_3CN	$CDCl_3$	1:1
Bu_4N^+	295.5	3,300	4,000	190
	245.0 (253.7)	14,000	3,300	330
	333.2 (337.1)	870	10,000	310
	ΔH	-5.1	-9.1	-2.3
	ΔS	-2.7	-12.8	2.8
	ΔC_p	-72.9	342	119
$(Ph_3P)_2N^+$	295.5	650	5,600	150
	245.0 (253.7)	3,900	$> 10^5$	280
	333.2 (337.1)	920	15,000	300
	ΔH	-5.3	–	-2.6
	ΔS	-4.3	–	1.6
	ΔC_p	187	–	150

[a]Temperatures in parentheses are for the $CDCl_3$ measurements.

Solvent mixtures are often used in chemical reactions to manipulate the properties of the solvent and differentially solvate the various solutes in a synergistic manner.[29] This strategy has not been employed for studying anion receptors even though it provides a systematic way of varying physical properties of the solvent. For example, the dielectric constant, polarity, and donor and acceptor numbers of binary solvent mixtures are expected to be intermediate to those of the two pure liquids, but generally are not linearly

dependent on the composition of the mixture. To systematically probe the impact of going from a non–polar solvent to a polar medium, the binding of **1** with Bu_4NCl was explored in three acetonitrile–solvent mixtures (i.e., CD_3CN–S, where S = $CDCl_3$, CD_2Cl_2, and $C_6D_5CD_3$) and in one instance $(Ph_3P)_2NCl$ was also employed (Table 3).

Table 3. Binding constants of **1** with Cl^- in different solvent mixtures at room temperature.

	K (M^{-1})			
CD_3CN (%)	$CDCl_3$	CD_2Cl_2 (Bu_4N^+)	$C_6D_5CD_3$	$CDCl_3$ ($(Ph_3P)_2N^+$)
0	4,000	25,000	-	5,600
10	870	22,000	-	1,300
25	270	5,900	68,000	1,200
50	190	1,900	21,000	150
75	160	1,200	7,200	200
90	460	1,400	970	290
100	3,300	3,300	3,300	650

We expected to observe a monotonic increase in going from the pure solvent with the smaller equilibrium constant (CD_3CN) to the liquid with the larger value, but surprisingly a minimum value was found in all four instances. It ranged from being ~3 to 21 times smaller than the binding constant in acetonitrile and its relative position varied depending upon the differences between the pure solvents. That is, when the two *K* values are similar the minimum is near the center (i.e., the equal composition point), whereas when

there is a large difference the minimum is closer to the composition of the lower binding medium (Figure 2).

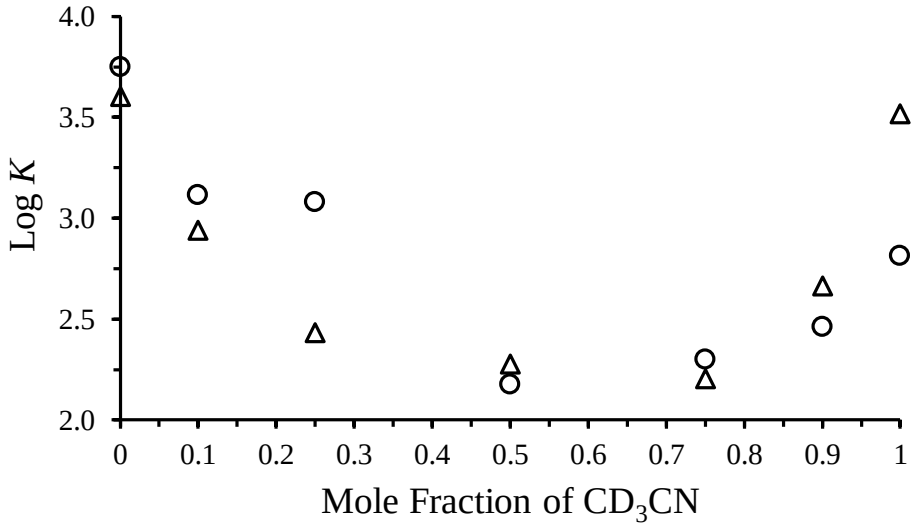

Figure 2. A logarithmic plot of the binding constants of **1** with Bu_4NCl (triangles) and $(Ph_3P)_2NCl$ (circles) versus the mole fraction of CD_3CN–$CDCl_3$ mixtures.

To explain this behavior we suggest that two counterbalancing effects are involved, the hydrogen bond strength in the host–guest complex and the solvation energies of the anion and the cation (i.e., the salt).[30] The former term is dominant in chloroform whereas the latter one is expected to be more important in acetonitrile for the tetrabutylammonium salts. In mixtures of the two solvents *K* is reduced, but its value varies with the mole fraction of CD_3CN as the relative contributions of the hydrogen bonds and the hydrophobic effect change. This is why binding constants can decrease dramatically upon

the addition of small amounts of water (e.g., 0.5%), and the solvation of F^- drops sharply in aqueous solvent mixtures when the water concentration becomes sufficiently low.[18] The thermodynamic parameters for the binding of **1** with Bu_4NCl and $(Ph_3P)_2NCl$ were also measured in a 1:1 CD_3CN–$CDCl_3$ solvent mixture. All three of them (ΔH, ΔS, and C_p) were found to be insensitive to the counterion and both the enthalpy and entropy of binding are favorable. The heat capacity is unfavorable (i.e., it has a positive value), but, interestingly, is approximately the average of the numbers obtained in the pure solvents. These new observations may play a critical role in understanding ion transporters, enzyme–receptor interactions, and the supramolecular chemistry of anion–binding events. To gain further insights into the effects of binary mixtures on molecular recognition processes, dynamics computations will be of value.

Bibliography

References for chapter 1

1. Jeffrey, G. A.; Saenger W. *Hydrogen Bonding in Biological Structures*, Springer-Verlag: Berlin, 1991.

2. Jeffrey, G. A. *An Introduction to Hydrogen Bonding*, Oxford University Press: New York, 1997.

3. Desiraju, G. R.; Steiner, T. *The Weak Hydrogen Bond in Structural Chemistry and Biology*, Oxford University Press: Oxford, 1999.

4. Scheiner, S. *Hydrogen Bonding: A Theoretical Perspective*, Oxford University Press: Oxford, 1997.

5. Pauling, L. *The Nature of the Chemical Bond*, Cornell University Press: Ithaca, New York, 1960.

6. Buckingham, A. D.; Legon, A. C.; Roberts, S. M. *Principles of Molecular Recognition*, Blackie Academic & Professional: London, 1993.

7. Pople, J. A.; Schneider, W. G.; Bernstein, H. J. *High Resolution Nuclear Magnetic Resonance*, McGraw-Hill: New York, 1959.

8. Kollman, P. A. Hydrogen bonding and donor-acceptor interactions in: *Applications of Electronic Structure Theory*, edited by Schaefer, H. F. III, Plenum, New York, 1977, pp. 109–152.

9. Pines, A.; Ruben, D. J.*;* Vega, S.*;* Mehring M. *Phys. Rec. Lett.* **1976**, *36*, 110-113.

10. Hinton, J. F.; Guthrie, P.; Pulay, P.; Wolinski, K. *J. Am. Chem. Soc.* **1992**, *114*, 1604-1605.

11. Chesnut, D. B. *J. Phys. Chem. A* **2002**, *106*, 6876-6879.

12. Ramanadham, M.; Chidambaram, R. in: *Advances in Crystallography*, edited by. R Srinivasan, Oxford University Press & IBH: New Delhi, 1978, pp. 81-103.

13. Schuster, P.; Zundel. G.; Sandorfy, C. *The Hydrogen Bond: Recent Developments in Theory and Experiments*. North-Holland: Amsterdam, 1976.

14. Perrin, C. L.; Nielson, J. B. *Annu. Rev. Phys. Chem.* **1997**, *48*, 511-544.

15. Fersht, A. R.; Shi, J. P.; Knill-Jones, J.; Lowe, D. M.; Wilkinson, A. J., et al. *Nature* **1985**, *314*, 235-238.

16. Serrano, L.; Kellis, J. T. J.; Cann, P.; Matouschek, A.; Fersht, A. R. *J. Mol. Biol.* **1992**, *224*, 783-804.

17. Thorson, J. S.; Chapman, E.; Schultz, P. G. *J. Am. Chem. Soc.* **1995**, *117*, 9361-9362.

18. Sampson, N. S.; Knowles, J. R. *Biochemistry* **1992**, *31*, 8488-8494.

19. Gerlt, J. A.; Gassman, P. G. *Biochemistry* **1993**, *32*, 11934-11952.

20. Gerlt, J. A.; Gassman, P. G. *J. Am. Chem. Soc.* **1993**, *115*, 11552-11568.

21. Cleland, W. W.; Kreevoy, M. M. *Science* **1994**, *264*, 1887-1890.

22. Frey, P. A.; Whitt, S.; Tobin, J. *Science* **1994**, *264*, 1927-1930.

23. Cleland, W. W.; Frey, P. A.; Gerlt, J. A. *J. Biol. Chem.* **1998**, *273*, 25529-25532.

24. Cho H. S.; Ha, N. C.; Choi, G.; Kim, H. J.; Lee, D.; Oh, K. S.; Kim, K. S.; Lee, W; Choi, K. Y.; Oh, B. H. *J. Biol. Chem.* **1999**, *274*, 32863-32868.

25. Zhao, Q.; Abeygunawardana, C.; Talalay, P.; Mildvan, A. S. *Proc. Nat. Acad. Sci. U.S.A.* **1996**, *93*, 8220-8224.

26. Warshel, A.; Papazyan, A.; Kollman, P. A. *Science* **1995**, *269*,102-103.

27. Warshel, A.; Russell, S. *J. Am. Chem. Soc.* **1986**, *108*, 6569-6579.

28. Warshel, A.; Naray-Szabo, G.; Sussman, F.; Hwang, J. K. *Biochemistry* **1989**, *28*, 3629-3637.

29. Kreevoy, M. M.; Liang, T. M.; *J. Am. Chem. Soc.* **1980**, *102*, 3315-3322.

30. Magonski, J.; Pawlak, Z.; Jasinski, T. *J. Chem. Soc. Faraday Trans* **1993**, *89*, 119-122.

31. Gunnarsson, G.; Wennerstrom, H.; Egan, W.; Forsen, S. *Chem. Phys. Lett.* **1976**, *38*, 96-99.

32. Kresge, A. J.; Chiang, Y. *J. Phys. Chem.* **1973**, *77*, 822-825.

33. a) Shan, S. O.; Herschlag, D. *Proc. Natl. Acad. Sci. U.S.A.* **1996**, *93*, 14474-14479. b) Shan, S. O.; Herschlag, D. *J. Am. Chem. Soc.* **1996**, *118*, 5515-5518.

34. Scheiner, S.; Kar, T. *J. Am. Chem. Soc.* **1995**, *117*, 6970-6975.

35. (a) Guthrie, J. P.; *Chem. Biol.* **1996**, *3*, 163-170. (b) Scheiner, S.; Kar, T. *J. Am. Chem. Soc.* **1995**, *117*, 6970-6975. (c) Alagona, G.; Ghio, C.; Kollman, P. *J. Am. Chem. Soc.* **1995**, *117*, 9855-9862. (d) Usher, K.; Remington, S. J.; Martin, D. P.; Drueckhammer, D. G. *Biochemistry* **1994**, *33*, 7753-7759. (e) Kolthoff, L. M.; Chantooni, M. *J. Am. Chem. Soc.* **1975**, *97*, 1376-1381. (f) Kolthoff, L. M.; Chantooni, M. *J. Am. Chem. Soc.* **1976**, *98*, 5063-5068.

36. Olmstead, W. N.; Margolin, Z.; Bordwell, F. G. *J. Org. Chem.* **1980**, *45*, 3295-3299.

37. Ervin, K. M.; DeTuri, F. *J. Phys. Chem. A* **2002**, *106*, 9947-9956.

38. Bartmess, J. E. *NIST Chemistry WebBook, NIST Standard Reference Database Number 6;* Mallard, W. G.; Linstrom, P. J. Eds.; National Institute of Standards and Technology: Gaithersburg, MD 20899 (http://webbook.nist.gov).

39. Kass, S. R.; Fattahi, A.; Tian, Z.; Lis, L. *J. Am. Chem. Soc.* **2009**, *131*, 16984-16988.

40. Kim, E. H.; Bradforth, S. E.; Arnold, D. W.; Metz, R. B.; Neumark, D. M. *J. Chem. Phys.* **1995**, *103*, 7801-7814.

41. Gupta, N.; Linchitz, H. *J. Am. Chem. Soc.* **1997**, *119*, 6384-6391.

42. Bordwell, F. G. *Acc. Chem. Res.* **1988**, *21*, 456-463.

43. Bordwell, F. G.; McCallum, R. J.; Olmstead, W. N. *J. Org. Chem.* **1984**, *49*, 1424-1427.

44. Wang, X. B.; Nicholas, J. B.; Wang, L. S. *J. Phys. Chem. A* **2000**, *104*, 504-508.

45. Koppel, I. A.; Taft, R. W.; Anvia, F.; Zhu, S. Z.; Hu, L. Q.; Sung, K. S.; Desmarteau, D. D.; Yagupolskii, L. M. *J. Am. Chem. Soc*. **1994**, *116*, 3047-3057.

46. A more acidic carborane with an estimated $\Delta H°_{acid}$ = 241 ± 29 kcal mol^{-1} recently was determined. See, Meyer, M. M., Wang, X. B., Reed, C. A., Wang, L. S., Kass, S. R. *J. Am. Chem. Soc*. **2009**, *131*, 18050-18051.

47. Fubini, D.; Aréan, L. O. *Chem. Soc. Rev.* **1999**, *28*, 373-381.

48. Bergbreiter, D. E. *Chem. Rev.* **2002**, *102*, 3345-3384.

49. Lipman, C. B.; Wilson, F. H. *Botanical Gazette **1913**, 55, 409-420.*

50. Brown, J. S.; Gläser, R.; Liotta, C. L.; Eckert, C. A. *Chem. Commun.* **2000**, 1295–1296.

51. Smith M. B. *March's Advanced Organic Chemistry: Reactions, Mechanisms, and Structure*, Wiley-Interscience: New Jersey, 2007.

52. Stoyanov, E. S.; Stoyanova, I. V.; Reed, C. A. *J. Am. Chem. Soc.* **2010**, *132*, 1484-1485.

53. Bronsted, J. N. *Chem. Rev.* **1928**, *5*, 231-338.

54. Akiyama, T.; Itoh, J.; Fuchibe, K. *adv. synth. catal.* **2006**, *9*, 999-1010.

55. Quirk, D. J.; Raines, R. T. *Biophys. J.* **1999**, *76*, 1571-1579.

56. Taylor, M. S.; Jacobsen, E. N. *Angew. Chem. Int. Ed.* **2006**, *45*, 1520-1543.

57. Sigman, M. S.; Jacobsen, E. N. *J. Am. Chem. Soc.* **1998,** *120*, 4901-4902.

58. Yoon, T. P.; Jacobsen, E. N. *Angew. Chem. Int. Ed.* **2005**, *44*, 466-468.

59. Vachal, P.; Jacobsen, E. N. *J. Am. Chem. Soc.* **2002**, *124*, 10012-10014.

60. Berkessel, A.; Roland, K.; Neudorfl, J. *Org. Lett*. **2006**, *8*, 4195-4198.

61. Sessler, J. L.; Gale, P. A.; Cho, W. S. *Anion receptor chemistry,* RSC publishing: Cambridge, 2006.

62. McLaurin, J.; Franklin, T.; Fraser, P. E.; Chakrabartty, A. *J. Biol. Chem.* **1998**, *273*, 4506-4515.

63. Davis, A. P.; Sheppard, D. N.; Smith, B. D. *Chem. Soc. Rev.* **2007**, *36*, 348-357.

64. (a) Kavallieratos, K.; de Gala, S. R.; Austin, D. J.; Crabtree, R. H.; *J. Am Chem. Soc.* **1997**, *119*, 2325-2326. (b) Kavallieratos, K.; Bertao, C.M.; Crabtree, R. H. *J. Org. Chem*. **1999**, *64*, 1675-1683. (c) Sessler, J. L.; Camiolo, S.; Gale, P. A. *Coord. Chem. Rev*. **2003**, *240*, 17-55. (d) Chmielewski, M. J.; Jurczak, J. *Chem. Eur. J*. **2005**, *11*, 6080-6094. (e) Esteban-Gomez, D.; Fabbrizzi, L.; Licchelli, M. *J. Org. Chem.* **2005**, *70*, 5717-5720. (f) Kang, S. O.; Begum, R. A.; Bowman-James, K. *Angew. Chem. Int. Ed*. **2006**, *45*, 7882-

7894. (g) Garcia-Garrido, S. E.; Caltagirone, C.; Light, M. E.; Gale, P. A. *Chem. Commun*. **2007**, 1450-1452.

65. Smith, D. K. *Org. Biomol. Chem*. **2003**, *1*, 3874-3877.

66. Davis, A. P.; Perry, J. J.; Wareham, R. S. *Tetrahedron Lett*. **1998**, *39*, 4569-4572.

67. Shimasaki, T.; Kato, S. I.; Ideta, K.; Goto, K.; Shinmyozu, T. *J. Org. Chem.* **2007**, *72*, 1073-1087.

68. Kondo, S.; Okada, N.; Tanaka, R.; Yamamura, M.; Unno, M. *Tetrahedron Lett.* **2009**, *50*, 2754-2757.

References for chapter 2

1. (a) Childs, W.; Boxer, S. G. *Biochemistry* **2010**, *49*, 2725-2731. (b) Simon, L.; Goodman, J. M. *J. Org. Chem*. **2010**, *75*, 1831-1840. (b) Sigala, P. A.; Kraut, D. A.; Caaveiro, J. M. M.; Pybus, B.; Rubin, E. A.; Ringe, D.; Petsko, G. A.; Herschlag, D. *J. Am. Chem. Soc.* **2008**, *130*, 13696-13708. (c) Zhang, Y.; Kua, J.; McCammon, J. A. *J. Am. Chem. Soc.* **2002**, *124*, 10572-10577. (d) Whiting, A. K.; Peticolas, W. L. *Biochemistry* **1994**, *33*, 552-561.

2. (a) Gerlt, J. A.; Gassman, P. G. *Biochemistry* **1993**, *32*, 11943-11952. (b) Gerlt, J. A.; Gassman, P. G. *J. Am. Chem. Soc.* **1993**, *115*, 11552-11568. (c) Cleland, W. W.; Kreevoy, M. M. *Science* **1994**, *264*, 1887-1890. (d) Frey, P. A.; Whitt, S. A.; Tobin, J. B. *Science* **1994**, *264*, 1927-1930. (e) Cleland, W. W.; Frey, P. A.; Gerlt, J. A. *J. Biol. Chem*. **1998**, *273*, 25529-25532. (f) Schwans, J. P.; Kraut, D. A.; Herschlag, D. *Proc. Natl. Acad. Sci. U.S.A.* **2009**, *106*, 14271-14275.

3. (a) Shan, S. O.; Herschlag, D. *Proc. Natl. Acad. Sci. U.S.A.* **1996**, *93*, 14474-14479. (b) Shan, S. O.; Herschlag, D. *J. Am. Chem. Soc.* **1996**, *118*, 5515-5518. (c) Shan, S. O.; Loh, S.; Herschlag, D. *Science* **1996**, *272*, 97-101. (d) Shan, S. O.; Herschlag, D. *Methods Enzymol*. **1999**, *308*, 246-276.

4. Tian, Z.; Fattahi, A.,; Lis, L.; Kass, S. R. *J. Am. Chem. Soc.* **2009**, *131*, 16984-16988.

5. (a) Jencks, W. P. *Adv. Enzymol. Relat Areas Mol. Biol*. **1975**, *43*, 219-410. (b) Jencks, W. P. *Methods Enzymol.* **1989**, *171*, 145-164.

6. Wang, X. B.; Wang, L. S. *Rev. Sci, Instrum*. **2008**, *79*, 073108.

7. (a) Becke, A. D. *J. Chem. Phys.* **1993**, *98*, 5648-5652. (b) Lee, C.; Yang, W.; Parr, R. G. *Phys. Rev. B* **1988**, *37*, 785-789.

8. Dunning, Jr., T. H. *J. Chem. Phys.* **1989**, *90*, 1007-1023.

9. (a) Zhao, Y.; Truhlar, D. G. *J. Phys. Chem. A* **2008**, *112*, 1095-1099. (b) Zhao, Y.; Truhlar, D. G. *Theor. Chem. Acc.* **2008**, *120*, 215-241. (c) Zhao, Y.; Truhlar, D. G. *Acc. Chem. Res.* **2008**, *41*, 157-167.

10. Papajak, E.; Truhlar, D. G. *J. Chem. Theory Comput.* **2010**, *6*, 597-601.

11. Frisch, M. J., *et al. Gaussian 09*, Gaussian, Inc., Pittsburgh, PA, 2009.

12. Woolley, E. M.; Tomkins, J.; Hepler, L. G. *J. Solution Chem.* **1972**, *1*, 341-351.

13. Vibrational resolution is required to obtain a precise value for the electron affinity, but given that the anion and radical geometries are predicted to be in similar bonding configurations, we anticipate that the adiabatic electron affinities reported herein are accurate to within 0.10 eV.

14. Ellison, G. B.; Engleking, P. C.; Lineberger, W. C. *J. Phys. Chem*. **1982**, *86*, 4873-4878.

15. Both the B3LYP and M06-2X ADEs with the aug-cc-pVDZ basis set are also underestimated, but in these cases the average error is 0.23 eV. This leads to corrected predictions of 2.64 (B3LYP) and 2.63 eV (M06-2X) for $HOCH_2CH_2CH_2O^-$ which are the same as the M06-2X/maug-cc-pVT(+d)Z value given in the text (to within 0.01 eV).

16. For examples, see: (a) Tian, Z.; Fattahi, A.; Lis, L.; Kass, S. R. *Croat. Chem. Acta* **2009**, *82*, 41-45. (b) Meot-Ner (Mautner), M. *Chem. Rev*. **2005**, *105*, 213-284.

17. This percentage is the average of pK_a $(\mathbf{2} - \mathbf{3})_{DMSO}/\Delta G^\circ_{acid}$ $(\mathbf{2} - \mathbf{3})_{gas\ phase}$ and pK_a $(\mathbf{3} - \mathbf{4})_{DMSO}/\Delta G^\circ_{acid}$ $(\mathbf{3} - \mathbf{4})_{gas\ phase}$ where the experimental values come from ref. 4.

18. Meot-Ner (Mautner), M.; Speller, C. V. *J. Phys. Chem*. **1986**, *90*, 6616-6624.

19. Lu, Z.; Continetti, R. E. *J. Phys. Chem. A* **2004**, *108*, 9962-9969.

20. Berzinsh, U.; Gustafsson, M.; Hanstorp, D.; Klinkmuller, A.; Ljungblad, U.; Martensson-Pendrill, A. M. *Phys. Rev*. *A* **1995**, *51*, 231-238.

21. Weaver, A.; Arnold, D. W.; Bradforth, S. E.; Neumark, D. M. *J. Chem. Phys*. **1991**, *94*, 1740-1751.

22. Wang, X. B.; Wang, L. S. *J. Chem. Phys*. **2000**, *113*, 10928-10933.

23. Wang, X. B.; Vorpagel, E. R.; Yang, X.; Wang, L. S. *J. Phys. Chem*. *A*, **2001**, *105*, 10468-10474.

24. Meot-Ner (Mautner), M. *J. Am. Chem. Soc*. **1986**, *108*, 6189-6197.

25. For related studies that report multiple intramolecular hydrogen bonding interactions, see: (a) Wu, R.; McMahon, T. B. *J. Phys. Chem. B* **2009**, *113*, 8767-8775. (b) Wu, R.;

McMahon, T. B. *J. Am. Chem. Soc.* **2007**, *129*, 11312-113.13. (c) Norrman, K.; McMahon, T. B. *J. Phys. Chem.* A **1999**, *103*, 7008-7016. (d) Meot-Ner (Mautner), M.; Sieck, L. W.; Scheiner, S.; Duan, X. *J. Am. Chem. Soc.* **1994**, *116*, 7848-7856. (e) Campbell, S.; Rodgers, M. T.; Marzluff, E. M.; Beauchamp, J. L. *J. Am. Chem. Soc.* **1995**, *117*, 12840-12854. (f) Sharma, R. B.; Blades, A. T.; Kebarle, P. *J. Am. Chem. Soc.* **1984**, *106*, 510-516. (g) Meot-Ner (Mautner), M. *J. Am. Chem. Soc.* **1983**, *105*, 4906-4911.

26. Xantheas, S. S. *J. Am. Chem. Soc.* **1995**, *117*, 10373-10380.

27. Bruice, T. C.; Pandit, U. K. *Proc. Natl. Acad. Sci. U.S.A.* **1960**, *46*, 402-404.

28. Ionic hydrogen bond networks were modeled for the trypsin active site and were found to contribute 65 kcal mol^{-1} in the resting state conformation and 32 kcal mol^{-1} in the transition structure. For more details, see: Meot-Ner (Mautner), M. *J. Am. Chem. Soc.* **1988**, *110*, 3075-3080.

29. For reviews, see: (a) Joyce, L. A.; Shabbir, S. H.; Anslyn, E. V. *Chem. Soc. Rev.* **2010**, *39*, 3621-3632. (b) Takemoto, Y. *Yuki Gosei Kagaku Kyokaishi* **2006**, *64*, 1139-1147. (c) Schreiner, P. R. *Chem. Soc. Rev.* **2003**, *32*, 289-296. (d) Betschmann, P.; Lerner, C.; Sahli, S.; Obst, U.; Diederich, F. *Chimia* **2000**, *54*, 633-639.

References for chapter 3

1. (a) Jencks, W. P. *Adv. Enzymol. Relat Areas Mol. Biol*. **1975**, *43*, 219-410. (b) Jencks, W. P. *Acc. Chem. Res*. **1976**, *9*, 425-432. (c) Jencks, W. P. *Catalysis in Chemistry and Enzymology*, Dover: New York, 1987, pp 864. (d) Fersht, A. *Structure and Mechanism in Protein Science*, Freeman: New York, 1998, pp 650.

2. Guthrie, J. P. *Chem. Biol.* **1996**, *3*, 163-170.

3. (a) Cleland, W. W. *Biochemistry* **1992**, *31*, 317-319. (b) Gerlt, J. A.; Gassman, P. G. *Biochemistry* **1993**, *32*, 11943-11952. (c) Gerlt, J. A.; Gassman, P. G. *J. Am. Chem. Soc.* **1993**, *115*, 11552-11568. (d) Cleland, W. W.; Kreevoy, M. M. *Science* **1994**, *264*, 1887-1890. (e) Frey, P. A.; Whitt, S. A.; Tobin, J. B. *Science* **1994**, *264*, 1927−1930. (f) Cleland, W. W.; Frey, P. A.; Gerlt, J. A. *J. Biol. Chem.* **1998**, *273*, 25529−25532.

4. For recent reviews in support of the LBHB proposal, see: (a) Cleland, W. W. *Adv. Phys. Org. Chem.* **2010**, *44*, 1-17. (b) Frey, P. A. *Isotope Effects in Chemistry and Biology*; Kohen, A., Limbach, H. H. Eds., CRC Press: Boca Raton, 2006, Chpt. 40, pp 975-993. (c) Frey, P. A. *Encylopedia of Biological Chemistry* **2004**, *2*, 594-598. (d) Northrop, D. B. *Acc. Chem. Res.* **2001**, *34*, 790-797.

5. For recent reviews, opposed to the LBHB proposal see ref. 2 and the following: (a) Perrin, C. L. *Acc. Chem. Res*. **2010**, *43*, 1550-1557. (b) Warshel, A.; Sharma, P. K.; Kato, M.; Xiang, Y.; Liu, H.; Olsson, M. H. M. *Chem. Rev*. **2006**, *106*, 3210-3235. (c) Schutz, C. N.; Warshel, A. *Proteins: Struct., Funct., Bioinf.* **2004**, *55*, 711-723.

6. (a) Shan, S. O.; Herschlag, D. *Proc. Natl. Acad. Sci. U.S.A.* **1996**, *93*, 14474-14479. (b) Shan, S. O.; Herschlag, D. *J. Am. Chem. Soc.* **1996**, *118*, 5515-5518. (c) Shan, S. O.; Loh, S.; Herschlag, D. *Science* **1996**, *272*, 97-101. (d) Shan, S. O.; Herschlag, D. *Methods Enzymol*. **1999**, *308*, 246-276.

7. Tian, Z.; Fattahi, A.,; Lis, L.; Kass, S. R. *J. Am. Chem. Soc.* **2009**, *131*, 16984-16988.

8. For the gas phase acidities, see the following reference unless otherwise note. Ervin, K. M.; DeTuri, V. F. *J. Phys. Chem. A* **2002**, *106*, 9947-9956.

9. For DMSO pK_a's, see: Bordwell, F. G. *Acc. Chem. Res*. **1988**, *21*, 456-463.

10. Thorson, J. S.; Chapman, E.; Murphy, E. C.; Schultz, P. G. *J. Am. Chem. Soc.* **1995**, *117*, 1157–1158.

11. Kuliopulos, A.; Mildvan, A. S.; Shortle, D.; Talalay, P. *Biochemistry* **1989**, *28*, 149–159.

12. Kraut, D. A.; Sigala, P. A.; Fenn, T. D.; Herschlag, D. *Proc. Natl. Acad. Sci. U.S.A.* **2010**, *107*, 1960-1965.

13. Horovitz, A. *Fold Des.* **1996**, *1*, R121-R126.

14. The gas phase photoelectron spectra of $(HOCH_2CH_2)_2CHO^-$, $(HOCH_2CH_2)_3CO^-$, and $(HOCH_2CH_2CH(OH)CH_2)_3CO^-$ were reported in the following reference, Shokri, A.; Schmidt, J.; Wang, X. B.; Kass, S. R. *J. Am. Chem. Soc.* **2012**, *134*, 2094-2099.

15. Chu, Y.; Deng, H.; Cheng, J. P. *J. Org. Chem*. **2007**, *72*, 7790-7793.

16. 9-Carboxymethylfluorene was prepared as previously described. See: Matthews W. S.; Bares, J. E.; Bartmess J. E.; Bordwell F. G.; Cornforth, F. J.; Drucker, G. E.; Margolin, Z.; McCallum, R. J.; McCollum, G. J.; Vanier, N. R. *J. Am. Chem. Soc.* **1975**, *97*, 7006-7014.

17. Spartan '08 for Macintosh, Wavefunction, Inc., Irvine, CA.

18. (a) Becke, A. D. *J. Chem. Phys.* **1993**, *98*, 5648-5652. (b) Lee, C.; Yang, W.; Parr, R. G. *Phys. Rev. B* **1988**, *37*, 785-789.

19. (a) Zhao, Y.; Truhlar, D. G. *J. Phys. Chem. A* **2008**, *112*, 1095-1099. (b) Zhao, Y.; Truhlar, D. G. *Theor. Chem. Acc.* **2008**, *120*, 215-241. (c) Zhao, Y.; Truhlar, D. G. *Acc. Chem. Res.* **2008**, *41*, 157-167.

20. Papajak, E.; Truhlar, D. G. *J. Chem. Theory Comput.* **2010**, *6*, 597-601.

21. Frisch, M. J., *et al. Gaussian 09*, Gaussian, Inc., Pittsburgh, PA, 2009.

22. Guthrie, J. P. *J. Phys. Chem. A* **2001**, *105*, 8495-8499.

23. (a) Barone, V.; Cossi, M. Tomasi, J. *J. Chem. Phys.* **1997**, *107*, 3210-3221. (b) Cammi, R.; Mennucci, B.; Tomasi, J. *J. Phys. Chem. A* **1998**, *102*, 870-875. (c) Cammi, R.; Mennucci, B.; Tomasi, J. *J. Phys. Chem. A* **2000**, *104*, 4690-4698 . (d) Cossi, M.; Rega, N.; Scalmani, G.; Barone, V. *J. Comput. Chem.* **2003**, *24*, 669-681.

24. (a) Silva, C. O.; Silva, M. A.; Nascimento, M. A. C. *J. Phys. Chem. A* **1999**, *103*, 11194-11199. (b) Toth, A. M.; Liptak, M. D.; Phillips, D. L.; Shields, G. C. *J. Chem. Phys.* **2001**, *114*, 4595-4606. (c) Liptak, M. D.; Shields, G. C. *J. Am. Chem. Soc.* **2001**, *123*, 7314-7319. (d) Liptak, M. D.; Gross, K. C.; Seybold, P. G.; Feldgus, S.; Shields, G. C. *J. Am. Chem. Soc.* **2002**, *124*, 6421-6429.

25. This smaller basis set gave similar results to the B3LYP/6-311+G(d,p) pK_a's.

26. (a) Richard, J. P. *Biochemistry* **1998**, *37*, 4305-4309. (b) Kirby, A. J. *Acc. Chem. Res.* **1997**, *30*, 290-296.

27. (a) Fafarman, A. T.; Sigala, P. A.; Schwans, J. P.; Fenn, T. D.; Herschlag, D.; Boxer, S. G. *Proc. Natl. Acad. Sci. U.S.A.* **2012**, *109*, E299-E308. (b) Dong, J.; Zhuang, Z.; Song, F.; Dunaway-Mariano, D.; Carey, P. R. *J. Raman Spectrosc.* **2012**, *43*, 65-71. (c) Chenprakhon, P.; Panijpan, B.; Chaiyen, P. *J. Chem. Ed.* **2012**, *89*, 791-795. (d) Childs, W.; Boxer, S. G. *Biochemistry* **2010**, *49*, 2725-2731. (e) Zhao, G.; Jorns, M. S. *Biochemistry*, **2005**, *44*, 16866-16874. (f) Liang, T. C.; Abeles, R. H. *Biochemistry*, **1987**, *26*, 7603-7608.

28. The B3LYP/6-311+G(d,p) relative energies are similar and are as follows: 0.0 (3˚), 5.9 (2˚), and 18.1 (1˚) kcal mol^{-1} (gas phase) and 0.0 (3˚), 5.5 (2˚), and 16.9 (1˚) kcal mol^{-1} (DMSO).

29. (a) Ding, F.; Smith, J. M.; Wang, H. *J. Org. Chem.* **2009**, *74*, 2679-2691. (b) Fu, Y.; Liu, L.; Li, R. Q.; Liu, R.; Guo, Q. X. *J. Am. Chem. Soc.* **2004**, *126*, 814-822. (c) Namazian, M.; Heidary, H. *Theochem* **2003**, *620*, 257-263. (d) Saracino, G. A. A.; Improta, R.; Barone, V. *Chem. Phys. Lett.* **2003**, *373*, 411-415. (e) Cramer, C. J.; Truhlar, D. G. *Chem. Rev.* **1999**, *99*, 2161-2200.

30. Angel, L. A.; Ervin, K. M. *J. Phys. Chem. A.* **2006**, *110*, 10392-10403.

31. Wang, X. B.; Vorpagel, E. R.; Yang, X.; Wang, L. S. *J. Phys. Chem. A,* **2001**, *105*, 10468-10474.

32. Bartmess, J. E. *NIST Chemistry WebBook, NIST Standard Reference Database Number 6;* Mallard, W. G., Linstrom, P. J., Eds.; National Institute of Standards and Technology: Gaithersburg, MD 20899 (http://webbook.nist.gov).

33. Intermolecular free energies of hydration were reported previously for $OH^-(H_2O)_n$, where n = 1–6, and the second solvation shell (n = 4-6) is worth 36% of the inner one (n = 1-3). See: Meot-Ner (Mautner), M. *J. Phys. Chem.* **1986**, *90*, 6616-6624.

34. (a) Chen, J.; McAllister, M. A.; Lee, J. K.; Houk, K. N. *J. Org. Chem.* **1998**, *63*, 4611-4619. (b) Pan, Y.; McAllister, M. A. *J. Am. Chem. Soc.* **1998**, *120*, 166-169.

35. (a) Rueping, M.; Kuenkel A.; Atodiresei. I. *Chem. Soc. Rev.* **2011**, *40*, 4539-4549. (b) Akiyama, T. *Chem. Rev.* **2007**, *107*, 5744-5758. (c) Akiyama, T.; Itoh, J.; Fuchibe, K. *Adv. Synth. Catal.* **2006**, *348*, 999-1010. (d) Duhamel, L.; Duhamel, P.; Plaquevent, J. C.

Tetrahedronn: Asymmetry **2004**, *15*, 3653-3691. (e) Eames, J.; Weerasooriya, N. *Tetrahedron: Asymmetry* **2001**, *12*, 1-24. (f) Fehr, C. *Angew. Chem. lnt. Ed. Engl.* **1996**, *35*, 2566-2587.

36. We recognize that α-fluoroalcohols are inherently unstable, but offer these computations to indicate what might be achievable.

37. For example, see: (a) Van Arnam, E. B.; Lester, H. A.; Dougherty, D. A. *ACS Chem. Biol.* **2011**, *6*, 1063-1068. (b) Kohrer, C.; RajBhandary, U. L. *Nucleic Acids and Molecular Biology* **2009**, *22*, 205-229. (c) England, P. M. *Biochemistry* **2004**, *43*, 11623-11629. (d) Beene, D. L.; Dougherty, D. A.; Lester, H. A. *Curr. Opin Neurbiol.* **2003**, *13*, 264-270.

38. For examples in computational design of enzymes, see: (a) Siegel, J. B., *et al. Science* **2010**, *329*, 309-313. (b) Privett, H. K., *et al. Proc. Natl. Acad. Sci. U.S.A.* **2012**, *109*, 3790-3795.

References for chapter 4

1. (a) Sessler, J. L.; Gale, P. A.; Cho, W. S. In *Anion Receptor Chemistry (Monographs in Supramolecular Chemistry)*, Stoddart, J. F. Ed.; RSC: Cambridge, 2006; pp 1-413. (b) Hoffmann, E. K. *Biochem. Biophys. Acta* **1986**, *864*, 1-31.

2. (a) Dutzler, R.; Campbell, E. B.; Cadene, M.; Chait, B. T.; MacKinnon, R. *Nature* **2002**, *415*, 287-294. (b) Dutzler, R.; Campbell, E. B.; MacKinnon, R. *Science* **2003**, *300*, 108-112. (c) Accardi, A.; Miller, C. *Nature* **2004**, 427, 803-807. (d) Miller, C. *Nature* **2006**, *440*, 484-489.

3. (a) Omata, T. *Plant Cell Physiol.* **1995**, *36*, 207-213. (b)Koropatkin, N. M.; Pakrasi, H.

B.; Smith, T. *J. Proc. Natl. Acad. Sci. U.S.A.* **2006**, *103*, 9820-9825.

4. Luecke, H.; Quiocho, F. A. *Nature* **1990**, *347*, 402-406.

5. Pflugrath, J. W.; Quiocho, F. A. *Nature* **1985**, *314*, 257-260.

6. Ghuysen, J. M. *Annu. Rev. Microbiol.* **1991**, *45*, 37-67.

7. (a) Kavallieratos, K.; de Gala, S. R.; Austin, D. J.; Crabtree, R. H. *J. Am. Chem. Soc.* **1997**, *119*, 2325-2326. (b) Kavallieratos, K.; Bertao, C.M.; Crabtree, R. H. *J. Org. Chem.* **1999**, *64*, 1675-1683. (c) Sessler, J. L.; Camiolo, S.; Gale, P. A. *Coord. Chem. Rev.* **2003**, *240*, 17-55. (d) Chmielewski, M. J.; Jurczak, J. *Chem. Eur. J.* **2005**, *11*, 6080-6094. (e) Esteban-Gomez, D.; Fabbrizzi, L.; Licchelli, M. *J. Org. Chem.* **2005**, *70*, 5717-5720. (f) Kang, S. O.; Begum, R. A.; Bowman-James, K. *Angew. Chem., Int. Ed.* **2006**, *45*, 7882-7894. (g) Garcia-Garrido, S. E.; Caltagirone, C.; Light, M. E.; Gale, P. A. *Chem. Commun.* **2007**, 1450-1452.

8. (a) Coteron, J. M.; Hacket, F.; Schneider, H. J. *J. Org. Chem.* **1996**, *61*, 1429-1435. (b) Davis, A. P.; Perry, J. J.; Wareham, R. S. *Tetrahedron Lett.* **1998**, *39*, 4569-4572. (c) Kano, K.; Tanaka, N.; Negi, S. Eur. *J. Org. Chem.* **2001**, 3689-3694. (d) Smith, D. K. *Org. Biomol. Chem.* **2003**, *1*, 3874-3877. (e) Winstanley, K. J.; Smith, D. K. *J. Org. Chem.* **2007**, *72*, 2803-2815. (f) Kondo, S. I.; Okada, N.; Tanaka, R.; Yamamura, M.; Unno, M. *Tetrahedron Lett.* **2009**, 50, 2754-2757.

9. (a) Davis, A. P.; Joos, J. P. *Coord. Chem. Rev.* **2003**, *240*, 143-156. (b) Chmielewski, M. J.; Jurczak, J. *Chem. Eur. J.* **2006**, *12*, 7652–7667.

10. Shokri, A.; Schmidt, J.; Wang, X. B.; Kass, S. R. *J. Am. Chem. Soc.* **2012**, *134*, 2094-2099.

11. Schmidt, J.; Meyer, M. M.; Spector, I.; Kass, S. R. *J. Phys. Chem. A* **2011**, *115*, 7625-7632.

12. Coblentz Society, Inc., Evaluated Infrared Reference Spectra. NIST Chemistry WebBook, NIST Standard Reference Database Number 69; Mallard, W. G.; Linstrom, P. J. Eds.; National Institute of Standards and Technology: Gaithersburg, MD 20899 (http://webbook.nist.gov).

13. Shokri, A.: Abedin, A.; Fattahi, A.; Kass, S. R. *J. Am. Chem. Soc.* **2012**, *134*, 10646-10650.

14. (a) Becke, A. D. *J. Chem. Phys.* **1993**, *98*, 5648-5652. (b) Lee, C.; Yang, W.; Parr, R. G. *Phys. Rev. B* **1988**, *37*, 785-789.

15. Dunning, Jr., T. H. *J. Chem. Phys.* **1989**, *90*, 1007-1023.

16. (a) Zhao, Y.; Truhlar, D. G. *J. Phys. Chem. A* **2008**, *112*, 1095-1099. (b) Zhao, Y.; Truhlar, D. G. *Acc. Chem. Res.* **2008**, *41*, 157-167.

17. Papajak, E.; Truhlar, D. G. *J. Chem. Theory Comput.* **2010**, *6*, 597-601.

18. Wang, X. B.; Wang, L. S. *Rev. Sci, Instrum.* **2008**, *79*, 073108-1–073108-8.

19. Meyer, M. M.; Kass, S. R. *J. Phys. Chem. A* **2010**, *114*, 4086-4092.

20. Wang, X. B.; Dacres, J. E.; Yang, X.; Broadus, K. M.; Lis, L.; Wang, L. S.; Kass, S. R. *J. Am. Chem. Soc.* **2003**, *125*, 296-304.

21. Berzinsh, U.; Gustafsson, M.; Hanstorp, D.; Klinkmuller, A.; Ljungblad, U.; Martensson-Pendrill, A. M. *Phys. Rev. A* **1995**, *51*, 231-238.

22. Markovich, G.; Pollack, S.; Giniger, R.; Cheshnovsky, O. *J. Chem. Phys.* **1994**, *101*, 9344-9353.

23. Carbohydrate–chloride complexes have been observed by mass spectrometry, but computations indicate that they only have two short hydrogen bonds. (a) Kosevich, M. V.; Zobnina, V. G.; Chagovets, V. V.; Boryak, O. A. *Rapid Commun. Mass Spectrom.* **2011**, *25*, 713–718. (b) Jiang, Y.; Cole, R. B. *J. Am. Soc. Mass Spectrom.* **2005**, *16*, 60-70. (c) Cai, Y.; Cole, R. B. *Anal. Chem.* **2002**, *74*, 985-991.

24. (a) Xantheas, S. S. *J. Phys. Chem.* **1996**, *100*, 9703-9713. (b) Kemp, D. D.; Gordon, M. S. *J. Phys. Chem. A* **2005**, *109*, 7688-7699.

25. Hiraoka, K.; Mizuse, S. *Chem. Phys.* **1987**, *118*, 457-466 and for similar measurements and values, see: (a) Keesee, R. G.; Castleman, Jr., A. W. *Chem. Phys. Lett.* **1980**, *74*, 139-142. (b) Arshadi, M.; Yamdagni, R.; Kebarle, P. *J. Phys. Chem.* **1970**, *74*, 1475-1482.

26. Fielding, L. *Tetrahedron* **2000**, *56*, 6151-6170.

27. Connors, K. *A. Binding Constants: The Measurement of Molecular Complex Stability*, Wiley-Interscience: New York, 1987; pp 432.

28. An α and β anomeric derivative of D-ribose has been found to bind Cl^- in CD_3CN with binding constants of 33 and 235 M^{-1}, respectively. See: Kondo, S.; Kobayashi, Y.; Unno, M. *Tetrahedron Lett.* **2010**, *51*, 2512-2514.

29. (a) Iwamoto, H.; Niimi, K.; Haino, T.; Fukazawa, Y. *Tetrahedron* **2009**, *65*, 7259-7267.(b) Tobey, S. L.; Anslyn, E. V. *J. Am. Chem. Soc.* **2003**, *125*, 14807-14815. (c) Hayashi, T.; Miyahara, T.; Koide, N.; Kato, Y.; Masuda, H.; Ogoshi, H. *J. Am. Chem. Soc.* **1997**, *119*, 7281-7290.

References for chapter 5

1. (a) Akiyama, T. *Chem. Rev.* **2007**, *107*, 5744-5758. (b) Taylor, M. S.; Jacobsen E. N. *Angew. Chem. Int. Ed.* **2006**, *45*, 1520-1543. (c) Akiyama, T. *Adv. Synth. Cat.* **2006**, *348*, 999-1010. (d) List, B.; Yang, J. W. *Science* **2006**, *313*, 1584-1586.

2. (a) Uraguchi, D.; Terada, M. *J. Am. Chem. Soc.* **2004**, *126*, 5356-5357. (b) Akiyama, T.; Itoh, J.; Yokota, K.; Fuchibe, K. *Angew. Chem. Int. Ed.* **2004**, *43*, 1566-1568.

3. Garcia-Garcia, P.; Lay, F.; Garcia-Garcia, P.; Rabalakos, C.; List, B. *Angew. Chem. Int. Ed.* **2009**, *48*, 4363-4366.

4. (a) Nakashima, D.; Yamamoto, H. *J. Am. Chem. Soc.* **2006**, 128, 9626-9627. (b) Cheon, C. H.; Yamamoto, H. *J. Am. Chem. Soc.* **2008**, *130*, 9246-9247.

5. Juhasz, M.; Hoffmann, S.; Stoyanov, E.; Kim, K. C.; Reed, C. A. *Angew. Chem. Int. Ed.* **2004**, *43*, 5352-5355.

6. (a) Wenzel, A. G.; Jacobsen, E. N. *J. Am. Chem. Soc.* **2002**, *124*, 12964-12965. (b) Joly, G. D.; Jacobsen, E. N. *J. Am. Chem. Soc.* **2004**, *126*, 4102-4103. (c) Okino, T.; Hoashi, Y.; Takemoto, Y. *J. Am. Chem. Soc.* **2003**, *125*, 12672-12673. (d) Inokuma, T.; Hoashi, Y.; Takemoto, Y. *J. Am. Chem. Soc.* **2006**, *128*, 9413-9419.

7. (a) Hine, J.; Linden, S. M.; Kanagasabapathy, V. M. *J. Org. Chem.* **1985**, *50*, 5096-5099. (b) Kelly, T. R.; Meghani, P.; Ekkundi, V. S. *Tetrahedron Lett.* **1990**, *31*, 3381-3384.

8. (a) Huang, Y.; Rawal, V. H. *J. Am. Chem. Soc.* **2002**, *124*, 9662-9663. (b) Huang, Y.; Unni, A. K.; Thadani, A. N.; Rawal, V. H. *Nature* **2003**, *424*, 146. (c) Unni, A. K.; Takenaka, N.; Yamamoto, H.; Rawal, V. H. *J. Am. Chem. Soc.* **2005**, *127*, 1336-1337.

9. (a) Curran, D. P.; Kuo, L. H. *Tetrahedron Lett.* **1995**, *36*, 6647-6650. (b) Vakulya, B.; Varga, S.; Csmpai, A.; Sos, T. *Org. Lett.* **2005**, *7*, 1967-1969.

10. Tian, Z.; Fattahi, A.,; Lis, L.; Kass, S. R., *J. Am. Chem. Soc.* **2009**, *131*, 16984-16988.

11. Shokri, A.: Abedin, A.; Fattahi, A.; Kass, S. R. *J. Am. Chem. Soc.* **2012**, *134*, 10646-10650.

12. Loeb, S. J.; Martin, J. W. L.; Willis, C. J. *Can. J. Chem.* **1978**, *56*, 2369-2373.

13. (a) Murphy, K., Ph.D. Thesis, University of Minnesota, 2010; pp 125-127. (b) Jeulin, S.; Paule, S. D. D.; Ratovelomanana-Vidal, V.; Genet, J. P.; Champion, N.; Dellis, P. *Angew. Chem. Int. Ed.* **2004**, *43*, 320-325.

14. (a) Matthews W. S.; Bares, J. E.; Bartmess J. E.; Bordwell F. G.; Cornforth, F. J.; Drucker, G. E.; Margolin, Z.; McCallum, R. J.; McCollum, G. J.; Vanier, N. R. *J. Am. Chem. Soc.* **1975**, *97*, 7006-7014. (b). Chu, Y.; Deng, H.; Cheng, J. P. *J. Org. Chem.* **2007**, *72*, 7790-7793.

15. For the syntheses of the indicators, see ref. 14a and (a) Benedikt, G. M.; Traynor, L. *Tetrahedron Lett.* **1987**, *28*, 763-766. (b) Johnson, A. W.; Lee S. Y.; Swor, R. A.; Royer, L. D. *J. Am. Chem. Soc.*, **1966**, *88*, 1953-1958.

16. For DMSO pK_a's, see: Bordwell, F. G. *Acc. Chem. Res.* **1988**, *21*, 456-463.

17. Spartan '08 for Macintosh, Wavefunction, Inc., Irvine, CA.

18. (a) Becke, A. D. *J. Chem. Phys.* **1993**, *98*, 5648-5652. (b) Lee, C.; Yang, W.; Parr, R. G. *Phys. Rev. B* **1988**, *37*, 785-789.

19. (a) Zhao, Y.; Truhlar, D. G. *J. Phys. Chem. A* **2008**, *112*, 1095-1099. (b) Zhao, Y.; Truhlar, D. G. *Theor. Chem. Acc.* **2008**, *120*, 215-241. (c) Zhao, Y.; Truhlar, D. G. *Acc. Chem. Res.* **2008**, *41*, 157-167.

20. Papajak, E.; Truhlar, D. G. *J. Chem. Theory Comput.* **2010**, *6*, 597-601.

21. Frisch, M. J., *et al. Gaussian 09*, Gaussian, Inc., Pittsburgh, PA, 2009.

22. (a) Barone, V.; Cossi, M. Tomasi, J. *J. Chem. Phys.* **1997**, *107*, 3210-3221. (b) Cammi, R.; Mennucci, B.; Tomasi, J. *J. Phys. Chem. A* **1998**, *102*, 870-875.

23. Wang, X. B.; Wang, L. S. *Rev. Sci, Instrum*. **2008**, *79*, 073108-1-073108-8.

24. (a) Shokri, A.; Schmidt, J.; Wang, X. B.; Kass, S. R. *J. Am. Chem. Soc.* **2012**, *134*, 2094-2099. (b) Tian, Z.; Fattahi, A.; Lis, L.; Kass, S. R. *Croat. Chem. Acta* **2009**, *82*, 41-45.

25. The conjugate base of **3** (**3a**) was only examined computationally because its ADE is predicted to be between those for **1a** and **2a**, and the acidities follow the same trend (i.e., **1** (least acidic) < **3** < **2** (most acidic)).

26. The higher binding energy feature in the spectrum of **1a** is due to a higher electronic state of the corresponding radical, presumably, due to the loss of a lone pair electron from a fluorine atom or the OH group.

27. (a) Ramond, T.M.; Davico, G. E.; Schwartz, R. L.; Lineberger, W. C. ***J. Chem. Phys.*** **2000**, *112*, 1158-1169. (b) Mihalick, J. E.; Gatev, G. G.; Brauman, J. I. ***J. Am. Chem. Soc.*** **1996**, *118*, 12424-12431.

28. Crowder, C.; Bartmess, J. ***J. Am. Soc. Mass Spectrom.*** **1993**, *4*, 723-726.

29. Lu, Z.; Continetti, R. E. *J. Phys. Chem. A* **2004**, *108*, 9962-9969.

30. Berzinsh, U.; Gustafsson, M.; Hanstorp, D.; Klinkmuller, A.; Ljungblad, U.; Martensson-Pendrill, A. M. *Phys. Rev. A* **1995**, *51*, 231-238.

31. Weaver, A.; Arnold, D. W.; Bradforth, S. E.; Neumark, D. M. ***J. Chem. Phys.*** **1991**, *94*, 1740-1751.

32. Wang, X. B.; Nicholas, J. B.; Wang, L. S. ***J. Phys. Chem. A***, **2000**, *104*, 504-508.

33. Stewart, R. *The Proton: Applications to Organic Chemistry*, Academic: New York, 1985, pp 313.

34. Davis, A. P.; Sheppard, D. N.; Smith, B. D. *Chem. Soc. Rev.* **2007**, *36*, 348-357.

35. Shokri, A.; Schmidt, J.; Wang, X. B.; Kass, S. R. *J. Am. Chem. Soc.* **2012**, *134*, 16944-16947.

36. Kondo, S.; Kobayashi, Y.; Unno, M. *Tetraheron Lett*. **2010**, *51*, 2512-2514.

37. Smith, D. K. *Org. Biomol. Chem*. **2003**, *1*, 3874-3877.

38. Herrera, R. P.; Sgarzani, V.; Bernard, L.; Ricci, A. *Angew. Chem., Int. Ed.* ***2005***, *44*, *6576-6579.*

39. Jakab, G.; Tancon, C.; Zhang, Z.; Lippert, K. M.; Schreiner, P. R. *Org. Lett.*, **2012**, *14*, 1724-1727.

References for chapter 6

1. Shan, S. O.; Herschlag, D. *J. Am. Chem. Soc.* **1996**, *118*, 5515-5518.

2. Tian, Z.; Fattahi, A.; Lis, L.; Kass, S. R. *J. Am. Chem. Soc.* **2009**, *131*, 16984-16988.

3. Richard, J. P. *Biochemistry* **1998**, *37*, 4305-4309.

4. Kirby, A. J. *Acc. Chem. Res.* **1997**, *30*, 290-296.

5. Cleland, W. W.; Frey, P. A.; Gerlt, J. A. *J. Biol. Chem.* **1998**, *273*, 25529-25532.

6. Guthrie, J. P.; Kluger, R. *J. Am. Chem. Soc.* **1993**, *115*, 11569-11572.

7. Cui, Q.; Karplus, M. *J. Phys. Chem. B* **2002**, *106*, 1768-1798.

8. (a) Gerlt, J. A.; Gassman, G. G. *J. Am. Chem. Soc.* **1993**, *115*, 11552-11568. (b) Harris, T. K.; Abeygunawardana, C.; Mildvan, A. S. *Biochemistry* **1997**, *36*, 14661-14675.

9. (a) Frey, P. A.; Whitt, S. A.; Tobin, J. B. *Science* **1994**, *264*, 1927-1930. (b) Schwans, J. P.; Kraut, D. A.; Herschlag, D. *Proc. Natl. Acad. Sci. U.S.A.* **2009**, *106*, 14271-14275. (c) Yamaguchi, S.; Kamikubo, H.; Kurihara, K.; Kuroki, R.; Niimura, N.; Shimizu, N.; Yamazaki, Y.; Kataoka, M. *Proc. Natl. Acad. Sci. U.S.A.* **2009**, *106*, 440-444.

10. (a) Perrin, C. L. *Acc. Chem. Res.* **2010**, *43*, 1550-1557. (b) Warshel, A.; Sharma, P. K.; Kato, M.; Xiang, Y.; Liu, H.; Olsson, M. H. M. *Chem. Rev.* **2006**, *106*, 3210-3235. (c) Schutz, C. N.; Warshel, A. *Proteins: Struct. Funct. Bioinf.* **2004**, *55*, 711-723.

11. (a) Cleland, W. W. *Adv. Phys. Org. Chem.* **2010**, *44*, 1-17. (b) Frey, P. A. In *Isotope Effects in Chemistry and Biology*; Kohen, A., Limbach, H. H., Eds.; CRC Press: Boca Raton, FL, 2006; Chapter 40, pp 975−993. (c) Frey, P. A. *Encyl. Biol. Chem.* **2004**, *2*, 594-598. (d) Northrop, D. B. *Acc. Chem. Res.* **2001**, *34*, 790−797.

12. Wenthold, P.; Squires, R. *J. Phys. Chem.* **1995**, *99*, 2002-2005.

13. Gerlt, J. A.; Gassman, P. G. *J. Am. Chem. Soc.* **1993**, *115*,11552–11568.

14. (a) Kolthoff, L. M.; Chantooni, M. *J. Am. Chem. Soc.* **1975**, *97*, 1376-1381. (b) Kolthoff, L. M.; Chantooni, M. *J. Am. Chem. Soc.* **1976**, *98*, 5063-5068

15. Shokri, A.: Abedin, A.; Fattahi, A.; Kass, S. R. *J. Am. Chem. Soc.* **2012**, *134*, 10646-10650.

16. *Bordwell, F. G.; Fried, H. E. J. Org. Chem*. **1991**, *56*, 4218-4223.

17. Wang, X. B.; Wang, L. S. *Rev. Sci. Instrum.* **2008**, *79*, 073108.

18. Spartan'08 for Macintosh; Wavefunction, Inc.: Irvine, CA.

19. (a) Becke, A. D. *J. Chem. Phys.* **1993**, *98*, 5648-5652. (b) Lee, C.; Yang, W.; Parr, R. G. *Phys. Rev. B* **1988**, *37*, 785-789.

20. (a) Zhao, Y.; Truhlar, D. G. *J. Phys. Chem. A* **2008**, *112*, 1095-1099. (b) Zhao, Y.; Truhlar, D. G. *Theor. Chem. Acc.* **2008**, *120*, 215-241. (c) Zhao, Y.; Truhlar, D. G. *Acc. Chem. Res.* **2008**, *41*, 157-167.

21. Papajak, E.; Truhlar, D. G. *J. Chem. Theory Comput.* **2010**, *6*, 597-601.

22. Frisch, M. J.; et al. Gaussian 09; Gaussian, Inc.: Pittsburgh, PA, 2009.

23. (a) Barone, V.; Cossi, M.; Tomasi, J. *J. Chem. Phys.* **1997**, *107*, 3210-3221. (b) Cammi, R.; Mennucci, B.; Tomasi, J. *J. Phys. Chem. A* **1998**, *102*, 870-875

24. Wang, Y.; O'Doherty, G. A. *J. Am. Chem. Soc.* **2013**, *135*, 9334-9337.

25. Shokri, A.; Schmidt, J.; Wang, X. B.; Kass, S. R. *J. Am. Chem. Soc*. **2012**, *134*, 2094-2099.

26. Lu, Z.; Continetti, R. E. *J. Phys. Chem. A* **2004**, *108*, 9962-9969.

27. Weaver, A.; Arnold, D. W.; Bradforth, S. E.; Neumark, D. M. *J. Chem. Phys.* **1991**, *94*, 1740-1751.

28. Berzinsh, U.; Gustafsson, M.; Hanstorp, D.; Klinkmuller, A.; Ljungblad, U.; Martensson-Pendrill, A. M. *Phys. Rev. A* **1995**, *51*, 231-238.

29. The most stable conformer of the C3 deprotonated alcohol distorts from the linear structure to form three primary hydrogen bonds to the alkoxide center and one secondary hydrogen bond between two non-charged hydroxyl groups.

30. Bordwell, F. G. *Acc. Chem. Res.* **1988**, *21*, 456-463.

31. The pK_a of isopropanol in DMSO is 30.3. See: Olmstead, W. N.; Margolin, Z.; Bordwell, F. G. *J. Org. Chem.* 1980, *45*, 3295-3299.

32. (a) Bailey, S. *Trans. Faraday Soc.* **1951**, *47*, 509-517. (b) Maricic, S.; Pifat, G.; Pravdic, V. *Biochim. Biophys. Acta* **1964**, *79*, 293-300. (c) Takashima, S.; Schwan, H. P. *J. Phys. Chem.* **1965**, *69*, 4176-4182. (d) Tanaka, A.; Ishida, Y. *J. Polym. Sci. Phys.* **1973**, *11*, 1117-1123. (e) Karplus, M.; McCammon, J. A. *CRC Crit. Rev. Biochem.* **1991**, *9*, 293-349. (f) King, G.; Lee, F. S.; Warshel, A. *J. Chem. Phys.* **1991**, *95*, 4366-4377. (g) Simonson, T.; Perahia, D.; Bricogne, G. *J. Mol. Biol.* **1991**, *218*, 859-886. (h) Simonson, T.; Perahia, D.; Brunger, A. T. *Biophys. J.* **1991**, *59*, 670-690. (I) Smith, P. E.; Brunne, R. M.; Mark, A. E.; van Gunsteren, W. F. *J. Phys. Chem.* **1993**, *97*, 2009-2014. (j) Simonson, T.; Perahia, D. *Proc. Natl. Acad. Sci. U.S.A.* **1995**, *92*, 1082-1086.

References for chapter 7

1. Sessler, J. L.; Gale, P. A.; Cho, W. S. In *Anion Receptor Chemistry* (Monographs in Supramolecular Chemistry) Stoddart, J. F. Ed., RSC: Cambridge, 2006.

2. Gale, P. A. *Acc. Chem. Res.* **2006**, *39*, 465-475.

3. Bowman-James, K. *Acc. Chem. Res.* **2005**, *38*, 671-678.

4. Ooi, T.; Maruoka, K. *Angew. Chem. Int. Ed.* **2007**, *46*, 4222–4266.

5. (a) Davis, A. P.; Sheppard, D. N.; Smith, B. D. *Chem. Soc. Rev.* **2007**, *36*, 348-357. (b) Gorteau, V.; Bollot, G.; Mareda, J.; Perez-Velasco, A.; Matile, S. *J. Am. Chem. Soc.* **2006**, *128*, 14788-14789.

6. Welsh, M. J.; Ramsey, B. W.; Accurso F.; Cutting, G. R. In *The Metabolic and Molecular Basis of Inherited Disease*, Scriver, C. R.; Beaudet, A. L.; Sly, W. S.; Valle, D. ed., McGraw-Hill: New York, 2001.

7. Ashcroft, F. M. *Ion Channels and Disease Channelopathies* Academic Press: San Diego, 2000.

8. (a) Jentsch, T. J.; Hubner, C. A.; Fuhrmann, J. C. *Nat. Cell Biol.* **2004**, *6*, 1039-1047. (b) Jentsch, T. J.; Maritzen, T.; Zdebik, A. A. *J. Clin. Invest.* **2005**, *115*, 2039-2046.

9. (a) Davis, J. T.; Okunola, O.; Quesada, R. *Chem. Soc. Rev.* **2010**, *39*, 3843-3862. (b) Brotherhood, P. R.; Davis, A. P. *Chem. Soc. Rev.* **2010**, *39*, 3633-3647. (c) Gokel, G. W.; Barkey, N. *New J. Chem.* **2009**, *33*, 947-963. (d) Gale, P. A. *Acc. Chem. Res.* **2011**, *44*, 216-226.

10. (a) Kavallieratos, K.; de Gala, S. R.; Austin, D. J.; Crabtree, R. H. *J. Am. Chem. Soc.* **1997**, *119*, 2325-2326. (b) Kavallieratos, K.; Bertao, C. M.; Crabtree, R. H. *J. Org. Chem.* **1999**, *64*, 1675-1683. (c) Sessler, J. L.; Camiolo, S.; Gale, P. A. *Coord. Chem. Rev.* **2003**, *240*, 17-55. (d) Chmielewski, M. J.; Jurczak, J. *Chem. Eur. J.* **2005**, *11*, 6080-6094. (e) Esteban-Gomez, D.; Fabbrizzi, L.; Licchelli, M. *J. Org. Chem.* **2005**, *70*, 5717-5720. (f) Kang, S. O.; Begum, R. A.; Bowman-James, K. *Angew. Chem., Int. Ed.* **2006**, *45*, 7882-7894. (g) Garcia-Garrido, S. E.; Caltagirone, C.; Light, M. E.; Gale, P. A. *Chem. Commun.* **2007**, 1450-1452.

11. (a) Coteron, J. M.; Hacket, F.; Schneider, H. J. *J. Org. Chem.* **1996**, *61*, 1429-1435. (b) Davis, A. P.; Perry, J. J.; Wareham, R. S. *Tetrahedron Lett.* **1998**, *39*, 4569-4572. (c) Kano, K.; Tanaka, N.; Negi, S. Eur. *J. Org. Chem.* **2001**, 3689-3694. (d) Smith, D. K. *Org. Biomol. Chem.* **2003**, *1*, 3874-3877. (e) Winstanley, K. J.; Smith, D. K. *J. Org. Chem.* **2007**, *72*, 2803-2815. (f) Kondo, S. I.; Okada, N.; Tanaka, R.; Yamamura, M.; Unno, M. *Tetrahedron Lett.* **2009**, 50, 2754-2757.

12. (a) Hedge, V.; Madhukar, P.; Madura, J. D.; Thummel, R. P. *J. Am. Chem. Soc.* **1990**, *112*, 4549-4550. (b) Hedge, V.; Hung, C. Y.; Madhukar, P.; Cummingham, R.; Hopfner, T.; Thummel, R. P. *J. Am. Chem. Soc.* **1993**, *115*, 872-878. (c) Bell, T. W.; Hou, Z.; Zimmerman, S. C.; Thiessen, P. A.; *Angew. Chem., Int. Ed.* **1995**, *34*, 2163-2165. (d) Bell, T. W.; Hext, N. M.; Khasanov, A. B. *Pure Appl. Chem.* **1998**, *70*, 2371-2377.

13. Santacroce, P. V.; Davis, J. T.; Light, M. E.; Gale, P. A.; Iglesias-Sanchez, J. C.; Prados, P.; Quesada, R. *J. Am. Chem. Soc.* **2007**, *129*, 1886-1887.

14. Lee, S.; Hua, Y.; Park, H.; Flood, A. H. *Org. Lett.* **2010**, *12*, 2100-2102.

15. (a) Jestin, J. -L.; Pecorari, F. *Foldamers: Structure, Properties and Applications*; Wiley-VCH: Weinheim, Germany, 2007. (b) Saraogi, I.; Hamilton, A. D. *Chem. Soc. Rev.* **2009**, *38*, 1726-1743.

16. (a) Hamuro, Y.; Geib, S. J.; Hamilton, A. D. *Angew. Chem. Int. Ed.* **1994**, *33*, 446-448. (b) Berl, V.; Huc, I.; Khoury, R. G.; Krische, M. J.; Lehn, J.-M. *Nature* **2000**, *407*, 720-723. (c) Gong, B.; Zeng, H.; Zhu, J.; Yua, L.; Han, Y.; Cheng, S.; Furukawa, M.; Parra, R. D.; Kovalevsky, A. Y.; Mills, J. L.; Skrzypczack-Jankun, E.; Martinovic, S.; Smith, R. D.; Zheng, C.; Szyperski, T.; Zeng, X. C. *Proc. Natl. Acad. Sci. U.S.A.* **2002**, *99*, 11583-11588.

17. (a) Sinkeldam, R. W.; vanHoutem, M. H. C. J.; Koeckelberghs, G.; Vekemans, J. A. J. M.; Meijer, E. W. *Org. Lett.* **2006**, *8*, 383-385. (b) Zhang, A.; Han, Y.; Yamato, K.; Zeng, X. C.; Gong, B. *Org. Lett.* **2006**, *8*, 803-806.

18. (a) Li, C.; Wang, G.-T.; Yi, H.-P.; Jiang, X.-K.; Li, Z.-T.; Wang, R. -X. *Org. Lett.* **2007**, *9*, 1797-1800. (b) Cai, W.; Wang, G. -T.; Xu, Y. -X.; Jiang, X. -K.; Li, Z. -T. *J. Am. Chem. Soc.* **2008**, *130*, 6936-6937.

19. (a) Amendola, V.; Esteban-Gomez, D.; Fabbrizzi, L.; Licchelli, M. *Acc. Chem. Res.* **2006**, *39*, 343-353. (b) Hunter, C. A. *Angew. Chem., Int. Ed.* **2004**, *43*, 5310-5324.

20. Busschaert, N.; Wenzel, M.; Light, M. E.; Iglesias-Hernandez, P.; Perez-Tomas, R.; Gale, P. A. *J. Am. Chem. Soc.* **2011**, *133*, 14136-14148.

21. (a) Boiocchi, M.; Del Boca, L.; Gomez, D. E.; Fabbrizzi, L.; Licchelli, M.; Monzani, E. *J. Am. Chem. Soc.* **2004**, *126*, 16507-16514. (b) Bergamaschi, G.; Boiocchi, M.; Monzani, E.; Amendola, V., *Org. biomol. Chem.* **2011,** *9*, 8276-8283

22. Shokri, A.; Wang, X. B.; Kass, S. R. *J. Am. Chem. Soc.* **2013**, *135*, 9525-9530.

23. Shokri, A.: Abedin, A.; Fattahi, A.; Kass, S. R. *J. Am. Chem. Soc.* **2012**, *134*, 10646-10650.

24. Shokri, A.; Schmidt, J.; Wang, X. B.; Kass, S. R. *J. Am. Chem. Soc.* **2012**, *134*, 2094-2099.

25. Tian, Z.; Fattahi, A.; Lis, L.; Kass, S. R. *J. Am. Chem. Soc.* **2009**, *131*, 16984-16988.

26. Wang, X. B.; Wang, L. S. *Rev. Sci. Instrum.* **2008**, *79*, 073108.

27. Frisch, M. J.; et al. Gaussian 09; Gaussian, Inc.: Pittsburgh, PA, 2009.

28. Spartan'08 for Macintosh; Wavefunction, Inc.: Irvine, CA.

29. (a) Becke, A. D. *J. Chem. Phys.* **1993**, *98*, 5648-5652. (b) Lee, C.; Yang, W.; Parr, R. G. *Phys. Rev. B* **1988**, *37*, 785-789.

30. Dunning, T. H., Jr. *J. Chem. Phys.* **1989**, *90*, 1007-1023.

31. (a) Zhao, Y.; Truhlar, D. G. *J. Phys. Chem. A* **2008**, *112*, 1095-1099. (b) Zhao, Y.; Truhlar, D. G. *Theor. Chem. Acc.* **2008**, *120*, 215-241. (c) Zhao, Y.; Truhlar, D. G. *Acc. Chem. Res.* **2008**, *41*, 157-167.

32. Papajak, E.; Truhlar, D. G. *J. Chem. Theory Comput.* **2010**, *6*, 597-601.

33. Li, H.; Homan, E. A.; Lampkins, A. J.; Ghiviriga, I.; Castellano, R. K. *Org. Lett.* **2005**, *7*, 443-446.

34. (a) Zhong, Z. L.; Ikeda, A.; Shinkai, S. In *Calixarenes*, Asfari, Z.; Bohmer, V.; Harrowfield, J.; Vicens, J. *Kluwer Academic Publishers*: Dodrecht, 2001. (b) Molenveld, P.; Engbersen, J. F. J.; Reinhoudt, D. N. *Chem. Soc. Rev.* **2000**, 75-86.

35. (a) Boyce, R.; Li, G.; Nestler, P.; Suenaga, T.; Still, W. C. *J. Am. Chem. Soc.* **1994**, *116*, 7955-7956. (b) Davies, T. A. P.; Perry, J. J.; Williams, R. P. *J. Am. Chem. Soc.* **1997**, *119*, 1793- 1794.

36. (a) Kemp, D. S.; Petrakis, K. S. *J. Org. Chem.* **1981**, *46*, 5140-5143; (b) Kocis, P.; Issakova, O.; Sepetov, N. F.; Leibl, M. *Tertahedron Lett.* **1995**, *36*, 6623-6626. (c) Rodgers, R. D.; Brechbiel, M. W. *Inorg. Chem.* **2001**, *40*, 493-498.

37. Bogdanov, B.; Peschke, M.; Tonner, D. S.; Szulejko, J. E.; McMahon, T. B. ***Int. J. Mass Spectrom.*** **1999**, *187*, 707-725.

38. Upon removal of HCl from **1** • Cl˙ the resulting alkoxy radical underwent a hydrogen atom shift to form a phenoxyl radical upon carrying out a B3LYP/aug-cc-pVDZ optimization.

39. Guniona, . F.; Gilles, M. K.; Polak, M. L.; Lineberger W. C. *Int. J. Mass Spectrom. Ion Processes* **1992**, *117*, 601-620.

40. (a) Iwamoto, H.; Niimi, K.; Haino, T.; Fukazawa, Y. *Tetrahedron* **2009**, *65*, 7259-7267.(b) Tobey, S. L.; Anslyn, E. V. *J. Am. Chem. Soc.* **2003**, *125*, 14807-14815. (c) Hayashi, T.; Miyahara, T.; Koide, N.; Kato, Y.;Masuda, H.;Ogoshi, H. *J. Am. Chem. Soc.* **1997**, *119*, 7281-7290.

41. For hydrophobic effect review see: (a) Southall, N. T.; Dill, K. A.; Haymet, A. D. J. *J. Phys. Chem. B* **2002**, *106*, 521–533. (b) Blokzijl, W.; Engberts, J. B. F. N. *Angew. Chem., Int. Ed.* **1993**, *32*, 1545-1579. (c) Chandler, D. *Nature* **2005**, *437*, 640-647.

42. Steed, J. W.; Atwood, J. L. In *Supramolecular Chemistry*, 2nd Ed. John Wiley and Sons: Wiltshire, 2009.

43. Riddickand, A. J.; Bunger, W. B. *Organic Solvents, Vol. II* of *Techniques of Organic Chemistry*, 3rd Ed.; Wiley-Interscience: New York, 1970.

44. Sawyer, D. T.; Roberts, J. L. In *Experimental electrochemistry for chemists.* John Wiley & Sons, Inc., 1974.

References for chapter 8

1. Davis, A. P.; Sheppard, D. N.; Smith, B. D. *Chem. Soc. Rev.* **2007**, *36*, 348-357.

2. Kaplan, R. S. *J. Membr. Biol.* **2001**, *179*, 165-183.

3. Sessler, J. L.; Gale, P. A.; Cho, W. S. In *Anion Receptor Chemistry* (Monographs in Supramolecular Chemistry) Stoddart, J. F. Ed.; RSC: Cambridge, 2006.

4. Pflugrath, J. W.; Quiocho, F. A. *Nature* **1985**, *314*, 257-260.

5. Pflugrath, J. W.; Quiocho, F. A. *J. Mol. Biol.* 1988, *200*, 163-180.

6. He, J. J.; Quiocho, F. A. *Science* **1991**, *251*, 1479-1481.

7. Alexandre, H.; Geuskens, M. *Arch. Biol.* ***1984****, 95*, 55-70.

8. Quigley, G. J.; Teeter, M. M.; Rich, A. *Proc. Natl. Acad. Sci. U.S.A.* **1978**, *75*, 64-68.

9. de Silva, A. P.; Gunaratne, H. Q. N.; Gunnlaugsson, T.; Huxley, A. J. M.; McCoy, C. P.; Rademacher, J. T.; Rice, T. E. *Chem. Rev.* **1997**, *97*, 1515-1566.

10. Schmidtchen, F. P.; Berger, M. *Chem. Rev.* **1997**, *97*, 1609-1646.

11. Gale, P. A. *Chem. Soc. Rev.* **2010**, *39*, 3746-3771.

12. Gale, P. A. *Chem. Commun.* **2011**, *47*, 82-86.

13. Gale, P. A. *Acc. Chem. Res.* **2011**, *44*, 216-226.

14. Mangani, S.; Ferraroni, M. In *Supramolecular Chemistry of Anions*, Bianchi, A.; Bowman-James, K.; Garcia-Espana, E. Eds: p. 63 Wiley-VCH: New York, 1997.

15. Beer, P. D.; Gale, P. A. *Angew. Chem. Int. Ed.* **2001**, *40*, 486-516.

16. Skwierczynski, R. D.; Connors, K. A. *J. Chem. Soc. Perkin Trans. 2* **1994**, 467-472.

17. Shokri, A.; Wang, X. B.; Kass, S. R. *J. Am. Chem. Soc.* **2013**, *135*, 9525-9530.

18. Steed, J. W.; Atwood, J. L. In *Supramolecular Chemistry*, 2nd Ed.: John Wiley and Sons: Wiltshire, 2009.

19. Riddickand, A. J.; Bunger, W. B. *Organic Solvents, Vol. II of Techniques of Organic Chemistry*, 3rd Ed.; Wiley-Interscience: New York, 1970.

20. Sessler, J. L.; Gross, D. E.; Cho, W.-S.; Lynch, V. M.; Schmidtchen, F. P.; Bates, G. W.; Light, M. E.; Gale, P. A. *J. Am. Chem. Soc.* **2006**, *128*, 12281-12288.

21. Adrian, J. C.; Wilcox, C. S. *J. Am. Chem. Soc.* **1991**, *113*, 678-680.

22. Williams, D. H.; Cox, J. P. L.; Doig, A. J.; Gardner, M.; Gerhard, U.; Kaye, P. T.; Lal, A. R.; Nicholls, I. A.; Salter, C. J.; Mitchell, R. C. *J. Am. Chem. Soc.* **1991**, *113*, 7020-7030.

23. Perrin, C. L.; Nielson, J. B. *Annu. Rev. Phys. Chem.* **1997**, *48*, 511-544.

24. Alunni, S.; Pero, A.; Reichenbach, G. *J. Chem. Soc. Perkin Trans. 2* **1998**, 1747-1750.

25. Tanford, C. H. *The Hydrophobic Effect*, John Wiley and Sons: New York, 1980.

26. Privalov, P. L.; Gill, S. J. *Adv. Protein Chem.* **1988**, *39*, 191-234.

27. Tobey, S. L.; Anslyn, E. V. *J. Am. Chem. Soc.* **2003**, *125*, 14807-14815.

28. Hayashi, T.; Miyahara, T.; Koide, N.; Kato, Y.; Masuda, H.; Ogoshi, H. *J. Am. Chem. Soc.* ***1997***, 119, 7281-7290.

29. Markus, Y. In *Solvent mixtures properties and selective solvation*, Marcel Dekker, Inc: Basel, Switzerland, 2002.

30. Bowman-James, K.; Bianchi, A.; García-España, E. In *Anion coordination Chemistry*, Wiley-VCH: Weinheim, 2012.

Appendices

Appendix for chapter 2

For XYZ coordinates and electronic energies see:

http://pubs.acs.org/doi/suppl/10.1021/ja2081907

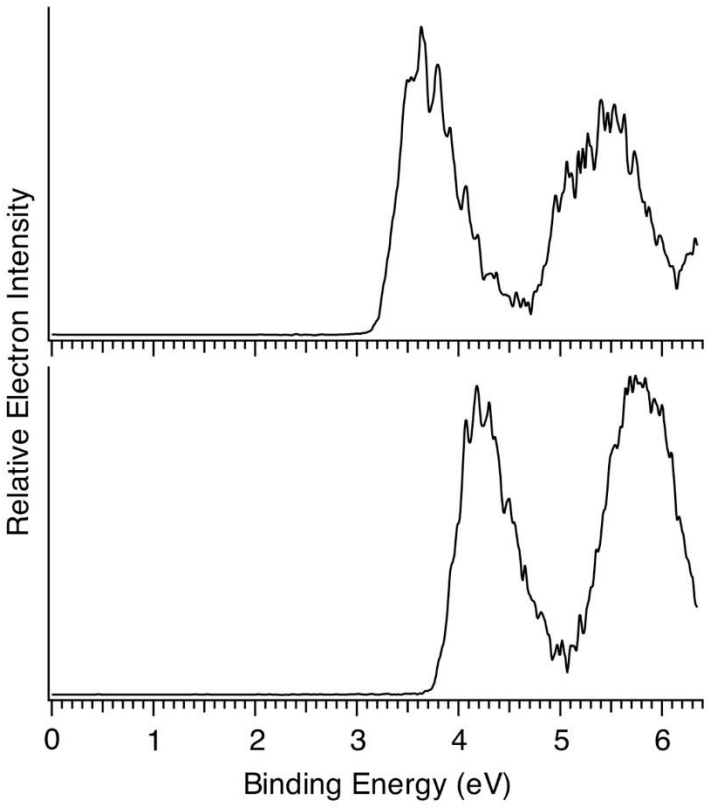

Figure S1. Low temperature (20 K) photoelectron spectra of $(HOCH_2CH_2)_2CHO^-$ (top) and $(HOCH_2CH_2)_3CO^-$ (bottom) at 193 nm (6.424 eV).

Appendix for chapter 3

For XYZ coordinates and electronic energies see:

http://pubs.acs.org/doi/suppl/10.1021/ja3037349

Table S1. Experimental and Theoretical DMSO pK_a Values based on the solution optimized structures.

Compound	B3LYP/ 6-311+G (d,p)[a]	M062X/ maug-cc-pVT(+d)Z[a]	Exptl
CH_3OH	30.2 (-1.2)	30.9 (-1.9)	29.0[c]
$(CH_3)_3COH$	28.4(3.8)	30.2(2.0)	32.2[c]
$HOCH_2CH_2CH_2O\mathit{H}$ (**2**)	24.1(1.3)	23.6(1.8)	25.4 ± 0.3[b]
$(HOCH_2CH_2)_2CHO\mathit{H}$ (**3**)	20.6(-0.9)	19.5(0.2)	19.7 ± 0.2[b]
$(HOCH_2CH_2)_3CO\mathit{H}$ (**4**)	16.4(-0.3)	14.8(1.3)	16.1 ± 0.2[b]
$(HOCH_2CH_2CH(OH)CH_2)_3CO\mathit{H}$ (**1**)	13.6(-2.2)	12.7(-1.3)	11.4 ± 0.2
$PhO\mathit{H}$	15.9(2.1)	16.1(1.9)	18.0[c]
$CH_3CO_2\mathit{H}$	9.4(3.2)	9.4(3.2)	12.6[c]
Average unsigned error	1.9	1.7	

[a]Parenthetical values correspond to the error in pK_a units (i.e. pK_a (expt – calc)). [b]Ref. 5 [c]Ref. 26

Appendix for chapter 4

For XYZ coordinates and electronic energies see:

http://pubs.acs.org/doi/suppl/10.1021/ja3075456

Materials and Methods:

General. Heptaol **1** was synthesized as previously reported (10). Acetonitrile-d_3 and tetrabutylammonium chloride (TBACl) were purchased from Cambridge Isotope Laboratories and Sigma Aldrich, respectively. The former compound was dried over activated 3 Å molecular sieves for several days and the latter one was stored in a vacuum desiccator containing phosphorous pentoxide before use. Proton NMR spectra were recorded on Varian VI-500 and VI-300 MHz instruments at different temperatures as indicated, and the resulting chemical shifts are reported in parts per million (δ) relative to the residual solvent peak. A Bruker BioTOF II electrospray ionization–time of flight mass spectrometer with polyethylene glycol 300 as an internal standard was used to obtain an exact mass measurement of the heptaol **1** · Cl^- complex.

Binding Constant Determinations. Various amounts of a 0.1 M tetrabutylammonium chloride stock solution in acetonitrile-d_3 were added to 1.00 ml of a 0.135 mM non-aggregating diastereomeric mixture (~3 RRS/SSR to 1 RRR/SSS) of **1** in CD_3CN. Changes in the chemical shift of the tertiary hydroxyl group at three different temperatures were followed to calculate the binding constants (Table S1 and Figures S1-S3).

Table S1. Titration data for chloride binding to **1**.[1]

Temp. (˚C)	µl Cl^{-2}	$[Cl^-]_0$	$[Cl^-]_{ub}$	$[\mathbf{1}]_o$	$[\mathbf{1}]_{ub}$	δ	Δδ	$\Delta\delta/[Cl^-]_0$	%bound[3]
22.0	0	0	0	0.135	0.135	5.091			
	5	0.498	0.478	0.134	0.114	5.196	0.105	0.211	15.3
	20	1.96	1.91	0.132	0.0780	5.372	0.281	0.143	41.1
	30	2.91	2.85	0.131	0.0642	5.440	0.349	0.120	51.0
	60	5.66	5.57	0.127	0.0428	5.545	0.454	0.0802	66.4
	100	9.09	8.99	0.123	0.0300	5.608	0.517	0.0569	75.6
	200	16.7	16.6	0.113	0.0178	5.667	0.576	0.0346	84.2
	300	23.1	23.0	0.104	0.0114	5.700	0.609	0.0264	89.0
	700	41.2	41.1	0.0794	0.00362	5.744	0.653	0.0159	95.4
56.2	0	0	0	0.135	0.135	4.952			
	10	0.990	0.968	0.134	0.114	5.056	0.104	0.105	15.0
	20	1.96	1.92	0.132	0.0957	5.144	0.192	0.0979	27.7
	40	3.85	3.79	0.130	0.0722	5.260	0.308	0.0801	44.4
	80	7.41	7.33	0.125	0.0514	5.361	0.409	0.0552	58.9
	200	16.7	16.6	0.113	0.0274	5.477	0.525	0.0315	75.6
	450	31.0	31.0	0.0931	0.0124	5.554	0.602	0.0194	86.7
-22.0	0	0	0	0.135	0.135	5.288			
	10	0.990	0.931	0.134	0.0770	5.554	0.266	0.269	42.4
	20	1.96	1.88	0.132	0.0512	5.673	0.385	0.196	61.3
	40	3.85	3.75	0.130	0.0299	5.771	0.483	0.126	77.0
	80	7.41	7.30	0.125	0.0185	5.823	0.535	0.0722	85.2
	200	16.7	16.6	0.113	0.00783	5.872	0.584	0.0350	93.0
	450	31.0	30.9	0.0931	0.00366	5.891	0.603	0.0194	96.1

[1]Chemical shifts and concentrations are given in ppm and mM, respectively. The abbreviation ub stands for unbound. [2]Total amount added. [3]Bound (%) = 100 x $\Delta\delta/\delta_{max}$, where δ_{max} = 0.628 (-22.0 ˚C), 0.684 (22.0 ˚C), and 0.694 (56.2 ˚C) ppm.

Figure S1. Nonlinear 1:1 binding isotherm for **1** and Cl^- at 22.0 ˚C. Circles are the experimental data and the line is the calculated isotherm.

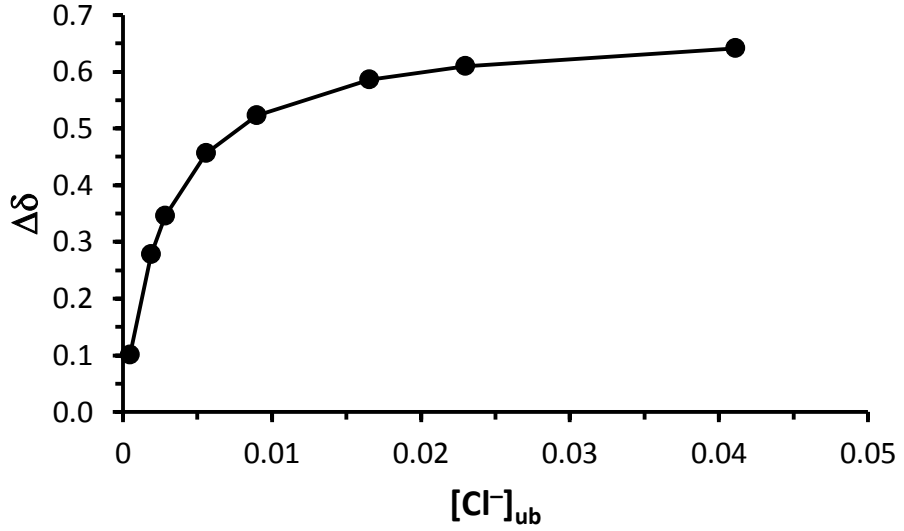

Figure S2. Nonlinear 1:1 binding isotherm for **1** and Cl^- at 56.2 ˚C. Circles are the experimental data and the line is the calculated isotherm.

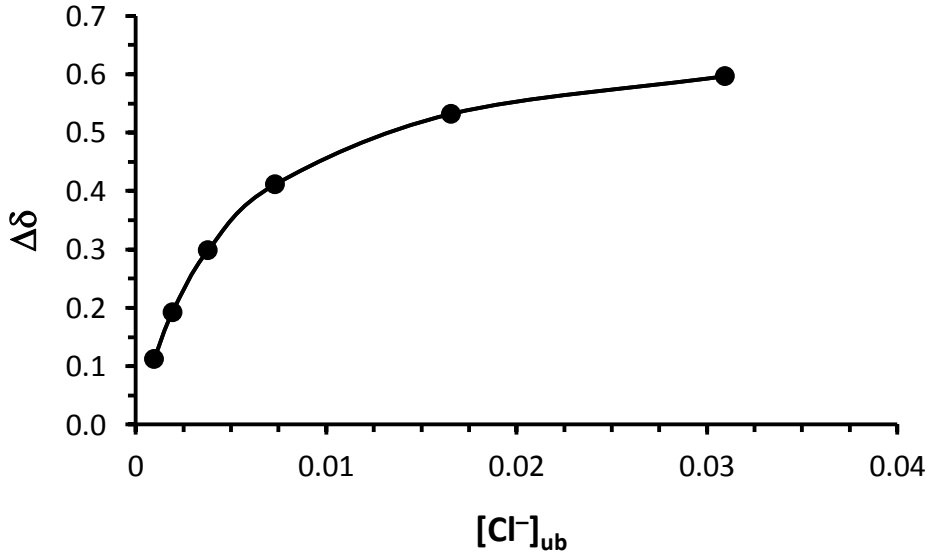

Figure S3. Nonlinear 1:1 binding isotherm for **1** and Cl^- at -23.0 ˚C. Circles are the experimental data and the line is the calculated isotherm.

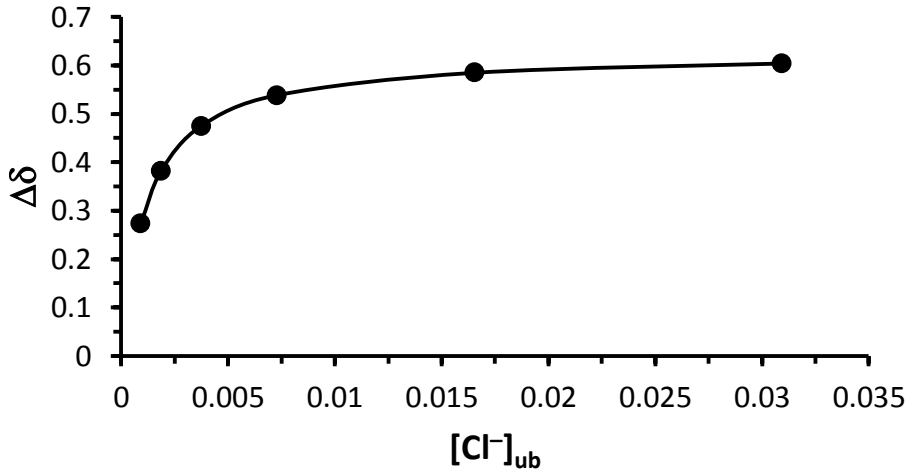

Infrared Photodissociation Spectra. A previously described LaserVision tunable IR laser system pumped by a Continuum Surelite II Nd:YAG laser was used in conjunction with a 3 T IonSpec Fourier transform mass spectrometer (FTMS) in these studies.[11] Heptaol **1** (RRR/SSS) and one equivalent of NH_4Cl were dissolved in methanol : water or CD_3OD : D_2O (3:1) to afford an ~2 mM solution. The **1** • Cl^- complex was generated by electrospray ionization (ESI) at a flow rate of 10 mL min^{-1} and transferred into the FTMS with the assistance of a pulse of argon gas. It was then isolated by ejecting unwanted ions with short duration RF bursts (chirps) and subsequently irradiated with tunable IR light for 10 s at 10 Hz in 5 cm^{-1} steps from 2800 - 3800 cm^{-1}. Each spectrum datum point was comprised of a single sequence, that is, new ions were generated, transferred, isolated, cooled, and irradiated. A simple moving average was used to smooth the fragmentation percentage and

this quantity was ploted vs. the IR wavelength. No corrections for the photon energy or changes in the laser power over the scanned range were applied except for an anomalous increase between 3070 and 3090 cm^{-1} that has previously been addressed. Fragmentation vs. time studies were also carried out at 3400 cm^{-1} from 0.5 to 150 s and there was no evidence of a second ion structure up to 94% conversion.

Photoelectron Spectroscopy. An ESI front end with a cryogenic ion-trap coupled to a photoelectron spectrometer was used to obtain 20 K photoelectron spectra in this work.[18] The desired cluster was generated from an ~10^{-3} M solution of **1** in methanol : water (7:3) along with a small amount of tetrabutylammonium chloride. The mass selected ion was cooled to 20 K for 20-80 ms before being photodetached with a 193 nm ArF laser or a 157 nm F_2 excimer laser. Data were recorded at 20 Hz so that shot-to-shot background subtraction could be carried out, and the resulting ADE was obtained from a linear extrapolation of the onset region. It has an estimated uncertainty of ± 0.1 eV.

Computations. Extensive B3LYP/aug-cc-pVDZ geometry optimizations were carried out on the RRS/SSR diastereomer of **1** • Cl^- using starting points generated by molecular mechanics and AM1 with Spartan,[S1,14,15] as well as additional conformations produced by inspection. The most favorable structures were converted to their RRR/SSS diastereomer and reoptimized. Vibrational frequencies of the lowest energy conformer of both diastereomers were computed and the unscaled values were used to obtain the zero-point energies and thermal corrections to the enthalpy at 298 K. Single-point energies were also calculated with the M06-2X functional and the maug-cc-pVT(+d)Z basis set.[16,17] To obtain ADEs, the radicals derived from the most favorable anion of both diastereomers were also

optimized (B3LYP/aug-ccpVDZ), their vibrational frequencies were computed, and M06-2X/maug-cc-pVT(+d)Z single-point energies were calculated. The resulting ADEs for both diastereomers are predicted to be within 0.04 eV of each other and the computed IR spectra are qualitatively the same. All of the B3LYP and M06-2X computations were carried out using Gaussian 09.[S2]

References

S1. Spartan '08 for Macintosh, Wavefunction, Inc., Irvine, CA.

S2. Frisch, M. J.; Trucks, G. W.; Schlegel, H. B.; Scuseria, G. E.; Robb, M. A.; Cheeseman, J. R.; Scalmani, G.; Barone, V.; Mennucci, B.; Petersson, G. A.; Nakatsuji, H.; Caricato, M.; Li, X.; Hratchian, H. P.; Izmaylov, A. F.; Bloino, J.; Zheng, G.; Sonnenberg, J. L.; Hada, M.; Ehara, M.; Toyota, K.; Fukuda, R.; Hasegawa, J.; Ishida, M.; Nakajima, T.; Honda, Y.; Kitao, O.; Nakai, H.; Vreven, T.; Montgomery, Jr., J. A.; Peralta, J. E.; Ogliaro, F.; Bearpark, M.; Heyd, J. J.; Brothers, E.; Kudin, K. N.; Staroverov, V. N.; Kobayashi, R.; Normand, J.; Raghavachari, K.; Rendell, A.; Burant, J. C.; Iyengar, S. S.; Tomasi, J.; Cossi, M.; Rega, N.; Millam, J. M.; Klene, M.; Knox, J. E.; Cross, J. B.; Bakken, V.; Adamo, C.; Jaramillo, J.; Gomperts, R.; Stratmann, R. E.; Yazyev, O.; Austin, A. J.; Cammi, R.; Pomelli, C.; Ochterski, J. W.; Martin, R. L.; Morokuma, K.; Zakrzewski, V. G.; Voth, G. A.; Salvador, P.; Dannenberg, J. J.; Dapprich, S.; Daniels, A. D.; Farkas, O.; Foresman, J. B.; Ortiz, J. V.; Cioslowski, J.; Fox, D. J. Gaussian 09, Gaussian, Inc., Wallingford, CT, 2009.

Appendix for chapter 5

For XYZ coordinates and electronic energies see:

http://pubs.acs.org/doi/suppl/10.1021/ja4036384

Figure S1. Non-linear plot for the binding of **1** with chloride ion. Circles are the experimental data and the line is the calculated isotherm.

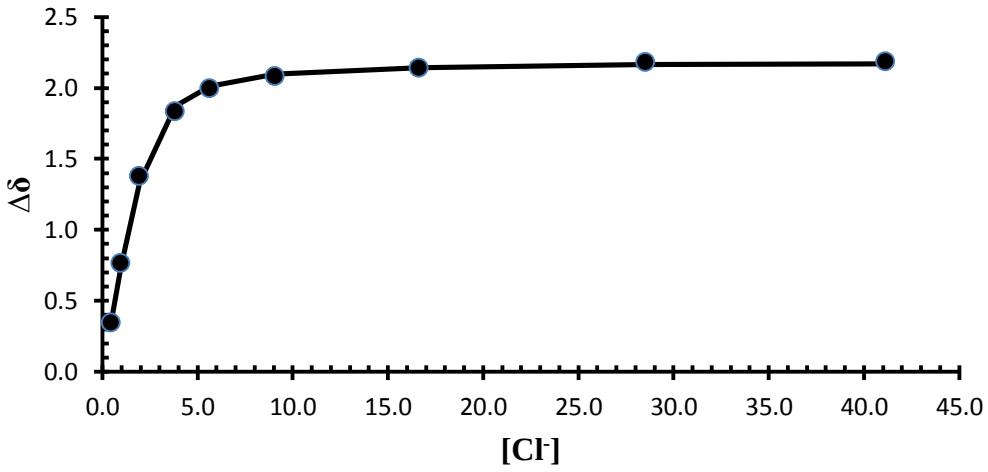

Table S1. Titration data for chloride binding to **1**.[a]

µL (Cl^- added)	[Cl^-]	[**1**]	δ (OH)	Δδ	%bound
0	0.0	2.50	4.251	0.000	0.0
5	0.50	2.49	4.597	0.346	15.8
10	0.99	2.48	5.017	0.766	35.1
20	1.96	2.45	5.629	1.378	63.1
40	3.85	2.40	6.085	1.834	83.9
60	5.66	2.36	6.246	1.995	91.3
100	9.09	2.27	6.333	2.082	95.3
200	16.67	2.08	6.392	2.141	98.0
400	28.57	1.79	6.432	2.181	99.8
700	41.18	1.47	6.436	2.185	100.0

[a]Chemical shifts and concentrations are given in ppm and mM, respectively.

Figure S2. Non-linear plot for the binding of **2** with chloride ion. Circles are the experimental data and the line is the calculated isotherm.

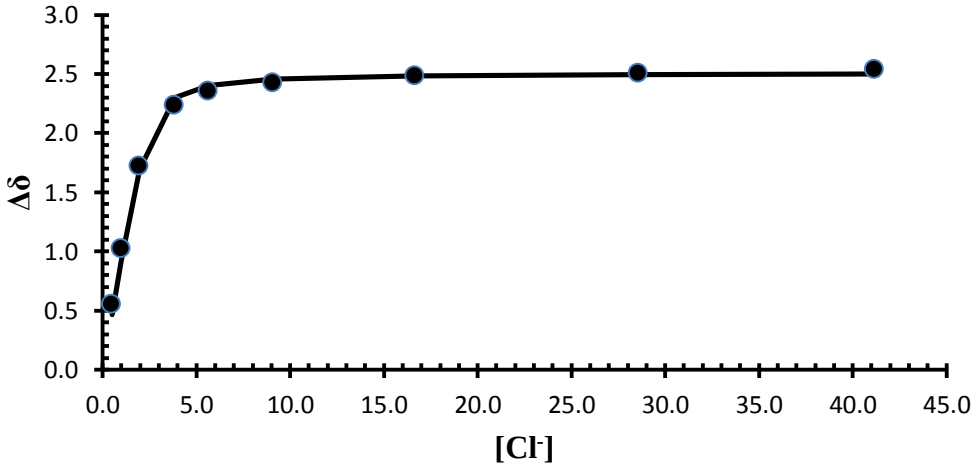

Table S2. Titration data for chloride binding to **2**.[a]

µL (Cl^- added)	[Cl^-]	[**2**]	δ (OH)	Δδ	%bound
0	0.0	2.50	6.533	0.000	0.0
5	0.50	2.49	7.090	0.557	21.9
10	0.99	2.48	7.560	1.027	40.4
20	1.96	2.45	8.255	1.722	67.8
40	3.85	2.40	8.769	2.236	88.1
60	5.66	2.36	8.890	2.357	92.8
100	9.09	2.27	8.958	2.425	95.5
200	16.67	2.08	9.021	2.488	98.0
400	28.57	1.79	9.043	2.510	98.9
700	41.18	1.47	9.072	2.539	100.0

[a]Chemical shifts and concentrations are given in ppm and mM, respectively.

Appendix for chapter 6

Figure S1. Synthetic route for the preparation of pentaol **P**.

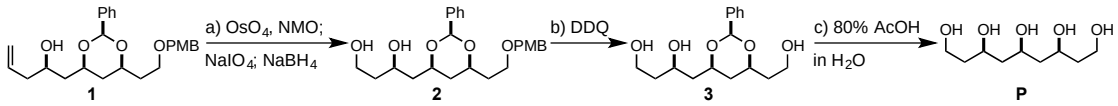

Reagents and conditions: a) OsO_4, NMO, THF, 0 °C to rt; $NaIO_4$, 0 °C; $NaBH_4$, 0 °C, 69%. b) DDQ, CH_2Cl_2, H_2O, 0 °C, 43%. c) AcOH/H_2O (4:1), 80 °C, 22%.

Experiment Procedures

(R)-4-((2S,4R,6S)-6-(2-((4-Methoxybenzyl)oxy)ethyl)-2-phenyl-1,3-dioxan-4-yl)butane-1,3-diol (**2**):

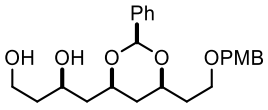

To a stirred solution of **1** (1.19 g, 2.89 mmol) in tetrahydrofuran (10 mL) at 0 °C was added osmium tetroxide (18.3 mg, 72.1 µmol), followed by *N*-methylmorpholine *N*-oxide (4.8 mol/L, 3.0 mL, 14.5 mmol) in water. The resulting mixture was warmed to room temperature and stirred for 3 h. The mixture was cooled to 0 °C, and $NaIO_4$ (3.09 g, 14.5 mmol) was added in one portion. After 1 h, $NaBH_4$ (2.19 g, 57.8 mmol) was added slowly at 0 °C. After an additional 5 min, the reaction was quenched by adding water (10 mL). The mixture was filtered through Celite and the filtrate was extracted with EtOAc (3 × 30 mL). The combined organic layers were washed with brine, dried over anhydrous Na_2SO_4,

and filtered and concentrated under reduced pressure. The crude residue was purified by flash chromatography (60 to 100% EtOAc in hexanes) on silica gel (40 mL) to afford **2** (0.823 g, 69%) as a colorless oil.

Data for **2:** R_f = 0.20 (80% EtOAc in hexanes);

$[\alpha]_D^{20}$ = –18.4 (CH_2Cl_2, *c* = 1.85);

IR (neat) 3387, 2941, 2917, 2863, 1611, 1512, 1453, 1342, 1245, 1174, 1099, 1027 cm^{-1};

^1H NMR (500 MHz, $CDCl_3$) δ 7.42–7.40 (m, 2H), 7.37–7.33 (m, 3H), 7.25 (d, *J* = 8.5 Hz, 2H), 5.86 (d, *J* = 8.5 Hz, 2H), 5.55 (s, 1H), 4.46 (d, *J* = 11.5 Hz, 1H), 4.43 (d, *J* = 11.5 Hz, 1H), 4.19 (dddd, *J* = 9.5, 7.0, 4.5, 2.5 Hz, 1H), 4.13 (dddd, *J* = 11.0, 11.0, 3.0, 3.0 Hz, 1H), 4.05 (dddd, *J* = 11.0, 8.0, 4.5, 2.5 Hz, 1H), 3.85–3.80 (m, 2H), 3.78 (s, 3H), 3.65 (ddd, *J* = 9.5, 8.0, 5.0 Hz, 1H), 3.67 (br, 1H), 3.55 (ddd, *J* = 9.5, 5.5, 5.5 Hz, 1H), 2.72 (br s, 1H), 1.95–1.79 (m, 3H), 1.75–1.69 (m, 2H), 1.65 (ddd, *J* = 14.5, 2.5, 2.5 Hz, 1H), 1.60 (ddd, *J* = 13.0, 2.5, 2.5 Hz, 1H), 1.50 (ddd, *J* = 13.0, 11.0, 11.0 Hz, 1H);

^{13}C NMR (100 MHz, $CDCl_3$) δ 159.3, 138.3, 130.6, 129.5, 129.0, 128.4, 126.1, 113.9, 100.8, 77.6, 74.0, 72.8, 71.6, 65.6, 61.4, 55.4, 42.9, 38.8, 37.2, 36.1;

HRMS (ESI) calcd for $C_{24}H_{32}O_6Na$ $[M + Na]^+$: 439.2091, found 439.2094.

*(R)-4-((2S,4R,6S)-6-(2-Hydroxyethyl)-2-phenyl-1,3-dioxan-4-yl)butane-1,3-diol (**3**):*

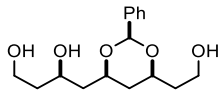

To a stirred solution of **2** (0.660 g, 1.59 mmol) in dichloromethane (8 mL) at 0 °C was added water (0.4 mL), followed by 2,3-dichloro-5,6-dicyano-1,4-benzoquinone (1.08 g, 4.75 mmol) under N_2. The resulting mixture was stirred at the same temperature for 2 h. The reaction was quenched by adding saturated aqueous sodium bicarbonate (20 mL), and filtered through a pad of Celite. The filtrate was extracted with EtOAc (3 × 30 mL) and the combined organic layers were washed with brine, dried over anhydrous Na_2SO_4, and filtered and concentrated under reduced pressure. The crude residue was purified by flash chromatography (1 to 10% MeOH in EtOAc) on silica gel (40 mL) to afford **3** (0.203 g, 43%) as a colorless oil.

Data for **3:** R_f = 0.26 (10% MeOH in EtOAc);

$[\alpha]_D^{19}$ = +1.6 (CH_2Cl_2, *c* = 0.64);

IR (neat) 3341, 2923, 2871, 1453, 1406, 1343, 1215, 1102, 1057, 1027;

^{1}H NMR (500 MHz, $CDCl_3$) δ 7.44–7.42 (m, 2H), 7.38–7.33 (m, 3H), 5.59 (s, 1H), 4.21–4.15 (m, 2H), 4.15–4.09 (m, 1H), 3.87–3.78 (m, 4H), 3.55 (br s, 1H), 2.71 (br s, 1H), 2.10 (br s, 1H), 1.93–1.87 (m, 2H), 1.84–1.78 (m, 1H), 1.74–1.70 (m, 2H), 1.66 (ddd, *J* = 15.0, 3.0, 3.0 Hz, 1H), 1.63–1.56 (m, 2H);

^{13}C NMR (100 MHz, $CDCl_3$) δ 138.1, 129.2, 128.6, 126.1, 101.0, 77.6, 75.9, 71.5, 61.4, 60.1, 42.9, 38.8, 38.1, 37.1;

HRMS (ESI) calcd for $C_{16}H_{24}O_5Na$ $[M + Na]^+$: 319.1516, found 319.1526.

*nonane-1,3,5,7,9-pentaol (**P**)*

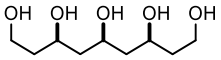

To a flask with **2** (0.456 g, 1.54 mmol) was added a solution of acetic acid (8 mL, 80%) in water. The resulting mixture was heated to 90 °C and stirred for 1 h. The solvent was removed under reduced pressure and the resulting residue was purified by flash chromatography (2 to 20% MeOH in EtOAc) on silica gel (30 mL) to afford **P** (70.0 mg, 22%) as a colorless oil.

Data for **P:** R_f = 0.44 (30% MeOH in EtOAc);

IR (neat) 3342, 2955, 2925, 2854, 1734, 1647, 1508, 1457, 1260, 1107;

^{1}H NMR (500 MHz, CD_3OD) δ 3.98 (dddd, *J* = 7.5, 7.5, 5.0, 5.0 Hz, 1H), 3.93 (dddd, *J* = 9.0, 9.0, 4.5, 4.5 Hz, 2H), 3.69 (t, *J* = 6.5 Hz, 4H), 1.72 (ddd, *J* = 14.0, 7.0, 7.0, 4.0 Hz, 2H), 1.66–1.56 (m, 6H);

^{13}C NMR (100 MHz, CD_3OD) δ 70.2, 68.8, 60.1, 45.5, 41.0;

HRMS (ESI) calcd for $C_9H_{20}O_5Na$ $[M + Na]^+$: 231.1203, found 231.1201.

^{1}H and ^{13}C NMR Spectra

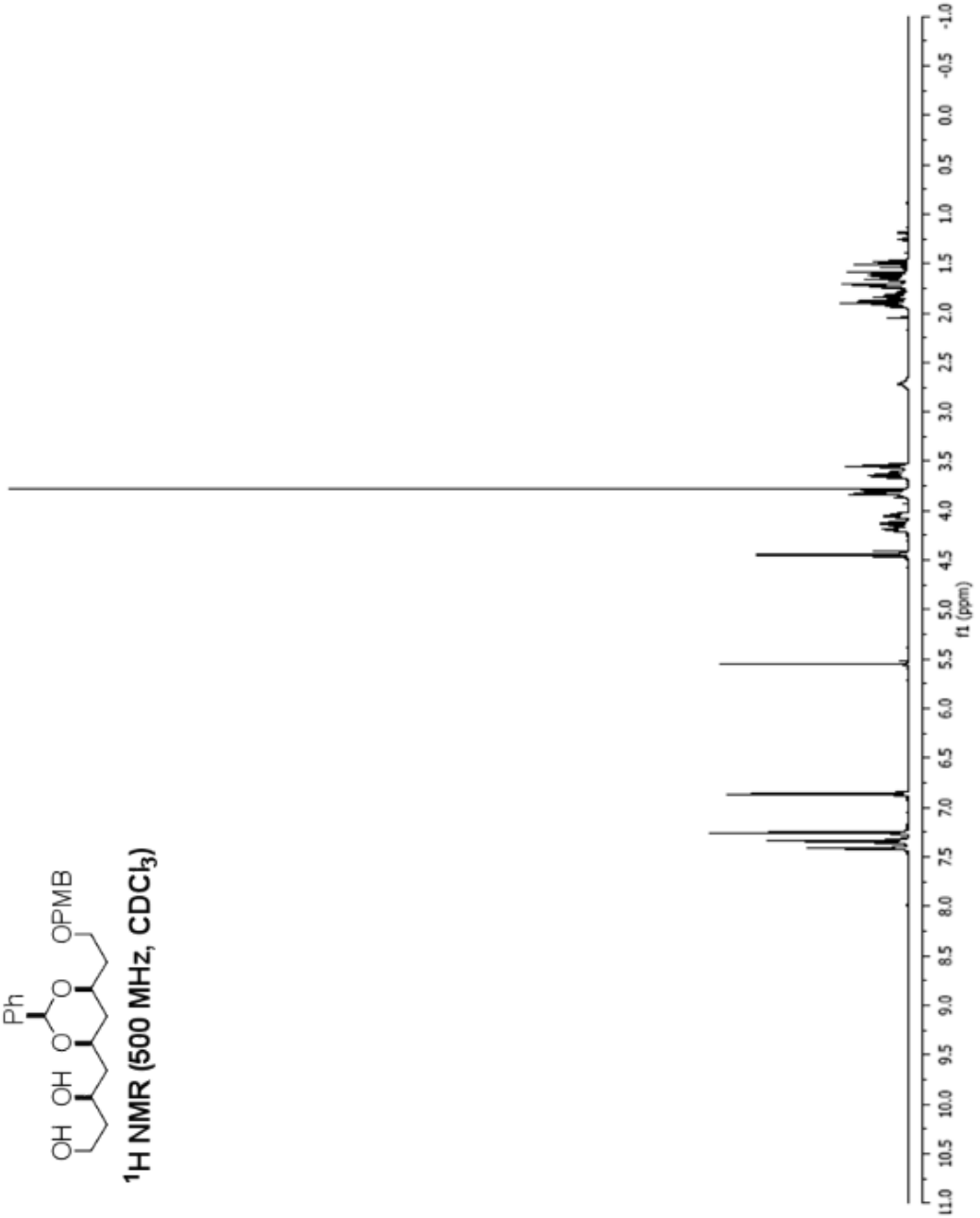

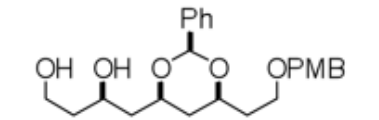

^{13}C NMR (100 MHz, $CDCl_3$)

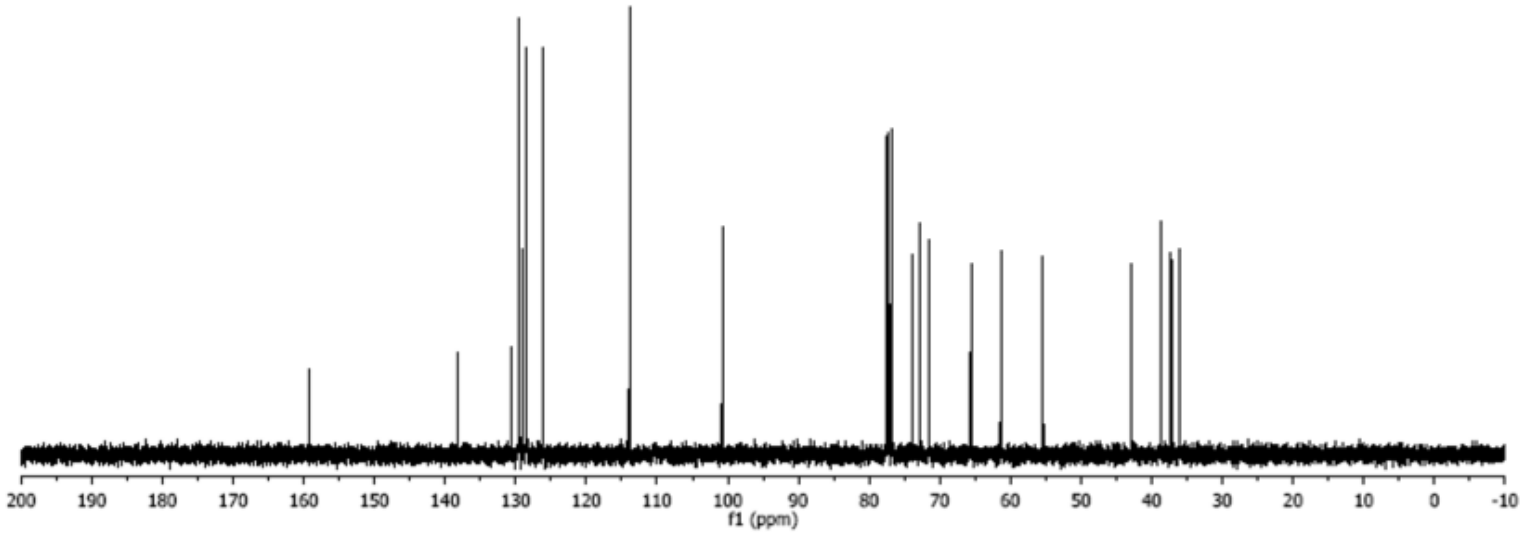

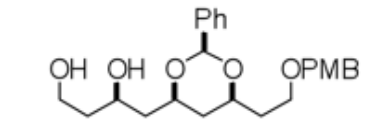

^{13}C NMR (100 MHz, $CDCl_3$)

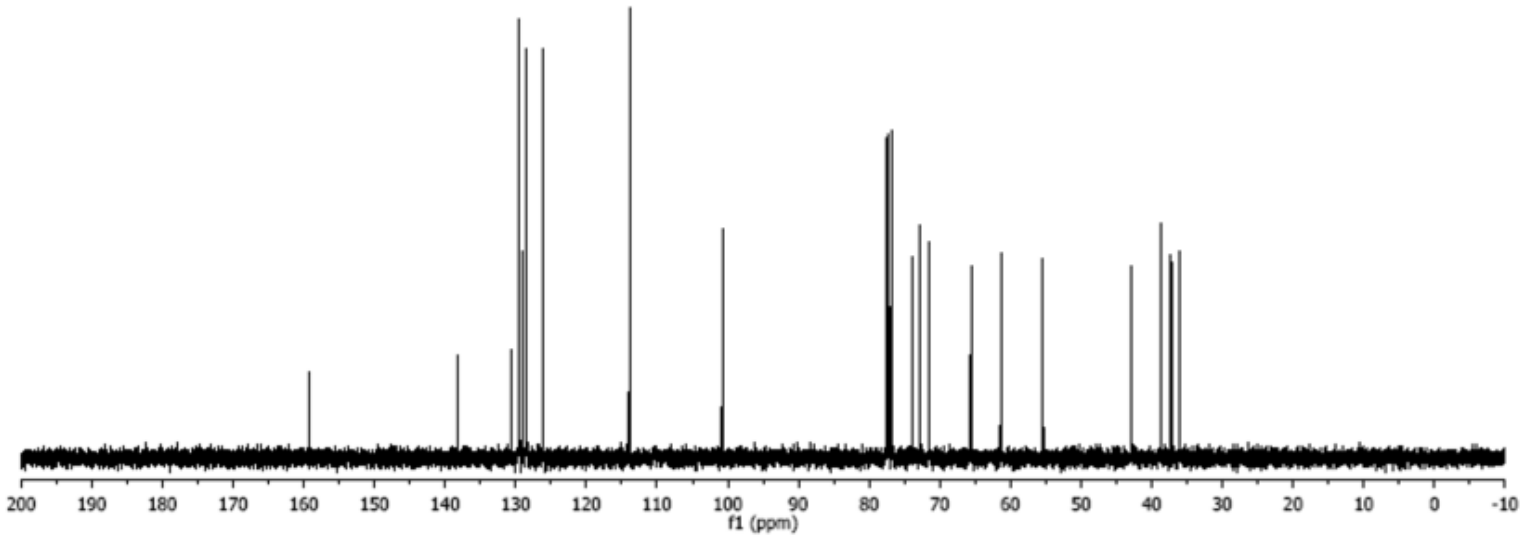

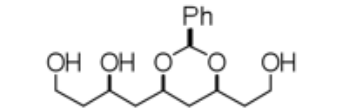

^{1}H NMR (500 MHz, $CDCl_3$)

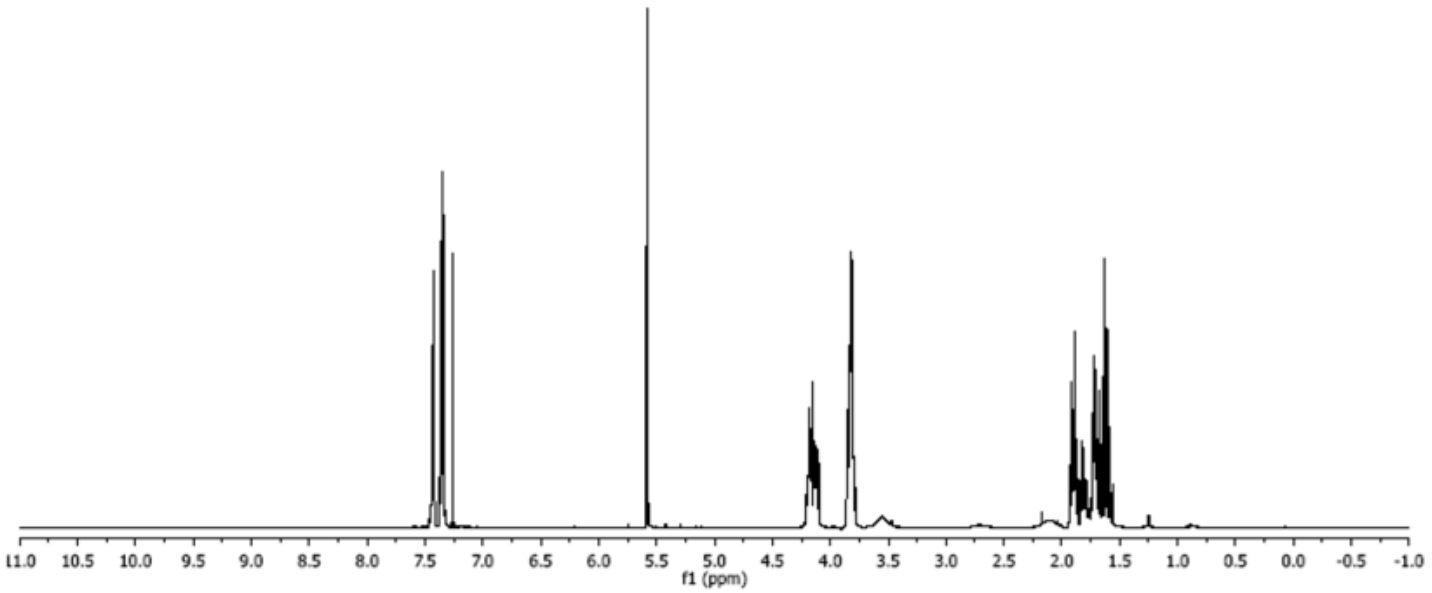

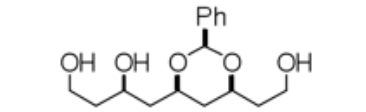

^{13}C NMR (100 MHz, $CDCl_3$)

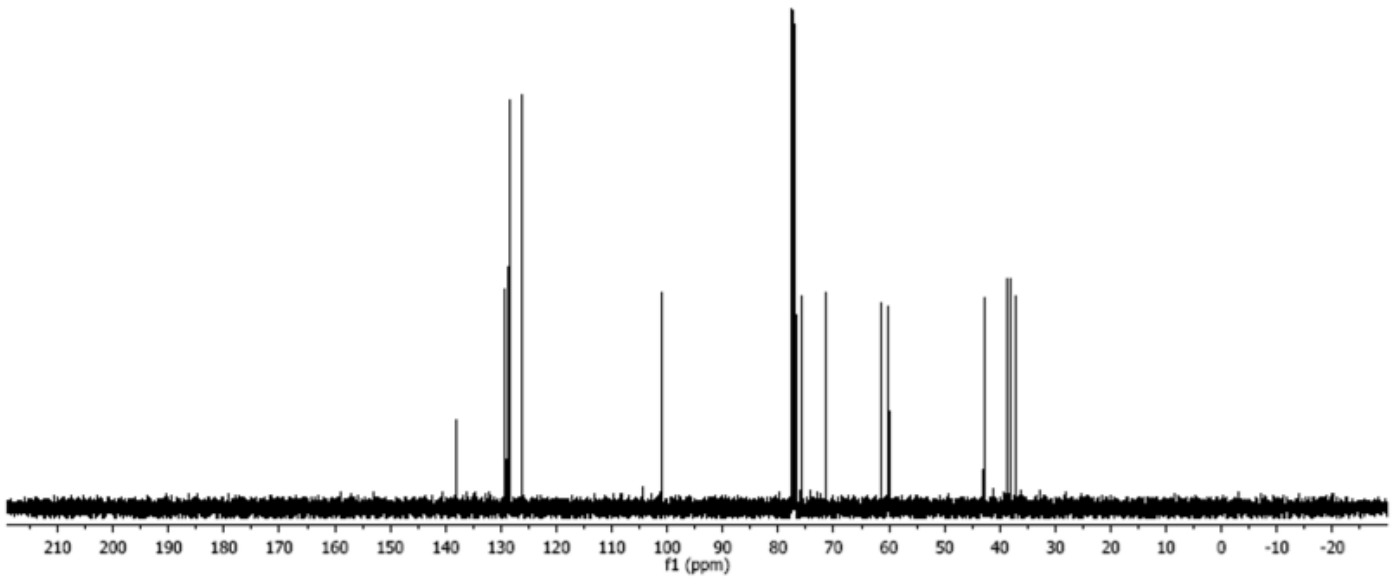

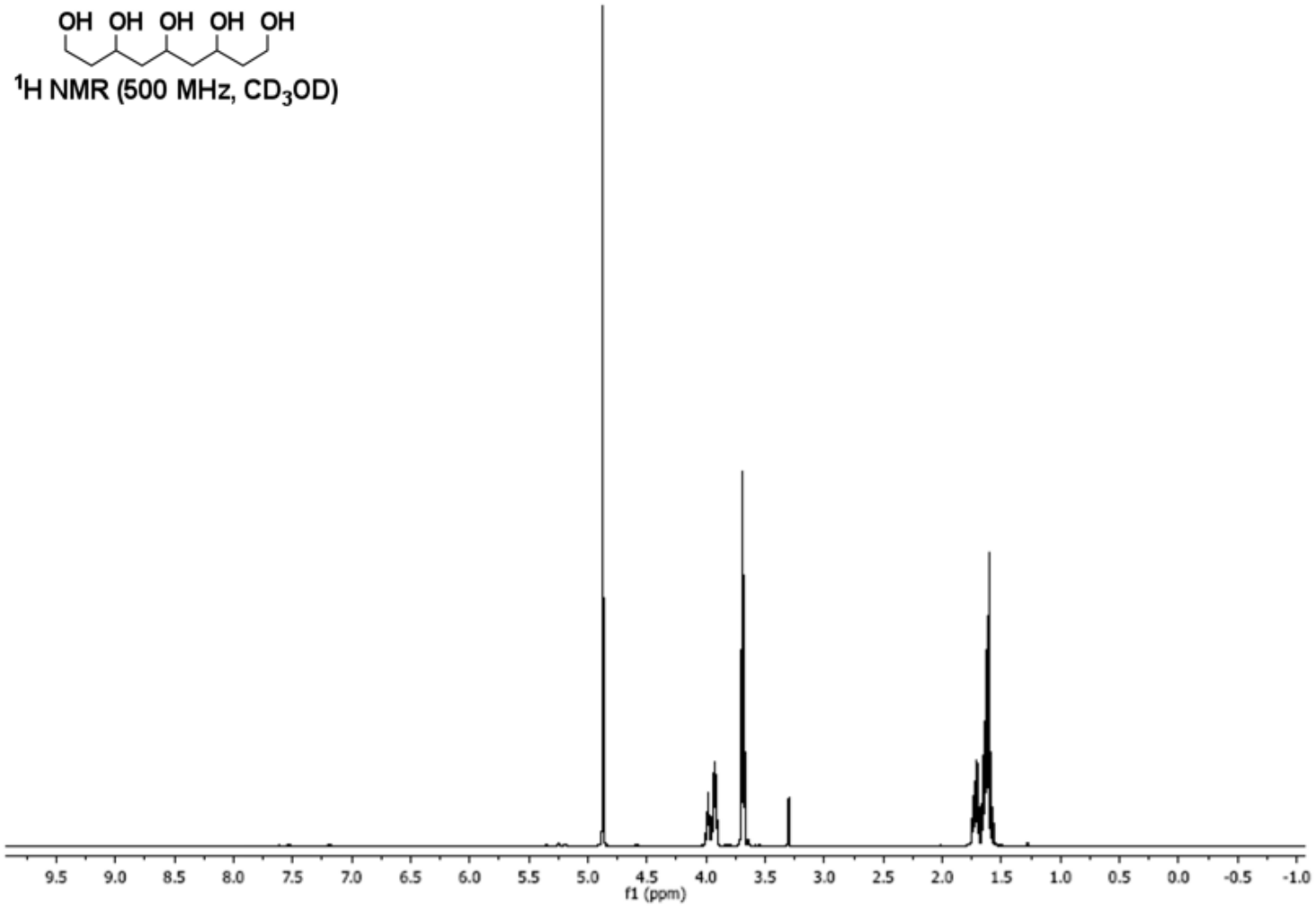
OH OH OH OH OH
^{1}H NMR (500 MHz, CD_3OD)
9.5 9.0 8.5 8.0 7.5 7.0 6.5 6.0 5.5 5.0 4.5 4.0 3.5 3.0 2.5 2.0 1.5 1.0 0.5 0.0 -0.5 -1.0
f1 (ppm)

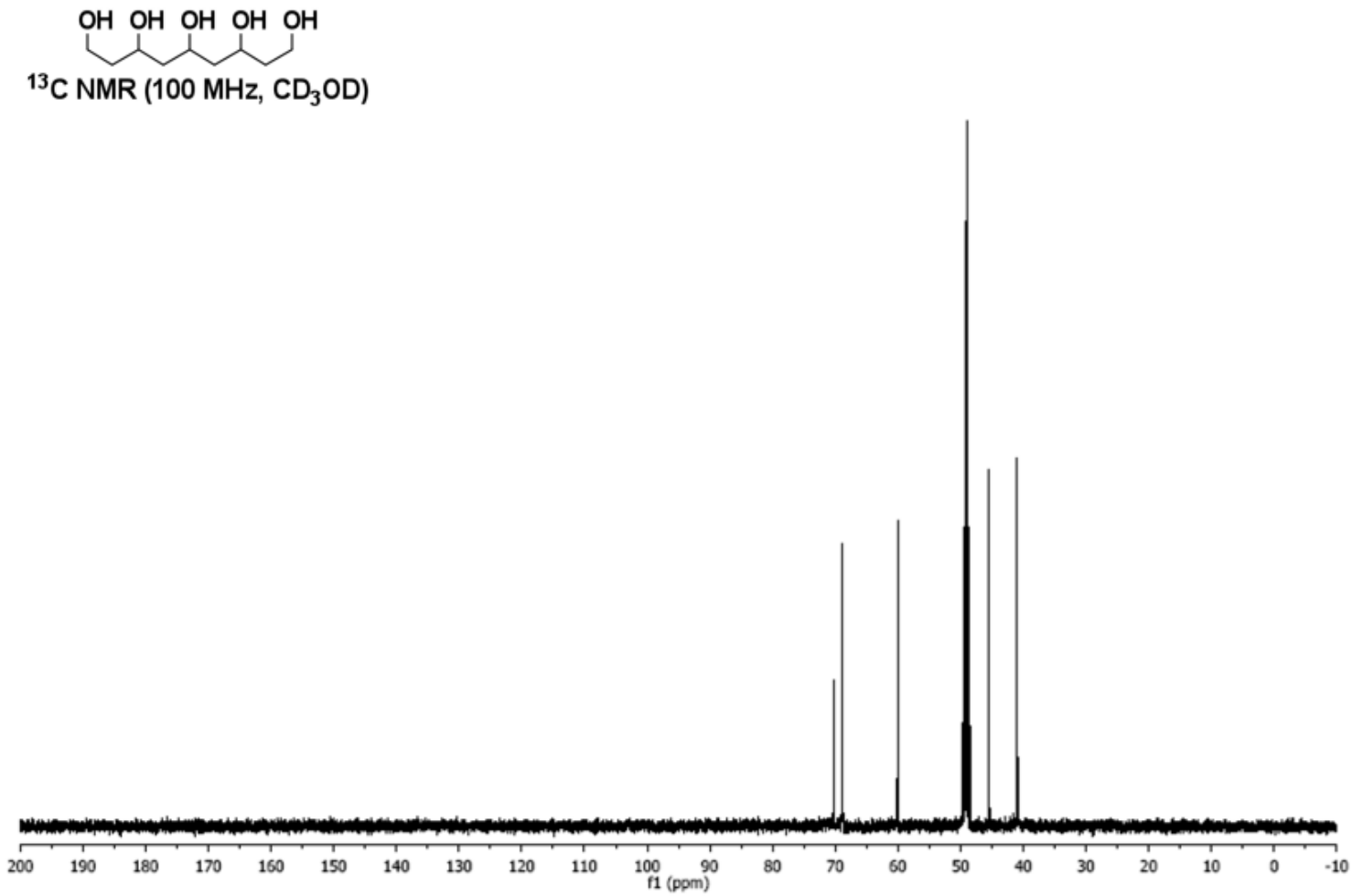
OH OH OH OH OH
13C NMR (100 MHz, CD3OD)
200 190 180 170 160 150 140 130 120 110 100 90 80 70 60 50 40 30 20 10 0 -10
f1 (ppm)

Computed Energies and Geometries

CH_3OH

B3LYP/6-311+g(d,p) = -115.764994, ZPE = 0.051036, thermal correction to the enthalpy = 0.0553315, entropy = 57.0 cal mol^{-1} K^{-1}
B3LYP/6-311+g(d,p)/CPCM (DMSO) = -115.770867
B3LYP/6-311+g(d,p)/CPCM (Acetone) = -115.7707007
B3LYP/6-311+g(d,p)/CPCM (CH_2Cl_2) = -115.7702779
B3LYP/6-311+g(d,p)/CPCM (THF) = -115.7701276
B3LYP/6-311+g(d,p)/CPCM ($CHCl_3$) = -115.76962
B3LYP/6-311+g(d,p)/CPCM (Benzene) =-115.7681798

M06-2X/maug-cc-pVT(+d)Z = -115.717019, ZPE = 0.051823, thermal correction to the enthalpy = 0.056111, entropy = 56.9 cal mol^{-1} K^{-1}
M06-2X/maug-cc-pVT(+d)Z/ CPCM (DMSO) = -115.722209
M06-2X/maug-cc-pVT(+d)Z/ CPCM (Acetone) = -115.72206
M06-2X/maug-cc-pVT(+d)Z/ CPCM (CH_2Cl_2) = -115.72168
M06-2X/maug-cc-pVT(+d)Z/ CPCM (THF) = -115.72154
M06-2X/maug-cc-pVT(+d)Z/ CPCM ($CHCl_3$) = -115.72109
M06-2X/maug-cc-pVT(+d)Z/ CPCM (Benzene) = -115.71979

B3LYP

C	0.66766900	-0.02030600	0.00002400
H	1.08393800	0.98743300	0.00006100
H	1.02859900	-0.54495400	-0.89321900
H	1.02853300	-0.54499200	0.89327100
O	-0.74978100	0.12211700	-0.00002500
H	-1.14883500	-0.75259100	-0.00005800

M06-2X

C	0.66316400	-0.02059000	0.00002400
H	1.08308000	0.98202700	0.00006100
H	1.01993500	-0.54462000	-0.88959600
H	1.01986900	-0.54465800	0.88964800
O	-0.74435000	0.12229500	-0.00002500
H	-1.14706800	-0.74757100	-0.00005700

CH_3O^-

B3LYP/6-311+g(d,p) = -115.145920, ZPE = 0.034696, thermal correction to the enthalpy = 0.038551, entropy = 52.7 cal mol^{-1} K^{-1}
B3LYP/6-311+g(d,p)/CPCM (DMSO) = -115.253637
B3LYP/6-311+g(d,p)/CPCM (Acetone) = -115.2550117
B3LYP/6-311+g(d,p)/CPCM (CH_2Cl_2) = -115.2475416
B3LYP/6-311+g(d,p)/CPCM (THF) = -115.2448683
B3LYP/6-311+g(d,p)/CPCM ($CHCl_3$) = -115.2357595
B3LYP/6-311+g(d,p)/CPCM (Benzene) =-115.2092646

M06-2X/maug-cc-pVT(+d)Z = -115.095347, ZPE = 0.035972, thermal correction to the enthalpy = 0.039821, entropy = 52.7 cal mol^{-1} K^{-1}
M06-2X/maug-cc-pVT(+d)Z/CPCM (DMSO) = -115.206898
M06-2X/maug-cc-pVT(+d)Z/ CPCM (Acetone) = -115.20389
M06-2X/maug-cc-pVT(+d)Z/ CPCM (CH_2Cl_2) =-115.19645
M06-2X/maug-cc-pVT(+d)Z/ CPCM (THF) = -115.19379
M06-2X/maug-cc-pVT(+d)Z/ CPCM ($CHCl_3$) = -115.18472
M06-2X/maug-cc-pVT(+d)Z/ CPCM (Benzene) = -115.15832

B3LYP

C	0.00000000	0.00000000	-0.54046500
H	0.00000000	1.02642800	-1.03789900
H	-0.88891200	-0.51321400	-1.03789900
H	0.88891200	-0.51321400	-1.03789900
O	0.00000000	0.00000000	0.79456100

M06-2X

C	0.00000000	0.00000000	-0.54348400
H	0.00000000	1.02017600	-1.02784800
H	-0.88349800	-0.51008800	-1.02784800
H	0.88349800	-0.51008800	-1.02784800
O	0.00000000	0.00000000	0.79305600

$(HOCH_2CH_2)_2CHOH$

B3LYP/6-311+g(d,p) = -423.557601, ZPE = 0.176081, thermal correction to the enthalpy = 0.185443, entropy = 94.3 cal mol^{-1} K^{-1}
B3LYP/6-311+g(d,p)/CPCM (DMSO) = -423.569883
B3LYP/6-311+g(d,p)/CPCM (Acetone) = -423.569480
B3LYP/6-311+g(d,p)/CPCM (CH_2Cl_2) = -423.568568
B3LYP/6-311+g(d,p)/CPCM (THF) = -423.568246
B3LYP/6-311+g(d,p)/CPCM ($CHCl_3$) = -423.567163
B3LYP/6-311+g(d,p)/CPCM (Benzene) = -423.564146

M06-2X/maug-cc-pVT(+d)Z = -423.410785, ZPE = 0.178269, thermal correction to the enthalpy = 0.187609, entropy = 94.3 cal mol^{-1} K^{-1}
M06-2X/maug-cc-pVT(+d)Z/ CPCM (DMSO) = -423.4219742
M06-2X/maug-cc-pVT(+d)Z/ CPCM (Acetone) = -423.4216512
M06-2X/maug-cc-pVT(+d)Z/ CPCM (CH_2Cl_2) = -423.4208189
M06-2X/maug-cc-pVT(+d)Z/ CPCM (THF) = -423.4205248
M06-2X/maug-cc-pVT(+d)Z/ CPCM ($CHCl_3$) = -423.4195366
M06-2X/maug-cc-pVT(+d)Z/ CPCM (Benzene) = -423.4167563

B3LYP

C	-0.01462800	0.31022100	0.23877300
C	1.28255700	1.00504400	-0.17574100
C	2.54485800	0.34764100	0.39313000
H	1.35488900	1.02475800	-1.26902000
H	1.23999900	2.04408200	0.17217300
H	3.40410500	1.00363100	0.23179500
H	2.43276900	0.21911000	1.48159700
H	-0.10924900	0.38091100	1.33517500
C	-1.25561600	0.94709200	-0.40038800
C	-2.57448200	0.46403900	0.18856300
H	-1.21160300	2.03363300	-0.26494300
H	-3.41497700	0.96015300	-0.31055800
H	-1.23845000	0.75150900	-1.47778300
H	-2.61895800	0.70405100	1.25895100
O	0.10236200	-1.07505600	-0.12158400
O	2.87032100	-0.88706900	-0.22776200
H	2.05594700	-1.40916500	-0.25035800
H	-0.77287700	-1.48058200	-0.04171000
O	-2.66688300	-0.96088700	0.00439900
H	-3.46413500	-1.29221800	0.42822900

M06-2X

C	-0.02058300	0.29910600	0.23815400
C	1.26821200	1.00264300	-0.15517500
C	2.51430600	0.33540900	0.41680100
H	1.35054900	1.02677100	-1.24508500
H	1.21652700	2.03433100	0.20063700
H	3.36894900	1.00408000	0.31616200
H	2.36685900	0.15101200	1.48931400
H	-0.13471400	0.36974600	1.32988500
C	-1.24259300	0.92859800	-0.42351500
C	-2.55739700	0.46610900	0.17183400
H	-1.18974500	2.01439200	-0.31840900
H	-3.39459100	0.94618700	-0.34074400
H	-1.21635600	0.69612200	-1.49064900
H	-2.59963700	0.73959000	1.23103500
O	0.10984200	-1.07187300	-0.12270200
O	2.86172200	-0.85534200	-0.25365700
H	2.06141200	-1.39066300	-0.30680600
H	-0.75775100	-1.48599300	-0.04306400
O	-2.64513000	-0.95122200	0.03284300
H	-3.45464700	-1.26926600	0.43726400

$(HOCH_2CH_2)_2CHO^-$

B3LYP/6-311+g(d,p) = -422.993405, ZPE = 0.160789, thermal correction to the enthalpy = 0.169281, entropy = 89.9 cal mol^{-1} K^{-1}
B3LYP/6-311+g(d,p)/CPCM (DMSO) = -423.0797198
B3LYP/6-311+g(d,p)/CPCM (Acetone) = -423.0772373
B3LYP/6-311+g(d,p)/CPCM (CH_2Cl_2) = -423.0713543
B3LYP/6-311+g(d,p)/CPCM (THF) = -423.0692559
B3LYP/6-311+g(d,p)/CPCM ($CHCl_3$) = -423.0621314
B3LYP/6-311+g(d,p)/CPCM (Benzene) = -423.0416068

M06-2X/maug-cc-pVT(+d)Z = -422.845823, ZPE = 0.162713, thermal correction to the enthalpy = 0.171110, entropy = 89.8 cal mol^{-1} K^{-1}
M06-2X/maug-cc-pVT(+d)Z/ CPCM (DMSO) = -422.9321233
M06-2X/maug-cc-pVT(+d)Z/ CPCM (Acetone) = -422.9296616
M06-2X/maug-cc-pVT(+d)Z/ CPCM (CH_2Cl_2) = -422.923794
M06-2X/maug-cc-pVT(+d)Z/ CPCM (THF) = -422.9217005
M06-2X/maug-cc-pVT(+d)Z/ CPCM ($CHCl_3$) = -422.9145899
M06-2X/maug-cc-pVT(+d)Z/ CPCM (Benzene) = -422.8940853
B3LYP

C	0.00005500	0.35243300	0.29413000
C	1.27747400	1.02705700	-0.26269600
C	2.54249600	0.31637200	0.23189200
H	1.25078200	0.97831700	-1.35978300
H	1.31384700	2.08813000	0.03035800
H	3.44375900	0.80979200	-0.16116200
H	2.58813100	0.40434700	1.33450100
H	0.00011800	0.56419300	1.39616700
C	-1.27749600	1.02718200	-0.26243200
C	-2.54236600	0.31630800	0.23222600
H	-1.31376300	2.08820400	0.03082400
H	-3.44379500	0.81005700	-0.16005800
H	-1.25096000	0.97862100	-1.35951700
H	-2.58750400	0.40356800	1.33490700
O	-0.00002000	-1.01025200	0.04419400
O	2.57402500	-1.04173100	-0.16276700
H	1.60039900	-1.30632300	-0.11492700
O	-2.57416000	-1.04156300	-0.16329500
H	-1.60075600	-1.30665900	-0.11507800

M06-2X

C	0.00004500	0.34869500	0.28748300
C	1.26629300	1.02319100	-0.26524600
C	2.51846800	0.31328500	0.23981500
H	1.24258300	0.95825300	-1.35838700
H	1.29395800	2.08212100	0.01822700
H	3.42301400	0.80246900	-0.14127000
H	2.54812600	0.40113400	1.33919800
H	0.00011700	0.54712400	1.38564200
C	-1.26618300	1.02332900	-0.26506100
C	-2.51836500	0.31333700	0.23988300
H	-1.29379500	2.08220300	0.01862100
H	-3.42286900	0.80268200	-0.14110100
H	-1.24250000	0.95860200	-1.35821500
H	-2.54803200	0.40100000	1.33928100
O	-0.00015000	-1.00700000	0.02384800
O	2.53497000	-1.03412100	-0.15460100
H	1.55194800	-1.28246700	-0.11947100
O	-2.53506100	-1.03403300	-0.15477100
H	-1.55217800	-1.28291200	-0.11957800

$(HOCH_2CH_2CH(OH)CH_2)_2CHOH$

B3LYP/6-311+g(d,p) = -731.351938, ZPE = 0.299823, thermal correction to the enthalpy = 0.314414 , entropy = 130.4 cal mol^{-1} K^{-1},
B3LYP/6-311+g(d,p)/CPCM (DMSO) = -731.3689709
B3LYP/6-311+g(d,p)/CPCM (Acetone) = -731.3685069
B3LYP/6-311+g(d,p)/CPCM (CH_2Cl_2) = -731.3672229
B3LYP/6-311+g(d,p)/CPCM (THF) = -731.3667699
B3LYP/6-311+g(d,p)/CPCM ($CHCl_3$) = -731.365251
B3LYP/6-311+g(d,p)/CPCM (Benzene) = -731.3610324

M06-2X/maug-cc-pVT(+d)Z = -731.107955, ZPE = 0.303528, thermal correction to the enthalpy = 0.318070, entropy = 130.4 cal mol^{-1} K^{-1},
M06-2X/maug-cc-pVT(+d)Z/ CPCM (DMSO) = -731.1234684
M06-2X/maug-cc-pVT(+d)Z/ CPCM (Acetone) = -731.1230361
M06-2X/maug-cc-pVT(+d)Z/ CPCM (CH_2Cl_2) = -731.121874
M06-2X/maug-cc-pVT(+d)Z/ CPCM (THF) = -731.1214638
M06-2X/maug-cc-pVT(+d)Z/ CPCM ($CHCl_3$) = -731.1200871
M06-2X/maug-cc-pVT(+d)Z/ CPCM (Benzene) = -731.1162137

B3LYP

C	-0.01226400	0.12879100	0.18399500
H	-0.09115900	0.18219300	1.28202700
C	-1.26176300	0.77700200	-0.42855900
H	-1.25773500	0.59238800	-1.50879800
H	-1.20688500	1.86068300	-0.27724400
C	1.27661300	0.83585700	-0.24076300
H	1.23106200	1.87054600	0.11711500
H	1.33637200	0.86570700	-1.33480200
C	2.55545600	0.18205600	0.30135800
H	2.43016200	0.01194000	1.38359700
C	3.79260300	1.05756200	0.09524400
H	3.64898000	1.99153100	0.65186200
H	3.88682800	1.31558400	-0.96579600
C	5.09651600	0.40229900	0.56323800
H	4.97476100	0.04207200	1.59736200
H	5.89897100	1.14475600	0.57152800
C	-2.57835400	0.28049800	0.17193300
H	-2.59667800	0.54986200	1.24050500
C	-3.80439300	0.90000800	-0.51061100
H	-3.86500500	0.52515700	-1.53772500
H	-3.67401900	1.98645700	-0.56634700
C	-5.11734100	0.62988700	0.21298600
H	-5.08458400	1.05275200	1.22540500
H	-5.94855800	1.09577800	-0.32831200
O	-5.31576900	-0.79435200	0.28559900
H	-6.11219700	-0.98797900	0.78891000
O	-2.59354800	-1.15220700	0.06223600
H	-3.49396500	-1.45983400	0.24403600

O	0.10014100	-1.24901000	-0.20028300
H	-0.77529400	-1.65471800	-0.09810000
O	2.80611800	-1.07867300	-0.33455400
H	1.96617000	-1.56388200	-0.35569700
O	5.53843300	-0.64759600	-0.28477700
H	4.76734300	-1.21005400	-0.44822300

M06-2X

C	-0.01799300	0.09729400	0.17222300
H	-0.11477300	0.15063800	1.26608100
C	-1.25105400	0.73563400	-0.46039500
H	-1.24603500	0.50804700	-1.53032300
H	-1.18884600	1.82037700	-0.34818200
C	1.26120400	0.81275400	-0.23369400
H	1.20914200	1.84130900	0.13084100
H	1.33039000	0.84650800	-1.32501200
C	2.52796900	0.15626100	0.30735100
H	2.38362700	-0.05952800	1.37612500
C	3.74358900	1.05781900	0.16044400
H	3.57754200	1.95725200	0.75823000
H	3.84495500	1.36294900	-0.88463000
C	5.04083700	0.39155900	0.60502300
H	4.89282300	-0.06623800	1.59220600
H	5.82472600	1.14189500	0.70815700
C	-2.56188000	0.26818200	0.15242800
H	-2.58772100	0.58573900	1.20467100
C	-3.77007500	0.85719400	-0.56827300
H	-3.84020300	0.39887000	-1.55738800
H	-3.61857400	1.92951000	-0.70870200
C	-5.07247500	0.66361400	0.18247900
H	-5.01794400	1.16543800	1.15372600
H	-5.90164500	1.09593500	-0.38236400
O	-5.28242200	-0.73521500	0.36994900
H	-6.09049100	-0.88145600	0.86576000
O	-2.57873200	-1.15539200	0.10203000
H	-3.47233300	-1.45329500	0.31250100
O	0.10873300	-1.26671500	-0.21235900
H	-0.75686600	-1.68236000	-0.10327000
O	2.80888600	-1.06017200	-0.37377600
H	1.98530600	-1.56408100	-0.41628500
O	5.51984000	-0.55836400	-0.32072100
H	4.77574200	-1.13250800	-0.53863600

$(HOCH_2CH_2CH(OH)CH_2)_2CHO^-$

B3LYP/6-311+g(d,p) = -730.807292 , ZPE = 0.283983, thermal correction to the enthalpy = 0.297547, entropy = 125.1 cal mol^{-1} K^{-1}
B3LYP/6-311+g(d,p)/CPCM (DMSO) = -730.883987
B3LYP/6-311+g(d,p)/CPCM (Acetone) = -730.881791
B3LYP/6-311+g(d,p)/CPCM (CH_2Cl_2) = -730.876456
B3LYP/6-311+g(d,p)/CPCM (THF) = -730.874559
B3LYP/6-311+g(d,p)/CPCM ($CHCl_3$) = -730.868134
B3LYP/6-311+g(d,p)/CPCM (Benzene) = -730.849768

M06-2X/maug-cc-pVT(+d)Z = -730.5632552, ZPE = 0.287413, thermal correction to the enthalpy = 0.300832, entropy = 124.7 cal mol^{-1} K^{-1}
M06-2X/maug-cc-pVT(+d)Z/ CPCM (DMSO) = -730.6393946
M06-2X/maug-cc-pVT(+d)Z/ CPCM (Acetone) =-730.6372199
M06-2X/maug-cc-pVT(+d)Z/ CPCM (CH_2Cl_2) = -730.631943
M06-2X/maug-cc-pVT(+d)Z/ CPCM (THF) = -730.6300648
M06-2X/maug-cc-pVT(+d)Z/ CPCM ($CHCl_3$) = -730.6237034
M06-2X/maug-cc-pVT(+d)Z/ CPCM (Benzene) = -730.6054948

B3LYP

H	-0.00000500	0.65010700	1.47232500
C	-0.00000200	0.39782800	0.38390000
C	1.27631000	1.03964400	-0.20871100
H	1.31525900	2.11081600	0.03651600
H	1.24673400	0.94116900	-1.30201600
C	-1.27631100	1.03964100	-0.20871900
H	-1.24673600	0.94114800	-1.30202300
H	-1.31525500	2.11081700	0.03649100
C	-2.54462100	0.34854200	0.30819400
H	-2.57671200	0.47613800	1.40735300
C	2.54461700	0.34853000	0.30819200
H	2.57669800	0.47609400	1.40735600
C	3.83724600	0.94076100	-0.26411500
H	3.91382600	1.99195100	0.04514700
H	3.79068000	0.91847900	-1.35977700
C	5.09447000	0.19573900	0.19366900
H	5.11998500	0.17371000	1.29653400
H	5.99314400	0.72777300	-0.13924000
C	-3.83724600	0.94075600	-0.26414100
H	-3.79067100	0.91844500	-1.35980100
H	-3.91383100	1.99195400	0.04509300
C	-5.09447100	0.19574200	0.19365100
H	-5.99314600	0.72776400	-0.13927700
H	-5.11999500	0.17374000	1.29651700
O	5.18248900	-1.12249400	-0.33058600
H	4.27366100	-1.47704800	-0.27619700

O	2.50394400	-1.04340200	0.00464800
H	1.50444600	-1.27622600	0.06226900
O	-5.18248000	-1.12250300	-0.33057300
H	-4.27365100	-1.47704900	-0.27615600
O	-2.50394500	-1.04340000	0.00469300
O	0.00000000	-0.98153400	0.19369300
H	-1.50445000	-1.27622500	0.06234700

M06-2X

H	-0.00000600	0.64394900	1.46018600
C	-0.00000400	0.39814100	0.37612100
C	1.26573000	1.03368500	-0.21627300
H	1.30339000	2.10373200	0.01554300
H	1.23857000	0.91564000	-1.30523200
C	-1.26573600	1.03368700	-0.21627800
H	-1.23857700	0.91563500	-1.30523500
H	-1.30339100	2.10373600	0.01553100
C	-2.52081100	0.34303900	0.30783700
H	-2.54944900	0.47665000	1.40363500
C	2.52080200	0.34302600	0.30783700
H	2.54944300	0.47663800	1.40363600
C	3.80428900	0.93424500	-0.26232100
H	3.87434200	1.98526600	0.03424600
H	3.76135300	0.89229900	-1.35471000
C	5.04799300	0.19176600	0.20926900
H	5.04543900	0.15439400	1.30827600
H	5.95014600	0.72783600	-0.09525500
C	-3.80429600	0.93425500	-0.26232300
H	-3.76135600	0.89231400	-1.35471100
H	-3.87435900	1.98527400	0.03424900
C	-5.04799400	0.19175800	0.20925600
H	-5.95015300	0.72780200	-0.09529700
H	-5.04546100	0.15440500	1.30826300
O	5.14034700	-1.10918700	-0.32998700
H	4.23526400	-1.46531200	-0.29027900
O	2.47108500	-1.03633500	0.00639900
H	1.46038100	-1.25414000	0.05893300
O	-5.14030300	-1.10920800	-0.32997800
H	-4.23521700	-1.46531800	-0.29021900
O	-2.47110100	-1.03632300	0.00639800
O	-0.00000200	-0.97623300	0.18101300
H	-1.46040400	-1.25412200	0.05893500

$(HOCH_2CH_2CH(OH)CH_2CH(OH)CH_2)_2CHOH$

B3LYP/6-311+g(d,p) = -1039.146894, ZPE = 0.423514, thermal correction to the enthalpy = 0.443311, entropy = 166.4 cal mol^{-1} K^{-1}
B3LYP/6-311+g(d,p)/CPCM (DMSO) = -1039.168162
B3LYP/6-311+g(d,p)/CPCM (Benzene) = -1039.158206

M06-2X/maug-cc-pVT(+d)Z = -1038.805728, ZPE = 0.428828, thermal correction to the enthalpy = 0.448537, entropy = 165.9 cal mol^{-1} K^{-1}
M06-2X/maug-cc-pVT(+d)Z/ CPCM (DMSO) = -1038.825041
M06-2X/maug-cc-pVT(+d)Z/ CPCM (Benzene) = -1038.815987

B3LYP

C	0.01025700	0.06081700	0.09485400
H	0.07626300	-0.05440900	1.18893400
C	-1.27126400	-0.62459400	-0.38514000
H	-1.22943300	-1.67690800	-0.08278000
H	-1.31594600	-0.59546700	-1.47990800
C	-2.55728400	-0.00065800	0.17401400
H	-2.45074500	0.10279800	1.26618900
C	-3.79255500	-0.85834800	-0.10947300
H	-3.65483200	-1.82760700	0.38291500
H	-3.87314300	-1.04221100	-1.18708600
C	-5.10849700	-0.23833700	0.38069400
H	-4.97514400	0.08445300	1.42661500
C	-6.27579100	-1.22554900	0.33048400
H	-6.04658700	-2.06292400	1.00064400
H	-6.37093900	-1.62975900	-0.68386800
C	-7.61787000	-0.61503400	0.74819500
H	-7.50407200	-0.11238400	1.72207300
H	-8.35889900	-1.40841200	0.87811100
C	1.26964900	-0.54664300	-0.53797000
H	1.27440400	-0.30631800	-1.60728600
H	1.22121400	-1.63708700	-0.44332200
C	2.57599000	-0.06977600	0.10130400
H	2.58679300	-0.39622800	1.15379000
C	3.81321900	-0.64361000	-0.60278200
H	3.88299600	-0.20163500	-1.60314700
H	3.67992300	-1.72397800	-0.72620800
C	5.12233300	-0.40978600	0.15393300
H	5.06378500	-0.93464600	1.12122700
C	6.34398200	-0.93047100	-0.61347900
H	6.48343300	-0.32117300	-1.51261800
H	6.15147400	-1.95797900	-0.94146600

C	7.62923100	-0.94016400	0.20426400
H	7.51660000	-1.59508900	1.07789200
H	8.45947000	-1.31657500	-0.40383400
O	-0.10308200	1.45793800	-0.21177300
H	0.77291000	1.85711500	-0.08193100
O	2.57664400	1.36483200	0.06728700
H	3.47068000	1.66408400	0.29882200
O	5.23124300	1.00072300	0.40620700
H	6.13809600	1.18828800	0.69144000
O	7.90674500	0.40514200	0.63556500
H	8.68757700	0.41425800	1.19718100
O	-2.79084500	1.29871800	-0.38773700
H	-1.94592000	1.77765600	-0.37346600
O	-5.47218600	0.90305300	-0.40784900
H	-4.67221300	1.44096300	-0.52180400
O	-8.15847000	0.27667100	-0.21597200
H	-7.43652600	0.86746400	-0.47630000

M06-2X

C	0.01460400	0.11707100	0.08414700
H	0.09304100	-0.02963300	1.17085200
C	-1.25433300	-0.56486200	-0.40427900
H	-1.20680800	-1.61981200	-0.12469900
H	-1.30249300	-0.50867200	-1.49577900
C	-2.53210000	0.04459900	0.16419900
H	-2.41165100	0.16630800	1.25024300
C	-3.74421300	-0.83821600	-0.09018600
H	-3.58930800	-1.79015900	0.42307200
H	-3.82787300	-1.04412400	-1.16144200
C	-5.05810300	-0.22460300	0.38436800
H	-4.91772500	0.16150200	1.40459900
C	-6.18712400	-1.24287500	0.40861400
H	-5.92861200	-2.02432800	1.12726900
H	-6.27680300	-1.70879600	-0.57651700
C	-7.53306600	-0.63610900	0.78871900
H	-7.41230800	-0.02587000	1.69372900
H	-8.24306000	-1.42935200	1.02308900
C	1.26115200	-0.45995700	-0.57931700
H	1.26879500	-0.14770100	-1.62773300
H	1.20621800	-1.55064300	-0.55484400
C	2.55902500	-0.03102600	0.08802900
H	2.57447000	-0.43277300	1.11117900
C	3.78134700	-0.55123200	-0.66208400
H	3.86483500	-0.00428100	-1.60569300

H	3.63256300	-1.60713200	-0.89876800
C	5.07869200	-0.41594800	0.11980600
H	5.01228200	-1.04605600	1.01822200
C	6.28644600	-0.85557300	-0.70094000
H	6.45011600	-0.12356300	-1.49511600
H	6.07071100	-1.81615600	-1.17338500
C	7.54938700	-1.01247700	0.12245900
H	7.40012400	-1.78102200	0.88742500
H	8.38039000	-1.31963900	-0.51655800
O	-0.11237600	1.50878400	-0.18377300
H	0.75284100	1.91340200	-0.03114200
O	2.56136100	1.39055900	0.15207200
H	3.44794800	1.66942400	0.41864700
O	5.19936300	0.94539800	0.52177100
H	6.09779800	1.08526900	0.84620200
O	7.84230800	0.23891400	0.74208100
H	8.63061400	0.16060000	1.28310200
O	-2.79477500	1.31757800	-0.41466700
H	-1.96724600	1.81804100	-0.39958800
O	-5.46123000	0.84575900	-0.46102500
H	-4.68682600	1.40686300	-0.60314400
O	-8.11178200	0.12038400	-0.25144900
H	-7.42527100	0.71655900	-0.57451800

$(HOCH_2CH_2CH(OH)CH_2CH(OH)CH_2)_2CHO^-$

B3LYP/6-311+g(d,p) = -1038.611433, ZPE = 0.407319, thermal correction to the enthalpy = 0.425997, entropy = 160.7 cal mol^{-1} K^{-1},
B3LYP/6-311+g(d,p)/CPCM (DMSO) = -1038.684268,
B3LYP/6-311+g(d,p)/CPCM (Benzene) = -1038.651475

M06-2X/maug-cc-pVT(+d)Z = -1038.270388, ZPE = 0.412064, thermal correction to the enthalpy = 0.430564, entropy = 160.7 cal mol^{-1} K^{-1},
M06-2X/maug-cc-pVT(+d)Z/ CPCM (DMSO) = -1038.342379,
M06-2X/maug-cc-pVT(+d)Z/ CPCM (Benzene) = -1038.309940

B3LYP

C	0.47630500	-0.44165100	0.00000000
H	0.79776800	-1.51035100	0.00000000
C	1.07294500	0.19378500	-1.27648900
H	2.15748000	0.02061600	-1.31963400
H	0.90163100	1.27775800	-1.24526100
C	0.41189500	-0.36830400	-2.54148300
H	0.61985700	-1.45414700	-2.58058300
C	0.95068300	0.25648800	-3.83432100

H	2.02028300	0.02628500	-3.91937000
H	0.84646000	1.34713900	-3.78063300
C	0.23087500	-0.24202400	-5.09272600
H	0.26831000	-1.34524600	-5.09920900
C	0.87022300	0.26125400	-6.38920700
H	1.89822900	-0.11924100	-6.43947600
H	0.92281600	1.35625200	-6.36818200
C	0.12168600	-0.17626800	-7.65177600
H	-0.00175700	-1.27176100	-7.63991300
H	0.70962300	0.07359000	-8.54093800
C	1.07294500	0.19378500	1.27648900
H	0.90163100	1.27775800	1.24526100
H	2.15748000	0.02061600	1.31963400
C	0.41189500	-0.36830400	2.54148300
H	0.61985700	-1.45414700	2.58058300
C	0.95068300	0.25648800	3.83432100
H	0.84646000	1.34713900	3.78063300
H	2.02028300	0.02628500	3.91937000
C	0.23087500	-0.24202400	5.09272600
H	0.26831000	-1.34524600	5.09920900
C	0.87022300	0.26125400	6.38920700
H	0.92281600	1.35625200	6.36818200
H	1.89822900	-0.11924100	6.43947600
C	0.12168600	-0.17626800	7.65177600
H	-0.00175700	-1.27176100	7.63991300
H	0.70962300	0.07359000	8.54093800
O	-0.91515700	-0.34300800	0.00000000
O	-0.99842700	-0.16911600	2.48588400
H	-1.21896900	-0.23859700	1.47793700
O	-1.14334200	0.16729800	5.09494900
H	-1.45271800	0.08206500	4.16601300
O	-1.13765700	0.46409400	7.81152400
H	-1.55285500	0.44964800	6.93280900
O	-0.99842700	-0.16911600	-2.48588400
H	-1.21896900	-0.23859700	-1.47793700
O	-1.14334200	0.16729800	-5.09494900
H	-1.45271800	0.08206500	-4.16601300
O	-1.13765700	0.46409400	-7.81152400
H	-1.55285500	0.44964800	-6.93280900

M06-2X

C	0.47725900	-0.42928400	0.00000000
H	0.80192100	-1.49121700	0.00000000
C	1.06166700	0.21118400	-1.26587400

H	2.14561100	0.06109200	-1.30791500
H	0.86153500	1.28779100	-1.23657600
C	0.40670000	-0.36319300	-2.51783100
H	0.62842200	-1.44366600	-2.55334800
C	0.93907800	0.26281500	-3.80173800
H	2.00882200	0.05017500	-3.88648700
H	0.81109500	1.34885800	-3.75152100
C	0.22334900	-0.24716300	-5.04653400
H	0.25964500	-1.34766800	-5.04160200
C	0.86840200	0.24223700	-6.33474900
H	1.89183900	-0.13989400	-6.37645400
H	0.91717000	1.33478500	-6.32047200
C	0.11654900	-0.20089900	-7.58361900
H	-0.04719200	-1.28644700	-7.53793200
H	0.71523400	0.00107500	-8.47359000
C	1.06166700	0.21118400	1.26587400
H	0.86153500	1.28779100	1.23657600
H	2.14561100	0.06109200	1.30791500
C	0.40670000	-0.36319300	2.51783100
H	0.62842200	-1.44366600	2.55334800
C	0.93907800	0.26281500	3.80173800
H	0.81109500	1.34885800	3.75152100
H	2.00882200	0.05017500	3.88648700
C	0.22334900	-0.24716300	5.04653400
H	0.25964500	-1.34766800	5.04160200
C	0.86840200	0.24223700	6.33474900
H	0.91717000	1.33478500	6.32047200
H	1.89183900	-0.13989400	6.37645400
C	0.11654900	-0.20089900	7.58361900
H	-0.04719200	-1.28644700	7.53793200
H	0.71523400	0.00107500	8.47359000
O	-0.91034600	-0.33845100	0.00000000
O	-0.99259500	-0.17541900	2.45450400
H	-1.19861500	-0.24210900	1.43481600
O	-1.13677800	0.16665000	5.05208000
H	-1.44334400	0.08578000	4.12516400
O	-1.10836300	0.47878000	7.75971200
H	-1.53415300	0.48751400	6.89019400
O	-0.99259500	-0.17541900	-2.45450400
H	-1.19861500	-0.24210900	-1.43481600
O	-1.13677800	0.16665000	-5.05208000
H	-1.44334400	0.08578000	-4.12516400
O	-1.10836300	0.47878000	-7.75971200
H	-1.53415300	0.48751400	-6.89019400

Appendix for chapter 7

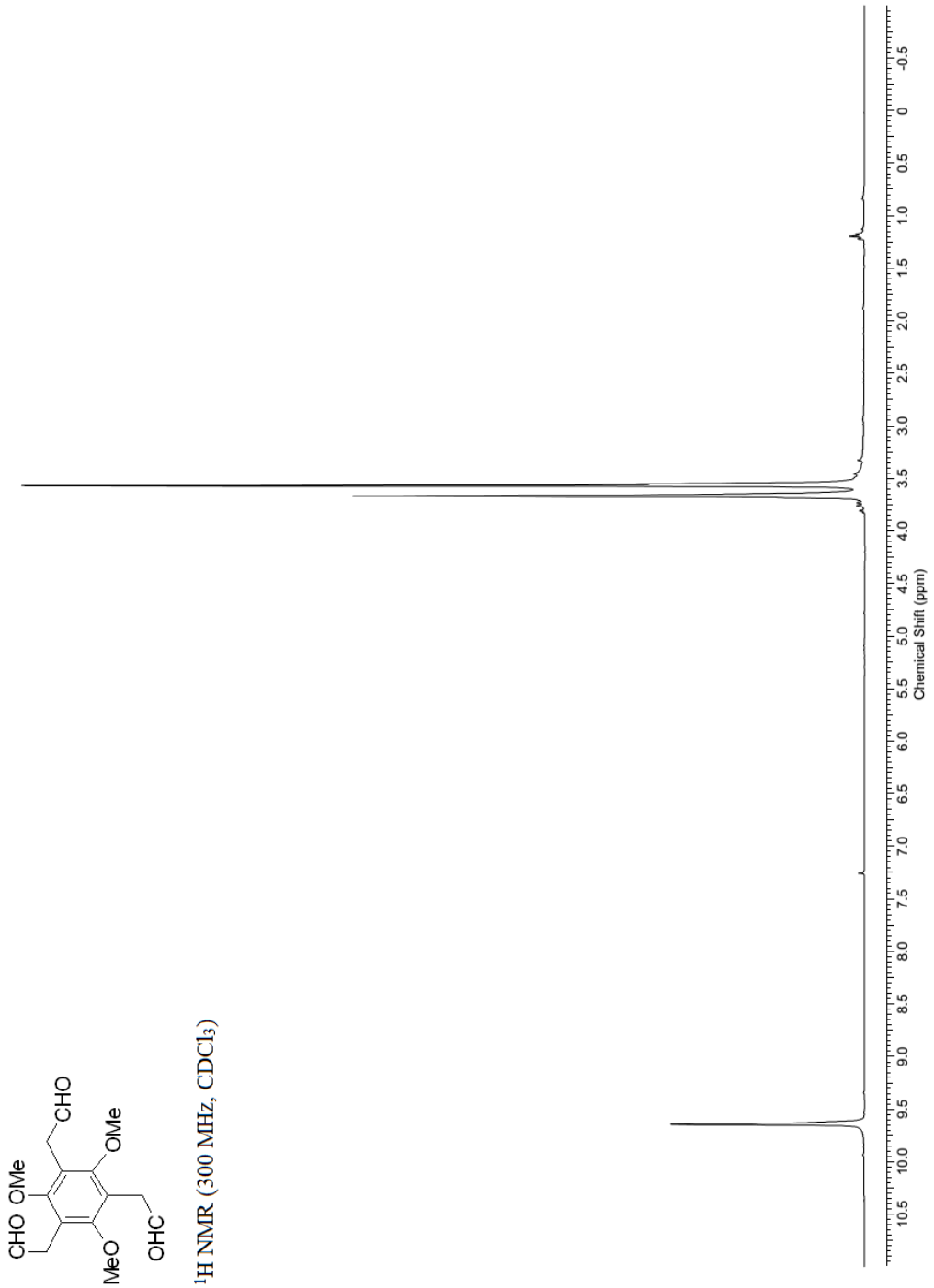

^{1}H NMR (300 MHz, $CDCl_3$)

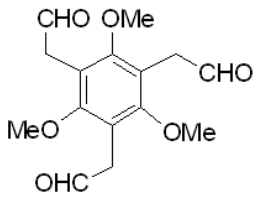

^{13}C NMR (75 MHz, $CDCl_3$)

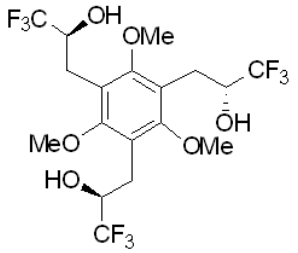

^{1}H NMR (300 MHz, $CDCl_3$)

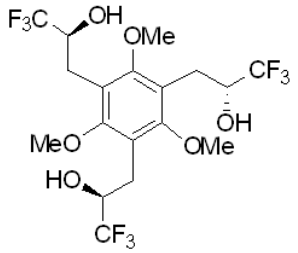

^{13}C NMR (75 MHz, $CDCl_3$)

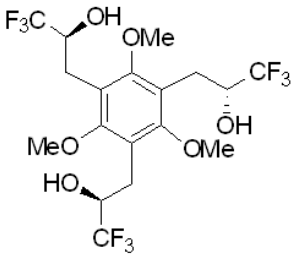

^{19}F NMR (282 MHz, $CDCl_3$)

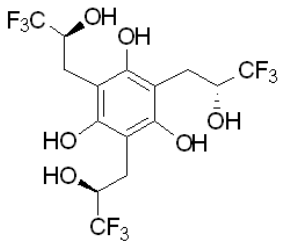

^{1}H NMR (300 MHz, CD_3CN)

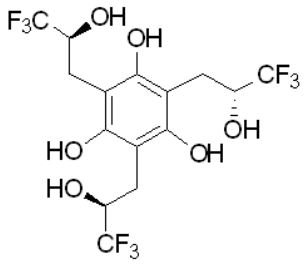

^{13}C NMR (75 MHz, CD_3CN)

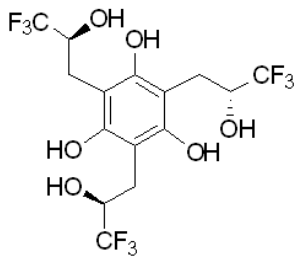

^{19}F NMR (282 MHz, CD_3CN)

1

B3LYP/ aug-cc-pVDZ = -1930.874134, ZPE = 0.311664, thermal correction to the enthalpy = 0.336652

C	0.57158800	1.26938900	-0.39088700
C	-0.67030800	-1.23674100	-0.08889000
C	-0.79138000	1.16725200	-0.05810200
C	1.29712400	0.07276200	-0.54144300
C	0.68854600	-1.19218500	-0.44953800
C	-1.42806700	-0.07251300	0.13445700
C	1.17920100	2.62387700	-0.69205800
H	0.36707300	3.32690700	-0.90285400
H	1.81485700	2.56718600	-1.58765300
C	-2.84568900	-0.17818800	0.65697000
H	-3.01990800	0.57223400	1.44154300
H	-2.97807500	-1.16842200	1.10446800
C	-3.92448800	0.00923000	-0.41280900
H	-3.72043200	-0.63785900	-1.27859400
C	1.47608500	-2.43777700	-0.80362500
H	2.33753800	-2.14771600	-1.41304700
H	0.85825100	-3.11912500	-1.40580000
C	1.98973400	-3.22162600	0.40672000
C	2.02758800	3.20184200	0.44308100
H	1.47303600	3.16523500	1.39247000
O	3.22944800	2.43332600	0.52692300
O	-3.92764400	1.38584300	-0.79663500
H	-4.47426200	1.51733400	-1.58118900
O	0.86810800	-3.84607300	1.03417000
H	1.12301700	-4.22420400	1.88488400
H	3.73253400	2.67655600	1.31397900
C	2.39289400	4.67157600	0.21543000
C	-5.32178800	-0.36891100	0.08716900
C	3.00746100	-4.29976700	0.02301000
F	4.14984400	-3.74892800	-0.44779700
F	2.54670400	-5.15658900	-0.91257800
F	3.34127000	-5.04437500	1.11728100
F	-5.67785900	0.28595600	1.21310400
F	-6.25884900	-0.07396600	-0.85971700
F	-5.41013000	-1.69569600	0.33642700
F	3.00268200	4.89027100	-0.96900700
F	1.29692800	5.46243100	0.26792000
F	3.24692900	5.10173800	1.18957800
O	-1.32376000	-2.43131100	0.06314900
H	-0.69053000	-3.11193500	0.35351200
O	-1.47370500	2.34401500	0.10383800
H	-2.41110600	2.20590700	-0.12250400
O	2.63020600	0.08730000	-0.85508900

H	3.03363400	0.90373600	-0.51113700
H	2.50447300	-2.54752700	1.10726100

1a (Hexaol anion)

B3LYP/ aug-cc-pVDZ = -1930.361405, ZPE = 0.297738, thermal correction to the enthalpy = 0.322021, M06-2X/maug-cc-pVT(+d)Z = -1930.225304

C	1.42739400	-0.06562000	-1.12282800
C	-1.24452700	0.15577500	-0.14050800
C	0.82487600	1.21815200	-0.95685700
C	0.63404900	-1.23791300	-0.92773900
C	-0.65561400	-1.08853000	-0.41545000
C	-0.47626300	1.29426000	-0.44590200
C	1.18467900	-2.56723000	-1.40319300
H	1.62330200	-2.41396100	-2.40133600
H	0.37453200	-3.29808400	-1.53635600
C	2.31456100	-3.22925900	-0.58384900
H	2.50976600	-4.22434400	-1.02576300
C	1.58034000	2.43402100	-1.45706200
H	0.89614600	3.28200100	-1.60187400
H	1.98357600	2.19524600	-2.45353200
C	2.80696300	2.92495500	-0.65573200
C	-2.60131500	0.26640100	0.51784700
H	-2.66865900	1.23251600	1.02998700
H	-2.71861800	-0.52610800	1.27024500
C	-3.78003700	0.16824000	-0.46894900
H	-3.68905800	0.96502500	-1.22490100
O	2.68173300	-0.17040300	-1.48573600
O	-1.08914400	2.51423800	-0.20533900
O	-1.46251100	-2.19764800	-0.15039200
C	-5.11870300	0.42321500	0.22969800
C	1.89855700	-3.54692400	0.86025700
O	-3.87964700	-1.08098500	-1.12998000
H	-3.16721200	-1.65943000	-0.81066300
F	0.68107200	-4.21121100	0.88357400
F	2.78033600	-4.38449500	1.46564500
F	1.76221400	-2.47347700	1.65677800
F	-5.37297100	-0.45202600	1.23654900
F	-6.16666900	0.34146500	-0.63200900
F	-5.16632300	1.67362200	0.77378700
H	-0.41191000	3.18821400	-0.07015900
H	-0.91257900	-2.97421100	0.01200600
O	3.50536800	-2.49597900	-0.57411400
H	3.29789000	-1.57140700	-0.90813800
H	3.15277700	3.86740500	-1.12036300

C	2.46039200	3.33526400	0.78300700
O	3.86845700	2.01420100	-0.63645100
H	3.51507800	1.12694700	-0.94753400
F	2.15149900	2.31470800	1.60139500
F	3.47698200	4.02190600	1.36803800
F	1.37484200	4.19550200	0.79824800

1$^{\bullet}$ (Hexaol Radical)

B3LYP/ aug-cc-pVDZ = -1930.225801, ZPE = 0.298749, thermal correction to the enthalpy = 0.323314, M06-2X/maug-cc-pVT(+d)Z = -1930.082474

C	-1.41662200	0.05365100	-1.16462200
C	1.17755700	-0.11021300	-0.07163200
C	-0.80195500	-1.25305100	-0.97668600
C	-0.65170000	1.27571200	-0.94807900
C	0.59982200	1.15765600	-0.37293300
C	0.45523200	-1.29638100	-0.40176600
C	-1.22675600	2.58958100	-1.42672200
H	-1.68208900	2.42577900	-2.41284900
H	-0.41440400	3.31131400	-1.58081500
C	-2.33094300	3.26782100	-0.57928600
H	-2.49473100	4.27287400	-1.00033400
C	-1.53005800	-2.48004300	-1.47826600
H	-0.81041900	-3.29139700	-1.64837400
H	-1.96227200	-2.24511300	-2.46049700
C	-2.70709000	-3.03799600	-0.64137900
C	2.52940700	-0.19968300	0.57625900
H	2.57205700	-1.09134300	1.21017600
H	2.69308300	0.68620200	1.20041700
C	3.66660600	-0.29297800	-0.46917900
H	3.58484400	-1.23308900	-1.02892300
O	-2.62960100	0.13110500	-1.51813700
O	1.11303000	-2.45654900	-0.11545000
O	1.38472900	2.23590400	-0.06321500
C	5.03564500	-0.32437000	0.22447800
C	-1.89685400	3.51968200	0.87196800
O	3.63838000	0.74229000	-1.42833400
H	3.47653400	1.58614700	-0.98319100
F	-0.66308700	4.15082200	0.89504100
F	-2.74966100	4.32973000	1.52014900
F	-1.76320400	2.39306100	1.60030900
F	5.28326000	0.83043900	0.89693900
F	6.03787000	-0.49651700	-0.66124500
F	5.11041800	-1.33933800	1.12384800
H	0.49209400	-3.19368500	-0.03128000

H	0.84279000	3.02493200	0.08036200
O	-3.55747400	2.58790800	-0.58296400
H	-3.40979200	1.67269400	-0.89311800
H	-2.99044300	-4.00737200	-1.08220600
C	-2.30558700	-3.37015700	0.80295200
O	-3.84347500	-2.21595900	-0.62847200
H	-3.58778500	-1.31951100	-0.92216400
F	-2.03223400	-2.28265600	1.55218000
F	-3.25379000	-4.07873400	1.43854700
F	-1.16228000	-4.15029800	0.80920400

1 • Cl^-

B3LYP/ aug-cc-pVDZ = -2391.239338, ZPE = 0.312803, thermal correction to the enthalpy = 0.338147, M06-2X/maug-cc-pVT(+d)Z = -2391.095834

C	1.55375300	0.01718800	-1.44348900
C	-1.23881600	0.29321200	-1.54814500
C	0.95028000	1.27939700	-1.47855100
C	0.71145900	-1.10700400	-1.42850800
C	-0.68239400	-0.99563100	-1.50580500
C	-0.44321100	1.44715000	-1.54368100
C	3.04200600	-0.12320000	-1.22470000
H	3.56836200	0.73647700	-1.65147800
H	3.41325400	-1.03403300	-1.71329700
C	-1.05090200	2.82940000	-1.51350100
H	-2.08081600	2.78733600	-1.88078900
H	-0.48142400	3.47639100	-2.19473400
C	-1.03147700	3.52708100	-0.11539700
H	-0.90707200	4.60764800	-0.27505700
C	-1.56206900	-2.20976500	-1.32658000
H	-1.05877800	-3.10392900	-1.70791900
H	-2.50455400	-2.08019700	-1.87436000
C	-1.87031700	-2.40485400	0.17609100
H	-0.94669800	-2.67898500	0.70519100
C	3.34629200	-0.20237800	0.28822500
H	3.09671600	0.75726200	0.76282900
O	2.63047500	-1.25635200	0.91302100
O	0.04998700	3.14176300	0.71138300
H	-0.04947400	2.21375200	1.04641800
O	-2.43829800	-1.23934900	0.75184800
H	-1.71833300	-0.75042900	1.22224100
Cl	0.09701200	0.19102800	2.00943900
H	1.82899800	-0.86181400	1.34702400
C	4.83033400	-0.43736800	0.55966000
C	-2.36055600	3.42966000	0.64348000
C	-2.85077100	-3.55125600	0.41149000

F	-2.38188700	-4.71642100	-0.12353700
F	-4.06764300	-3.32734300	-0.15157300
F	-3.06533600	-3.78848900	1.72784400
F	-2.70132200	2.17860300	1.00367300
F	-2.33201500	4.17845100	1.77794200
F	-3.38140500	3.92815400	-0.11736400
F	5.27507100	-1.62238100	0.06387600
F	5.59507000	0.53725100	-0.01391900
F	5.12285000	-0.43082600	1.88224600
O	-2.60926400	0.45273200	-1.52574100
H	-2.93266500	-0.07825200	-0.77249900
O	1.77339500	2.38768500	-1.36976300
H	1.40690100	2.92282800	-0.63940600
O	1.24288700	-2.36813000	-1.25063100
H	1.89083000	-2.29111700	-0.52178100

1 • $Cl^{\bullet}$

B3LYP/ aug-cc-pVDZ = -2391.071480 , ZPE = 0.313350, thermal correction to the enthalpy = 0.338914, M06-2X/maug-cc-pVT(+d)Z = -2390.911790

C	0.02665600	1.43973900	-1.39055800
C	-0.04111300	-1.34957500	-1.26573500
C	-1.22030900	0.70813400	-1.34605200
C	1.24070200	0.71687400	-1.35931200
C	1.24089400	-0.67102500	-1.31614900
C	-1.27606400	-0.67928900	-1.37866400
C	0.02446000	2.92662400	-1.23412800
H	-0.90174900	3.35831600	-1.62353100
H	0.87956400	3.35853300	-1.76902100
C	-2.57822000	-1.43201300	-1.23981300
H	-2.47893800	-2.43822600	-1.65880100
H	-3.36454300	-0.91192800	-1.80305300
C	-2.99475700	-1.52650600	0.24454000
C	2.52303700	-1.44675300	-1.20087300
H	3.34758000	-0.84839300	-1.59825800
H	2.45966200	-2.37894300	-1.77829700
C	2.81827300	-1.79740100	0.27985000
H	3.01097500	-0.88129200	0.85245000
C	0.15014800	3.27833700	0.28066500
H	-0.77402100	2.99745200	0.80232400
O	1.26994500	2.64202300	0.86902900
O	-3.00254800	-0.23463200	0.84365900
H	-2.16429100	-0.13351600	1.35222100
O	1.73449500	-2.51606700	0.85750500
H	1.19658200	-1.87475600	1.38795400
Cl	0.01854200	-0.11181600	1.91487400

H	0.95801200	1.83948500	1.35069300
C	0.31969300	4.78834300	0.46880100
C	4.06918100	-2.67098000	0.40062100
F	5.13906000	-2.04247600	-0.15029400
F	3.92192400	-3.85610500	-0.23926700
F	4.36733700	-2.93380400	1.68661800
F	1.46094800	5.24469400	-0.10011900
F	-0.71451200	5.45701100	-0.10503000
F	0.34845000	5.12403900	1.77209800
O	-0.07714600	-2.65177900	-1.02219800
H	0.69084500	-2.88943500	-0.42369400
O	-2.31160900	1.46008000	-1.13682000
H	-2.90835200	0.95778500	-0.52793100
O	2.43427800	1.36900300	-1.29402600
H	2.35671200	2.03935400	-0.58169500
C	-4.39606000	-2.11781700	0.39982900
F	-4.45784900	-3.34462500	-0.18265300
F	-4.73823500	-2.26510200	1.69418200
F	-5.34151500	-1.34493100	-0.18879700
H	-2.31218300	-2.19104600	0.78981100

1 • OAc^-

B3LYP/ aug-cc-pVDZ = -2159.886483, ZPE = 0.363353, thermal correction to the enthalpy = 0.391139, M06-2X/maug-cc-pVT(+d)Z = -2159.360753

C	-0.51818200	1.27581500	-1.47976400
C	0.58146400	-1.30499200	-1.52888800
C	-1.33113600	0.13928400	-1.50280700
C	0.87131700	1.07912200	-1.46753600
C	1.43990300	-0.19648900	-1.52348500
C	-0.81314200	-1.16271600	-1.50868700
C	-1.11296300	2.65990800	-1.36717500
H	-2.13449400	2.65752900	-1.74785700
H	-0.53177100	3.37177600	-1.96104900
C	-1.71201000	-2.36445200	-1.33073800
H	-2.58101800	-2.31479900	-2.00052600
C	-2.19090100	-2.51607200	0.14150600
H	-2.52947700	-1.54096200	0.51836000
C	2.93431400	-0.37033300	-1.38917700
H	3.44544800	0.52093800	-1.75153800
H	3.27455200	-1.22644900	-1.97868900
C	3.29873100	-0.60677300	0.09267800
C	-1.11589800	3.13943300	0.10058300
H	-1.72028900	2.45277100	0.70341500
O	0.19497100	3.23893200	0.61921900
O	-1.22798800	-3.07972900	0.98378700
H	-0.63534100	-2.38261600	1.35449900
O	2.68444200	-1.78139800	0.58817600

H	1.90950300	-1.51890200	1.16404800
H	0.37382100	2.47095000	1.22890000
C	-1.77673200	4.51006100	0.24993900
C	-3.43047700	-3.40840500	0.22003200
C	4.80523200	-0.75253900	0.28927800
F	5.46804200	0.35078600	-0.15212200
F	5.32435600	-1.80841700	-0.38425200
F	5.14313100	-0.91258300	1.58658000
F	-3.22520700	-4.65402100	-0.25562100
F	-3.90030300	-3.53299500	1.47712500
F	-4.45198300	-2.87338200	-0.51909500
F	-1.13388700	5.47990500	-0.43856400
F	-3.05755000	4.48797900	-0.20796900
F	-1.83461800	4.91114100	1.53821400
O	1.09324200	-2.57519000	-1.50825600
H	1.79311800	-2.58878800	-0.82289000
O	-2.69526700	0.36134100	-1.46324400
H	-3.16167000	-0.46738900	-1.61184900
O	1.72311200	2.15065700	-1.39279000
H	1.35019700	2.77921600	-0.74303300
H	2.98838600	0.25989900	0.68635200
O	0.48173000	-1.17394300	1.94746100
C	0.15669000	0.01002900	2.27654500
O	0.79464800	1.04189100	1.96082400
H	-1.16589300	-3.27006500	-1.59166100
C	-1.07856900	0.15724500	3.16716900
H	-1.80055200	-0.64110400	2.98854200
H	-1.54751100	1.13409000	3.03892300
H	-0.75180400	0.07895100	4.20913900

1 • OAc˙

B3LYP/ aug-cc-pVDZ = -2159.713432, ZPE = 0.362310, thermal correction to the enthalpy = 0.390054, M06-2X/maug-cc-pVT(+d)Z = -2159.180609

C	-1.02699400	0.98964500	-1.33927400
C	1.00234400	-0.95895400	-1.45161100
C	-1.37369600	-0.35268200	-1.42272100
C	0.38324900	1.33121300	-1.30139500
C	1.39608800	0.37476700	-1.43614100
C	-0.39088300	-1.35808600	-1.45540000
C	-2.07633000	2.06277100	-1.26922500
H	-3.02553900	1.66810500	-1.62825600
H	-1.79442300	2.90489600	-1.90858700
C	-0.75128700	-2.79980000	-1.32396800
H	-1.60902400	-3.04347500	-1.96076800
C	-1.09232700	-3.16738500	0.17189300
H	-1.72487300	-2.38176500	0.60520400
C	2.85038000	0.77534000	-1.34969100
H	2.96897300	1.81145000	-1.66360400
H	3.44922700	0.15315500	-2.02140300

C	3.36640900	0.59829300	0.09203700
C	-2.25496500	2.59480700	0.17612200
H	-2.59594500	1.78566200	0.82874200
O	-1.05252100	3.15404400	0.66383300
O	0.03794600	-3.40240700	0.93692900
H	0.34234200	-2.56443200	1.36154200
O	3.20543100	-0.75090400	0.50540600
H	2.39963800	-0.80702000	1.08998000
H	-0.61421300	2.48681900	1.26367500
C	-3.33768800	3.67693700	0.23110500
C	-1.95994400	-4.43182100	0.19569200
C	4.84692900	0.95625700	0.21304100
F	5.05457100	2.23855800	-0.17519800
F	5.62584300	0.17314400	-0.56390300
F	5.28669200	0.84160100	1.47659200
F	-1.35914200	-5.48843500	-0.37423100
F	-2.31030800	-4.77077700	1.44235500
F	-3.11687000	-4.20499400	-0.49769400
F	-3.02637900	4.74273600	-0.53242200
F	-4.51670300	3.18565500	-0.21987400
F	-3.53354900	4.11112500	1.48537700
O	1.87258000	-1.95853400	-1.38556100
H	2.64136600	-1.66713300	-0.81847300
O	-2.70488800	-0.64492300	-1.41202300
H	-2.86419300	-1.58494500	-1.55458000
O	0.74114500	2.59402200	-1.14988100
H	0.06889100	3.07446400	-0.58743300
H	2.82189100	1.26529700	0.76633700
O	0.87204500	-0.97976100	1.79346000
C	0.16728300	0.00753200	2.18289700
O	0.25661700	1.15685000	1.68104400
H	0.07829200	-3.43477200	-1.62797800
C	-0.79456300	-0.23210500	3.33547900
H	-1.19737500	-1.24570200	3.31335300
H	-1.60084100	0.50181400	3.34594400
H	-0.23246400	-0.12741800	4.26858700

1 • $H_2PO_4^-$

B3LYP/ aug-cc-pVDZ = -2575.035205, ZPE = 0.353598, thermal correction to the enthalpy = , M06-2X/maug-cc-pVT(+d)Z = 0.382507

C	0.32475000	1.38100100	-1.60697800
C	-0.43760700	-1.29936800	-1.40356200
C	1.27788700	0.35519900	-1.62228000
C	-1.02949100	1.01800000	-1.59275800
C	-1.43303600	-0.32432600	-1.52158700
C	0.91980500	-0.99778700	-1.54053900
C	0.73756300	2.82447200	-1.43696400
H	-0.15485400	3.44882900	-1.46877300
H	1.40198800	3.14248800	-2.24521900

C	1.95890000	-2.09615500	-1.51449200
H	1.50070400	-3.02838700	-1.84583700
C	2.55403900	-2.29995500	-0.10850400
H	1.77109700	-2.64589900	0.57390500
C	-2.89294700	-0.72122800	-1.50962200
H	-2.98207200	-1.74741700	-1.86806900
H	-3.45838300	-0.07374300	-2.18728000
C	-3.51891300	-0.62806100	-0.10807300
C	1.48227500	3.05879300	-0.09880900
O	0.81985300	2.51581800	1.03045000
O	3.14013700	-1.10651400	0.38128800
H	2.50101600	-0.71510600	1.03113600
O	-3.46239200	0.70467700	0.38744900
H	-2.75221200	0.73303900	1.06112900
C	3.63246600	-3.38094600	-0.09778200
C	-4.98519000	-1.05187600	-0.10417800
F	-5.75984100	-0.27071300	-0.89295400
F	-5.52367900	-1.01521300	1.13457200
F	-5.12686500	-2.32537800	-0.55423500
F	3.14214400	-4.56567200	-0.54922000
F	4.69010600	-3.07262800	-0.88525400
F	4.11792100	-3.60850100	1.14090200
O	-0.80456100	-2.59453400	-1.08701900
H	-0.86133600	-2.58672900	-0.10604600
O	2.60299900	0.72491400	-1.63596600
H	3.08212400	0.11283400	-1.04218800
O	-1.96467900	2.02400300	-1.59416700
H	-2.69725100	1.75414900	-1.00967400
H	-2.99700800	-1.30600000	0.57394100
H	2.77193900	-1.85179200	-2.20546200
P	-0.17229800	-0.54365800	2.21671600
H	1.23593500	1.66538900	1.29342100
O	1.21924000	-0.04039200	1.87511200
O	-0.76360600	-1.77698000	1.58361600
O	-1.20038000	0.72568800	1.95256500
H	-0.71918100	1.51973500	1.64735500
O	-0.23465800	-0.72419700	3.83938300
H	-0.88371900	-1.39896800	4.06637000
H	2.48926300	2.64382600	-0.17802600
C	1.66979900	4.54981200	0.17237400
F	2.30549400	5.15678400	-0.86672800
F	2.42442600	4.77726200	1.27052500
F	0.50351600	5.20664700	0.35343700

1 • $H_2PO_4^{\bullet}$

B3LYP/ aug-cc-pVDZ = -2574.860015, ZPE = 0.352295, thermal correction to the enthalpy = 0.381211, M06-2X/maug-cc-pVT(+d)Z = -2574.343551

C	0.16891500	1.41210300	-1.61906200
C	-0.13277300	-1.42777300	-1.28643500

C	1.26989600	0.56693400	-1.54834700
C	-1.09202700	0.80546500	-1.52749700
C	-1.26542200	-0.63619600	-1.43478300
C	1.14479100	-0.87729200	-1.44962100
C	0.31982800	2.90869200	-1.49421300
H	-0.64876900	3.37550900	-1.66618500
H	1.01454100	3.28812300	-2.24624900
C	2.35653400	-1.75857600	-1.45894800
H	2.06276800	-2.76504300	-1.75562400
C	3.02784700	-1.82371300	-0.06068700
H	2.36785100	-2.34106900	0.64036100
C	-2.63328100	-1.25931200	-1.47413900
H	-2.53112900	-2.30141100	-1.77786500
H	-3.25274000	-0.74271000	-2.21363500
C	-3.35300800	-1.20553300	-0.10830200
C	0.84746800	3.30985200	-0.08570600
O	0.23317800	2.59373000	0.96393800
O	3.33669000	-0.52806100	0.41390700
H	2.61528600	-0.27636700	1.04929200
O	-3.48481900	0.14573600	0.31956400
H	-2.90061800	0.27280800	1.09585600
C	4.32776200	-2.63036100	-0.11808300
C	-4.75500500	-1.81203000	-0.19711400
F	-5.53825000	-1.15357600	-1.07638900
F	-5.37198300	-1.79244000	0.99497800
F	-4.68483600	-3.10040900	-0.60277000
F	4.08739500	-3.87768000	-0.58444500
F	5.23688500	-2.06163200	-0.93690900
F	4.88491700	-2.74906500	1.09546200
O	-0.25129400	-2.74355000	-0.96550800
H	-0.42149500	-2.73825500	0.01300200
O	2.48024400	1.11581700	-1.47719300
H	3.06864100	0.55005300	-0.90656500
O	-2.15658600	1.58484300	-1.45034000
H	-2.87270700	1.13899300	-0.91959100
H	-2.79268800	-1.78215300	0.63108300
H	3.08828900	-1.37678100	-2.17666100
P	-0.12495400	-0.65964400	2.19589300
H	0.75523400	1.79160700	1.17376200
O	1.08235600	0.08142600	1.64375000
O	-0.61831700	-1.93369400	1.55941400
O	-1.40100700	0.39718600	2.13218900
H	-1.12097300	1.32660900	2.15849300
O	0.14427400	-0.87777000	3.77389400
H	-0.42380900	-1.55813000	4.15487700
H	1.93253900	3.17901300	-0.05538400
C	0.60503600	4.79640600	0.17491700
F	1.15261600	5.54191900	-0.81733600
F	1.16202800	5.19687200	1.33095800
F	-0.70688700	5.10229500	0.22776600

2

B3LYP/ aug-cc-pVDZ = -2048.745852, ZPE = 0.393657, thermal correction to the enthalpy = 0.422290

C	-0.83720200	-1.10701600	-0.03088200
C	0.65968200	1.20886300	0.50311600
C	0.49213600	-1.24487100	0.40227900
C	-1.46369900	0.14855700	-0.14596300
C	-0.68788600	1.28749900	0.11289200
C	1.20717100	-0.06884400	0.68725400
C	-2.91206800	0.25730000	-0.57420100
H	-3.07060400	-0.29629700	-1.50739300
H	-3.15602200	1.30464600	-0.77590200
C	-3.89869200	-0.29149300	0.46454800
H	-3.64112600	-1.33058000	0.71140200
C	1.12961300	-2.60707300	0.58144100
H	0.36871300	-3.38278500	0.45219800
H	1.52080200	-2.70377400	1.60213400
C	2.28790700	-2.88322900	-0.38663400
H	3.03696700	-2.08330600	-0.31240200
C	1.49983400	2.45831000	0.65743700
H	2.35243800	2.26026700	1.31161600
H	0.91385200	3.26424900	1.11337900
C	2.05385900	2.95935500	-0.69290400
H	2.75189600	2.21456800	-1.10374900
O	-1.59715900	-2.23824000	-0.27681600
O	2.52967000	-0.18272900	1.09756900
O	-1.22743500	2.55123200	-0.11590600
C	-1.86492900	3.17177800	1.02114300
H	-2.70580400	2.56205300	1.36953300
H	-2.21884400	4.14702900	0.67194300
H	-1.14707000	3.31207100	1.84206600
C	2.71398500	-0.18513500	2.52074700
H	2.36050400	0.75497600	2.96895100
H	3.78998700	-0.29210000	2.69256400
H	2.18102300	-1.02542900	2.98907100
C	-1.56292100	-2.72685800	-1.63314500
H	-1.90736200	-1.95574900	-2.33720800
H	-2.25000200	-3.57875500	-1.66119800
H	-0.55050400	-3.04431500	-1.90732300
C	3.01882800	-4.17981700	-0.02207800
C	2.88235200	4.23541900	-0.49039300
C	-5.32677800	-0.32936700	-0.08892100
O	1.77330100	-2.98606600	-1.70610100
H	2.50624300	-2.99623600	-2.33415700
O	1.06750800	3.20655500	-1.67038900
H	0.20271000	3.29402700	-1.23683400
F	-5.43404000	-1.20804600	-1.11712700
F	-6.19878800	-0.73672700	0.87633100
F	-5.76131300	0.87035900	-0.53269000
F	2.14612700	5.25312300	0.02492000
F	3.41847100	4.67408300	-1.64852700

F	3.91682800	4.01612000	0.37057000
F	2.20576000	-5.25755000	0.02794400
F	3.98841500	-4.45329500	-0.93856700
F	3.63208400	-4.07631300	1.18530900
O	-3.86180600	0.53626500	1.61935500
H	-4.37947300	0.12324800	2.32173700

2 • Cl^-

B3LYP/ aug-cc-pVDZ = -2509.108688, ZPE = 0.392721, thermal correction to the enthalpy = 0.422134, M06-2X/maug-cc-pVT(+d)Z = -2508.935269

C	1.20529100	0.28387200	1.19379300
C	-1.45437300	-0.57714900	1.13776600
C	0.94856800	-1.09293400	1.14322800
C	0.19087500	1.25238700	1.18879400
C	-1.13180500	0.78840100	1.19498100
C	-0.39654500	-1.50014600	1.14524300
C	2.07719100	-2.07659900	0.93658400
H	2.90834100	-1.86684100	1.62074600
H	1.72508800	-3.09665700	1.11507500
C	0.52248200	2.71561900	1.01128500
H	-0.34980600	3.33342400	1.24336600
H	1.34812700	3.01331100	1.66834900
C	-2.88493100	-1.00883100	0.91383100
H	-2.98748400	-2.08417600	1.08523000
H	-3.56379600	-0.47598400	1.59047500
O	-0.68593300	-2.85470800	1.09172500
O	2.53049700	0.71445700	1.13820000
O	-2.17550400	1.70643700	1.16964800
C	-0.83060100	-3.46553000	2.36959100
H	-1.65598200	-3.01070100	2.94192100
H	0.09670300	-3.38534900	2.96088500
H	-1.05461600	-4.52279700	2.18578500
C	-2.61309900	2.12324200	2.46006100
H	-2.95862900	1.26783500	3.06293600
H	-3.44727800	2.81572200	2.29852400
H	-1.80875200	2.64056100	3.00763300
C	3.14207400	0.89265400	2.41450600
H	3.16172400	-0.04993500	2.98361200
H	2.61334600	1.65460700	3.00853400
H	4.16901100	1.22563900	2.22579900
C	-3.30661400	-0.72343800	-0.55321900
C	0.92034400	2.99988500	-0.46199100
H	1.76569900	2.35327000	-0.74004000
C	2.59630100	-2.00841300	-0.52484800
H	2.89325600	-0.97491700	-0.75635300

O	1.66665100	-2.50017600	-1.45015400
O	-0.15617500	2.85111900	-1.34618600
H	-0.13426500	1.94289300	-1.73572400
H	-3.15602000	0.34384400	-0.77280900
O	-2.63996700	-1.54372200	-1.47358600
H	-1.83627800	-1.08055300	-1.81084900
C	1.43484300	4.43268100	-0.60827200
C	3.86928200	-2.84220700	-0.67706700
C	-4.80498600	-0.97110000	-0.73309600
F	4.38692800	-2.77477800	-1.92478400
F	4.85269400	-2.40574200	0.17249800
F	3.68115600	-4.15866300	-0.39661700
F	-5.54335600	-0.18441500	0.11186000
F	-5.23060900	-0.68929800	-1.98551800
F	-5.16781100	-2.25500900	-0.47121900
F	2.51415100	4.65816900	0.20574800
F	1.84213800	4.71108500	-1.86738000
F	0.50590500	5.36810200	-0.27626100
Cl	-0.03809900	-0.06105000	-2.46130400
H	1.12616500	-1.75202600	-1.80004600

2 • $Cl^{\bullet}$

B3LYP/ aug-cc-pVDZ = -2508.932582, ZPE = 0.393950, thermal correction to the enthalpy = 0.423476, M06-2X/maug-cc-pVT(+d)Z = -2508.748768

C	1.28541200	-0.01666800	1.19442200
C	-1.50017500	-0.32021800	1.02512700
C	0.71994400	-1.32463800	1.13297400
C	0.54447300	1.15825900	1.10098500
C	-0.87917300	0.99533400	1.01550400
C	-0.68447100	-1.44421900	1.12546200
C	1.59909500	-2.50999300	0.86850600
H	2.49441100	-2.49517100	1.49841600
H	1.05026700	-3.43913800	1.03720200
C	1.30293200	2.46565800	1.02260900
H	0.74206300	3.30125100	1.43875600
H	2.22045800	2.37142100	1.60869600
C	-2.99269800	-0.43914900	0.92582500
H	-3.28995000	-1.46128200	1.17147900
H	-3.46258000	0.25796600	1.63033700
O	-1.25592000	-2.68919500	1.09698600
O	2.65626100	0.08245100	1.20100600
O	-1.80430500	1.94417900	1.02128900
C	-1.41183100	-3.31383100	2.38046800
H	-2.08618800	-2.72663600	3.02182400
H	-0.44232600	-3.43420100	2.88667400

H	-1.85016100	-4.29711700	2.18611600
C	-1.63253700	3.38128700	0.96942400
H	-2.65074400	3.75857100	0.84498900
H	-1.00351900	3.65751600	0.11847400
H	-1.22319500	3.73913700	1.92098900
C	3.28709700	-0.04280200	2.48983800
H	3.00321100	-0.98190300	2.98370300
H	3.01383000	0.80377100	3.13592400
H	4.36431900	-0.03356800	2.30145000
C	-3.53671000	-0.13334600	-0.50264700
C	1.70402100	2.80558400	-0.43880000
H	2.32201200	1.99124800	-0.84316500
C	2.05265300	-2.49584100	-0.62807400
H	2.59717000	-1.56367200	-0.83551300
O	0.98516800	-2.69156700	-1.51211100
O	0.59234700	3.06453700	-1.26058100
H	0.30009300	2.22269800	-1.67529900
H	-3.18907600	0.85712500	-0.82827000
O	-3.19380400	-1.12568700	-1.42741400
H	-2.34461100	-0.86922800	-1.83644500
C	2.58321300	4.05874400	-0.46539800
C	3.05848900	-3.62616100	-0.87116400
C	-5.06551800	-0.05030200	-0.46534000
F	3.52003300	-3.61896800	-2.13590300
F	4.13939300	-3.48643300	-0.04822300
F	2.53367100	-4.84905500	-0.63003500
F	-5.46966400	0.93469600	0.39118800
F	-5.57995000	0.24407800	-1.67473700
F	-5.64032300	-1.20025600	-0.04258900
F	3.69373500	3.88475300	0.30505400
F	3.00189300	4.35533000	-1.70900400
F	1.93316500	5.14776900	0.01940900
Cl	-0.39987200	0.22939300	-2.02989900
H	0.60150300	-1.82962200	-1.76621900

2 • OAc^-

B3LYP/ aug-cc-pVDZ = -2277.383435, ZPE =0.442481 , thermal correction to the enthalpy = 0.474212, M06-2X/maug-cc-pVT(+d)Z = -2277.192331

C	-1.13486100	0.40392800	-1.39107700
C	1.45112400	-0.65591600	-1.33838200
C	-0.04999600	1.29387900	-1.37112500
C	-0.98176200	-0.99034200	-1.38336800
C	0.32846500	-1.49661700	-1.38546100
C	1.23388600	0.73094300	-1.37793400
C	-0.26419500	2.77982000	-1.20322900

H	-1.10118700	3.12438000	-1.82074300
H	0.63518700	3.32857400	-1.49806900
C	2.83596600	-1.19715600	-1.07148500
H	3.58216600	-0.70152400	-1.70353500
H	2.86799500	-2.27373800	-1.26129100
C	-2.17883000	-1.89933700	-1.22495300
H	-1.91000500	-2.92669200	-1.48721900
H	-3.00190100	-1.57419400	-1.87206700
O	-2.42470900	0.92874100	-1.31969900
O	0.51478000	-2.87099200	-1.36630600
O	2.34421700	1.56534900	-1.34084600
C	2.83738000	1.92964700	-2.62660600
H	3.12954400	1.04304900	-3.21279800
H	3.71765300	2.56013800	-2.45622600
H	2.08531000	2.49852300	-3.19701900
C	0.66932100	-3.44998600	-2.65756300
H	1.54849800	-3.03945400	-3.18104500
H	-0.22417100	-3.28289100	-3.28197500
H	0.80819400	-4.52624500	-2.50205300
C	-3.02549900	1.18768200	-2.58720700
H	-2.44236600	1.92243400	-3.16410100
H	-4.02292100	1.59359800	-2.38376000
H	-3.11975400	0.26514400	-3.18143300
C	-2.66927700	-1.90451200	0.24819500
H	-2.89278300	-0.86932200	0.55133500
C	-0.55004300	3.12728900	0.28081400
H	-1.40271600	2.52906600	0.63659300
C	3.20384800	-0.96640500	0.42020300
H	3.14519300	0.11027500	0.64190800
O	2.42171900	-1.72762500	1.29891900
H	1.56511100	-1.27207600	1.48691800
C	4.65906800	-1.35791100	0.67667100
C	-3.99768500	-2.65288400	0.36436700
C	-1.00427200	4.58768600	0.39799200
O	0.58068800	2.94015400	1.07435900
O	-1.77272800	-2.52551500	1.12325300
H	-1.09030500	-1.86504400	1.43206300
F	-4.95908600	-2.08812200	-0.43160600
F	-4.49145400	-2.63651700	1.62548900
F	-3.91133300	-3.95633700	-0.00878000
F	-0.07707600	5.47198800	-0.06005100
F	-1.28646100	4.93956700	1.67311200
F	-2.14542900	4.82204200	-0.32781100
F	5.04138300	-1.12647900	1.95381400
F	4.91238200	-2.66865100	0.42020900
F	5.51193500	-0.63949400	-0.11814900
C	-0.29069700	0.05263100	2.91890700
O	-0.02670100	-0.66531900	1.89212500

O	-0.08005900	1.28577100	3.01376100
H	0.37576900	2.27672700	1.79673800
C	-0.89933000	-0.66490200	4.12294400
H	-1.26176500	0.05526000	4.86469300
H	-0.12556800	-1.29842000	4.58097400
H	-1.71224900	-1.32927200	3.80131800

2 • OAc$^{\bullet}$

B3LYP/ aug-cc-pVDZ = -2277.209273, ZPE = 0.443365, thermal correction to the enthalpy = 0.474990, M06-2X/maug-cc-pVT(+d)Z = -2277.009141

C	-1.30797400	0.25696900	-1.43082700
C	1.38396600	-0.56086100	-1.38696300
C	-0.36168000	1.27268300	-1.40314900
C	-0.98263600	-1.13978700	-1.39548300
C	0.38224600	-1.51566300	-1.44996500
C	1.01119800	0.84626600	-1.40399000
C	-0.84515500	2.69667200	-1.25163400
H	-1.84920100	2.78017300	-1.67281400
H	-0.21398500	3.40983300	-1.78129900
C	2.82112600	-0.94653500	-1.20931000
H	3.46708600	-0.33101600	-1.84444800
H	2.95249200	-2.00149900	-1.46036400
C	-2.04173600	-2.14690900	-1.10828000
H	-1.69642300	-3.15402300	-1.35080100
H	-2.96169500	-1.92048200	-1.65624000
O	-2.63495200	0.58986400	-1.35245200
O	0.70819200	-2.84410800	-1.43214800
O	2.08980700	1.60384100	-1.47446200
C	2.19085100	3.04795700	-1.56155000
H	3.26821200	3.22729300	-1.59359200
H	1.73809300	3.49611700	-0.67299500
H	1.72902600	3.39423900	-2.49244600
C	0.75172000	-3.47365400	-2.72264900
H	1.52825400	-3.01629600	-3.35371600
H	-0.22048900	-3.40400600	-3.23346200
H	0.99616300	-4.52352500	-2.53718800
C	-3.34798200	0.63789600	-2.60404400
H	-2.95768000	1.44700700	-3.23745800
H	-4.39240100	0.83597800	-2.34799100
H	-3.27054500	-0.31650900	-3.14270400
C	-2.39306500	-2.13657100	0.43036800
H	-2.71879400	-1.12302300	0.70937800
C	-0.90424200	3.08447400	0.25106900
H	-1.64328300	2.44628400	0.75891000
C	3.25598900	-0.76322700	0.28128900

H	3.11669600	0.28826200	0.57661000
O	2.59466600	-1.63948600	1.14083300
H	1.71792500	-1.25565300	1.38511300
C	4.75791000	-1.03222900	0.41400700
C	-3.60657300	-3.04530000	0.66274400
C	-1.42290900	4.52172200	0.39186300
O	0.35262600	2.98099800	0.84593600
O	-1.35666300	-2.60280000	1.22333800
H	-0.74191800	-1.84857000	1.44847000
F	-4.67404700	-2.62163500	-0.07630500
F	-3.99085100	-3.03489900	1.95346400
F	-3.36929500	-4.32976500	0.31283100
F	-0.61093900	5.42067900	-0.22736400
F	-1.53104900	4.89538000	1.67916500
F	-2.65830100	4.65559700	-0.17433500
F	5.19006600	-0.84438700	1.67581700
F	5.09719400	-2.28941300	0.04629500
F	5.46778600	-0.17943000	-0.38323500
C	0.06465800	0.16201300	2.76872200
O	0.18880400	-0.48093800	1.65694500
O	0.10276300	1.41040700	2.86074100
H	0.29644000	2.35074600	1.64126100
C	-0.12453000	-0.65752700	4.03378000
H	-0.33007000	-0.00680000	4.88882600
H	0.79151200	-1.23467200	4.22437800
H	-0.93952600	-1.38157500	3.90173400

2 • $H_2PO_4^-$

B3LYP/ aug-cc-pVDZ = -2692.49481202, ZPE = 0.430847, thermal correction to the enthalpy = 0.472980, M06-2X/maug-cc-pVT(+d)Z = -2692.344694

C	-1.11341400	0.24781600	-1.52691100
C	1.59656800	-0.43982700	-1.44018400
C	-0.16317900	1.28181000	-1.48920300
C	-0.76615600	-1.11147400	-1.52705600
C	0.60301900	-1.42834700	-1.51691200
C	1.18772400	0.90442500	-1.46675000
C	-0.59595200	2.72689500	-1.38096900
H	-1.44663700	2.91771300	-2.04443300
H	0.22264700	3.39315700	-1.66837600
C	3.04620600	-0.78948800	-1.19456800
H	3.70610200	-0.16412300	-1.80676900
H	3.23135100	-1.84013100	-1.43514000
C	-1.82583700	-2.18444000	-1.41926300
H	-1.42370600	-3.14682200	-1.74906400

H	-2.69175300	-1.93382000	-2.04202700
O	-2.46337100	0.58934100	-1.47949100
O	0.98039300	-2.76222500	-1.52275600
O	2.16832800	1.88546400	-1.39836800
C	2.63845800	2.33134800	-2.66746200
H	1.82907100	2.79567400	-3.25358500
H	3.06798200	1.50226400	-3.25292300
H	3.41604000	3.07710700	-2.46693600
C	1.22359400	-3.28826500	-2.82328300
H	2.04121500	-2.74957900	-3.32998900
H	0.32051500	-3.23452000	-3.45370600
H	1.50931900	-4.33757800	-2.68601200
C	-3.07947600	0.75079200	-2.75619700
H	-3.04133300	-0.18163000	-3.34078300
H	-2.59602600	1.55191700	-3.33680000
H	-4.12460500	1.01959600	-2.56624100
C	-2.29896500	-2.35693400	0.04887800
H	-2.64448000	-1.38882600	0.44181200
C	-0.98765000	3.10047000	0.07035500
H	-1.65841100	2.32973500	0.47905100
C	3.40449100	-0.58357700	0.30255800
H	3.14752300	0.44537900	0.59818600
O	2.81094100	-1.53622100	1.14140300
C	4.91569400	-0.70092900	0.50678900
C	-3.51620100	-3.28035200	0.10637400
C	-1.80657200	4.39714500	0.08041300
O	0.14423800	3.28295900	0.86796500
O	-1.31710300	-2.92587900	0.87068800
H	-0.74604500	-2.20795600	1.23808100
F	-3.26443600	-4.52507800	-0.38151600
F	-4.55320400	-2.78066200	-0.63634000
F	-3.98915400	-3.44018700	1.36306100
F	-1.13463100	5.45298700	-0.45182000
F	-2.18058900	4.75773400	1.33072300
F	-2.96220700	4.27297900	-0.64588000
F	5.28313300	-0.48989500	1.79106600
F	5.40695700	-1.91772200	0.14975900
F	5.59113100	0.22161600	-0.24588200
H	0.12295800	2.64506800	1.62959900
P	-0.32887500	0.08207000	2.86120400
H	1.90225200	-1.25140300	1.40202500
O	-1.98289500	-0.06654200	2.68590000
H	-2.40604500	0.69725100	3.09945600
O	-0.05364100	-0.48634800	4.39678700
H	0.04440400	-1.44708400	4.35541400
O	0.03764700	1.56001700	2.87414800
O	0.25092100	-0.93441600	1.86033700

2 • $H_2PO_4^{\bullet}$

B3LYP/ aug-cc-pVDZ = -2692.320330, ZPE = 0.431897, thermal correction to the enthalpy = 0.465122, M06-2X/maug-cc-pVT(+d)Z = -2692.163271

C	-1.40047600	-0.01460100	-1.36824400
C	1.46410700	0.20562200	-1.47063200
C	-0.79185600	1.26234500	-1.33235800
C	-0.65190300	-1.17863700	-1.43921500
C	0.79786300	-1.06222000	-1.54951500
C	0.64085700	1.32837000	-1.40625200
C	-1.62450900	2.48392600	-1.12785600
H	-2.52024700	2.42018100	-1.75525800
H	-1.07163300	3.39229200	-1.37068300
C	2.95813300	0.42053500	-1.35590100
H	3.19479200	1.42189000	-1.72135100
H	3.53464100	-0.28729200	-1.95070100
C	-1.30474100	-2.52635500	-1.35565300
H	-0.75275700	-3.26604200	-1.94121200
H	-2.32840300	-2.45732300	-1.73127900
O	-2.76433400	-0.09205000	-1.21264200
O	1.33731100	-2.24269000	-1.77847300
O	1.22002400	2.55914800	-1.31594900
C	1.35215100	3.29361500	-2.54774500
H	0.37902000	3.42525800	-3.04074800
H	2.04048400	2.77689500	-3.23223400
H	1.76292200	4.26840900	-2.27120800
C	2.73186200	-2.59408300	-1.94945700
H	3.11590600	-2.13341300	-2.86680300
H	2.71011500	-3.68088600	-2.05768900
H	3.29806000	-2.29399700	-1.06282900
C	-3.53334000	-0.08729800	-2.42935900
H	-3.29586900	-0.96401400	-3.04828600
H	-3.35039100	0.82687500	-3.01157300
H	-4.58211900	-0.12338800	-2.12197700
C	-1.37029800	-3.04831800	0.11877300
H	-1.84976100	-2.28760800	0.75229700
C	-2.10155000	2.65031200	0.36622400
H	-2.42281900	1.66988200	0.74824800
C	3.41762700	0.32440900	0.12586500
H	2.83839800	1.03596800	0.73227500
O	3.31385100	-0.98527400	0.62398100
C	4.88493400	0.74516600	0.24179800
C	-2.28127400	-4.28056000	0.17362000
C	-3.34854200	3.54218000	0.39346900
O	-1.14282200	3.25323700	1.16433700

O	-0.12033600	-3.42373400	0.61143000
H	0.25743000	-2.67737700	1.13883200
F	-1.82591000	-5.29497200	-0.60160600
F	-3.53665100	-3.97782900	-0.26766600
F	-2.40649600	-4.75211700	1.42907900
F	-3.11569100	4.77406900	-0.11660000
F	-3.81748900	3.69812900	1.64689400
F	-4.35773400	2.99232200	-0.34380700
F	5.32009700	0.71516100	1.51480400
F	5.70527100	-0.05715200	-0.48848800
F	5.06615900	2.01489300	-0.21844300
H	-0.51006700	2.55833800	1.49440100
P	0.27915700	-0.06509300	2.47633800
H	2.47304500	-1.08158600	1.14087200
O	-1.32679900	-0.47515600	2.58161700
H	-1.80704200	0.15047200	3.14165400
O	0.75773000	0.04804400	4.04661500
H	0.93479800	-0.82949400	4.41338700
O	0.46491400	1.30949300	1.84422200
O	0.94119400	-1.28684500	1.80534800

Figure S1. Non-linear plot for the binding of **1** with chloride ion. Circles are the experimental data and the line is the calculated isotherm.

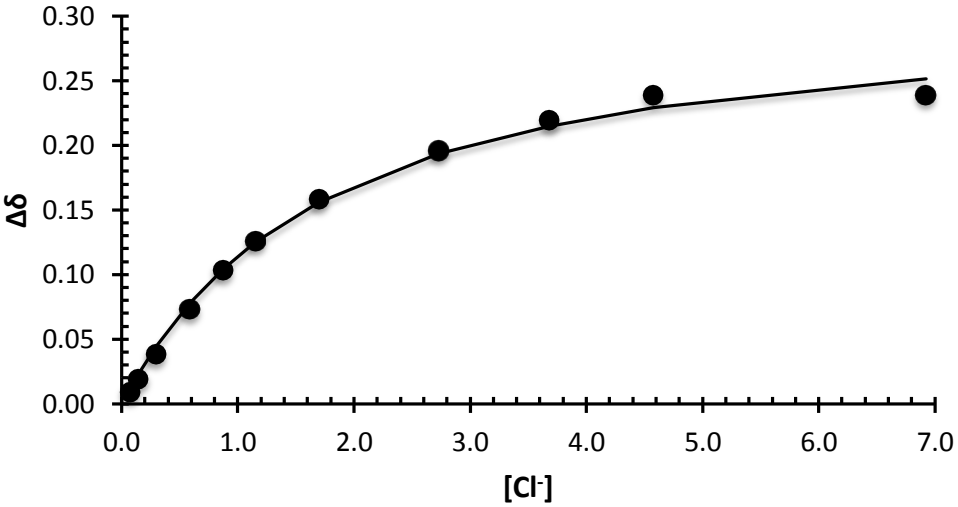

Table S1. Titration data for chloride binding to **1**.[a]

µL (Cl^-added)	[Cl^-]	[**1**]	δ (C-H)	Δδ	%bound
0	0.00	0.32	3.804	0.000	0.0
3	0.07	0.32	3.813	0.009	3.8
5	0.15	0.32	3.823	0.019	7.9
10	0.30	0.32	3.842	0.038	15.9
20	0.59	0.32	3.877	0.073	30.5
30	0.87	0.32	3.907	0.103	43.1
40	1.15	0.32	3.930	0.126	52.7
60	1.70	0.32	3.962	0.158	66.1
100	2.73	0.32	4.000	0.196	82.0
140	3.68	0.32	4.023	0.219	91.6
180	4.58	0.32	4.0430	0.239	100.0
300	6.92	0.32	4.0431	0.239	100.0

[a] Chemical shifts and concentrations are given in ppm and mM, respectively.

Figure S2. Non-linear plot for the binding of **2** with chloride ion. Circles are the experimental data and the line is the calculated isotherm.

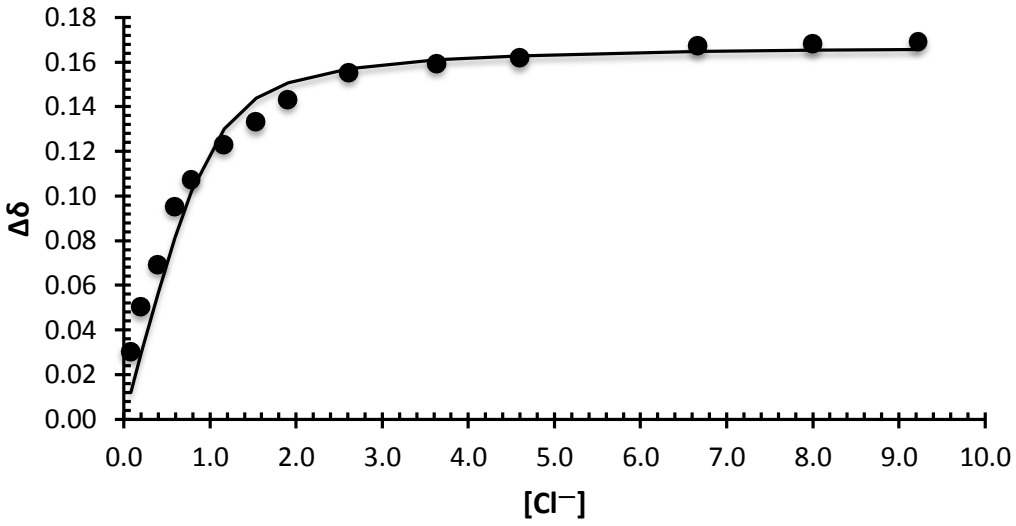

Table S2. Titration data for chloride binding to **2**.[a]

µL (Cl^- added)	[Cl^-]	[**2**]	δ (C-H)	Δδ	%bound
0	0.00	1.00	4.396	0.000	0.0
2	0.08	1.00	4.426	0.030	17.8
5	0.20	0.99	4.446	0.050	29.6
10	0.40	0.99	4.465	0.069	40.8
15	0.59	0.99	4.491	0.095	56.2
20	0.78	0.98	4.503	0.107	63.3
30	1.17	0.97	4.519	0.123	72.8
40	1.54	0.96	4.529	0.133	78.7
50	1.91	0.95	4.539	0.143	84.6
70	2.62	0.93	4.551	0.155	91.7
100	3.64	0.91	4.555	0.159	94.1
130	4.60	0.89	4.558	0.162	95.6
200	6.67	0.83	4.563	0.167	98.8
250	8.00	0.80	4.564	0.168	99.4
300	9.23	0.77	4.565	0.169	100.0

[a] Chemical shifts and concentrations are given in ppm and mM, respectively.

Appendix for chapter 8

Experimental section

General. All reactants and reagents including $(Ph_3P)_2NCl$ and Bu_4NX (X = Cl, OAc, NO_3, H_2PO_4, and HSO_4) were bought from Sigma–Aldrich. Tetrahydrofuran was dried by refluxing it over sodium metal under argon and subsequently was distilled. TLC analyses were performed on precoated (250 mm) silica gel 60 F-254 plates (Merck) and were visualized by staining with $KMnO_4$ or with a hand–held UV lamp. Diol **1** was synthesized as previously reported.[17] All deuterated solvents were purchased from Cambridge Isotope Laboratories and used from freshly opened bottles except for $CDCl_3$ and CD_3CN which were dried over activated 3 Å molecular sieves for several days. Proton NMR spectra were recorded on Varian VI-500 and VI-300 MHz instruments at different temperatures as indicated, and the resulting chemical shifts are reported in parts per million (δ) relative to the residual solvent peak. For ^{13}C spectra the residual acetonitrile signal at 1.39 ppm was used whereas for ^{19}F an extenal reference sample of $CFCl_3$ was set to 0.00 ppm. A Bruker BioTOF II electrospray ionization–time of flight mass spectrometer with polyethylene glycol 400 as an internal standard was used to obtain an exact mass measurement of **2**.

Binding Constant Determinations. Dilute solutions of **1** and **2** (2.5 mM) were titrated with anions salts (30-100 mM) at different temperatures. The changes in the chemical shifts of the hydroxyl groups in **1** and **2** were followed and nonlinear plots of the titration data (i.e., Δδ versus the concentration of the guest) were fit to a 1:1 binding equation

using the Solver add–on program to Microsoft Excel 2010 to obtain the binding constants.

Figure S1. Non-linear plot for the binding of **1** with Bu_4NCl in $CDCl_3$ at room temperature. Circles are the experimental data and the line is the calculated isotherm.

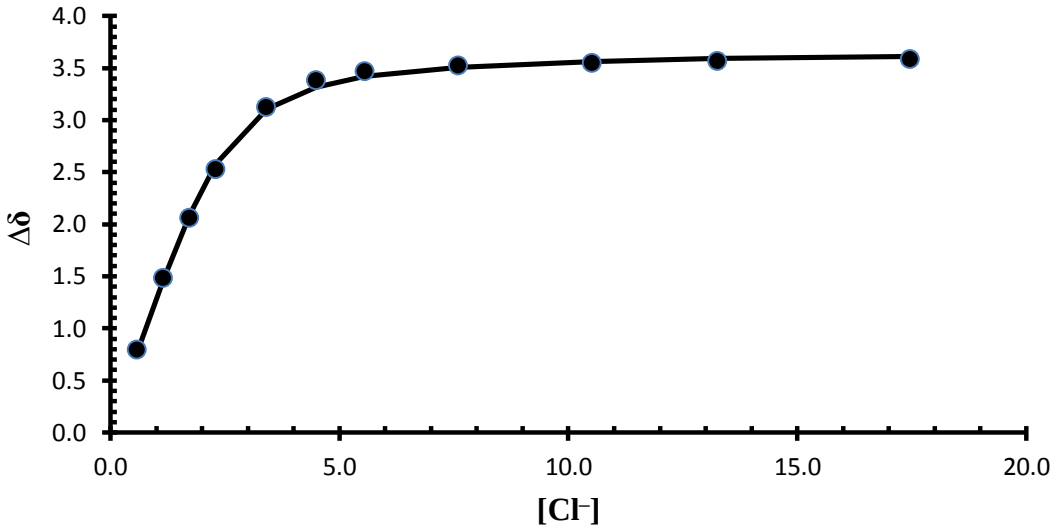

Table S1. Titration data for Bu_4NCl binding to **1** in $CDCl_3$.[1]

µL (Cl^- added)	[Cl^-]	[**1**]	δ (OH)	Δδ	%bound
0	0.0	2.50	2.562	0.000	0.0
5	0.58	2.49	3.354	0.792	22.1
10	1.16	2.47	4.044	1.482	41.4
15	1.73	2.46	4.619	2.057	57.4
20	2.30	2.44	5.090	2.528	70.5
30	3.41	2.41	5.683	3.121	87.1
40	4.49	2.39	5.940	3.378	94.3
50	5.56	2.36	6.026	3.464	96.7
70	7.61	2.31	6.083	3.521	98.2
100	10.53	2.24	6.111	3.549	99.0
130	13.27	2.17	6.126	3.564	99.4
180	17.48	2.06	6.146	3.584	100

[1]Chemical shifts and concentrations are given in ppm and mM, respectively. The chloride solution was 100 mM and the NMR initially contained 0.85 ml of a 2.5 mM solution of **1**.

Figure S2. Non-linear plot for the binding of **2** with Bu_4NCl in $CDCl_3$ at room temperature. Circles are the experimental data and the line is the calculated isotherm.

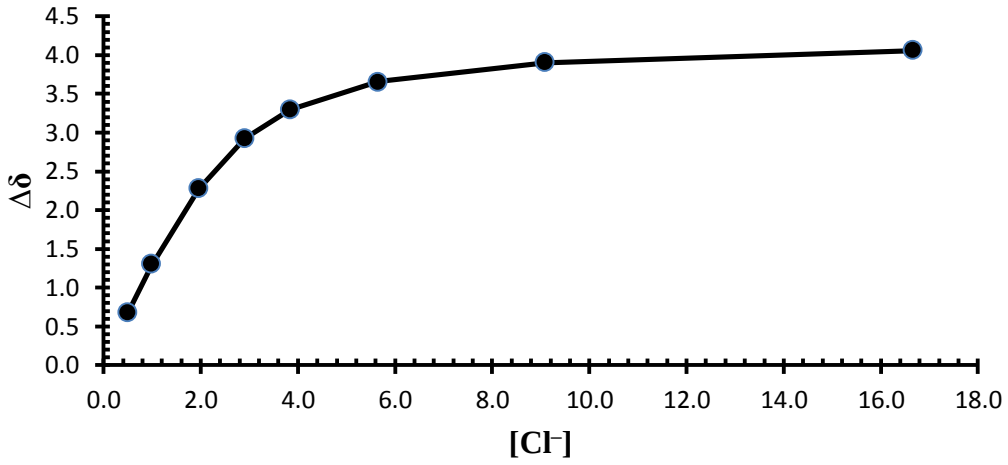

Table S2. Titration data for Bu_4NCl binding to **2** in $CDCl_3$.[1]

µL (Cl^- added)	[Cl^-]	[**2**]	δ (OH)	Δδ	%bound
0	0.0	2.50	2.395	0.000	0.0
5	0.50	2.49	3.072	0.677	16.1
10	0.99	2.47	3.699	1.304	31.0
20	1.96	2.45	4.671	2.276	54.1
30	2.91	2.43	5.316	2.921	69.4
40	3.85	2.40	5.691	3.296	78.4
60	5.66	2.36	6.040	3.645	86.6
100	9.09	2.27	6.300	3.905	92.8
200	16.66	2.08	6.456	4.061	96.5

[1]Chemical shifts and concentrations are given in ppm and mM, respectively. The chloride solution was 100 mM and the NMR initially contained 0.85 ml of a 2.5 mM solution of **1**.

Figure S3. Van't Hoff plot of complex formation of **1** with Cl^- at three different temperatures.

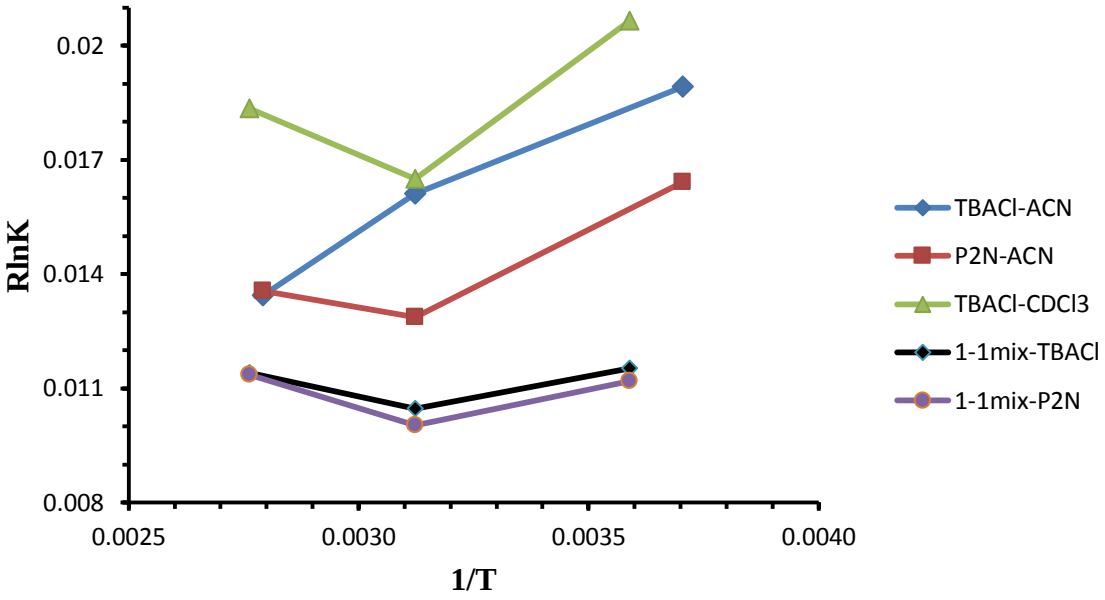

*(racemic)-1,1,1,6,6,6-Hexafluoro-2,5-diphenylhexane-2,5-diol (**2**):* A dry two-necked round-bottomed flask was equipped with a magnetic stirring bar, a reflux condenser with an argon inlet, and a rubber septum. The flask was charged with 0.95 g (4.0 mmol) of 1,4-diphenylbutane-1,4-dione dissolved in 5 ml of monoglyme and cooled to 0 °C. Trifluoromethyl(trimethylsilane) (1.85 g, 13.0 mmol) and a catalytic amount of CsF (0.012g, 0.10 mmol) were added sequentially with stirring and then the bath temperature was allowed to rise to room temperature before heating the reaction mixture at 60 °C for 3 h. The solvent was removed at reduced pressure and then 5 ml of THF was added to the residue. Tetrabutylammonium fluoride (12 ml of a 1 M solution in THF) was added dropwise and the resulting solution was stirred at room temperature for 2 h. Volatile compounds were removed at reduced pressure and the product was extracted with diethyl ether. The organic layer was dried over $MgSO_4$ and concentrated under vacuum to give the desired diol in a 2:1 (dl : meso) diastereomeric ratio. Purification and separation of the diastereomers was carried out via column chromatography (1:5 diethyl ether/pentane) to give 0.55 g (35%) of the desired dl-diol as a white solid. ^{1}H NMR (300 MHZ, CD_3CN) δ 1.60 (2H, dd, J = 13.8 and 4.0 Hz), 2.30 (2H, dd, J = 13.8 and 4.5 Hz), 4.41 (2H, br s), 7.46 (6H, m), 7.59 (4H, d, J = 7.2 Hz). ^{13}C NMR (75 MHZ, CD_3CN) δ 29.1, 77.8 (q, J = 28.2 Hz), 127.3 (CF_3, q, J = 284 Hz), 128.0, 129.7, 129.9, 137.7. ^{19}F-NMR (282 MHz, CD_3CN) δ -81.2. IR (ATR source) 3537 (OH), 3405 (OH, br). HRMS-ESI: calc for $C_{18}H_{15}F_6O_2^-$ $(M - H)^-$ 377.0982, found 377.0979.

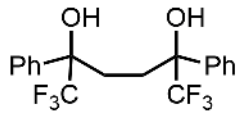

^{1}H NMR (300 MHz, CD_3CN)

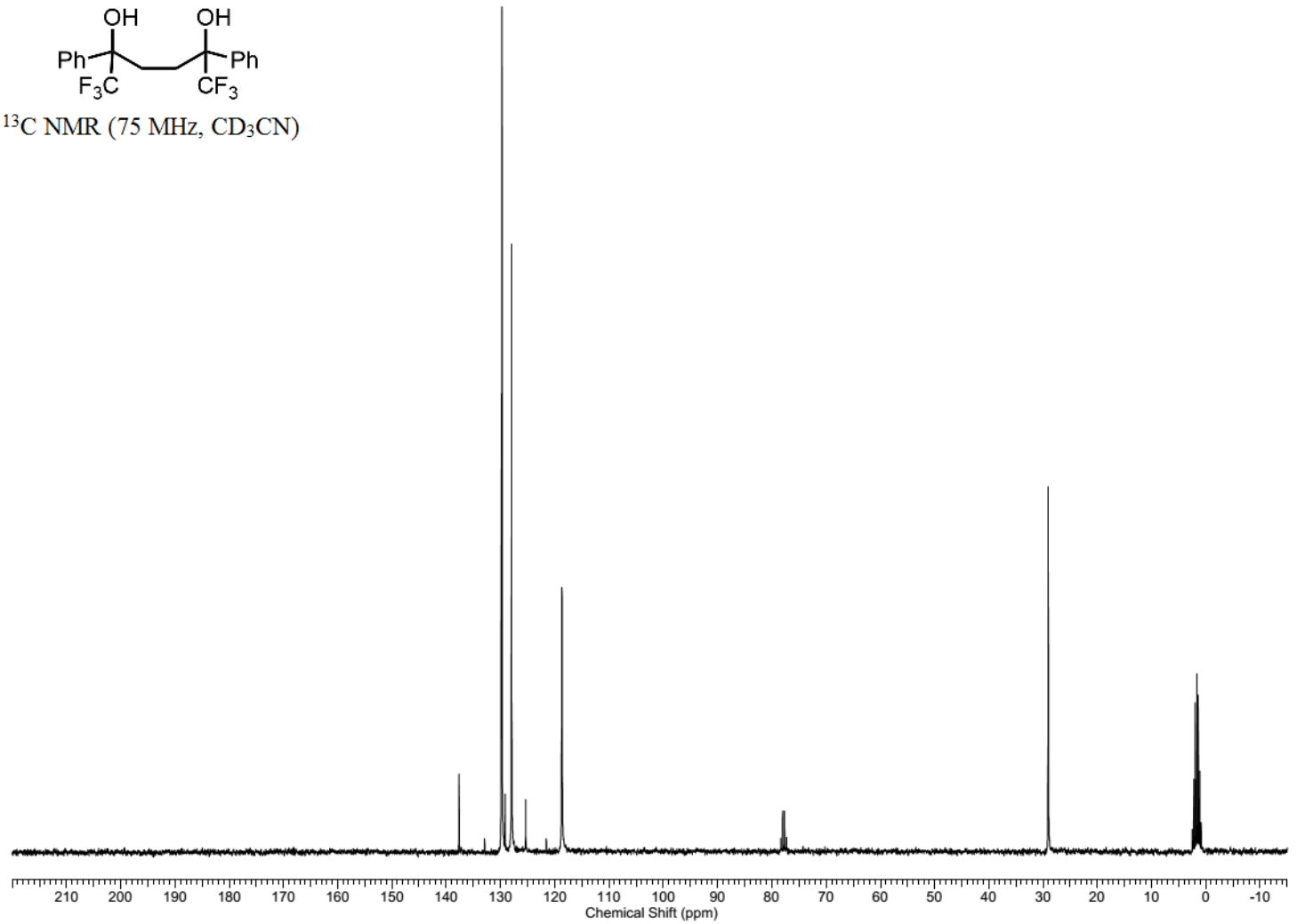
OH
OH
Ph
Ph
F3C
CF3
13C NMR (75 MHz, CD3CN)
210 200 190 180 170 160 150 140 130 120 110 100 90 80 70 60 50 40 30 20 10 0 -10
Chemical Shift (ppm)

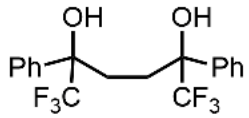

^{19}F NMR (282 MHz, CD_3CN)